SOME DESIGN AND OPTIMIZATION TECHNIQUES FOR EXTENDING THE OPERATING FREQUENCY RANGE OF ACTIVE-RC FILTERS

S. NATARAJAN

A THESIS

IN

THE FACULTY

OF

ENGINEERING

Presented in Partial Fulfillment of the Requirements

for the degree of Doctor of Philosophy at

Concordia University

Montreal, Quebec, Canada

December, 1978

© S. Natarajan, 1978

ABSTRACT

SOME DESIGN AND OPTIMIZATION TECHNIQUES FOR EXTENDING THE OPERATING FREQUENCY RANGE OF ACTIVE-RC FILTERS

S. Natarajan, Ph.D.
Concordia University, 1978

Two techniques for extending the frequency range of active-RC filters have been developed and studied in detail. The first technique increases considerably the frequency range of application of the active-RC filters employing finite gain amplifiers (FGA) as active elements while the second one maximizes the operating frequency range of any second order active-RC filter that uses operational amplifiers (OA).

A general theory of active compensation of FGA's using OA's, based on a control model having a single forward path and a single feedback path, is first presented. This requires, for stability reasons, the improved FGA's to have only a second order transfer function. A complete set of realizations of such a transfer function is thus given. Employing multiple feedback paths, it is then shown that stable FGA's of any order can be realized. However, considerations such as relative stability, the expected improvement in performance, indicate that it is fruitless to go beyond third order realizations.

The comparisons of the characteristics of the new FGA's with those of the conventional FGA's show that the bandwidth of second order FGA's is an order of magnitude more than that of the conventional FGA's. Further, the bandwidth of the third order FGA's is about twice that of

the second order FGA's. Experimental results are given that support these conclusions.

The properties of the new FGA's depend on the ratios of the resistors and the GB products of the OA's. These quantities are relatively unaffected by the variations in power supply voltage, temperature, etc. in IC technology. Thus, in IC technology, once tuned, the characteristics of the FGA's should remain independent of changing environmental conditions.

The utility of the new FGA's has been demonstrated by using them in two well known active-RC filter circuits. In these applications, the operating frequency range is extended atleast by 10 and 20 times when the conventional FGA's are replaced by the second order and third order FGA's respectively. The signal handling capabilities of these filters have also been found to be acceptable.

Three optimization algorithms are then given, each of which seeks to minimize the effect of the GB products of the OA's used in any given second order active-RC filter on its performance. In the process, the optimal set of values for the circuit elements are obtained that maximizes the operating frequency of the given filter. It has been demonstrated through an application that these optimization techniques extend the operating frequency range of active-RC filters significantly. These algorithms are compared as to the simplicity, accuracy of the results obtained and the execution time required. Algorithm I is the simplest and the most accurate but requires a considerably larger execution time. Algorithm II is the optimal one from the above considerations. Algorithm III is acceptable only for the highly selective filters, though it requires the least execution time. Extensive experimental results confirm the above conclusions.

ACKNOWLEDGEMENTS

The author wishes to record his appreciation and deep sense of gratitude to Dr. B.B. Bhattacharyya for his guidance and assistance during the entire preparation of this thesis.

Thanks are also due to Dr. P. Karivaratharajan for many useful discussions. The author also gratefully acknowledges the various sacrifices made, inspiration, understanding and patience accorded to him by his wife Mrs. Saroja Natarajan and his sons Sundaram and Senthilvelu, throughout the period of the study.

The author thanks Mr. B. Raman for reading and commenting on the manuscript and to Miss June Anderson for typing the thesis.

The author acknowledges the support given by the National Research Council of Canada under grant No. 7740, awarded to Dr. B.B. Bhattacharyya.

DEDICATED TO THE MEMORY OF MY FATHER

RM. SUNDARAM CHETTIAR

TABLE OF CONTENTS

LIST OF TABLES

LIST OF FIGURES

LIST OF IMPORTANT SYMBOLS AND ABBREVIATIONS.

CHAPTER I
INTRODUCTION

1.1 GENERAL

The evolution of active-RC filters dates back to the thirties when the twin-T RC network was used in the feedback path of an amplifier to realize a bandpass filter. However, the strongest incentive came from the rapidly developing technology of integrated circuits, where a complex network, with all its elements and interconnections, is fabricated in a single chip. The main advantages of integrated circuits are well known [1,2]. However, building inductors with reasonable values of the inductance and quality factors by integrated circuit techniques has not been successful thus far. Even in conventional technology, the inductors of reasonable values are quite heavy and bulky in size for low frequency applications. Further, the nonlinear frequency dependence of the quality factors (Q-factor) of the inductors, coupled with the variation of the Q-factor from one inductor to the other makes an accurate synthesis of filter functions fairly complicated.

The obvious solution to the above problem is to realize network functions with an active-RC circuit, which consists of resistors, capacitors and active elements and which does not require inductors. Depending upon the type of the active element used in the circuit, active-RC circuits can be classified into the following general classes [1,3]:

(a) Controlled-source realizations

(b) Negative-resistance realizations

(c) NIC, GIC, Gyrator realizations

(d) Infinite-gain realizations

(e) Multiple-amplifier realizations.

All the existing types of active elements are realizable with what are known as operational amplifiers. As this thesis is mainly concerned with such operational amplifiers, let us first discuss some of the important properties of operational amplifiers.

1.2 THE OPERATIONAL AMPLIFIER

The development of integrated circuit technology and particularly the low-cost high-gain operational amplifiers (OA) had a major impact on the realization of any type of active-RC filters. With continually increasing use of this element, its price has come down to a level which is comparable to that of a resistor or a capacitor. Furthermore, it is an element which is available as an "of-the-shelf component" [4]. Commercially available silicon monolithic integrated OA's are reliable, versatile, relatively inexpensive and have excellent properties. With further development of the IC technology, they are also available in the form of "quads" (four OA's in a single chip) and "duals" (two OA's in a single chip). The representation of the most commonly used OA element is shown in Fig. 1.1. Ideally, the model of this element is one of having a frequency independent infinite differential gain and one of possessing infinite input impedance and zero output impedance. Referring to Fig. 1.1, the above statement means that

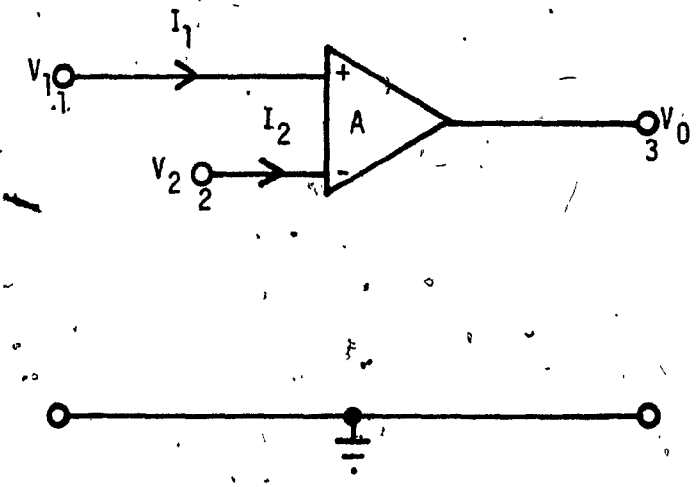

FIG. 1.1: The Representation for an Operational Amplifier

$$A \to \infty \tag{1.1}$$

$$I_1 = I_2 = 0 \tag{1.2}$$

Further, with this model, the OA should be capable of supplying any amount of power.

On the contrary, the practising engineer finds the commercially available OA to possess the following important non-ideal properties.

1. It has a finite (but very large) input impedance and a non-zero (but very low) output impedance.
2. The output voltage, V_o is related to the differential input voltage, V_i in Fig. 1.1 by

$$V_o = AV_i \tag{1.3}$$

where $V_i = (V_1 - V_2)$ and A is, in general, a frequency dependent gain.

For an internally frequency compensated OA, assuming a one pole model, the open-loop gain is given by

$$A = \frac{A_o \omega_c}{(s+\omega_c)} \tag{1.4}$$

where A_o, ω_c, s and $B = A_o \omega_c$ are the d.c. gain, the cut-off frequency, the generalized complex frequency and the gain-bandwidth product (GB product), respectively. Apart from the above, there are other imperfections such as d.c. off-set voltage and off-set current,

slew rate etc. Table 1.1 gives important parameters of interest of a commercially available OA, μA741.

The quantities A_0 , ω_c and B have large manufacturing tolerances in addition to their dependences on the temperature and the power supply voltage.

In most of the active-RC filter applications, the effects of the finite input and non-zero output impedances have been found to be negligible and can perhaps be eliminated with a good circuit design. However, the frequency dependence of the gain affects the performance of the filter to a significant level [5]. The frequency dependent characteristics of the OA's lead to the non-ideal performances of the active elements which are realized by using such OA's. As for example, ideal controlled sources are non-reciprocal elements and the gain factors of these elements must be constant without any change in magnitude and without any phase shift with frequency. However, when such controlled sources are realized using OA's having frequency dependent characteristics, they will also have frequency dependent characteristics. To particularize our discussion and also because of the fact that a large part of this thesis is concerned with realizations of finite gain amplifiers, let us now discuss the effect of the frequency dependence of the OA's in the conventional realizations of finite gain amplifiers.

1.3 FINITE GAIN AMPLIFIERS

The finite gain amplifiers are an important class of active elements, which are widely used in the realization of active-RC filters. These types of filters, such as Sallen and Key [6], Bach's circuit [7,8]

TABLE 1.1 Some Important Parameters of Fairchild μA741 Operational Amplifier

ELECTRICAL CHARACTERISTICS (V_S = ±15V, T_A = 25°C unless otherwise specified)

PARAMETERS	CONDITIONS	MIN.	TYP.	MAX.	UNITS
Input Offset Voltage	$R_S \leq 10k\Omega$		1.0	5.0	mV
Input Offset Current			20	200	nA
Input Bias Current			80	500	nA
Input Resistance		0.3	2.0		MΩ
Input Capacitance			1.4		pF
Offset Voltage Adjustment Range			±15		mV
Large-Signal Voltage Gain	$R_L \geq 2k\Omega$, V_{out}=±10V	50,000	200,000		
Output Resistance			75		Ω
Output Short-Circuit Current			25		mA
Supply Current			1.7	2.8	mA
Power Consumption			50	85	mW
Transient Response (unity gain)	V_{in}=20mV, R_L=2kΩ, $C_L \leq$100 pF				
Risetime			0.3		μs
Overshoot			5.0		%
Slew Rate	$R_L \geq 2k\Omega$		0.5		V/μs

and many others [5] are very popular for realizing second and higher order filter sections. It has been shown that all useful second order realizations and all pass realizations even with real zeros of transmission in the right hand side of the s-plane can be realized with a single finite gain amplifier [9,10]. They are also useful in the inductance realization schemes [11,12]. Further, these amplifiers find many other applications such as in the design of oscillators, in instrumentation and in A/D converters etc. [13].

Such finite gain amplifiers are usually realized employing OA's. The conventional realizations of positive and negative gain amplifiers using OA's are shown in Fig. 1.2. With ideal OA's in the circuits, these two circuits will realize gains of $+\mu_o$ and $-\mu_o$ respectively. These gains are constants for all frequencies without any phase shift being introduced. However, if the frequency dependent gains of the OA's are included in calculating the gain factors of the circuits of Fig. 1.2, it is obvious that these gains will also be frequency dependent.

From the actual transfer function, one can obtain approximate expressions for the change in magnitude of the gain from the nominal value of μ_o and the change in the phase of the gain from 0 or π for positive and negative gain amplifiers, respectively. It will be shown later that when the operating frequency, ω and the GB product, B are such that $(\omega/B) << 1$, the excess phase shift is of the order of (ω/B) and the change in magnitude is of the order of $(\omega/B)^2$.

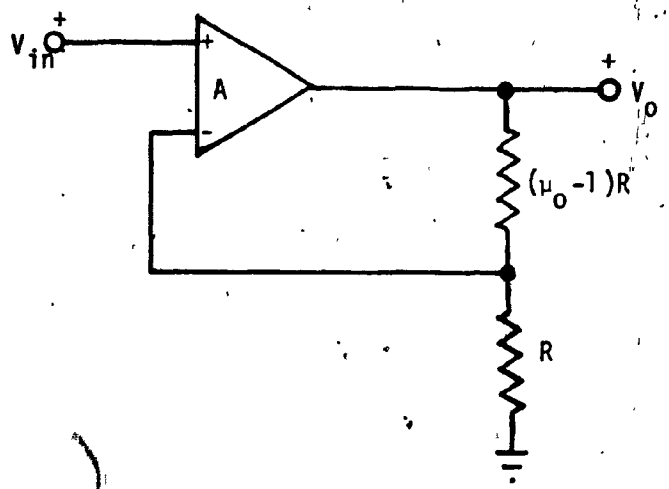

(a)

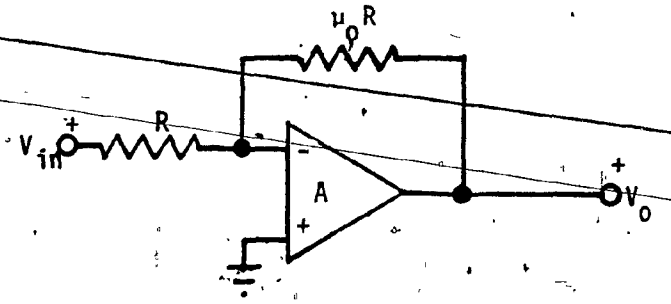

(b)

FIG. 1.2: Conventional Realizations of Finite Gain Amplifiers

(a) Positive Gain Amplifier

(b) Negative Gain Amplifier

In this case, obviously the excess phase shift will be the dominating factor in restricting the bandwidth of the amplifiers. However, in the case of some other active elements, both the change in magnitude of the gain and the excess phase shift introduced may be of importance. This fact will be established later. At this stage let us simply note that, in general, the changes, both in the magnitude and in the phase of the gain of these elements from their nominal values, due to the finite values of GB products of the OA's, have to be considered. These changes will have their effect on the performance of the active filters which use such elements. These effects have been examined in the literature [14]. The purpose of the next few sections is to consider such effects and briefly review the solutions that have been attempted so far.

1.4 THE EFFECTS OF FINITE GB PRODUCTS OF THE OA'S IN ACTIVE-RC FILTERS

The excess phase shift and the change in the magnitude, in the gains of the active elements using OA's, from their nominal values may cause the performance of the active filters to deviate drastically from the desired one. The circuit may even become unstable due to these effects. Generally speaking, the effect of finite GB products will be to cause the following in the realized filters:

(1) Change in the pole Q-factor (Q_p) (usually Q-enhancement).

(2) Change in the pole frequency (ω_p).

(3) A combination of the above two.

These factors limit the maximum operating frequency as well as the maximum Q_p attainable from the active filters. At this juncture,

it is worthwhile to note the following statement by Moschytz [15].

"In most cases, the maximum Q's feasible with active networks will be limited by the attainable stability of pole frequency, ω_p long before they are limited by the attainable stability of pole-Q."

Thus, even with OA's having GB products in excess of 1 MHz, the active-RC filters perform poorly, if the frequency of operation is beyond a few kilohertz. The effect of finite GB products of OA's has been analysed by several authors, some of which are given in [14, 16-20].

In an attempt to solve the problem of realizing active filters for high frequency applications, various forms of solutions have been given thus far. They can be broadly classified into the following categories.

1. Active-R Filters
2. Passive Compensation
3. Active Compensation

A brief account of the above techniques will be given and their merits and demerits will be examined in the following sections.

1.5 ACTIVE-R FILTER

In the recent past, several active-R networks have been proposed in the literature for the realization of high frequency filters, some of which are given in [21-23]. These filters use the 6db/octave roll-off characteristic of the OA's and thus eliminate the need for capacitors. The major disadvantage of these filters is the frequency stability. Though the OA has become an off-the-shelf component, the

stability of the GB products of the OA's is not accurately known, as it is known for resistors and capacitors. Moreover, the value of the GB product itself varies from one unit to the other even for the same type of OA's. This variation can be very large, even of the order of many tens of percent, unlike those of resistors and capacitors. The result is that the actual frequency of operation of the realized filter may be widely different from the desired one.

In addition, the GB products of the OA's vary significantly with changes in environmental conditions such as variations in power supply voltage, temperature etc. Thus the actual frequency of operation of the realized filter will be highly sensitive to changes in the environmental conditions. Though temperature compensated OA's such as LM 324 are available commercially, they are not yet inexpensive and do not achieve stability of the GB products comparable to those of resistors and capacitors. Unless the technology improves to a level such that the GB product of the OA's of a given type can be specified within a few percent and its stability properties are well established and controlled, these types of filters are not likely to find applications except under specified laboratory conditions.

Thus the only viable approach for the realization of insensitive high frequency filters appears to be one that uses compensation techniques in the existing active-RC networks. There are two types of compensation techniques (a) passive compensation and (b) active compensation.

1.6 PASSIVE COMPENSATION

In this technique, the compensation of the active elements or the overall network is achieved with the use of additional passive elements such as resistors and capacitors. These additional passive elements serve to reduce the effect of the finite GB products of the OA's on the filter performance. Such techniques have been described in [16,17,24-27]. This method suffers from the following disadvantages:

1. The values of the compensating elements have to be related to the GB products of the OA's used. Thus the values of the GB products must be accurately known and the passive components have to individually tailored for each OA.

2. Since the changes in the GB product do not usually track with those in the passive components, the compensation will not be effective under varying environmental conditions.

3. The circuit may have to be tuned for each set of ambient conditions. To enable this, the passive components have to be external to the circuit, when the whole circuit is fabricated in the IC form. Further, in many cases, the compensating elements turn out to be capacitors. This makes not only the tuning difficult but also the fabrication of the circuit costlier, as capacitors occupy the largest substrate area among all the components in IC technology.

On the other hand, there are several advantages offered by the technique of active compensation, in which only OA's and resistors are used.

1.7 ACTIVE COMPENSATION

In active compensation, the characteristics of one set of OA's are used to provide compensation for the detrimental effects of another set of OA's in a given circuit. Such active compensation techniques have been considered by several workers for improving the performance of active-RC filters [28-39]. The active compensation technique not only avoids all the problems that we encountered in the case of passive compensation but also possesses additional advantages. These are as follows:

1. The characteristics of the compensated circuit depend only on the ratios of resistors and the GB products of the OA's. As these ratios track closely with variations in the environmental conditions, once the circuit is tuned, the compensation is likely to be effective under varying environmental conditions, such as temperature and power supply voltage variations.

2. The compensating elements used are only OA's and resistors and thus these elements can be easily integrated along with the other parts of the circuit. This is attractive if the whole circuit is to be fabricated in monolithic IC form.

3. The tuning of such actively compensated circuits can be done with relative ease by trimming resistors only.

From the foregoing discussion, it appears that, at present, the method of active compensation is the only viable technique for the realization of high frequency filters. The improved performance can be

achieved in two ways:

(a) Compensating the overall network.

(b) Compensating the active elements.

Active compensation of an overall network may improve the performance of a given network as has been reported in [29,30,39]. However, by compensating the active elements, one can improve the performance of an entire class of active RC filters. Thus the latter technique becomes a more general approach than the first one. Such types of active compensation techniques have been suggested for finite gain amplifiers and integrators [31-38].

As has already been seen, the class of active-RC filters employing finite gain amplifiers is very popular and widely used. The high frequency performances of such filters can be upgraded by improving the performance of these amplifiers.

A major concern of this thesis is to consider various possibilities of active compensation of finite gain amplifiers. Thus in the following section active compensation techniques for these amplifiers, that have been attempted so far, are reviewed.

1.8 ACTIVE COMPENSATION OF FINITE GAIN AMPLIFIERS

Finite gain amplifiers are usually realized using OA's. When these amplifiers are designed with a single OA in the conventional method, the excess phase lag introduced in the amplifier circuit will limit the maximum frequency of operation of the active-RC filters employing such amplifiers. This phase lag is mainly determined by the first order term

of (ω/B). Actively compensated finite gain amplifiers with variable phase shift employing two OA's and four resistors were first suggested by Reddy [31]. These amplifiers can also be used, wherein the first order effect of GB product can be made zero. However, the circuit given by Reddy for realizing positive gain amplifiers can not improve the performance of an important class of positive gain amplifiers viz. unity gain amplifiers. Furthermore, as it will be shown later, these amplifiers have poor relative stability beyond a certain value of gain.

Later Geiger suggested a positive gain amplifier circuit [35] using two OA's and additional resistors. The design of this circuit is based on the monotonicity of the magnitude characteristic. Thus the phase deviation of this amplifier circuit is still dominated by the first order term of the GB products of the OA's. This, coupled with the fact that this amplifier has frequency dependent finite input impedance, limits the usefulness of this amplifier to low frequency applications of active-RC filters. Further, these designs not only fail to realize the class of unity gain amplifiers but can only be used to obtain amplifiers having a nominal d.c. gain greater than $(\sqrt{2} + 1)$.

Geiger also looked at the problem of increasing the operating frequency of active-RC filters employing finite gain amplifiers in another way [36]. However, the circuits, except for one, given by him in [36] are the same as those suggested earlier by Reddy in [31]. The only new circuit is for realizing a positive gain amplifier, which is again, a slightly modified version of the circuit given by Reddy. Unfortunately, this circuit possesses finite input impedance and for any

given gain, less bandwidth compared to the one in [31].

At this point one may become concerned at the increase in the number of OA's and resistors used. It will be later shown that the useful operating frequency range of active-RC filters can be increased by an order of magnitude or more by the new designs of the finite gain amplifiers. This, along with the fact that the cost of producing additional OA's and resistors is insignificant in IC technology, outweighs the increase in the component count, particularly in the days of MSI and LSI technologies.

1.9 THE SCOPE OF THE THESIS

The objective of this thesis is to present some techniques for extending the operating frequency range of active-RC filters. This is done by first presenting designs for a set of new finite gain amplifiers with improved bandwidth so that the class of filters employing these amplifiers will have an extended frequency range of operation and then to give some optimization algorithms so that the operating frequency range of any filter using OA's can be maximized.

Towards this end, Chapter II gives a general theory of active compensation for finite gain amplifiers (FGA). In this theory a basic block diagram employing a single forward as well as a single feedback path, the same as the one used by the conventional realizations of FGA's, is assumed. The required form of the transfer functions, for the FGA's to possess improved bandwidth, is obtained from this control diagram. The stability study of the transfer functions of these FGA's leads to the fact that only second order realizations are possible.

In Chapter III, all possible topological structures for realizing such second order transfer functions are obtained. These structures employ two OA's and resistors only. From these structures, "optimal" and in some cases additional non-optimal realizations are derived. The circuits given in [31] are shown to be special cases of these realizations. A comparison of all possible realizations will be made based on tunability, relative stability and the maximum bandwidth that can be obtained for a specified deviation in their magnitude and phase characteristics. Theoretical as well as experimental results are also provided for these circuits.

Some of the second order realizations are found to possess multiple feedback paths instead of the single feedback path assumed in Chapter II. Thus the problem of stability, encountered in Chapter II for higher order realizations, is re-examined in Chapter IV after introducing multiple feedback paths in the amplifier realizations. This leads to two general configurations (one for non-inverting and the other for inverting gain amplifiers) with which stable amplifiers realizing higher order transfer functions can be designed. However, for a good relative stability and from the point of view of improvement in the bandwidth, it is found that it is not worthwhile going beyond the third order realizations. These are realized using resistors and 3 OA's. These circuits possess wider bandwidth compared to the one given by 2 OA circuits developed in Chapter III. Theoretical and experimental characteristics of the 3 OA realizations of the FGA's are presented. Comparison of these characteristics with those of the 2 OA and conventional realizations establishes the superiority of the 3 OA realizations.

Some applications of these new elements in active-RC filters are considered in Chapter V, through which the superiority of these new amplifiers over the conventional amplifiers is further demonstrated. A method of comparison is also developed based on the maximum change in the magnitude characteristic of the actual transfer function from the ideally desired one. The theoretical predictions show that the operating frequency range of active-RC filters can be improved by more than an order of magnitude. These results are confirmed by computer simulations and experimental verifications.

In Chapters II through IV, the designs of the FGA's have been considered separately from the circuit in which they are used. However when an FGA is employed in a particular filter circuit, the design of the given FGA can also be done so as to maximize the operating frequency range of the filter circuit. This is not only true for the case of active filters employing FGA's but also true for active filters using other types of active elements. In particular, the design of a circuit employing compensation can be so done as to "match" the amount of compensation required by the given circuit. Specifically, the compensating parameters can be chosen through an optimization procedure which will maximize the operating frequency of that particular filter for a specified change in the performance characteristics. Thus, in Chapter VI, three different algorithms for optimizing the performance of any filter such that it will have the maximum operating frequency range for a specified deviation in the magnitude characteristic of the actual transfer function are developed. In order to emphasize the fact that these algorithms are useful to produce an optimized design for

any type of filter, simulation results, based on these algorithms, are provided for an actively compensated double integrator loop [39]. Experimental verifications of these results are also given. Finally, a detailed comparison of these algorithms, as to their accuracy and the execution time required, is made through the same application. Based on these results, it is found that only two algorithms are competitive and the usefulness of these algorithms is shown to depend on the nominal value of the pole-Q factor desired. Finally, the appropriate algorithm for a given pole-Q factor is suggested.

Chapter VII contains a summary of the results obtained in this thesis and includes suggestions for potentially useful directions for further research work.

CHAPTER II

A GENERAL THEORY OF ACTIVE COMPENSATION FOR FINITE GAIN AMPLIFIERS

2.1 INTRODUCTION

The aim of this Chapter is to provide a general and a systematic theory of active compensation for finite gain amplifiers [33]. For this purpose a control diagram, which has a single feedback path and where the forward path is provided by a single internally compensated OA, is assumed. Analysis of this control model leads to the required transfer function for the feedback element for realizing FGA's having improved bandwidth. The type of control diagram is, in fact, suggested by the conventional realizations of the FGA's. Thus, let us start by considering the conventional realizations of the FGA's and their properties. The results of such an analysis will also be useful later for purposes of comparison.

2.2 CONVENTIONAL REALIZATIONS OF FINITE GAIN AMPLIFIERS

The conventional realizations of positive and negative gain amplifiers using OA's are shown in Fig. 1.2. For convenience they are reproduced in Fig. 2.1. Since we are interested in the effects of the frequency dependent characteristics of the OA's used on the FGA's, let us assume that the OA is ideal except that its gain is frequency dependent. We shall also assume that all the OA's are internally frequency compensated and can be represented by a single pole model. Then the gain equation of an OA is given by (1.4). Generally the value of ω_c is few

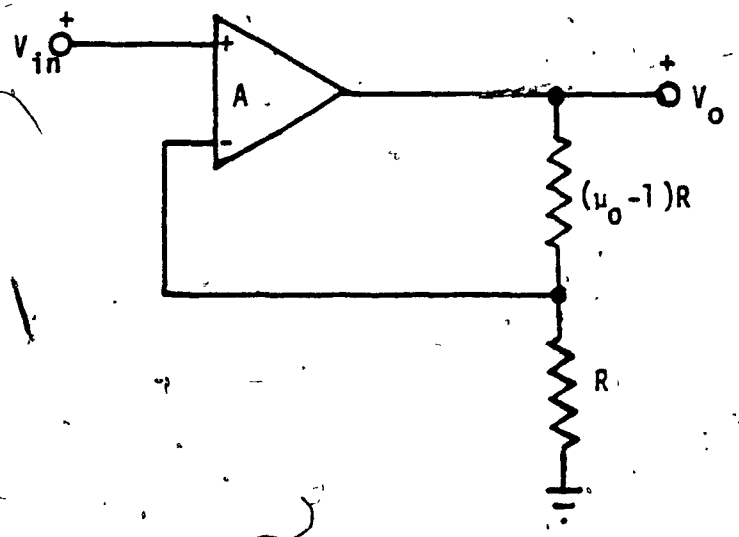

(a)

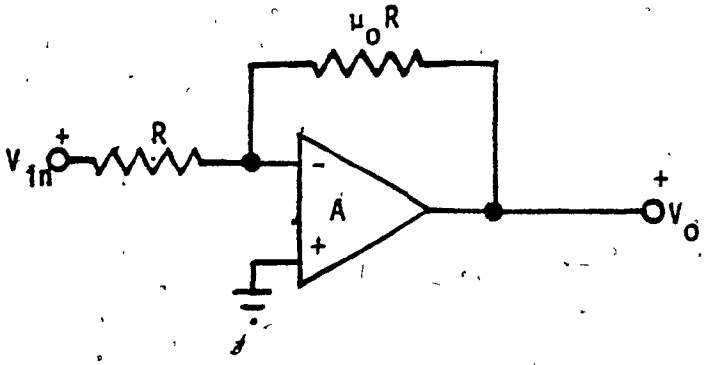

(b)

FIG. 2.1 : Conventional Realizations of Finite Gain Amplifiers

(a) Positive Gain Amplifier

(b) Negative Gain Amplifier

radians/sec for commercially available OA's and the operating frequency of the FGA's for active-RC filter applications is such that

$$\omega_c << \omega << B \tag{2.1}$$

where ω is the frequency of operation of the FGA's. Then the gain equation of the OA given by (1.4) can be simplified to the one given below.

$$A(s) \cong \frac{B}{s} \tag{2.2}$$

The transfer function of the positive gain amplifier, $G_p(s)$ can be derived using (2.2) and it is given below as

$$G_p(s) = \frac{\mu_o}{(1+\mu_o \frac{s}{B})} \tag{2.3}$$

Similarly the gain of an inverting amplifier is described by the following equation.

$$G_n(s) = \frac{-\mu_o}{\{1+(1+\mu_o)\frac{s}{B}\}} \tag{2.4}$$

The circuit shown in Fig. 2.1(a) will behave close to a real positive gain amplifier with a constant gain of μ_o and with a negligible phase shift only when

$$(\mu_o \frac{\omega}{B}) << 1 \tag{2.5}$$

where ω is the frequency of operation.

In the case of the negative gain amplifier, the transfer function given by (2.4) suggests that the circuit of Fig. 2.1(b) will give a gain of μ_o with a phase shift close to π rads/sec, only when the operating frequency ω is such that

$$(\mu_o+1)\frac{\omega}{B} << 1 \tag{2.6}$$

The approximate expressions for the change in the magnitude and the phase shift of the gain can be derived when the operating frequency satisfies the inequalities 2.5 and 2.6. (The amplifier circuits are useful only under such conditions). Towards that end, let

$$G(j\omega) = \mu(\omega)\, e^{j\phi(\omega)} \tag{2.7}$$

where $G(j\omega)$ is $G_p(s)$ or $G_n(s)$ when $s=j\omega$ and $\mu(\omega)$ and $\phi(\omega)$ denote the magnitude and phase functions of the finite gain amplifiers. Nominally $\mu(\omega) = \mu_o$ and $\phi(\omega) = 0$ or π. However, the normalized changes in the magnitude and the phase for frequencies satisfying inequalities (2.5) and (2.6) are given as follows.

For the positive gain amplifier,

$$\left.\begin{aligned} (\Delta\mu/\mu_o) &\cong (1/2)\,(\mu_o\omega/B)^2 \\ \text{and} \\ \Delta\phi &\cong -(\mu_o\omega/B) \end{aligned}\right\} \tag{2.8}$$

In the case of negative gain amplifiers, these expressions turn out to be

$$\left.\begin{aligned} (\Delta\mu/\mu_0) &\cong (1/2)\,\{(\mu_0+1)\omega/B\}^2 \\ \text{and} \\ \Delta\phi &\cong -\{(\mu_0+1)\omega/B\} \end{aligned}\right\} \quad (2.9)$$

The equations (2.8) and (2.9) indicate that long before the effect of the change in the magnitude is felt, the effect of the deviation in the phase will be predominant in the case of the above amplifier circuits. In a general case, however, one has to consider the effects of the changes in both the magnitude and the phase. Thus, if amplifier circuits are developed wherein both the change in the magnitude and the phase deviation are theoretically zero, then by employing such amplifiers in active-RC filters, the effect of the GB products of the OA's on the performance of filters can be eliminated. For this purpose, a systematic theory for the design of actively compensated FGA's is presented next.

2.3 THEORY OF THE NEW FINITE GAIN AMPLIFIERS

To develop the theory of the new finite gain amplifiers (NFGA's) let us consider the block diagram shown in Fig. 2.2, where A is the gain of the forward path, α is a premultiplier and β is the gain of the feedback path. The transfer function of the system is given by

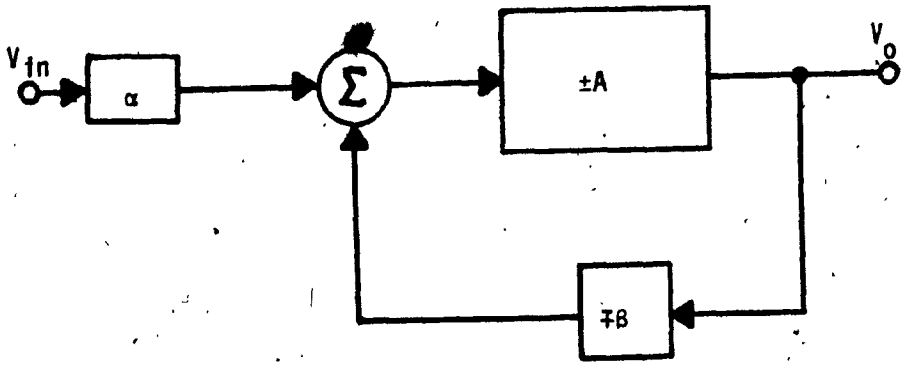

FIG. 2.2: The Basic Block Diagram

$$G(s) = \frac{V_o}{V_{in}} = \frac{\pm A\alpha}{1+A\beta} \tag{2.10}$$

Our aim is to develop amplifiers, whose gains are independent of frequency. Thus, $G(s)$ should be equated to a real constant, $\pm\mu_o$, which will be equal to the required value of the gain (i.e.) we should have

$$\frac{A\alpha}{1+A\beta} = \mu_o \quad \text{or} \quad \beta = \frac{\alpha}{\mu_o} - \frac{1}{A} \tag{2.11}$$

In the case of conventional realizations of finite gain amplifiers, the forward path gain is provided by an OA, as can be seen from Fig. 2.1. Let us also assume that the forward path gain A is provided by an OA and obtain the condition on the feedback factor, β. Thus, $A(s)$ is given by (2.2) and hence (2.11) becomes

$$\beta = \frac{\alpha}{\mu_o} - \frac{s}{B} \tag{2.12}$$

If the gain of the feedback factor of the loop is of the form given by (2.12), then one can realize the given gain $\pm\mu_o$ exactly at all frequencies without any phase shift or the change in magnitude. Unfortunately, such a realization is not possible with physical elements. However, the equation (2.12) can be modified and written in the form of a convergent series as follows:

$$\beta = \frac{(\frac{\alpha}{\mu_o})}{(1 - \frac{\mu_o s}{\alpha B})^{-1}}$$

$$= \frac{(\frac{\alpha}{\mu_o})}{1 + \sum_{i=1}^{\infty} (\frac{\mu_o s}{\alpha B})^i}, \text{ provided } |\frac{\mu_o s}{\alpha B}| < 1 \qquad (2.13)$$

In the case of conventional realization of positive gain amplifier shown in Fig. 2.1(a), we can show that

$$\alpha = 1 \quad \text{and} \quad \beta = \frac{1}{\mu_o} \qquad (2.14)$$

The resultant transfer function is given by (2.3). Similarly, for the case of conventional realization of negative gain amplifier

$$\alpha = \frac{\mu_o}{(1+\mu_o)} \quad \text{and} \quad \beta = \frac{1}{\mu_o} \qquad (2.15)$$

The resultant transfer function for this amplifier is given by (2.4).

As was mentioned earlier, the useful frequency range of the conventional realizations of positive and negative gain amplifiers is given by the inequalities (2.5) and (2.6), respectively. We note from (2.13), (2.14) and (2.15) that the feedback factor that is provided in the conventional OA realization of finite gain elements is just $\frac{\alpha}{\mu_o}$ and all other terms in the denominator of β in (2.13) are completely neglected. However, by retaining more terms in

the summation, better accuracy to the realization of FGA's can be achieved. Consequently, better frequency response of the amplifiers can be expected. By preserving the first $(m-1)$ terms in the summation for β, the overall transfer function, $G(s)$ becomes as follows:

$$G(s) = \pm \mu_o \frac{[1+(\frac{\mu_o s}{\alpha B})+ \ldots +(\frac{\mu_o s}{\alpha B})^{m-2}+(\frac{\mu_o s}{\alpha B})^{m-1}]}{[1+(\frac{\mu_o s}{\alpha B})+ \ldots +(\frac{\mu_o s}{\alpha B})^{m-2}+(\frac{\mu_o s}{\alpha B})^{m-1}+(\frac{\mu_o s}{\alpha B})^{m}]} \qquad (2.16)$$

In (2.16), the transfer function $\{G(s)/\pm\mu_o\}$ is of the form such that the coefficients of the numerator polynomial are same as those of the denominator polynomial up to the order of $(m-1)$. The finite gain amplifiers described by (2.16), when $m>1$, will possess better frequency response compared to the ones realized with a single OA and resistive feedback which corresponds to the case when $m=1$. This is because the limit on the operating frequency of the FGA's described by (2.16) is now given by

$$(\frac{\mu_o \omega}{\alpha B})^m << 1 \qquad (2.17)$$

instead of the inequalities (2.5) and (2.6).

Since $(\frac{\mu_o \omega}{\alpha \beta})$ is a quantity less than unity, the greater is the value of m, the larger is the bandwidth of the new FGA's. Unfortunately, as the value of m is increased beyond 2, the transfer function given by (2.16) becomes unstable as shown in the next section.

2.4 STABILITY OF THE NFGA'S

To determine the stability of the transfer function given by (2.16), let us consider the denominator polynomial, D(s) of (2.16). Now

$$D(s) = 1 + \frac{\mu_o s}{\alpha B} + \cdots + \left(\frac{\mu_o s}{\alpha B}\right)^m$$

Letting $\left(\frac{\mu_o s}{\alpha B}\right) = x$, we obtain

$$D(s) = 1 + x + \cdots + x^m$$

$$= \frac{(1-x^{m+1})}{(1-x)} \qquad (2.18)$$

It is obvious that $(1-x)$ is a factor of $(1-x^{m+1})$ and the zeros of $(1-x^{m+1})$ are the only zeros of D(s) except the one at $x=1$. These zeros are given by

$$x = e^{j2\pi n/(m+1)} \quad , \quad n=1,2,\ldots,m$$

(n=0 gives the root at $x=1$ as mentioned before).

Thus, the zeros of D(x) all lie on the unit circle $|x| = 1$. The phase angle $\theta = \{2\pi n/(m+1)\}$ from the real axis gives the position of the zero on the unit circle. In order that the transfer function given by (2.16) to be stable, those zeros can not lie in the R.H.S. of the x plane. Thus, this phase angle, θ , must be greater than $\pi/2$ for absolute stability (correspondingly, the poles of G(s) will lie in

the L.H.S. of the s-plane). This means that m should be such that

$$\frac{2\pi n}{(m+1)} > \frac{\pi}{2} \quad , \quad n=1,\ldots,m$$

or equivalently,

$$m < (4n-1) \quad , \quad n=1,\ldots,m \; . \tag{2.19}$$

The inequality (2.19) can be satisfied only for values of m up to 2 and for $m \geq 3$, this can not be satisfied. Thus when $m \geq 3$, the transfer function given by (2.16) becomes unstable. In particular, when m=3, there are a pair of poles on the $j\omega$ axis of the s-plane and the corresponding circuit realization of (2.16) yields a purely sinusoidal oscillator. It's practical implementation and related studies were reported earlier [40].

Thus, it is clear, from the stability considerations, $m \leq 2$. As we have seen already, the case m=1 corresponds to the conventional realizations of finite gain amplifiers. Hence, it is only required to find the realizations corresponding to the case m=2. The transfer function, for m=2, is given

$$G(s) = \pm\mu_o \frac{1+(\frac{\mu_o s}{\alpha B})}{1+(\frac{\mu_o s}{\alpha B}) + (\frac{\mu_o s}{\alpha B})^2} \tag{2.20}$$

In the next Chapter, we shall concern ourselves with practical circuits that implement the above transfer function. To lend generality to the discussion, we shall consider the realization of the transfer

function of the following form:

$$G(s) = \pm\mu_o \frac{1+\alpha_1 (\frac{s}{B})}{1+\alpha_1 (\frac{s}{B})+\alpha_2 (\frac{s}{B})^2} \qquad (2.21)$$

It is obvious that (2.20) is a special case of (2.21), where $\alpha_2 = \alpha_1^2$. It is also apparent that to maximize the bandwidth of the FGA, the coefficient α_2 in (2.21) should be as small as possible.

Since we are interested in the actively compensated FGA's, our circuit implementations of (2.21) must consist of OA's and resistors. Thus, in Chapter I.II, an attempt will be made to enumerate all possible topological structures that will realize (2.21) using OA's and resistors.

2.5 CONCLUSION

Assuming a control model with a single forward path and a single feedback path, a general form of the transfer function for FGA's to possess an improved operating bandwidth has been obtained. The stability considerations, however, reduce the transfer function to one of second order. The following chapter will consider, in detail, circuit implementation of second order FGA's.

CHAPTER III

REALIZATIONS OF ACTIVELY COMPENSATED SECOND ORDER FINITE GAIN AMPLIFIERS

3.1 INTRODUCTION

In the last Chapter, the study of active compensation of finite gain amplifiers led us to restrict ourselves to amplifiers with second order transfer functions. It is possible to realize such a transfer function in many different ways. Thus, in this Chapter, starting with a general amplifier configuration, all possible realizations for positive and negative gain amplifiers are investigated. It is shown that the amplifier circuits that have been suggested in the literature so far are only particular cases of this general configuration. The analysis also yields several new circuits. Finally, a comparison of all the useful circuits is made based on some practical considerations. The frequency response characteristics of the set of the 'best' amplifiers that emerge out of this analysis are then investigated in detail theoretically as well as experimentally.

3.2 ANALYSIS OF THE GENERAL SECOND ORDER FGA NETWORK

Our main concern in this Chapter is to realize actively compensated amplifier circuits having second order transfer functions. It is obvious that such FGA's will have at least two OA's and the other elements in the network must be resistors. A little thought will indicate that the most general network that one can think of for the FGA's, will

be a five-port active-R configuration. Let us therefore consider the five-port two OA active-R network shown in Fig. 3.1. It is assumed that the OA's have infinite input and zero output impedances. Furthermore, it is also assumed that the OA's embedded are internally frequency compensated for a single-pole roll-off. Thus each OA can be represented by a gain equation of the form given by (2.2). Let $\hat{V}'(s)$ and $\hat{V}(s)$ be column matrices of voltages defined by

$$\hat{V}'(s) = \begin{bmatrix} V_1'(s) \\ V_2'(s) \end{bmatrix} \quad \text{and} \quad \hat{V}(s) = \begin{bmatrix} V_1(s) \\ V_2(s) \end{bmatrix}$$

where $V_j'(s)$ and $V_j(s)$ are shown in Fig. 3.1.

Considering $\hat{V}$ and V_I as the driving voltages, $\hat{V}'$ can be obtained by applying the principle of superposition. This superposition is applied to the resistive network that remains after the OA's are removed from the active-R network. Thus,

$$\hat{V}'(s) = \hat{F}\,\hat{V}(s) + \hat{f}\,V_I(s) \qquad (3.1)$$

where

$$\hat{F} = \begin{bmatrix} F_{11} & F_{12} \\ F_{21} & F_{22} \end{bmatrix} \quad \text{and} \quad \hat{f} = \begin{bmatrix} f_1 \\ f_2 \end{bmatrix}$$

The voltages $\hat{V}'(s)$ and $\hat{V}(s)$ are related by the gain equations

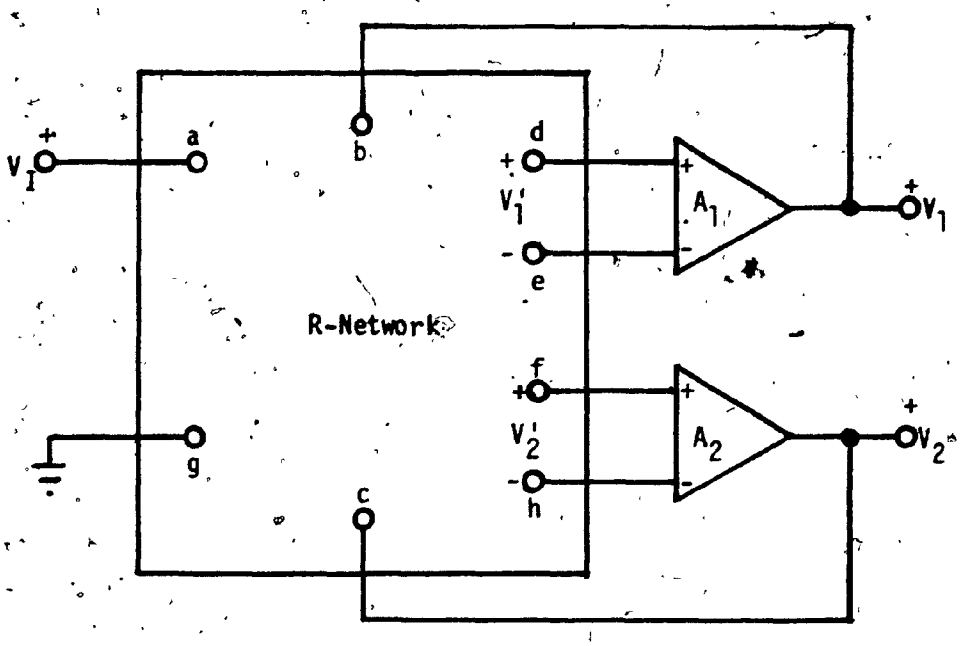

FIG. 3.1: The General Active-R Network to Realize a Second Order Transfer Function

of the OA's. Thus the following equation can be obtained.

$$\hat{V}(s) = \hat{A}(s)\,\hat{V}'(s) \tag{3.2}$$

where $\hat{A}$ is a 2×2 matrix given below:

$$\hat{A}(s) = \begin{bmatrix} B_1/s & 0 \\ 0 & B_2/s \end{bmatrix} \tag{3.3}$$

where B_1 and B_2 are the GB products of the two OA's A_1 and A_2 respectively.

As will be shortly seen, it can be assumed, without loss of generality that the output of the FGA's is taken at the output of the OA, A_1. Thus, the transfer function of the network, when V_1 is the output, can be obtained from (3.1), (3.2) and (3.3) as:

$$G(s) = \frac{V_1(s)}{V_I(s)} = \frac{(f_2F_{12}-f_1F_{22}) + f_1 s/B_2}{(F_{11}F_{22}-F_{12}F_{21}) - s\left(\frac{F_{11}}{B_2} + \frac{F_{22}}{B_1}\right) + \frac{s^2}{B_1B_2}} \tag{3.4}$$

where the definitions of various 'f' and 'F' functions can be obtained by using (3.1). As for example,

$$f_2 = \left.\frac{V_2'(s)}{V_I(s)}\right|_{V_1 = V_2 = 0}$$

Similarly,

$$\therefore F_{11} = \left.\frac{V_1'(s)}{V_1(s)}\right|_{V_I = V_2 = 0}$$

Clearly, the quantities f's and F's are functions of resistor ratios.

By considering the output V_2, an equation for the transfer function, similar to (3.4) can be obtained where the roles of f_1 and f_2, F_{11} and F_{22}; and F_{12} and F_{21} are interchanged. Thus, topologically, the resultant structures of the amplifier circuits will remain the same. Our aim, as mentioned before, is to find all possible realizations of second order FGA's. Therefore, in order to find the possible realizations, there is no loss of generality in assuming that the output is taken at the output of OA, A_1. Hence, let us focus our attention on (3.4). Further, it will be assumed for simplicity, that both the OA's have got the same GB products, equal to B. Then, the equation (3.4) can be written in the following form:

$$G(s) = a \frac{1+a_1(\frac{s}{B})}{1+b_1(\frac{s}{B})+b_2(\frac{s}{B})^2} \qquad (3.5)$$

where

$$a = \frac{(f_2F_{12} - f_1F_{22})}{(F_{11}F_{22} - F_{12}F_{21})}$$

$$a_1 = \frac{f_1}{(f_2F_{12} - f_1F_{22})}$$

$$b_1 = \frac{-(F_{11} + F_{22})}{(F_{11}F_{22} - F_{12}F_{21})}$$

and

$$b_2 = \frac{1}{(F_{11}F_{22} - F_{12}F_{21})}$$

The transfer function of the amplifier circuits that are to be developed, has been shown to be of the form given by (2.21). This function is reproduced below for convenience.

$$G(s) = G_0 \frac{1+\alpha_1(\frac{s}{B})}{1+\alpha_1(\frac{s}{B}) + \alpha_2(\frac{s}{B})^2} \tag{3.6}$$

where α_1 and α_2 are real constants, such that

$$\alpha_1 > 0 \tag{3.7}$$

$$\alpha_2 > 0 \tag{3.8}$$

and G_0 is the required d.c. gain.

In the case of positive gain amplifiers, the value of G_0 is positive and in the case of the negative gain amplifiers, G_0 is negative. Thus let $G_0 = \mu_0$ or $-\mu_0$ for the positive and the negative gain amplifiers respectively where $\mu_0 > 0$. Now comparing (3.5) and (3.6) along with the conditions (3.7) and (3.8), some equations and conditions that should be satisfied by the 'f' and 'F' constants can be obtained for both the positive and the negative gain amplifiers. These are given below:

3.2.1 The Conditions on 'f' and 'F' Constants for Positive Gain Amplifiers

$$\left.\begin{array}{ll} 1. & (F_{11}\,F_{22} - F_{12}\,F_{21}) > 0 \\ 2. & (f_2\,F_{12} - f_1\,F_{22}) > 0 \\ 3. & f_1 > 0 \\ 4. & \dfrac{(f_2F_{12} - f_1F_{22})}{(F_{11}F_{22} - F_{12}F_{21})} = \mu_0 \\ 5. & (F_{11} + F_{22}) = -\left(\dfrac{f_1}{\mu_0}\right) \end{array}\right\} \quad (3.9)$$

3.2.2 The Conditions on 'f' and 'F' constants for Negative Gain Amplifiers

$$\left.\begin{array}{ll} 1. & (F_{11}F_{22} - F_{12}F_{21}) > 0 \\ 2. & (f_2F_{12} - f_1F_{22}) < 0 \\ 3. & f_1 < 0 \\ 4. & \dfrac{(f_2F_{12} - f_1F_{22})}{(F_{11}F_{22} - F_{12}F_{21})} = -\mu_0 \\ 5. & (F_{11} + F_{22}) = \dfrac{f_1}{\mu_0} \end{array}\right\} \quad (3.10)$$

3.3 FURTHER COMMENTS, RESTRICTIONS AND SOME DEFINITIONS

As we mentioned earlier, the constants 'f' and 'F' are functions of resistor ratios. These constants can be negative or positive

depending upon the type of connection. Under certain circumstances, they can be zero as well. However, the absolute magnitudes of these constants must be less than or equal to 1 and greater than or equal to zero, that is, it is required that

$$0 \leq |f_k| \ , \quad |F_{ij}| \leq 1 \ , \quad k=1,2 \text{ and } i,j=1,2 \tag{3.11}$$

Depending upon the signs of 'f' and 'F' constants, further restrictions have to be imposed on them. For example it is shown below that these functions must satisfy the following:

$$|f_i| + |F_{i1}| + |F_{i2}| \leq 1 \quad i=1,2 \tag{3.12}$$

When all the three quantities f_i , F_{i1} and F_{i2} are of the same sign. When anyone of them has a sign opposite to those of the other two, then that particular quantity does not appear in (3.12). Any restriction on it, however, is taken care of by (3.11). To prove the above statement as well as (3.12), let us consider the R-network, which results after the removal of the OA's in Fig. 3.1. Let V_I , V_1 and V_2 be the impressed potentials at the terminals a, b and c respectively with reference to the ground terminal, g . Let V_1^+ , V_1^- , V_2^+ and V_2^- be the resultant potentials at d, e, f and h , respectively, with reference to the same ground terminal, g . Let us also define the following quantities:

$$f_i^{(x)} = \left. \frac{V_i^{(x)}}{V_I} \right|_{V_1 = V_2 = 0} \qquad i=1,2 \tag{3.13}$$

$$\left.\begin{aligned} F_{ij}^{(x)} &= \left.\frac{V_i^{(x)}}{V_j}\right|_{V_I = V_i = 0} \qquad \begin{matrix} i=1,2 \\ j=1,2 \\ i\neq j \end{matrix} \\ F_{11}^{(x)} &= \left.\frac{V_1^{(x)}}{V_1}\right|_{V_I = V_2 = 0} \\ F_{22}^{(x)} &= \left.\frac{V_2^{(x)}}{V_2}\right|_{V_I = V_1 = 0} \end{aligned}\right\} \quad (3.14)$$

and

where x stands for + or - sign.

The network of Fig. 3.1 can be considered as a seven port resistive network, where $f_i^{(x)}$ and $F_{ij}^{(x)}$ are all transfer constants. Clearly, these constants are all non-negative. Thus, let

$$\left.\begin{aligned} f_i^{(x)} &= \frac{P_{i.}^{(x)}}{Q_i^{(x)}} \\ F_{i1}^{(x)} &= \frac{P_{i1}^{(x)}}{Q_i^{(x)}} \qquad i=1,2 \\ F_{i2}^{(x)} &= \frac{P_{i2}^{(x)}}{Q_i^{(x)}} \end{aligned}\right\} \quad (3.15)$$

and

where $P_i^{(x)}$, $P_{i1}^{(x)}$, $P_{i2}^{(x)} \geq 0$ and $Q_i^{(x)} > 0$.

Since it is a resistive multiport network the following are true:

$$\left.\begin{aligned} & p_i^{(x)} + p_{i1}^{(x)} + p_{i2}^{(x)} \leq Q_i^{(x)} \\ & p_i^{(x)} + p_{i1}^{(x)} \leq Q_i^{(x)} \\ & p_{i1}^{(x)} + p_{i2}^{(x)} \leq Q_i^{(x)} \qquad i=1,2 \\ \text{and} \quad & p_{i2}^{(x)} + p_i^{(x)} \leq Q_i^{(x)} \end{aligned}\right\} \quad (3.16)$$

From (3.16), it follows that

$$\left.\begin{aligned} & f_i^{(x)} + F_{i1}^{(x)} + F_{i2}^{(x)} \leq 1 \\ & f_i^{(x)} + F_{i1}^{(x)} \leq 1 \qquad i=1,2 \\ & F_{i1}^{(x)} + F_{i2}^{(x)} \leq 1 \\ \text{and} \quad & F_{i2}^{(x)} + f_i^{(x)} \leq 1 \end{aligned}\right\} \quad (3.17)$$

Let us consider two particular combinations of 'f' and 'F' constants in (3.12). As a first combination, let f_i, F_{i1} and $F_{i2} \geq 0$. These constants, by the definitions of (3.13), (3.14) and using (3.1), can be expressed as follows:

$$\left.\begin{aligned} & f_i = f_i^+ - f_i^- \\ & F_{i1} = F_{i1}^+ - F_{i1}^- \\ \text{and} \quad & F_{i2} = F_{i2}^+ - F_{i2}^- \end{aligned}\right\} \quad (3.18)$$

Then,

$$f_i+F_{i1}+F_{i2} = (f_i^+-f_i^-) + (F_{i1}^+-F_{i1}^-) + (F_{i2}^+-F_{i2}^-)$$
$$\leq (f_i^++F_{i1}^++F_{i2}^+)$$

Then, using (3.17) it follows,

$$f_i + F_{i1} + F_{i2} \leq 1$$

Now another combination of 'f' and 'F' constants is considered, which are such that f_i and $F_{i2} \leq 0$ and $F_{i1} \geq 0$. Then,

$$|f_i| + |F_{i2}| = (f_i^- - f_i^+) + (F_{i2}^- - F_{i2}^+) \leq f_i^- + F_{i2}^-$$

Thus, it follows from (3.17),

$$|f_i| + |F_{i2}| \leq 1$$

Also $F_{i1} \leq 1$

Similarly, by considering other combinations of 'f' and 'F' constants, the general nature of (3.12) and the statement following it can be proved. It should be noted that this proof is independent of the mode of connections of resistances to realize a given set of 'f' and 'F' constants.

At this stage, let us note that it is desirable, whenever possible, to realize a particular set of 'f' and 'F' constants with a minimum number of resistors. As for example, if f_1, F_{11} and F_{12} are all non-negative, then for minimum resistor implementation, the voltages V_I, V_1 and V_2 should be mixed through a star connection of

resistors. The star point can then be connected to the + input of the OA, A_1 while the negative input terminal of the same is grounded. This means that f_1^-, F_{11}^- and F_{12}^- are all zero. However, one can also have connections such that both the groups f_1^+, F_{11}^+, F_{12}^+ and f_1^-, F_{11}^-, F_{12}^- have non-zero values. In such a case, however, a larger number of resistors will be required.

As an additional example, let us consider another situation, where two infinite-input impedance points are fed from the same source. They need not be fed through different potential divider connections and they can be connected through a single circuit. For an illustration of this, let us examine a situation, shown in Fig. 3.2(a), where only the part of the connections that are required to realize F_{12} (>0) and F_{22} (<0) are shown. (The constants f_1 and F_{11} are non-positive; and f_2 and F_{21} are both non-negative). The alternative and simpler ways of connections which use a minimum number of resistors are shown in Figs. 3.2(b) and 3.2(c) under two possible magnitude conditions that can exist between these two constants.

Let us now go back to our original discussion about the equations (3.11) and (3.12) and illustrate their use with an application. Let $f_1 = -\alpha$, $F_{11} = -\beta$ and $F_{12} = \gamma$, where $\alpha, \beta, \gamma \geq 0$. The equations (3.11) and (3.12) require the quantities α, β and γ to satisfy the following inequalities.

$$0 \leq \alpha, \beta, \gamma \leq 1$$

and

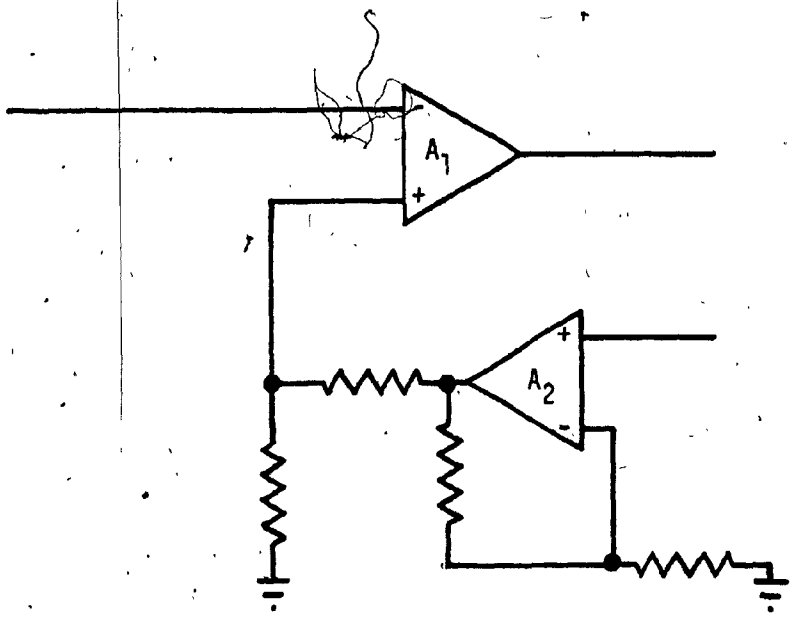

(a)

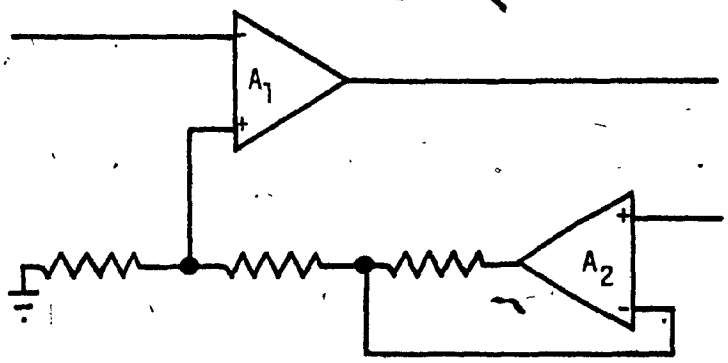

$|F_{22}| \geq |F_{12}|$

(b)

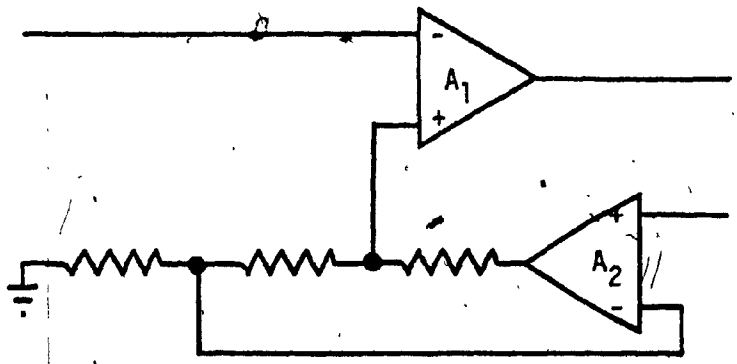

$|F_{12}| \geq |F_{22}|$

(c)

FIG. 3.2: Different Mode of Connections when $f_1 \leq 0$, $F_{11} \leq 0$, $F_{12} \geq 0$, $f_2 \geq 0$, $F_{21} \geq 0$ and $F_{22} \leq 0$

$$0 \leq (\alpha+\beta) \leq 1$$

The restrictions given by (3.11) and (3.12) must also be considered along with (3.9) or (3.10) for the appropriate realizations of the FGA's.

Now that all the restrictions and equations relating 'f' and 'F' constants and μ_0 (the nominal d.c. gain of the amplifier) have been obtained, we are in a position to obtain second order realizations of both the positive and the negative gain amplifiers.

It is easy to visualize that there are different combinations of 'f' and 'F' constants that can realize a given second order amplifier circuit, even after satisfying (3.9) or (3.10), (3.11) and (3.12). These different combinations will give rise to different topological configurations of networks. For a given topology, however, the choices for the different quantities can be made so as to maximize the amplifier bandwidth. Ideally, the maximum bandwidth is obtained for our amplifiers when $\alpha_2 = 0$ in (3.6). However, a simple study of both the equations (3.5) and (3.6) together, shows that it is impossible to achieve this condition in practice. Clearly then, one has to aim for minimizing α_2. Comparing (3.5) and (3.6), we obtain

$$\left(\frac{1}{\alpha_2}\right) = (F_{11}\, F_{22} - F_{12}\, F_{21}) \qquad (3.19)$$

For convenience, let us denote the R.H.S. of (3.19) by F. That is, let

$$F = F_{11}F_{22} - F_{12}F_{21} \tag{3.20}$$

Let us introduce the following definition, which is used later on.

Definition:

A suboptimal second order realization is a realization obtained from a given topology for which the constant F (as defined by (3.20)) is, for a given d.c. gain μ_0, maximum (i.e. α_2 is minimum) subject to the constraints given by (3.9) or (3.10) as the case may be and the constraints given by (3.11) and (3.12).

Clearly, there will be one realization among all the suboptimal realizations which will possess the maximum bandwidth. However, maximum bandwidth alone can not be the main consideration. Other practical considerations, such as relative stability, tunability, etc., are also important. One may achieve higher bandwidth at the risk of poor relative stability. However, when such amplifiers are used in practical applications, such as in active-RC filters, the whole circuit may start oscillating. Thus, the choice of the optimal circuit is influenced not only by the attainable bandwidth but also by various other considerations. This is why the amplifier realization possessing the maximum possible bandwidth for a given topology has been termed suboptimal and not optimal. Let us now proceed to enumerate various possible topological structures for the realization of second order FGA's.

3.4 TOPOLOGICAL STRUCTURES FOR POSITIVE GAIN AMPLIFIERS

We shall require all positive gain realizations to have an infinite input impedance. This requirement is imposed in order to be

consistent with the fact that the conventional realization of the positive gain amplifiers also has an infinite input impedance. Thus, invoking this requirement, one finds that there is only one value for f_1, which is 1. Furthermore, the same condition also restricts the constant f_2 to only discrete values of 0, -1 and +1. In addition, it is required that $F_{11}, F_{12} \leq 0$. Hence, there are only three combinations of f's and F's that are possible. These three combinations of conditions on the 'f' and 'F' constants are listed below:

1. $f_1 = 1$, $f_2 = 0$, $F_{11}, F_{12} \leq 0$

2. $f_1 = 1$, $f_2 = -1$, $F_{11}, F_{12} \leq 0$, $F_{21}, F_{22} \geq 0$

3. $f_1 = 1$, $f_2 = 1$, $F_{11}, F_{12}, F_{21}, F_{22} \leq 0$.

Since both F_{11} and $F_{12} \leq 0$ in all the cases, let us start with the assumption that

$$F_{11} = -\alpha \text{ and } F_{12} = -\beta \tag{3.21}$$

where $\alpha, \beta \geq 0$.

Using the relations (4) and (5) of (3.9), we obtain

$$\left.\begin{aligned} F_{22} &= \left(\alpha - \frac{1}{\mu_0}\right) \\ \text{and} \\ F_{21} &= \frac{\left(\alpha - \frac{1}{\mu_0}\right)^2}{\beta} - \frac{f_2}{\mu_0} \end{aligned}\right\} \tag{3.22}$$

Another quantity of interest, that should be maximized, is F and this is given by

$$F = -\frac{f_2\beta}{\mu_0} - \frac{(\alpha - \frac{1}{\mu_0})}{\mu_0} \tag{3.23}$$

The different possible cases will now be considered in detail.

Case I: $f_1 = 1$ and $f_2 = 0$

In this case one obtains,

$$\left.\begin{aligned} &f_1 = 1\ ,\ F_{11} = -\alpha\ ,\ F_{12} = -\beta \\ &f_2 = 0\ ,\ F_{21} = \frac{(\alpha - \frac{1}{\mu_0})^2}{\beta}\ ,\ F_{22} = (\alpha - \frac{1}{\mu_0}) \end{aligned}\right\} \tag{3.24}$$

The inequality (2) of (3.9) requires that

$$\alpha < (\frac{1}{\mu_0}) \tag{3.25}$$

The above condition suggests that $F_{22} < 0$ and $F_{21} > 0$.

All the realizability conditions can now be derived using (3.11) and (3.12) and they are listed below:

$$\left.\begin{aligned} &\text{(i)}\ \ 0 \le \alpha \le 1\ , \quad \text{(ii)}\ \ 0 \le \beta \le 1 \\ &\text{(iii)}\ \ \alpha < \left(\frac{1}{\mu_0}\right)\ , \quad \text{(iv)}\ \ \alpha \ge \left(\frac{1}{\mu_0} - 1\right) \\ &\text{(v)}\ \ \beta \le 1-\alpha\ , \quad \text{(vi)}\ \ \beta \ge \left(\alpha - \frac{1}{\mu_0}\right)^2 \end{aligned}\right\} \quad (3.26)$$

It is obvious that $\mu_0 \ge 1$. The topological structure to realize the 'f' and 'F' constants given by (3.24) is shown in Fig. 3.3.

To obtain the suboptimal realization, let us refer to (3.23) and note that when $f_2 = 0$, F is maximized by choosing $\alpha = 0$, for a given μ_0 . In that case, (3.24) and (3.26) become as follows:

$$\left.\begin{aligned} &f_1 = 1\ , \quad F_{11} = 0\ , \quad F_{12} = -\beta \\ &f_2 = 0\ , \quad F_{21} = \frac{1}{\beta\mu_0^2}\ , \quad F_{22} = -\frac{1}{\mu_0} \end{aligned}\right\} \quad (3.27)$$

where β is constrained by the following inequality

$$\left(\frac{1}{\mu_0}\right)^2 \le \beta \le 1$$

The quantity F is given by

$$F = \left(\frac{1}{\mu_0}\right)^2 \quad (3.28)$$

Obviously, there is an infinite number of values for the choice of β . Three particular values for β are of interest, in that they all minimize the number of resistors used. Those choices for β are

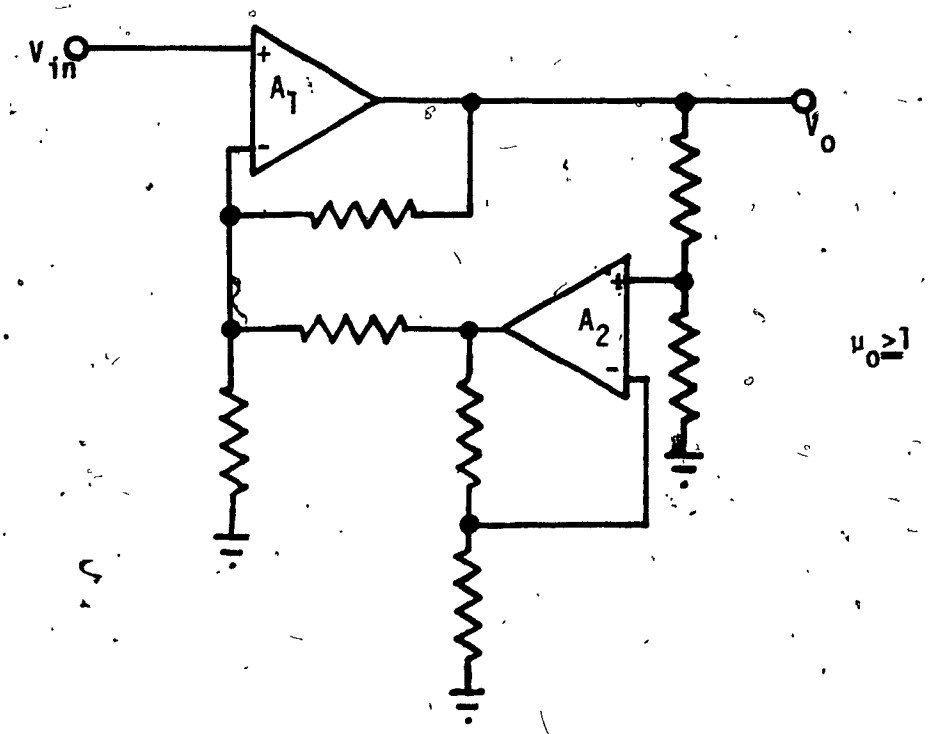

FIG. 3.3: Topological Structure of the Positive Gain Amplifier with $f_1=1$ and $f_2=0$

$(\frac{1}{\mu_0})^2$, $(\frac{1}{\mu_0})$ and 1 . The corresponding suboptimal realizations are given in Fig. 3.4. The circuits shown in Figs. 3.4(a) and 3.4(b) were reported earlier by this author and Bhattacharyya [33].

Case II: $f_1 = 1$, $f_2 = -1$

In this case, the quantities 'f' and 'F' are given below.

$$\left.\begin{aligned} & f_1 = 1 \ , \quad F_{11} = -\alpha \ , \quad F_{12} = -\beta \\ & f_2 = -1 \ , \quad F_{21} = \frac{1}{\mu_0} + \frac{(\alpha - \frac{1}{\mu_0})^2}{\beta} \ , \quad F_{22} = (\alpha - \frac{1}{\mu_0}) \end{aligned}\right\} \quad (3.29)$$

and

$$F = \frac{\beta}{\mu_0} - \frac{(\alpha - \frac{1}{\mu_0})}{\mu_0} \quad (3.30)$$

The realizability conditions are as follows:

$$\left.\begin{aligned} & \text{(i)} \ \ 0 \leq \alpha \leq 1 \ , \quad \text{(ii)} \ \ 0 \leq \beta \leq 1 \\ & \text{(iii)} \ \ \alpha \geq \frac{1}{\mu_0} \ , \quad \text{(iv)} \ \ \alpha+\beta \leq 1 \\ & \text{and} \quad \text{(v)} \ \ \beta \geq \frac{(\alpha - \frac{1}{\mu_0})^2}{(1-\alpha)} \end{aligned}\right\} \quad (3.31)$$

The topological structure for the realization of the 'f' and 'F' constants given by (3.29) is shown in Fig. 3.5. The realization is possible only when $\alpha < 1$ (to keep β finite) and this implies that

$$\mu_0 > 1 \quad (3.32)$$

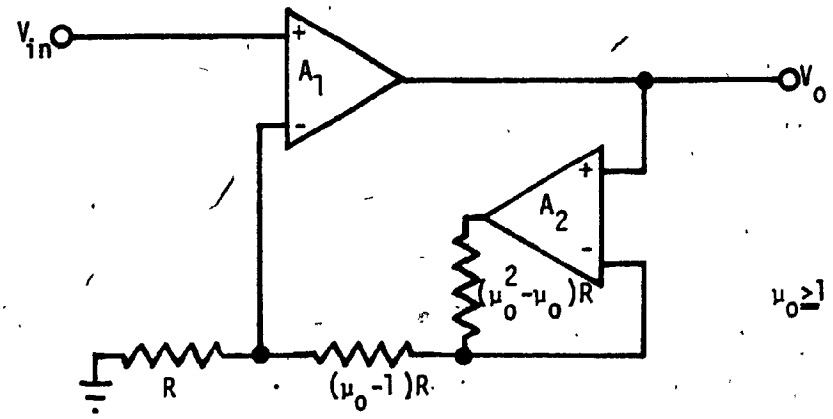

(a)

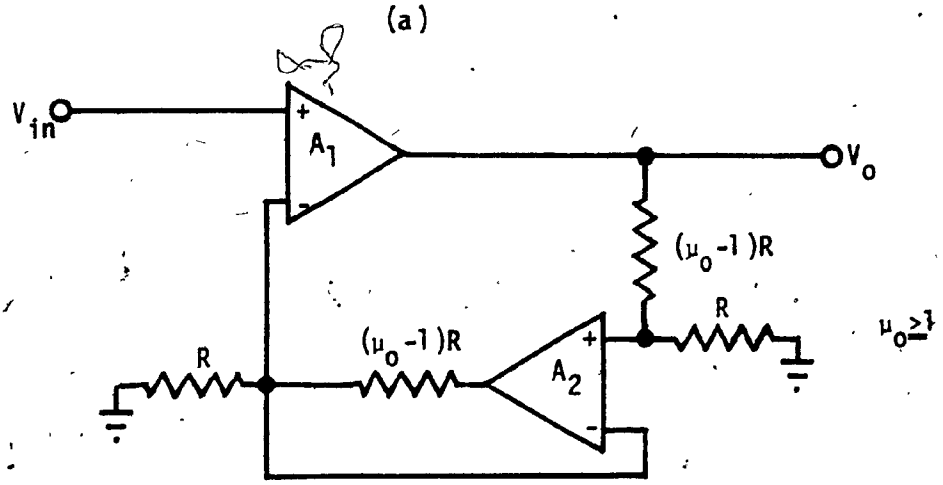

(b)

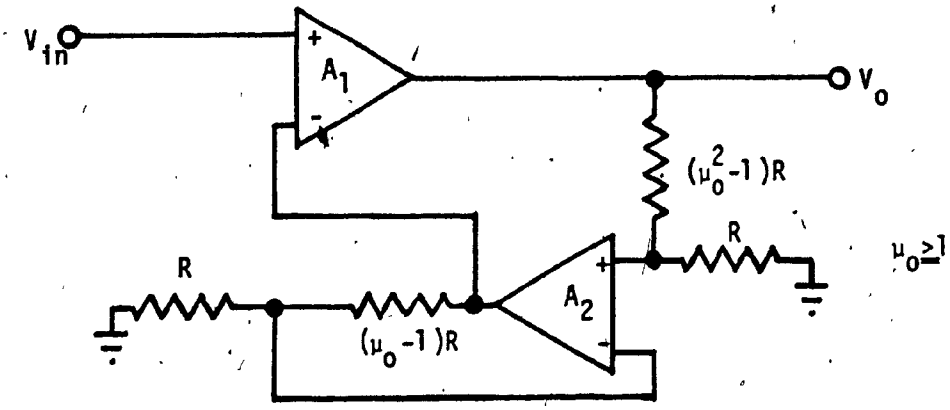

(c)

FIG. 3.4: Suboptimal Realizations of the Positive Gain Amplifiers with $f_1 \neq 1$ and $f_2 \neq 0$

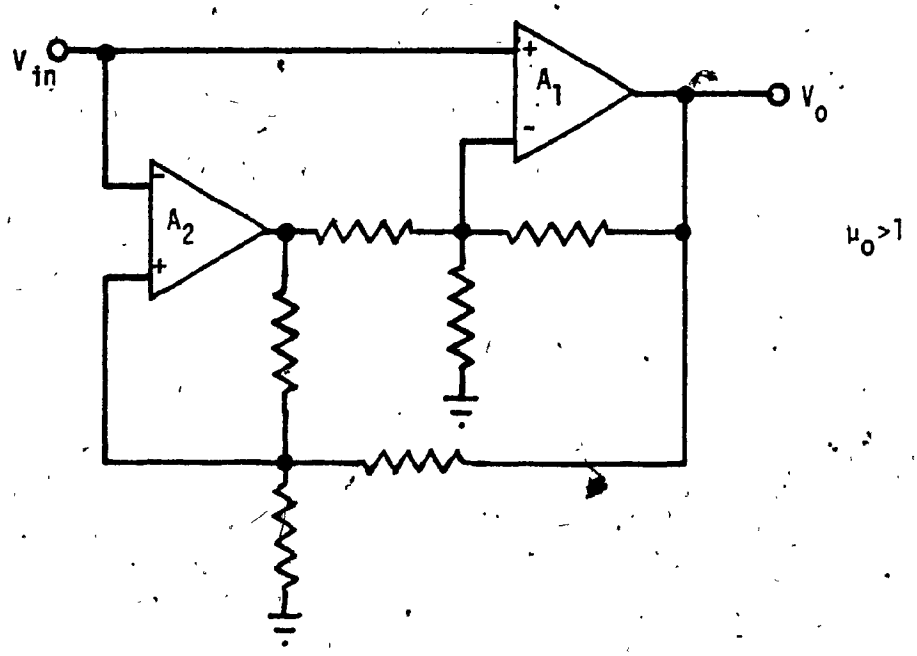

FIG. 3.5: Topological Structure of the Positive Gain Amplifier with $f_1=1$ and $f_2=-1$

For the suboptimal realization in this case, the value of α has to be chosen as $(\frac{1}{\mu_0})$. Choosing this value of α, the equations (3.29) and (3.30) become as given below:

$$\left.\begin{aligned} f_1 &= 1 \quad , \quad F_{11} = -(\tfrac{1}{\mu_0}) \quad , \quad F_{12} = -\beta \\ f_2 &= -1 \quad , \quad F_{21} = (\tfrac{1}{\mu_0}) \quad , \quad F_{22} = 0 \end{aligned}\right\} \tag{3.33}$$

and

$$F = (\tfrac{\beta}{\mu_0}) \tag{3.34}$$

The realizability conditions thus become

$$\text{(i)}\ \ 0 < \beta \leq (1 - \tfrac{1}{\mu_0}) \ \text{ and } \ \text{(ii)}\ \ \mu_0 > 1 \tag{3.35}$$

It is worth noting that a choice of $\beta = (\frac{1}{\mu_0})$ can be made which will satisfy the conditions given by (3.35) for $\mu_0 \geq 2$. With such a choice, the realization of a positive gain amplifier is shown in Fig. 3.6. However, the suboptimal realization is obtained when $\beta = (1 - \frac{1}{\mu_0})$ and this realization, originally suggested by Reddy [31], is shown in Fig. 3.7.

Case III: $f_1 = 1$ and $f_2 = 1$

In this case, the various 'f' and 'F' quantities are as follows:

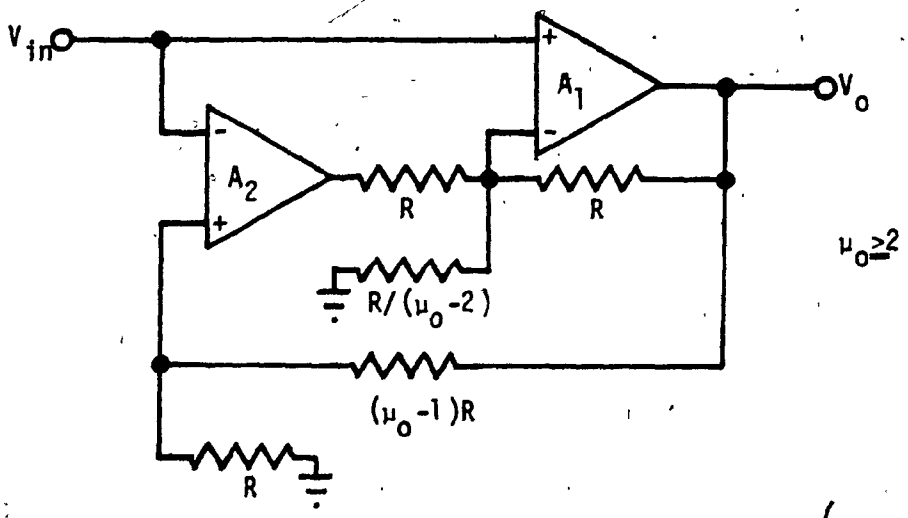

FIG. 3.6: Positive Gain Amplifier Realization with $f_1=1$, $f_2=-1$ and $\beta = \frac{1}{\mu_o}$ in (3.33)

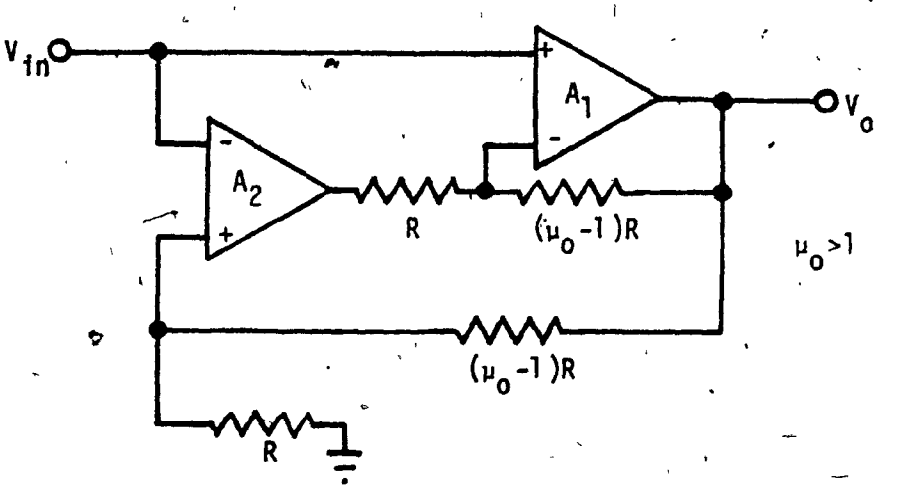

FIG. 3.7: Suboptimal Realization of the Positive Gain Amplifier with $f_1=1$ and $f_2=-1$

$$\left.\begin{aligned} f_1 &= 1\ , \quad F_{11} = -\alpha\ , \quad F_{12} = -\beta \\ f_2 &= 1\ , \quad F_{21} = \frac{(\alpha - \frac{1}{\mu_0})^2}{\beta} - \frac{1}{\mu_0}\ , \quad F_{22} = (\alpha - \frac{1}{\mu_0}) \end{aligned}\right\} \quad (3.36)$$

and

$$F = (\frac{1}{\mu_0})^2 - \frac{(\alpha+\beta)}{\mu_0} \quad (3.37)$$

The realizability conditions are given by the following:

$$\left.\begin{aligned} &\text{(i)}\ \ 0 \leq \alpha\ ,\ \beta \leq 1\ ,\ \text{(ii)}\ \ (\alpha+\beta) \leq \frac{1}{\mu_0} \\ &\text{(iii)}\ (\alpha+\beta) \leq 1\ \ ,\ \ \text{(iv)}\ \ \beta \geq \mu_0\,(\alpha - \frac{1}{\mu_0})^2 \\ &\text{(v)}\ \ \alpha < \frac{1}{\mu_0}\ \ ,\ \ \text{(vi)}\ \ \beta \leq \frac{(\alpha - \frac{1}{\mu_0})^2}{(\frac{2}{\mu_0} - \alpha - 1)} \end{aligned}\right\} \quad (3.38)$$

The condition (vi) in (3.38) does not apply when $\alpha > (2/\mu_0 - 1)$. It can be shown that $\alpha=0$ makes $\beta = \frac{1}{\mu_0}$, leading to $F=0$, while $\beta=0$ makes $\alpha = \frac{1}{\mu_0}$ in conflict with the requirement $\alpha < \frac{1}{\mu_0}$. Thus the choices for α and β have to be made such that $\alpha, \beta > 0$. After choosing the value of α such that $0 < \alpha < \frac{1}{\mu_0}$, the value of β can be chosen to satisfy (3.38). The topological structure to realize (3.36) is shown in Fig. (3.8). By combining conditions (iii) and (iv) in (3.38), it follows that

$$\alpha \leq \frac{(1+\sqrt{4\mu_0 - 3})}{2\mu_0}$$

In order that α is real, it follows that

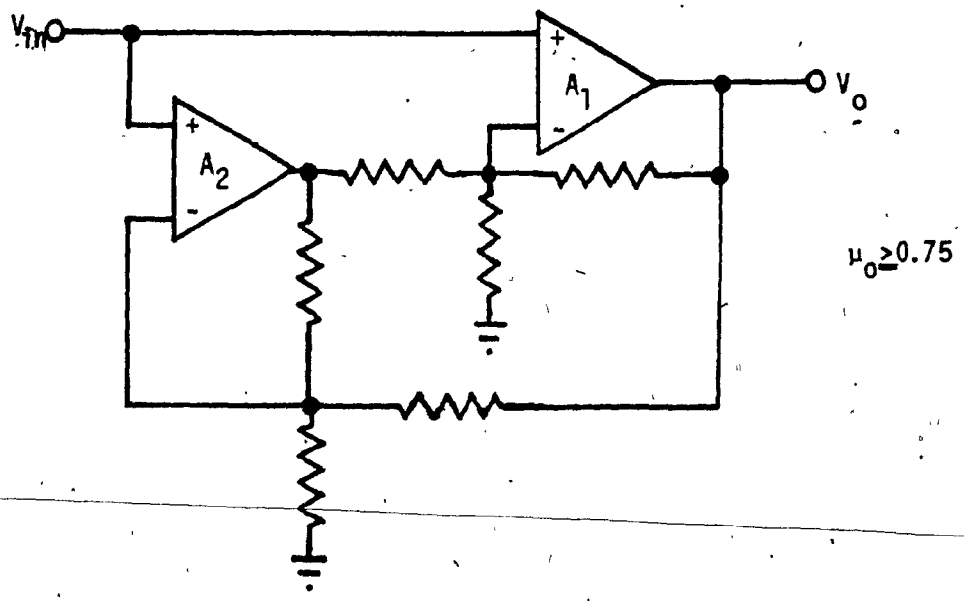

FIG. 3.8: Topological Structure of the Positive Gain Amplifier with $f_1 = f_2 = 1$

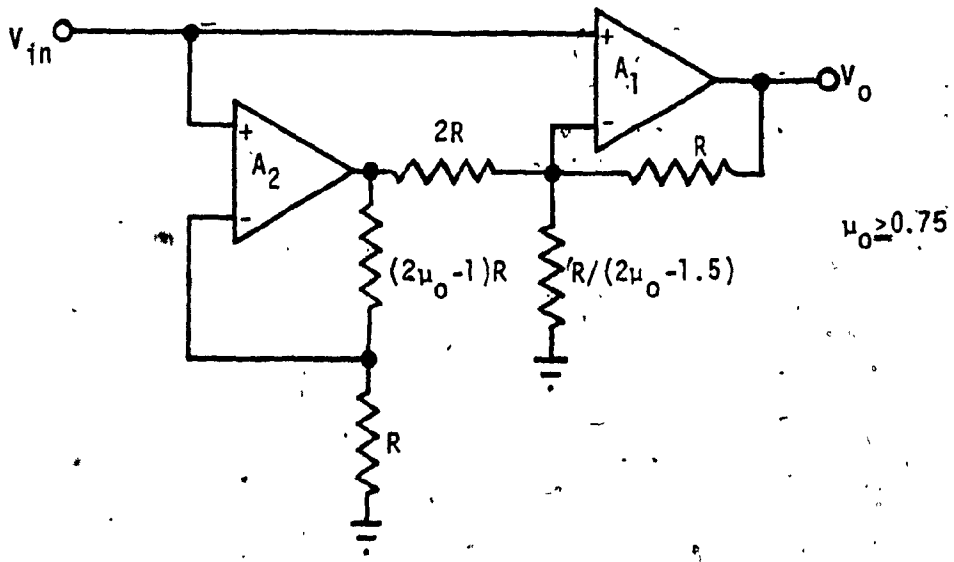

FIG. 3.9: Suboptimal Realization of the Positive Gain Amplifier with $f_1 = f_2 = 1$

$$\mu_0 \geq 0.75 \ .$$

The suboptimal realization is obtained with $\alpha = (1/2\mu_0)$, $\beta = (1/4\mu_0)$. Then the quantities 'f' and 'F' become as follows:

$$\left.\begin{aligned} f_1 &= 1 \ , \quad F_{11} = -\left(\frac{1}{2\mu_0}\right) \ , \quad F_{12} = -\left(\frac{1}{4\mu_0}\right) \\ f_2 &= 1 \ , \quad F_{21} = 0 \ , \quad F_{22} = -\left(\frac{1}{2\mu_0}\right) \end{aligned}\right\} \tag{3.39}$$

and

$$F = \left(\frac{1}{2\mu_0}\right)^2 \tag{3.40}$$

where, as shown above,

$$\mu_0 \geq 0.75 \tag{3.41}$$

The suboptimal realization corresponding to (3.39) is shown in Fig. 3.9.

Having obtained the possible topological structures and the corresponding suboptimal realizations for positive gain amplifiers, let us now proceed to derive the possible topological structures for the realization of negative gain amplifiers.

3.5 SOME GENERAL COMMENTS ABOUT NEGATIVE GAIN AMPLIFIERS

In the case of the conventional negative gain amplifier, the input impedance is finite. It is impossible to realize a negative gain amplifier with infinite input impedance using a single OA. However,

infinite input impedance can be obtained with a buffer amplifier at the input. Thus, for the realization of negative gain amplifiers with an infinite input impedance, at least, two OA's are required. As two OA's are also used for actively compensated second order FGA's, it may be possible to obtain improved negative gain amplifiers with an infinite input impedance. This leads to two possibilities.

(a) Negative gain amplifiers with an infinite input impedance

(b) Negative gain amplifiers with a finite input impedance.

Before proceeding with these two cases, let us prove the following theorem.

Theorem 3.1

It is impossible to realize an inverting amplifier with a second order transfer function as defined in (3.6) such that the following conditions are satisfied:

a) The amplifier should employ only two OA's.

b) It should have an infinite input impedance.

c) $\mu_0 \leq 1$.

Proof:

For infinite input impedance, the values of both f_1 and f_2 can take only discrete values of 1, 0, and -1 . In particular, since $f_1 < 0$ (Condition 3 of 3.10), the only possible value for f_1 is -1 . Also it implies that F_{11} , $F_{12} \geq 0$. Thus, let

$$F_{11} = \alpha \quad \text{and} \quad F_{12} = \beta \quad (0 \leq \alpha, \beta \leq 1)$$

From the relation (5) of (3.10), we get

$$F_{22} = -\frac{1}{\mu_0} - \alpha \tag{3.42}$$

The realizability condition of (3.11) requires that

$$|F_{22}| \leq 1 .$$

The above inequality and (3.42) imply that

$$\mu_0 \geq 1 .$$

Now we shall investigate the case $\mu_0=1$. Again the only possibility is that $F_{22} = -1$ and $\alpha=0$, that is,

$$F_{22} = -1 \quad \text{and} \quad F_{11} = 0 \tag{3.43}$$

Then the inequality (1) of (3.10) requires that

$$-F_{12} F_{21} > 0 \tag{3.44}$$

Since $F_{11} = 0$, neither F_{12} nor F_{21} can be zero in order to satisfy the inequality (3.44). From (2) of (3.10), one also gets with $f_1 = F_{22} = -1$,

$$f_2 F_{12} - 1 < 0 \tag{3.45}$$

Using (4) of (3.10) now, for $\mu_0=1$, it can be shown that

$$f_2 F_{12} - 1 = -F_{12} F_{21} \tag{3.46}$$

In view of (3.44) and (3.46), we can write

$$f_2 F_{12} - 1 > 0 \tag{3.47}$$

It is impossible to satisfy (3.45) and (3.47) simultaneously.

Thus, for an inverting FGA using two OA's and possessing an infinite input impedance, the magnitude of the d.c. gain, μ_0 must satisfy the condition $\mu_0 > 1$. Hence the theorem.

The above theorem implies that it is not possible to realize a second order inverter (unity gain inverting amplifier) with an improved bandwidth and possessing an infinite input impedance. Thus, we need only to investigate the possibilities of realizing non-unity gain inverting amplifiers with an infinite input impedance.

3.6 NEGATIVE GAIN AMPLIFIERS WITH INFINITE INPUT IMPEDANCE

In the case of infinite input impedance, it is required that

$$f_1 = -1 \ , \ F_{11} \ , \ F_{12} \geq 0 \tag{3.48}$$

Let $F_{11} = \alpha$ and $F_{12} = \beta$. Then, using the relation (5) of (3.10), we get

$$F_{22} = -\left(\alpha + \frac{1}{\mu_0}\right) \tag{3.49}$$

Since $F_{22} < 0$ for all possible values of μ_0, there are only two possible values for f_2, which are 1 and 0. These two cases will

be considered separately now.

Case I: $f_1 = -1$, $f_2 = 0$

With the use of relation (4) of (3.10), (3.48) and (3.49), the 'f' and 'F' constants are obtained as given below:

$$\left.\begin{aligned} & f_1 = -1 , \quad F_{11} = \alpha , \quad F_{12} = \beta \\ & f_2 = 0 , \quad F_{21} = \frac{-(\alpha + \frac{1}{\mu_0})^2}{\beta} , \quad F_{22} = -(\alpha + \frac{1}{\mu_0}) \end{aligned}\right\} \quad (3.50)$$

and

$$F = \frac{\alpha}{\mu_0} + (\frac{1}{\mu_0})^2 \quad (3.51)$$

The realizability conditions are as follows:

$$\left.\begin{aligned} & \text{(i)} \quad 0 \leq \alpha \leq 1 , \quad \text{(ii)} \quad 0 \leq \beta \leq 1 - \alpha \\ & \text{(iii)} \quad \beta \geq \frac{(\alpha + \frac{1}{\mu_0})^2}{(1 - \alpha - \frac{1}{\mu_0})} . \end{aligned}\right\} \quad (3.52)$$

Using (ii) and (iii) of (3.52), it can be shown that

$$\alpha \leq \frac{(1 - \frac{1}{\mu_0} - \frac{1}{\mu_0^2})}{(2 + \frac{1}{\mu_0})} .$$

Thus, $\mu_0 \geq \{(\sqrt{5}+1)/2\}$ in order that $\alpha \geq 0$. The topological structure to realize (3.50) is shown in Fig. 3.10. The suboptimal realization can be obtained with the following choices for α and β .

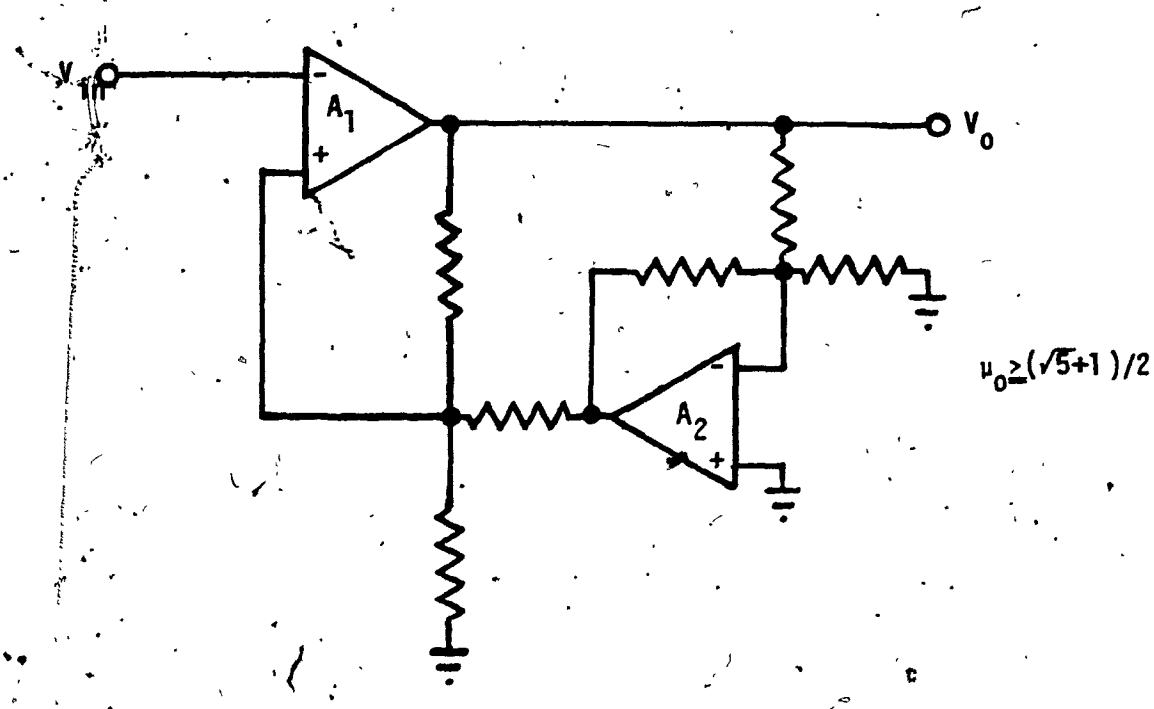

FIG. 3.10: Topological Structure of the Negative Gain Amplifier with $f_1=-1$ and $f_2=0$

$$\alpha = \frac{(\mu_0^2 - \mu_0 - 1)}{(2\mu_0^2 + \mu_0)}$$

and,

$$\beta = \frac{(\mu_0 + 1)^2}{(2\mu_0^2 + \mu_0)}$$

The resulting value of F is given by (3.53).

$$F = \frac{(\mu_0 + 1)}{(2\mu_0^2 + \mu_0)} \tag{3.53}$$

where

$$\mu_0 \geq \frac{(\sqrt{5}+1)}{2} \tag{3.54}$$

Two possible realizations are shown in Fig. 3.11.

Case II: $f_1 = -1$, $f_2 = 1$

In this case, the 'f' and 'F' constants are given below:

$$\left.\begin{aligned} &f_1 = -1 \ , \ F_{11} = \alpha \ , \ F_{12} = \beta \\ &f_2 = 1 \ , \ F_{21} = \frac{-(\alpha + \frac{1}{\mu_0})^2}{\beta} + \frac{1}{\mu_0} \ , \ F_{22} = -(\alpha + \frac{1}{\mu_0}) \end{aligned}\right\} \tag{3.55}$$

and

$$F = \frac{(\alpha-\beta)}{\mu_0} + (\frac{1}{\mu_0})^2 \tag{3.56}$$

The realizability conditions are as follows:

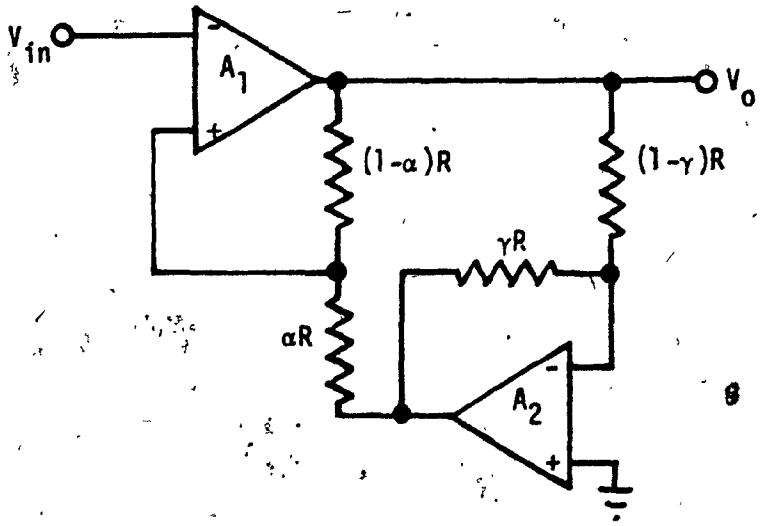

$$\alpha = \frac{(\mu_o^2-\mu_o-1)}{\mu_o(2\mu_o+1)}$$

$$\gamma = \frac{\mu_o}{(2\mu_o+1)}$$

$$\mu_o \geq (\sqrt{5}+1)/2$$

(a)

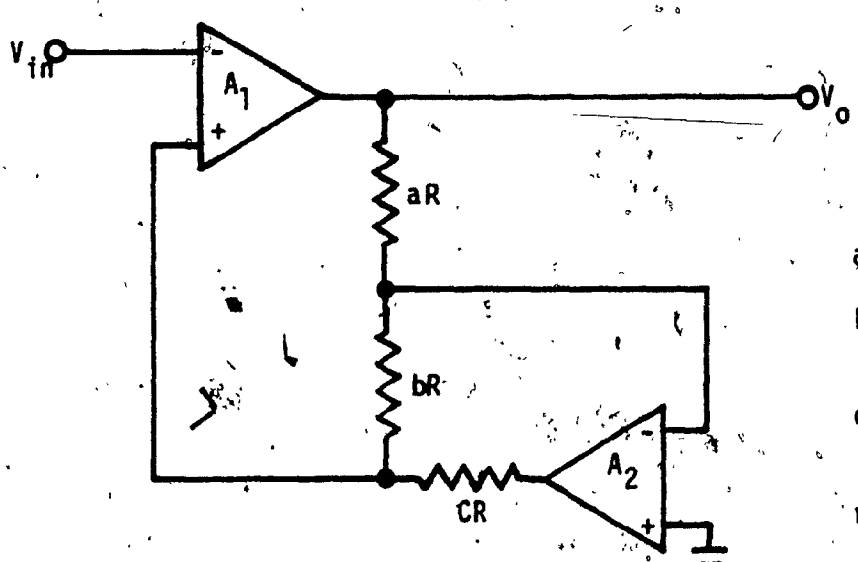

$$a = \mu_o$$

$$b = 1$$

$$c = \frac{\mu_o^2-\mu_o-1}{(\mu_o+1)}$$

$$\mu_o \geq (\sqrt{5}+1)/2$$

(b)

FIG. 3.11: Suboptimal Realizations of the Negative Gain Amplifier with $f_1=-1$ and $f_2=0$

$$\left.\begin{aligned} &\text{(i)}\ \ \beta < (\alpha + \frac{1}{\mu_0}) \ , \quad \text{(ii)}\ \ \beta < \mu_0 (\alpha + \frac{1}{\mu_0})^2 \\ &\text{(iii)}\ \ \beta \leq (1-\alpha) \ , \quad \text{(iv)}\ \ \beta \geq \frac{(\alpha + \frac{1}{\mu_0})^2}{(1-\alpha)} \end{aligned}\right\} \quad (3.57)$$

Using the Conditions (ii) and (iv) of (3.57), it can be shown that $\mu_0 > 1$. The topological structure realizing (3.55) is shown in Fig. 3.12. The quantity F can be maximized with the following choices for α and β.

$$\left.\begin{aligned} &\alpha = 1 - \frac{1}{\sqrt{2}}(1 + \frac{1}{\mu_0}) \\ &\text{and} \\ &\beta = \frac{(\sqrt{2}-1)^2}{\sqrt{2}} (1 + \frac{1}{\mu_0}) \end{aligned}\right\} \quad (3.58)$$

It is obvious that in order that α is non-negative

$$\mu_0 \geq (\sqrt{2}+1)$$

The maximum value of F becomes,

$$F = \frac{(1+\mu_0)(\sqrt{2}-1)^2}{\mu_0^2} \quad (3.59)$$

The topology of the suboptimal realization is same as shown in Fig. 3.12. However, as it will be seen later that this circuit is not suitable for practical adjustments, further consideration of this is omitted.

Before proceeding to find the topological structures and the corresponding suboptimal realizations of negative gain amplifiers with

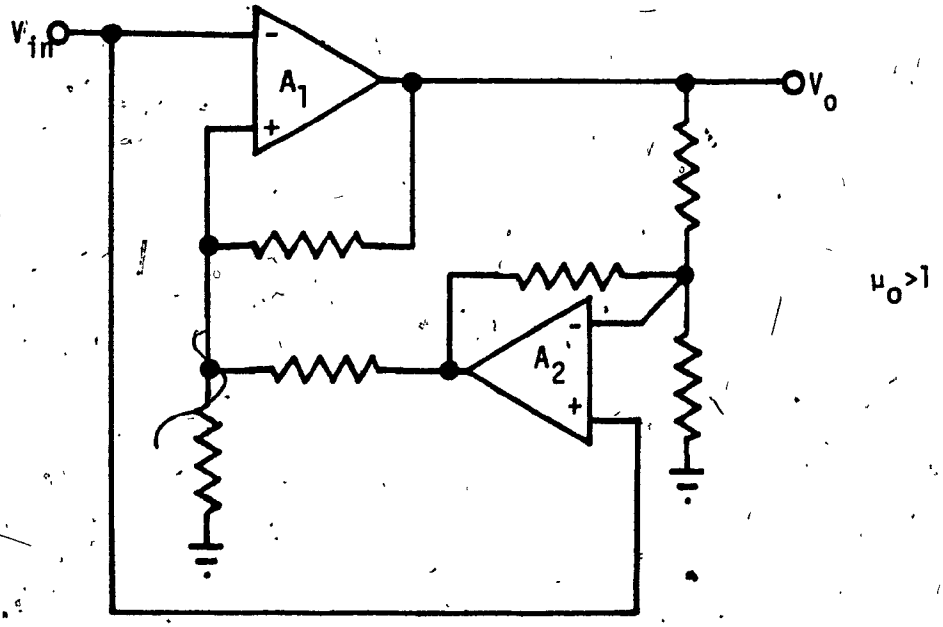

FIG. 3.12: Topological Structure of the Negative Gain Amplifier with $f_1 = -1$ and $f_2 = 1$

finite input impedance, some comments are now in order.

Since the input impedance can be finite, the resistors can be connected from the input to any of the input terminals of the OA's. There are only two equality relations in (3.10), while there are six parameters to be found. Thus, in general, four parameters are to be selected arbitrarily, while satisfying the inequality constraints of (3.10), (3.11) and (3.12). The other two parameters are fixed by the equality relations of (3.10).

3.7 NEGATIVE GAIN AMPLIFIERS WITH FINITE INPUT IMPEDANCE

Since we have to pick four parameters out of six arbitrarily, let us first choose the value of f_1 to satisfy the inequality (3) of (3.10). Thus, let

$$f_1 = -\alpha \qquad (0 < \alpha \leq 1) \tag{3.60}$$

The next choice can be made for F_{22} or F_{11}. Once the choice for one is made, the other one is fixed by the equality relation (5) of (3.10). Thus, let us choose F_{22} as follows:

$$F_{22} = \beta \tag{3.61}$$

Since $|F_{22}| \leq 1$, we have

$$-1 \leq \beta \leq 1 \tag{3.62}$$

The equation (3.62) implies that β can be negative, positive or zero.

Hence, the following two cases are to be considered.

$$\left.\begin{array}{l} 1.\ F_{22} \geq 0 \\ 2.\ F_{22} \leq 0 \end{array}\right\} \quad (3.63)$$

In each of the above cases, different subcases will arise depending upon how the other parameters are chosen. However, let us first consider the subcases which are common to both the above given by (3.63), that is, with $F_{22}=0$. For ease of later use and to maintain an order, we shall continue to serialize the cases in a continuously increasing order along with those considered in the previous section, that is, those with an infinite input impedance.

3.7.1 Negative Gain Amplifiers with $F_{22} = 0$

The use of the condition (1) of (3.63), (3.60) and (3.10) results in

$$F_{11} = -\frac{\alpha}{\mu_0} \quad (3.64)$$

The inequality (2) of (3.10) implies that

$$f_2 F_{12} < 0 \quad (3.65)$$

The inequality (3.65) can be satisfied in two ways as given below:

$$\left.\begin{array}{l} (a)\ f_2 < 0 \text{ and } F_{12} > 0 \\ (b)\ f_2 > 0 \text{ and } F_{12} < 0 \end{array}\right\}$$

Thus, we have two subcases when $F_{22} = 0$.

Case III: $f_1 < 0$, $F_{22} = 0$, $f_2 < 0$ and $F_{12} > 0$:

Let $F_{12} = \beta$ and $f_2 = -\gamma$. Then, the 'f' and 'F' constants are given below:

$$\left.\begin{aligned} f_1 &= -\alpha \ , \quad F_{11} = -\left(\frac{\alpha}{\mu_0}\right) \ , \quad F_{12} = \beta \\ f_2 &= -\gamma \ , \quad F_{21} = -\left(\frac{\gamma}{\mu_0}\right) \ , \quad F_{22} = 0 \end{aligned}\right\} \quad (3.66)$$

and

$$F = \frac{\beta\gamma}{\mu_0} \quad (3.67)$$

The realizability conditions are given below:

$$\left.\begin{aligned} &\text{(i)} \ 0 < \alpha, \beta, \gamma \leq 1 \ , \quad \text{(ii)} \ \alpha, \gamma \leq \frac{\mu_0}{(1+\mu_0)} \\ &\text{and} \\ &\text{(iii)} \ \mu_0 > 0 \end{aligned}\right\} \quad (3.68)$$

The topological structure realizing (3.66) is shown in Fig. 3.13. From (3.67) and (3.68), one can note that F is maximized with the following choices for β and γ :

$$\beta = 1 \quad \text{and} \quad \gamma = \frac{\mu_0}{(1+\mu_0)} \quad (3.69)$$

The choice for α is still arbitrary except that its value is restricted by (3.68). For a maximum first order coefficient (for better relative stability), it is always better to maximize α . Thus, the choice for

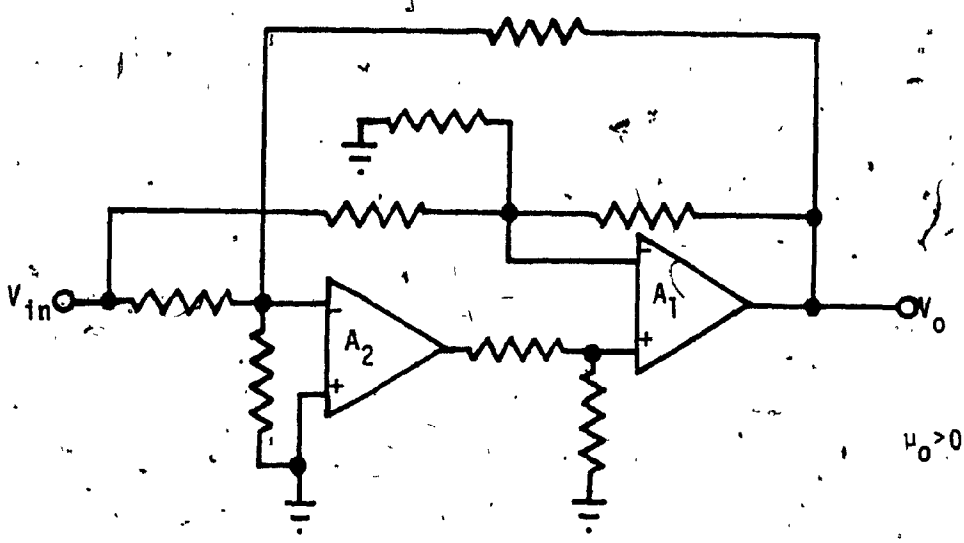

FIG. 3.13: Topological Structure of the Negative Gain Amplifier with $f_1<0$, $F_{22}=0$, $f_2<0$ and $F_{12}>0$

α can be made as follows:

$$\alpha = \frac{\mu_0}{(1+\mu_0)} \tag{3.70}$$

This choice for α will also reduce the number of resistors by 1. The resultant second order suboptimal realization is shown in Fig. 3.14 and the quantity F_b is given by

$$F = \frac{1}{(1+\mu_0)} \tag{3.71}$$

where

$$\mu_0 > 0 .$$

This realization was originally suggested by Reddy [31].

Case IV: $f_1 = -\alpha$, $F_{22} = 0$, $f_2 > 0$ and $F_{12} < 0$:

Let $F_{12} = -\beta$ and $f_2 = \gamma$. Then the 'f' and 'F' constants are given by the following:

$$\left.\begin{aligned} f_1 &= -\alpha , \quad F_{11} = -\left(\frac{\alpha}{\mu_0}\right) , \quad F_{12} = -\beta \\ f_2 &= \gamma , \quad F_{21} = \frac{\gamma}{\mu_0} , \quad F_{22} = 0 , \end{aligned}\right\} \tag{3.72}$$

and

$$F = \left(\frac{\beta\gamma}{\mu_0}\right) \tag{3.73}$$

The realizability conditions are as follows:

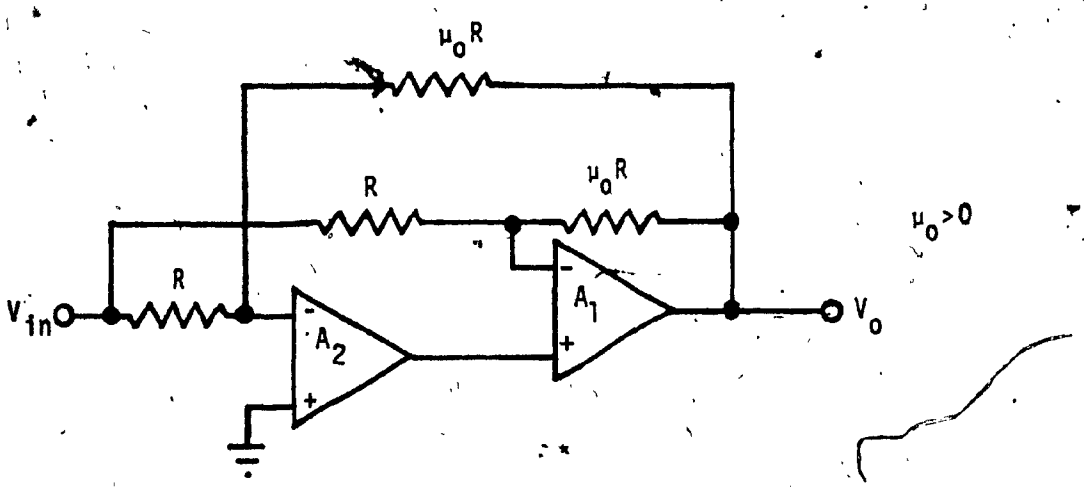

FIG. 3.14: Suboptimal Realization of the Negative Gain Amplifier with $f_1<0$, $F_{22}=0$, $f_2<0$ and $F_{12}>0$

$$\left.\begin{aligned} &\text{(i)}\quad 0 < \alpha,\ \beta,\ \gamma \leq 1\ , \quad \text{(ii)}\quad 0 < \beta \leq 1 - \alpha\left(1+\frac{1}{\mu_0}\right) \\ &\text{(iii)}\quad \gamma \leq \frac{\mu_0}{(1+\mu_0)}\ , \qquad \text{(iv)}\quad \mu_0 > 0\ . \end{aligned}\right\} \text{(3.74)}$$

The topological structure corresponding to (3.72) is shown in Fig. 3.15.

The suboptimal realization is obtained with the choice for γ as $\left(\frac{\mu_0}{1+\mu_0}\right)$ and the values of α and β tending to zero and one respectively. However, the choice for α has to be made with the following restriction.

$$0 < \alpha < \left(\frac{\mu_0}{1+\mu_0}\right)$$

Thus, an appropriate value of α subject to the above constraint should be chosen. Then the value of β can be chosen as

$$\beta = 1 - \frac{\alpha(1+\mu_0)}{\mu_0} \tag{3.75}$$

The resultant 'F' is given as below:

$$F = \frac{1}{(1+\mu_0)} - \frac{\alpha}{\mu_0} \tag{3.76}$$

The suboptimal realization is shown in Fig. 3.16. A suitable compromise between bandwidth and stability can be obtained by choosing α to be $\{\mu_0/(\mu_0+1)\}^2$. Then, the quantity F is given by

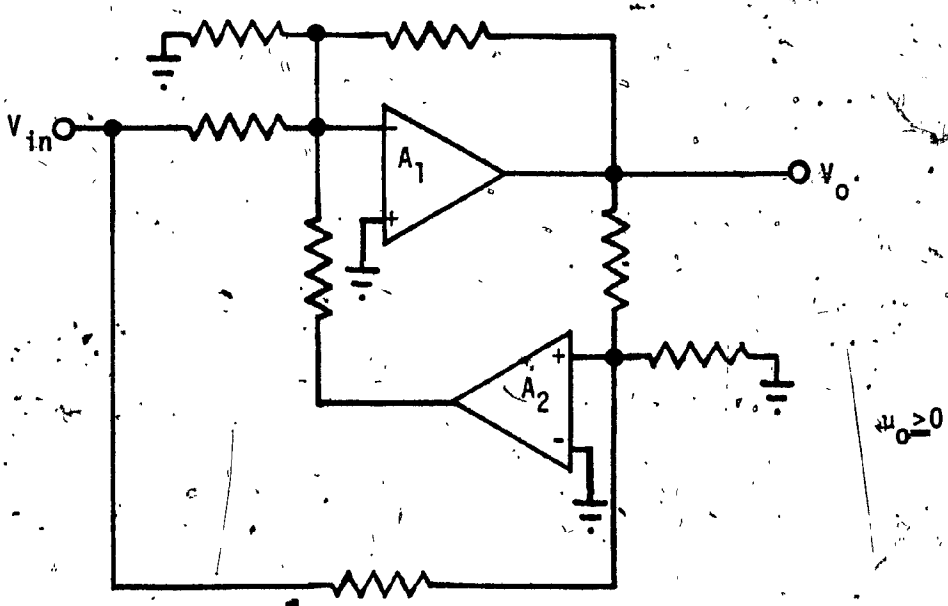

FIG. 3.15: Topological Structure of the Negative Gain Amplifier with $f_1<0$, $F_{22}=0$, $f_2>0$ and $F_{12}<0$

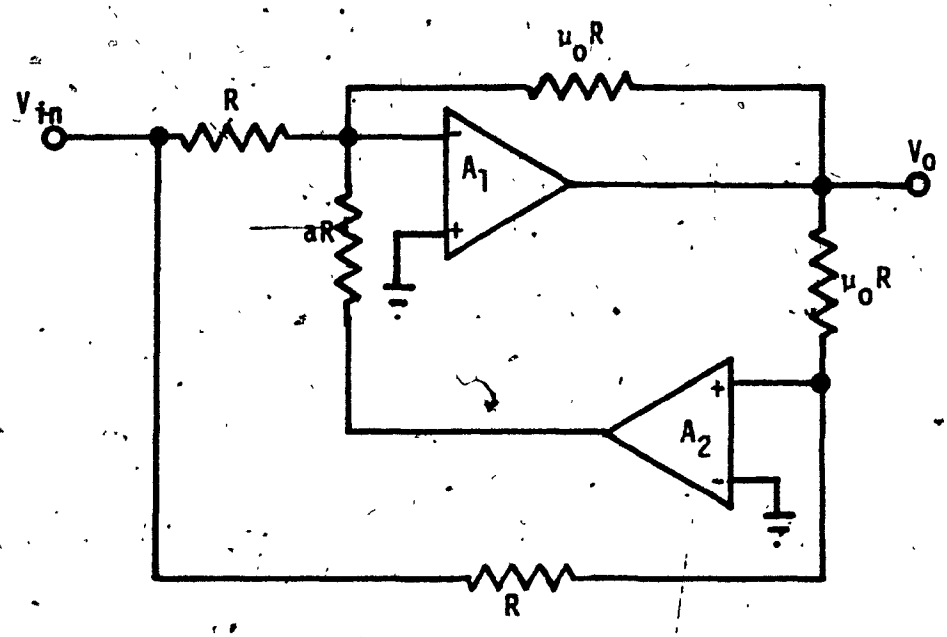

$$a = \frac{\mu_o \alpha}{\mu_o - \mu_o \alpha - \alpha}$$

$$0 < \alpha < \frac{\mu_o}{(1+\mu_o)}$$

$$\mu_o > 0$$

FIG. 3.16: Suboptimal Realization of the Negative Gain Amplifier with $f_1 < 0$, $F_{22} = 0$, $f_2 > 0$ and $F_{12} < 0$

$$F = \frac{1}{(1+\mu_0)^2} \tag{3.77}$$

3.7.2 Negative Gain Amplifiers with $F_{22} \geq 0$

Let

$$f_1 = -\alpha \text{ and } F_{22} = \beta \tag{3.78}$$

Then,

$$F_{11} = -(\beta + \frac{\alpha}{\mu_0}) \tag{3.79}$$

The condition (2) of (3.10) implies that there are only two possible cases when $F_{22} \geq 0$ and they are

(a) $f_2 < 0$ and $F_{12} > 0$

(b) $f_2 > 0$ and $F_{12} < 0$

Case V: $f_1 < 0$, $F_{22} \geq 0$, $f_2 < 0$ and $F_{12} > 0$:

Let $F_{12} = \gamma$ and $f_2 = -\delta$. Then the 'f' and 'F' constants are as given below:

$$\left.\begin{aligned} f_1 &= -\alpha \,, \quad F_{11} = -(\beta + \frac{\alpha}{\mu_0}) \,, \quad F_{12} = \gamma \\ f_2 &= -\delta \,, \quad F_{21} = -(\frac{\delta}{\mu_0} + \frac{\beta^2}{\gamma}) \,, \quad F_{22} = \beta \end{aligned}\right\} \tag{3.80}$$

and

$$F = \frac{(\gamma\delta - \alpha\beta)}{\mu_0} \tag{3.81}$$

The realizability conditions are as follows:

$$\left.\begin{aligned} &\text{(i)}\ 0 \leq \alpha, \gamma, \delta \leq 1\ , \quad \text{(ii)}\ 0 \leq \beta \leq 1 \\ &\text{(iii)}\ \gamma\delta > \alpha\beta\ , \quad \text{(iv)}\ \delta \leq \frac{(1-\frac{\beta^2}{\gamma})}{(1+\frac{1}{\mu_0})} \end{aligned}\right\} \quad (3.82)$$

and

$$\text{(v)}\ \alpha \leq \frac{(1-\beta)}{(1+\frac{1}{\mu_0})}$$

Two possible topological structures are shown in Fig. 3.17. The sub-optimal realization is obtained by choosing $\beta = 0$. This realization has already been obtained in case III.

Case VI: $f_1 < 0$, $F_{22} \geq 0$, $f_2 > 0$ and $F_{12} < 0$:

Let $F_{12} = -\gamma$ and $f_2 = \delta$. Then 'f' and 'F' constants can be obtained, which are given below:

$$\left.\begin{aligned} &f_1 = -\alpha\ , \quad F_{11} = -(\beta + \frac{\alpha}{\mu_0})\ , \quad F_{12} = -\gamma \\ &f_2 = \delta\ , \quad F_{21} = \frac{\delta}{\mu_0} + \frac{\beta^2}{\gamma}\ , \quad F_{22} = \beta \end{aligned}\right\} \quad (3.83)$$

and

$$F = \frac{(\gamma\delta - \alpha\beta)}{\mu_0} \quad (3.84)$$

The realizability conditions are given below:

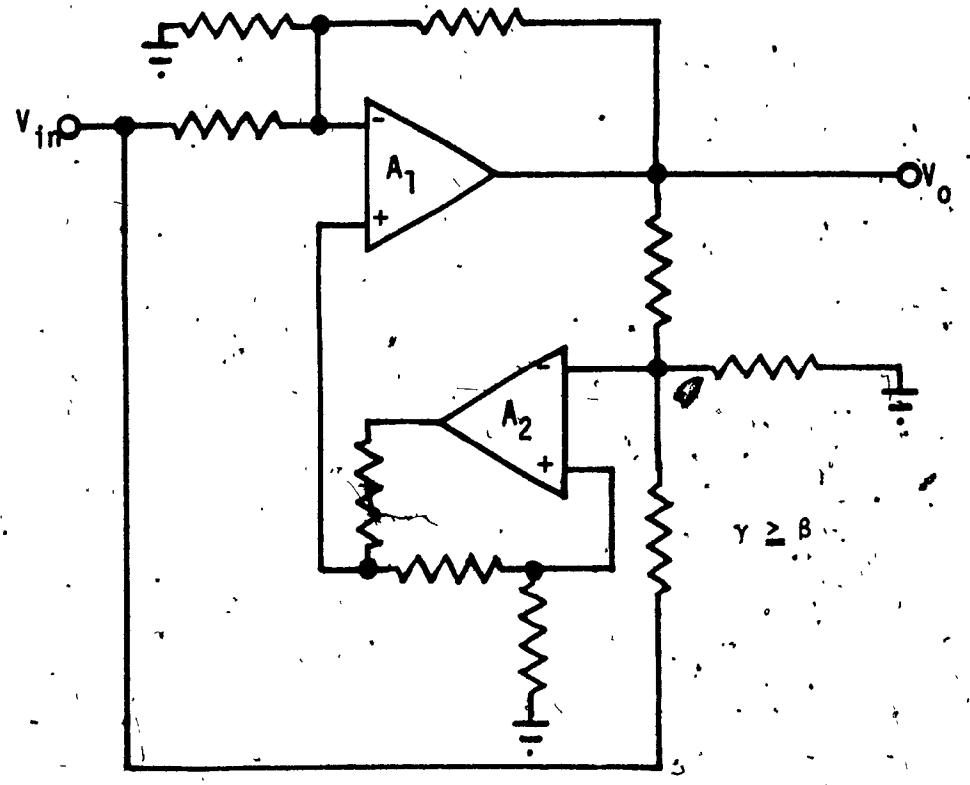

(a)

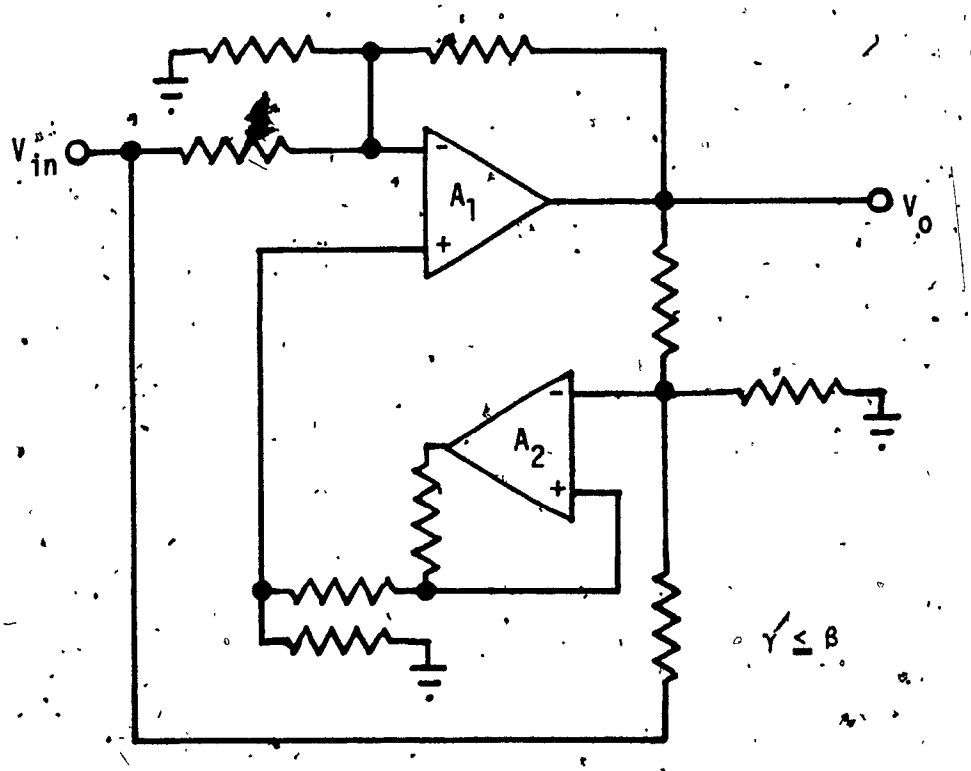

(b)

FIG. 3.17: Topological Structures of the Negative Gain Amplifier with $f_1<0$, $F_{22}\geq 0$, $f_2<0$ and $F_{12}>0$

$$\left.\begin{aligned} &\text{(i)}\ \ 0 < \alpha, \gamma, \delta \leq 1\ , \qquad \text{(ii)}\ \ 0 \leq \beta \leq 1 \\ &\text{(iii)}\ \ \gamma\,\delta > \alpha\,\beta\ , \qquad \text{(iv)}\ \ \alpha \leq \frac{(1-\beta-\gamma)\mu_0}{(1+\mu_0)} \end{aligned}\right\} \tag{3.85}$$

and

$$\text{(v)}\ \ \delta \leq \frac{\{1-\beta(1+\frac{\beta}{\gamma})\}\mu_0}{(1+\mu_0)}$$

The only possible topological structure to realize (3.83) is shown in Fig. 3.18. The suboptimal realization reduces to the one given in case IV.

3.7.3 Negative Gain Amplifiers with $F_{22} \leq 0$

Let us start with the following:

$$f_1 = -\alpha\ , \quad F_{22} = -\beta \tag{3.86}$$

Using (3.86) and the relation (5) of (3.10), it follows:

$$F_{11} = (\beta - \frac{\alpha}{\mu_0}) \tag{3.87}$$

For arbitrary choices of α and β, the equation (3.87) implies two possibilities.

$$\left.\begin{aligned} &\text{(a)}\ \ \beta \leq \frac{\alpha}{\mu_0}\ \ (F_{11} \leq 0) \\ &\text{(b)}\ \ \beta \geq \frac{\alpha}{\mu_0}\ \ (F_{11} \geq 0) \end{aligned}\right\} \tag{3.88}$$

The inequality (2) of (3.10) implies that

$$f_2\, F_{12} < \alpha\,\beta \tag{3.89}$$

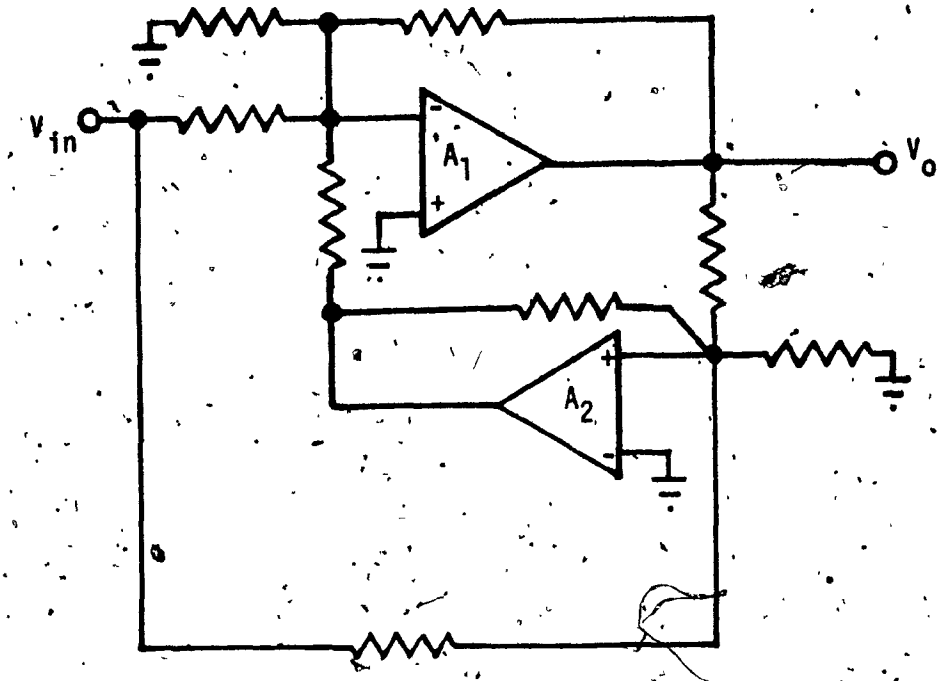

FIG. 3.18: Topological Structure of the Negative Gain Amplifier with $f_1<0$, $F_{22}\geq 0$, $f_2>0$ and $F_{12}<0$

The choices for f_2 and F_{12} can be made in the following four possible ways to satisfy (3.89).

(i) $f_2 \geq 0$, $F_{12} \geq 0$ but $f_2 F_{12} < \alpha\beta$

(ii) $f_2 \leq 0$, $F_{12} \leq 0$ but $f_2 F_{12} < \alpha\beta$

(iii) $f_2 \leq 0$ and $F_{12} \geq 0$

(iv) $f_2 \geq 0$ and $F_{12} \leq 0$

Thus it turns out that there are eight different cases that we have to consider. Whatever might be the choice for α, β , f_2 and F_{12} , one gets the following equations:

$$F = \frac{(\alpha\beta - f_2 F_{12})}{\mu_0} \qquad (3.90)$$

and

$$F_{21} = \frac{f_2}{\mu_0} - \frac{\beta^2}{F_{12}} \qquad (3.91)$$

Since the 'f' and 'F' constants are finite, the equation (3.91) suggests that neither F_{12} nor F_{21} can be made zero. Thus, from (3.90), when both f_2 and F_{12} are of the same sign, it is only possible to make f_2 equal to zero for maximizing F. Let us now examine the eight different cases in detail.

Case VII: $f_1 < 0$, $F_{22} \leq 0$, $F_{11} \leq 0$, $f_2 \geq 0$, $F_{12} > 0$.

Let $F_{12} = \delta$ and $f_2 = \gamma$. Then the quantities 'f' and 'F' are as follows:

$$\left.\begin{aligned} f_1 &= -\alpha \ , \quad F_{11} = -\left(\frac{\alpha}{\mu_0} - \beta\right) \ , \quad F_{12} = \delta \\ f_2 &= \gamma \ , \quad F_{21} = -\left(\frac{\beta^2}{\delta} - \frac{\gamma}{\mu_0}\right) \ , \quad F_{22} = -\beta \end{aligned}\right\} \quad (3.92)$$

and

$$F = \frac{(\alpha\beta - \gamma\delta)}{\mu_0}$$

Since $\beta \leq \frac{\alpha}{\mu_0}$ and $\alpha\beta > \gamma\delta$, these two conditions imply that $F_{21} < 0$. Then, the realizability conditions follow immediately:

$$\left.\begin{aligned} &\text{(i)} \quad 0 < \alpha, \delta \leq 1 \ , \qquad \text{(ii)} \quad 0 \leq \beta, \gamma \leq 1 \\ &\text{(iii)} \quad \alpha \geq \mu_0 \beta \ , \qquad \text{(iv)} \quad \alpha\beta > \gamma\delta \\ &\text{(v)} \quad \alpha \leq \frac{(1+\beta)\mu_0}{(1+\mu_0)} \quad \text{and} \quad \text{(vi)} \quad \gamma \geq \mu_0 \left\{\beta + \frac{\beta^2}{\delta} - 1\right\} \end{aligned}\right\} \quad (3.93)$$

Two possible topological structures are shown in Fig. 3.19 to realize (3.92). The suboptimal realization is obtained with $\gamma = 0$ and this realization is shown in Fig. 3.20. It is worth noting that this realization reduces to the high input impedance realization (Case I) when $\mu_0 = (\sqrt{5}+1)/2$. The quantity F is given by

$$F = \frac{1}{(1+\mu_0)} \quad (3.94)$$

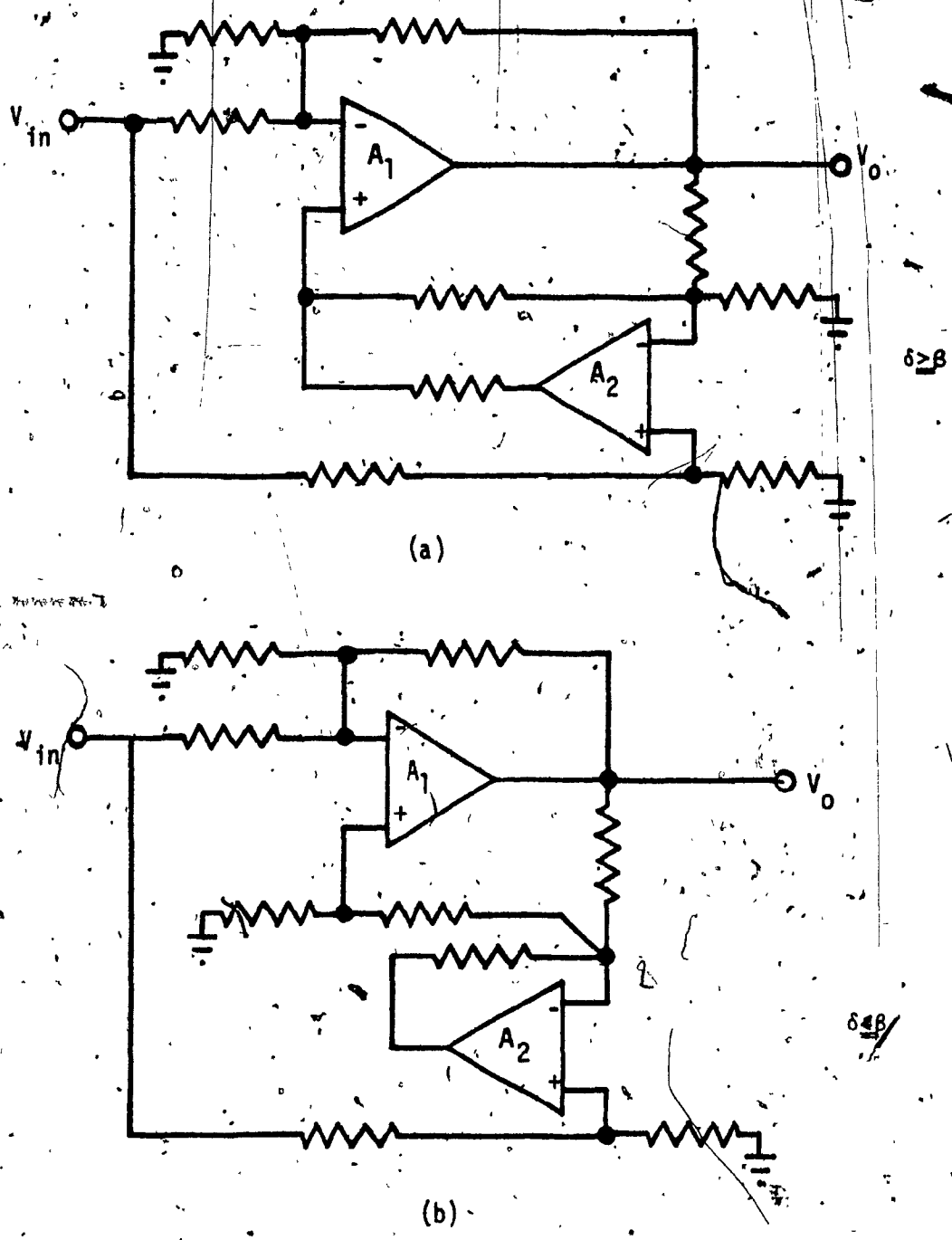

FIG. 3.19: Topological Structures of the Negative Gain Amplifier with $f_1<0$, $F_{22}\leq 0$, $F_{11}\leq 0$, $f_2\geq 0$ and $F_{12}>0$

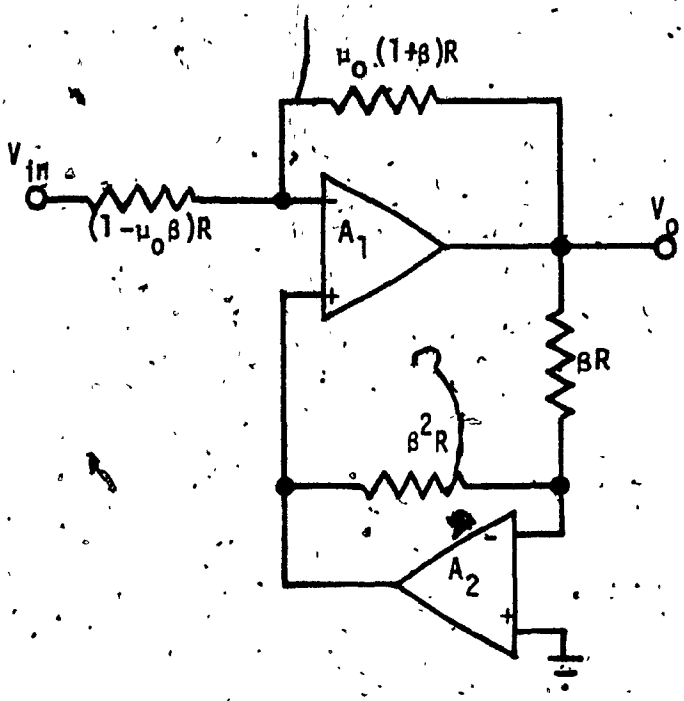

$\beta = (\sqrt{5}-1)/2$

$\mu_o \leq (\sqrt{5}+1)/2$

FIG. 3.20: Suboptimal Realization of the Negative Gain Amplifier with $f_1<0$, $F_{22}\leq 0$, $F_{11}\leq 0$, $f_2\geq 0$ and $F_{12}>0$

Case VIII: $f_1 < 0$, $F_{22} \leq 0$, $F_{11} \leq 0$, $f_2 \leq 0$ and $F_{12} < 0$.

Let $F_{12} = -\delta$ and $f_2 = -\gamma$. Then the 'f' and 'F' constants are obtained as given below:

$$\left.\begin{aligned} f_1 &= -\alpha \ , \quad F_{11} = -\left(\frac{\alpha}{\mu_0} - \beta\right) \ , \quad F_{12} = -\delta \\ f_2 &= -\gamma \ , \quad F_{21} = \frac{\beta^2}{\delta} + \frac{\gamma}{\mu_0} \ , \quad F_{22} = -\beta \end{aligned}\right\} \quad (3.95)$$

and

$$F = \frac{(\alpha\beta - \gamma\delta)}{\mu_0} \quad (3.96)$$

It can be shown that $F_{21} \geq 0$. The realizability conditions follow now.

(i) $0 < \alpha, \delta \leq 1$, (ii) $0 \leq \beta \leq 1$,

(iii) $\beta \leq \left(\frac{\alpha}{\mu_0}\right)$, (iv) $\alpha\beta > \gamma\delta$

(v) $\alpha \leq \frac{\mu_0(1+\beta-\delta)}{(1+\mu_0)}$, (vi) $1 \geq \delta \geq \frac{\beta^2}{(1+\frac{\gamma}{\mu_0})}$

and

(vii) $\beta \leq (1-\gamma)$.

Two possible topological structures are shown in Fig. 21. The sub-optimal realization in this case turns out to be with $f_2 = 0$. The quantity 'F' is given by the following:

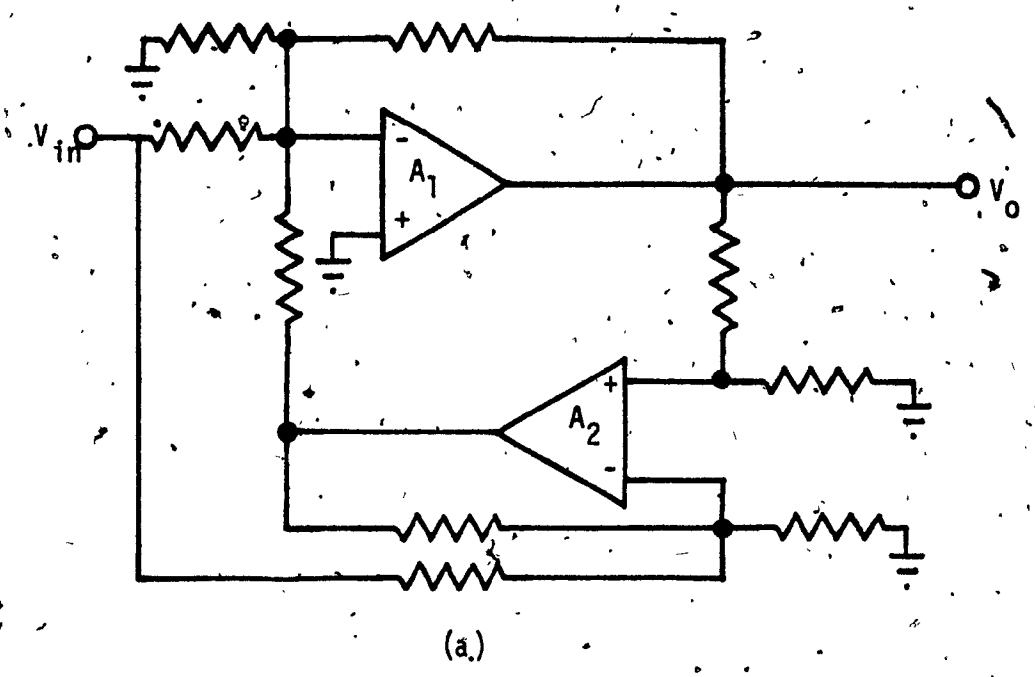

(a)

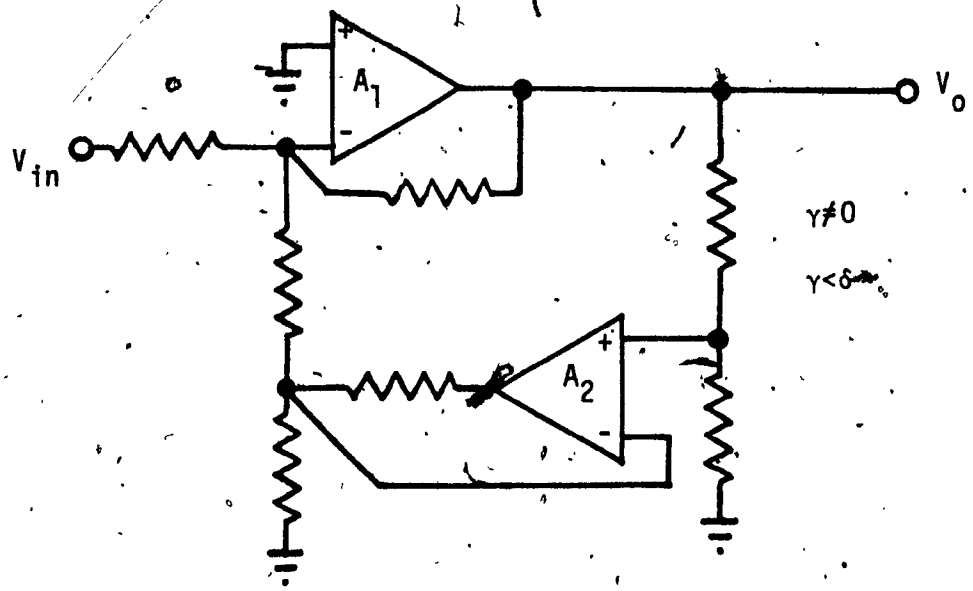

(b)

FIG. 3.21.: Topological Structures of the Negative Gain Amplifier with $f_1<0$, $F_{22}\leq 0$, $F_{11}\leq 0$, $f_2\leq 0$ and $F_{12}<0$

$$F = \beta^2 \tag{3.97}$$

where

$$\beta = \sqrt{\left(\frac{\mu_0}{2}\right)^2 + 1} - \left(\frac{\mu_0}{2}\right)$$

The suboptimal realization is shown in Fig. 3.22. Two more realizations of negative gain amplifiers, which can be derived from Fig. 3.21(b), are shown in Fig. 3.23. These networks of inverting amplifiers were originally suggested by this author and Bhattacharyya [33]. The quantity 'F' for the circuit shown in Fig. 3.23(a) is given by

$$F = \frac{(\mu_0+1)}{\{(\mu_0+1)^2-\mu_0\}} \tag{3.98}$$

and for the circuit shown in Fig. 3.23(b), F is given by

$$F = \frac{1}{(\mu_0^2 + \mu_0+1)} \tag{3.99}$$

Case IX: $f_1 < 0$, $F_{22} \leq 0$, $F_{11} \leq 0$, $f_2 \leq 0$ and $F_{12} > 0$.

Let $F_{12} = \delta$ and $f_2 = -\gamma$. Then the 'f' and 'F' constants can be obtained as given below:

$$\left.\begin{aligned} f_1 &= -\alpha\,, \quad F_{11} = -\left(\frac{\alpha}{\mu_0} - \beta\right)\,, \quad F_{12} = \delta \\ f_2 &= -\gamma\,, \quad F_{21} = \left(\frac{\beta^2}{\delta} + \frac{\gamma}{\mu_0}\right)\,, \quad F_{22} = -\beta \end{aligned}\right\} \tag{3.100}$$

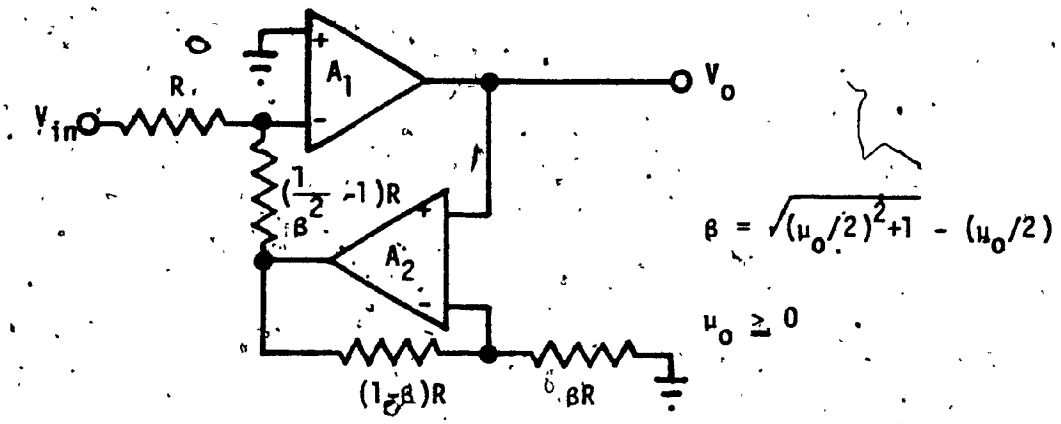

FIG. 3.22: Suboptimal Realization of the Negative Gain Amplifier - with $f_1<0$, $F_{22}\leq 0$, $F_{11}\leq 0$, $f_2\leq 0$ and $F_{12}<0$

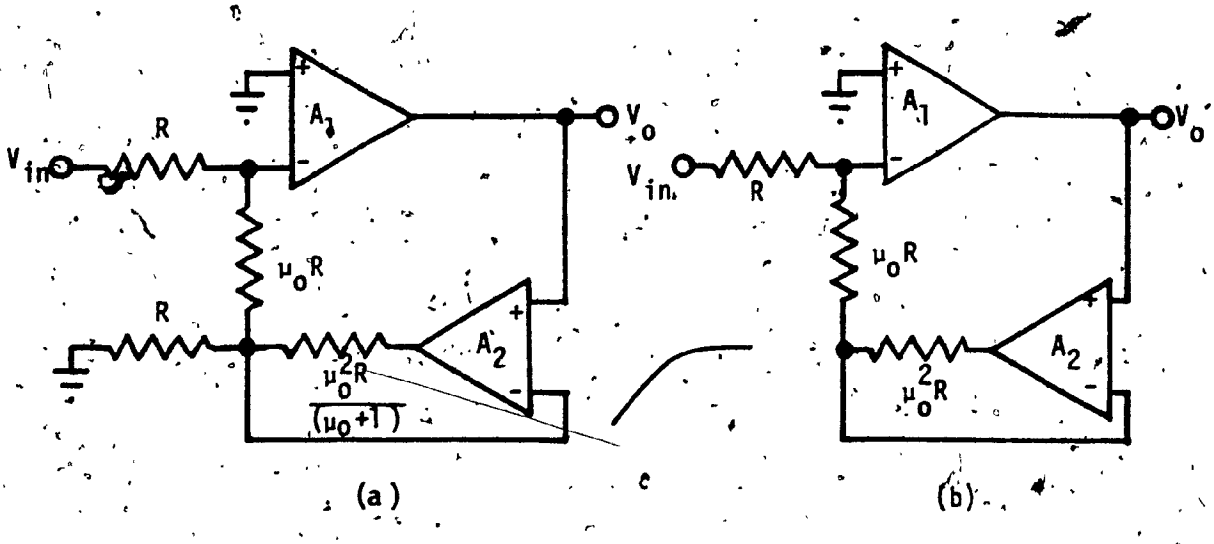

FIG. 3.23: Negative Gain Amplifiers Derived from Fig. 3.21(b)

and

$$F = \frac{(\alpha\beta + \gamma\delta)}{\mu_0} \tag{3.101'}$$

The realizability conditions are as follows:

$$\left.\begin{aligned} &\text{(i)}\ \ 0 < \alpha, \delta \leq 1\ , \qquad \text{(ii)}\ \ 0 \leq \beta, \gamma \leq 1 \\ &\text{(iii)}\ \ \beta \leq \left(\frac{\alpha}{\mu_0}\right)\ , \qquad \text{(iv)}\ \ \alpha \leq \frac{\mu_0(1+\beta)}{(1+\mu_0)} \end{aligned}\right\} \tag{3.102}$$

and

$$\text{(v)}\ \ \gamma \leq \frac{\mu_0(1-\beta-\beta^2)}{(1+\mu_0)}$$

Two possible topological structures are shown in Fig. 3.24. The sub-optimal realization is shown in Fig. 3.25 and the quantity 'F' for this realization is given by

$$F = \frac{1}{(1+\mu_0)} \tag{3.103}$$

and the realizability condition is given below:

$$\mu_0 \geq \frac{(\sqrt{5}+1)}{2} \tag{3.104}$$

Let us now consider the last case corresponding to the condition (a) of (3.88).

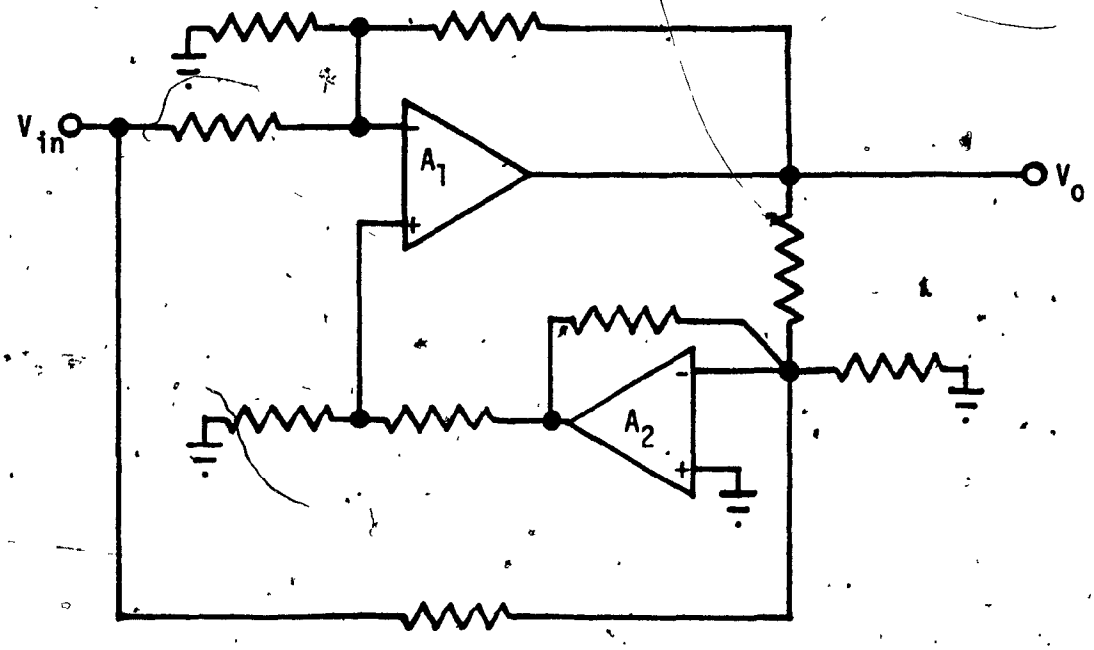

(a)

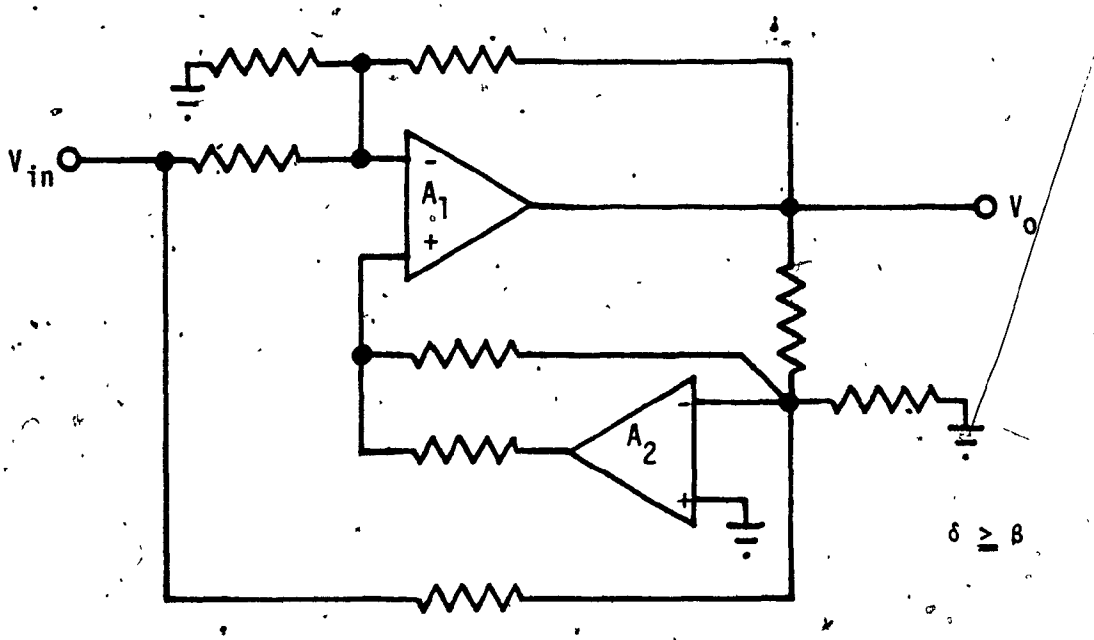

(b)

FIG. 3.24: Topological Structures of the Negative Gain Amplifier with $f_1<0$, $F_{22}\leq 0$, $F_{11}\leq 0$, $f_2\leq 0$ and $F_{12}>0$

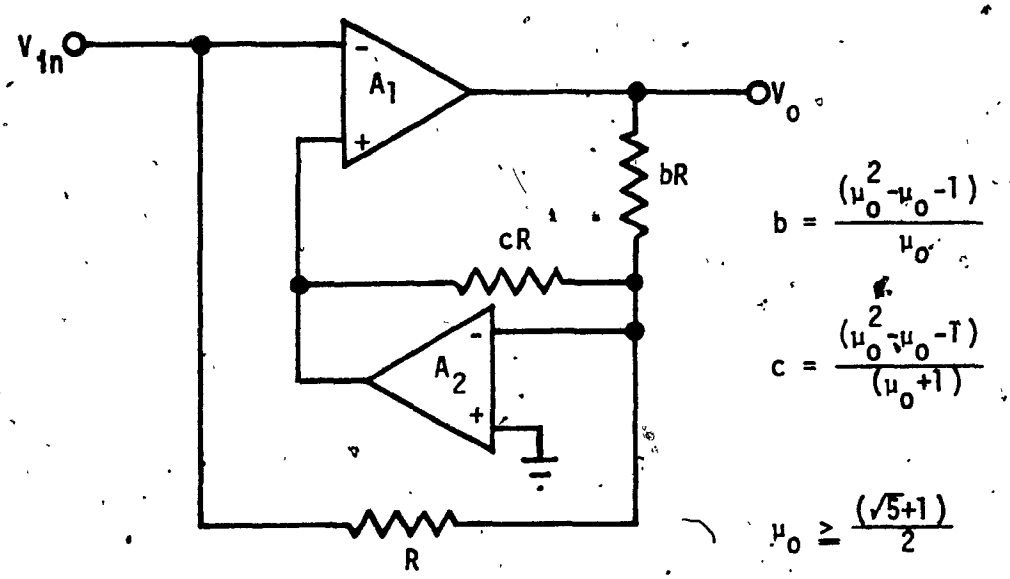

FIG. 3.25: Suboptimal Realization of the Negative Gain Amplifier with $f_1<0$, $F_{22}\leq 0$, $F_{11}\leq 0$, $f_2\leq 0$ and $F_{12}>0$

Case X: $f_1 < 0$, $F_{22} \leq 0$, $F_{11} \leq 0$, $f_2 \geq 0$ and $F_{12} < 0$.

Let $F_{12} = -\delta$ and $f_2 = \gamma$. Then the different 'f' and 'F' quantities are as follows:

$$\left.\begin{aligned} f_1 &= -\alpha \ , \quad F_{11} = -\left(\frac{\alpha}{\mu_0} - \beta\right) \ , \quad F_{12} = -\delta \\ f_2 &= \gamma \ , \quad F_{21} = \left(\frac{\gamma}{\mu_0} + \frac{\beta^2}{\delta}\right) \ , \quad F_{22} = -\beta \end{aligned}\right\} \quad (3.105)$$

and

$$F = \frac{(\alpha\beta + \gamma\delta)}{\mu_0} \quad (3.106)$$

The realizability conditions are given below:

$$\left.\begin{aligned} &\text{(i)} \ \ 0 < \alpha, \delta \leq 1 \ , \qquad \text{(ii)} \ \ 0 \leq \beta, \gamma \leq 1 \\ &\text{(iii)} \ \ \beta \leq \left(\frac{\alpha}{\mu_0}\right) \ , \qquad \text{(iv)} \ \ \alpha \leq \frac{\mu_0(1-\delta+\beta)}{(\mu_0 + 1)} \\ &\text{and} \\ &\text{(v)} \ \ \gamma \leq \frac{\mu_0(\delta-\beta^2)}{\delta(\mu_0+1)} \end{aligned}\right\} \quad (3.107)$$

Two possible topological structures are shown in Fig. 3.26. The amplifier networks shown in Fig. 3.23 can also be derived from Fig. 3.26(b). To obtain the suboptimal realization, from (3.106), it is obvious that F is maximum when γ and δ are maximum. Hence, choosing the upper bound for γ and δ (which are in terms of α, β and μ_0) using (v) and (iv) of (3.107) and substituting them in (3.106), the quantity 'F'

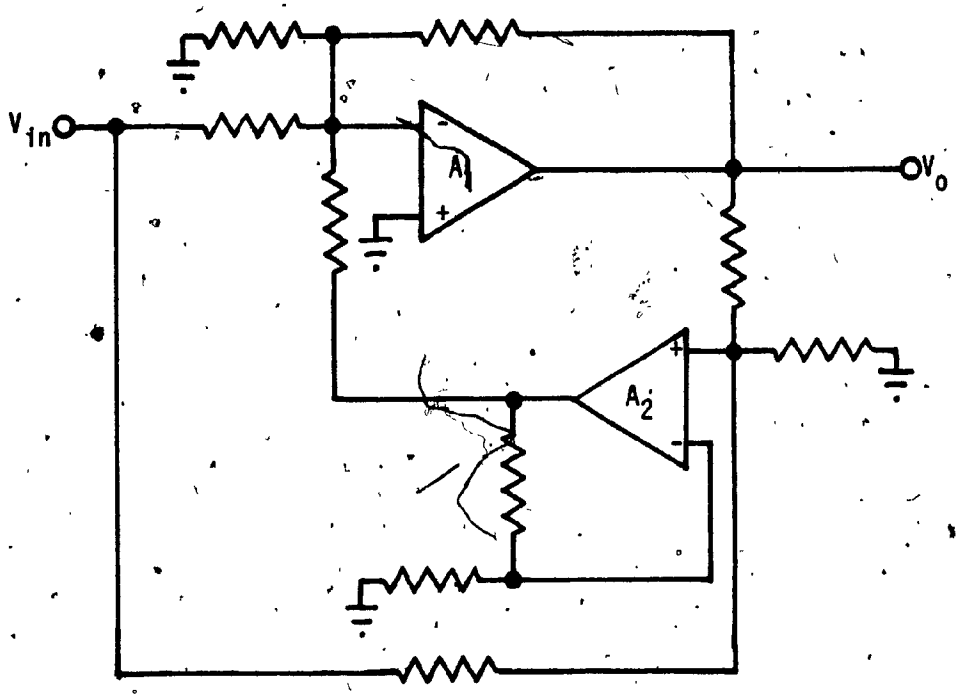

(a)

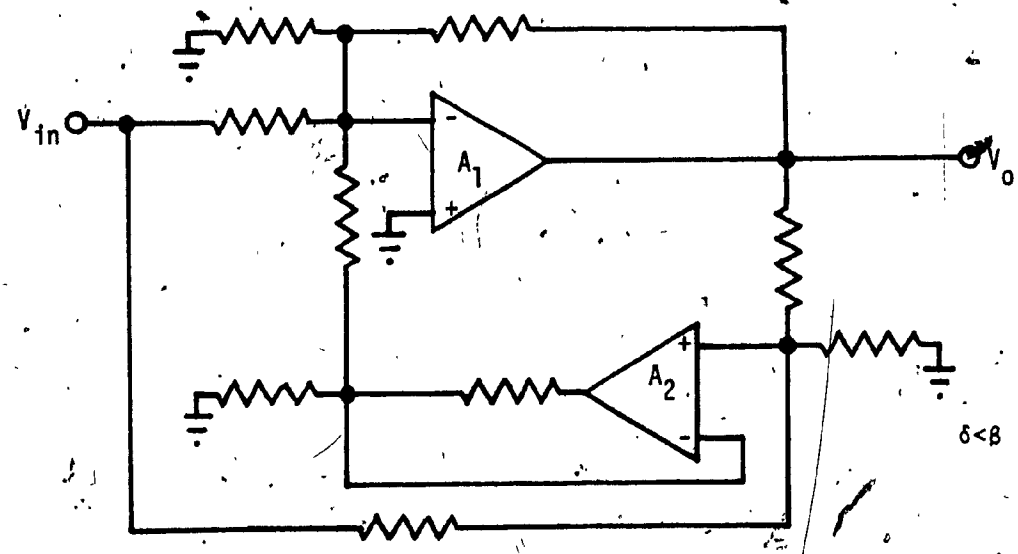

(b)

FIG. 3.26: Topological Structures of the Negative Gain Amplifiers with $f_1<0$, $F_{22}\leq 0$, $F_{11}\leq 0$, $f_2\geq 0$ and $F_{12}<0$

becomes

$$F = (1-\beta)\left(\frac{\beta}{1+\mu_0} - \frac{\alpha}{\mu_0}\right)$$

Now F is maximum for $\alpha = 0$. This condition contradicts (i) of (3.107), which requires $\alpha > 0$. Also, the amplifier circuit becomes unstable with $\alpha = 0$. Choosing the minimum bound for α from (iii) of (3.107), it can be shown that F becomes negative for $\mu_0 > 0$, again leading to an unstable mode. In order that F be positive, it is required that

$$\frac{\beta}{(\mu_0+1)} > \frac{\alpha}{\mu_0}$$

Using the above and (iii) of (3.107), it can be shown that $\alpha < 0$, contradicting again (i) of (3.107). Thus, there is no suboptimal realization, which will meet the conditions $f_2 > 0$ and $F_{12} < 0$. Hence, we start again with $f_2 = 0$. The suboptimal realization is obtained with $F_{11} = 0$ and is the same as shown in Fig. 3.22.

Let us now consider the cases when $F_{11} \geq 0$.

Case XI: $f_1 < 0$, $F_{22} \leq 0$, $F_{11} \geq 0$, $f_2 \geq 0$ and $F_{12} > 0$:

Let $F_{12} = \delta$ and $f_2 = \gamma$. Then the 'f' and 'F' constants are as given below:

$$\left.\begin{aligned} f_1 &= -\alpha, \quad F_{11} = \beta - \frac{\alpha}{\mu_0}, \quad F_{12} = \delta \\ f_2 &= \gamma, \quad F_{21} = \left(\frac{\gamma}{\mu_0} - \frac{\beta^2}{\delta}\right), \quad F_{22} = -\beta \end{aligned}\right\} \quad (3.108)$$

and

$$F = \frac{(\alpha\beta - \gamma\delta)}{\mu_0} \tag{3.109}$$

It can be shown that $F_{21} < 0$. Thus, the realizability conditions are obtained as given below:

$$\left.\begin{array}{ll} \text{(i)}\ \ 0 < \alpha, \delta \leq 1\,, & \text{(ii)}\ \ 0 \leq \beta, \gamma \leq 1 \\ \text{(iii)}\ \ \beta \geq \frac{\alpha}{\mu_0}\,, & \text{(iv)}\ \ \beta \leq 1 - \delta + \frac{\alpha}{\mu_0} \\ \text{(v)}\ \ \beta \leq \frac{(1+\frac{\gamma}{\mu_0})}{(1+\frac{\beta}{\delta})} \text{ and} & \text{(vi)}\ \ \alpha\beta > \gamma\delta \end{array}\right\} \tag{3.110}$$

The topological structure realizing (3.108) is shown in Fig. 3.27. The suboptimal realization is obtained with $\gamma = 0$ and $\alpha = 1$. Under such conditions, the various 'f' and 'F' constants given by (3.108) are the same as those of (3.50) except for symbol changes. Thus, the suboptimal realization in this case, turns out to be the one given in case I.

Case XII: $f_1 < 0$, $F_{22} \leq 0$, $F_{11} \geq 0$, $f_2 \leq 0$ and $F_{12} < 0$.

Let $F_{12} = -\delta$ and $f_2 = -\gamma$. Then, the following equation gives the 'f' and 'F' constants.

$$\left.\begin{array}{lll} f_1 = -\alpha\,, & F_{11} = \beta - \frac{\alpha}{\mu_0}\,, & F_{12} = -\delta \\ f_2 = -\gamma\,, & F_{21} = \frac{\beta^2}{\delta} - \frac{\gamma}{\mu_0}\,, & F_{22} = -\beta \end{array}\right\} \tag{3.111}$$

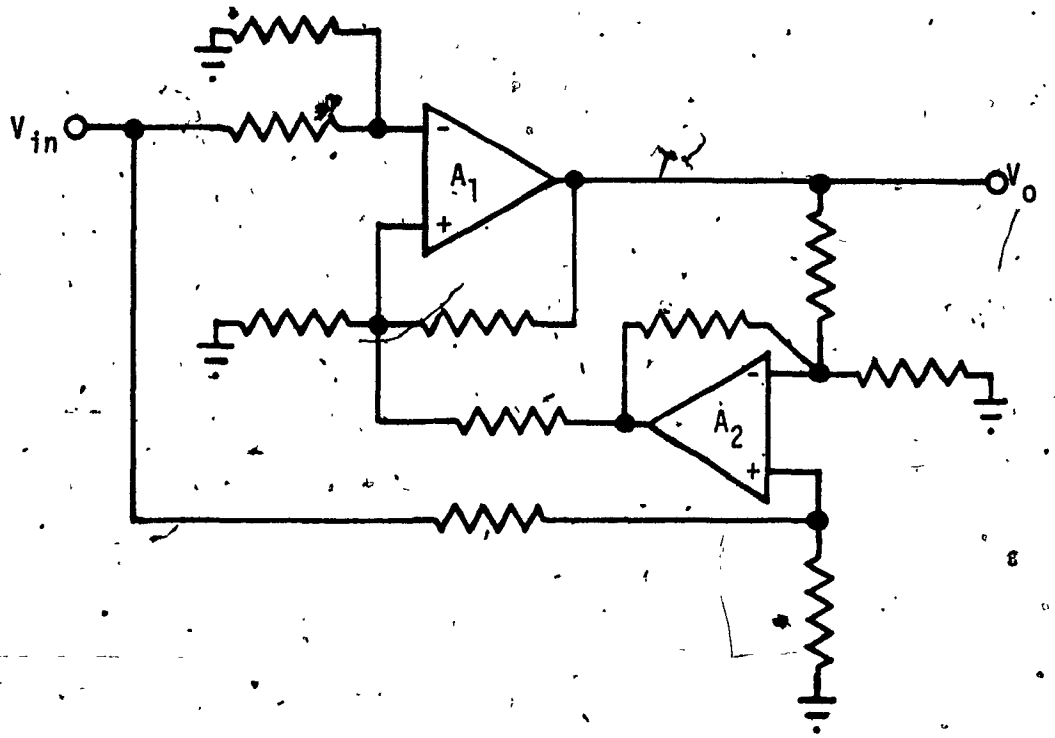

FIG. 3.27: Topological Structure of the Negative Gain Amplifier with $f_1<0$, $F_{22}\leq 0$, $F_{11}\geq 0$, $f_2\geq 0$ and $F_{12}>0$

and

$$F = \frac{(\alpha\beta - \gamma\delta)}{\mu_0} \tag{3.112}$$

It can be shown that $F_{21} > 0$. Then the realizability conditions are given below:

$$\left.\begin{array}{ll} \text{(i)}\ 0 < \alpha, \delta \leq 1\ , & \text{(ii)}\ 0 \leq \beta, \gamma \leq 1\ , \\ \text{(iii)}\ \beta \geq \left(\frac{\alpha}{\mu_0}\right)\ , & \text{(iv)}\ \alpha+\delta \leq 1 \\ \text{(v)}\ 0 \leq \left(\beta - \frac{\alpha}{\mu_0}\right) \leq 1\ , & \text{(vi)}\ \gamma+\beta \leq 1 \\ \text{(vii)}\ \beta^2 \leq \delta\left(1+\frac{\gamma}{\mu_0}\right) \text{ and } & \text{(viii)}\ \alpha\beta > \gamma\delta \end{array}\right\} \tag{3.113}$$

Two possible topological structures are shown in Fig. 3.28 to realize (3.111). The suboptimal realization is obtained with $\gamma = 0$, $\delta = \beta^2$ and $\beta^2 \leq (1-\alpha)$. But according to (iii) of (3.113) $\beta^2 \geq (\alpha^2/\mu_0^2)$. Thus, the value of α is restricted by

$$\alpha \leq \frac{\mu_0^2}{2}\left[\left(1+\frac{4}{\mu_0^2}\right)^{\frac{1}{2}} - 1\right].$$

F reaches its maximum value when α is maximum. Thus, α and β can be chosen as follows:

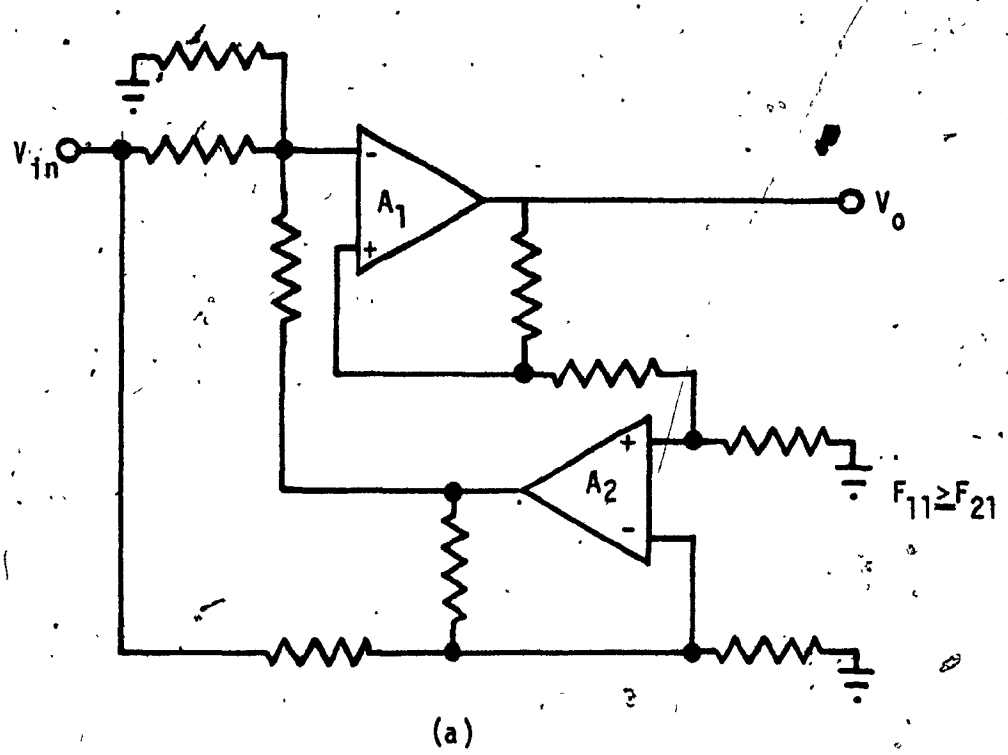

(a)

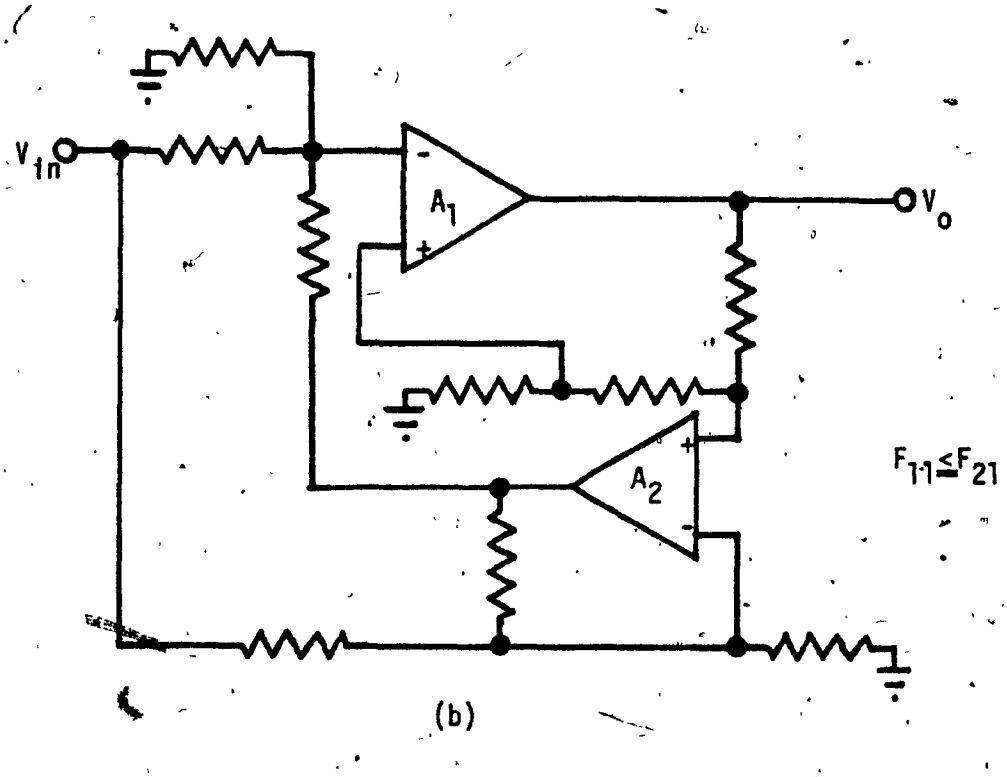

(b)

FIG. 3.28: Topological Structures of the Negative Gain Amplifier with $f_1<0$, $F_{22}\leq 0$, $F_{11}\geq 0$, $f_2\leq 0$ and $F_{12}<0$

$$\left.\begin{aligned} \alpha &= \frac{\mu_0^2}{2}\left[\left(1+\frac{4}{\mu_0^2}\right)^{\frac{1}{2}}-1\right] \\ \text{and} \\ \beta &= \frac{\alpha}{\mu_0} \end{aligned}\right\} \quad (3.114)$$

This case has already been dealt with in case VIII.

Case XIII: $f_1 < 0$, $F_{22} \leq 0$, $F_{11} \geq 0$, $f_2 \leq 0$ and $F_{12} > 0$.

With F_{12} and f_2 chosen as given below

$$F_{12} = \delta \quad \text{and} \quad f_2 = \gamma$$

one gets the various 'f' and 'F' constants as follows:

$$\left.\begin{aligned} f_1 &= -\alpha\,, \quad F_{11} = \beta - \frac{\alpha}{\mu_0}\,, \quad F_{12} = \delta \\ f_2 &= -\gamma\,, \quad F_{21} = -\left(\frac{\beta^2}{\delta} + \frac{\gamma}{\mu_0}\right)\,, \quad F_{22} = -\beta \end{aligned}\right\} \quad (3.115)$$

and

$$F = \frac{(\alpha\beta+\gamma\delta)}{\mu_0} \quad (3.116)$$

The realizability conditions follow immediately.

$$\left.\begin{aligned} &\text{(i)}\ 0 < \alpha, \delta \leq 1\,, \quad \text{(ii)}\ 0 \leq \beta, \gamma \leq 1 \\ &\text{(iii)}\ \gamma \leq \frac{\mu_0(1-\beta-\beta^2/\delta)}{(1+\mu_0)}\,, \quad \text{(iv)}\ \beta \geq \frac{\alpha}{\mu_0} \\ &\text{and} \\ &\text{(v)}\ \delta \leq \left(1+\frac{\alpha}{\mu_0}-\beta\right) \end{aligned}\right\} \quad (3.117)$$

One possible topological structure is shown in Fig. 3.29. The topological structure shown in Fig. 3.24(b) can also realize (3.115), though it was given for $F_{11} \leq 0$. The reason for this is that there are both positive and negative feedbacks in that circuit. Depending upon the relative magnitudes of these feedbacks, F_{11} can either be made positive or negative.

The suboptimal realization can be obtained by assigning maximum values to α, γ and δ. Thus choosing $\alpha = 1$, $\gamma = \{\mu_0(1+\beta-\beta^2/\delta)\}/(1+\mu_0)$ and $\delta = (1+\alpha/\mu_0-\beta)$, restricted by (i), (iii) and (v) of (3.117), F becomes

$$F = \frac{(\mu_0+1 - \mu_0\beta)}{\mu_0(\mu_0+1)}$$

The above is maximum, when $\beta = 0$. However, the value of β is restricted by (i) and (iv) of (3.117). Thus, one has to choose β such that

$$\frac{1}{\mu_0} \leq \beta \leq 1$$

However, F is maximum, when β is minimum. Thus, β can be chosen as $(1/\mu_0)$, in which case $F_{11} = 0$. This case has been dealt in case IX. However, another useful inverting amplifier configuration can be obtained from Fig. 3.24(b). It is shown in Fig. 3.30. In this amplifier, $F_{11} \geq 0$ for $\mu_0 \geq 1$ and $F_{11} < 0$ for $\mu_0 < 1$, when c is infinity. For $c < \infty$, the sign of F_{11} depends on the values of c and μ_0. The quantity 'F' for this amplifier circuit is given by

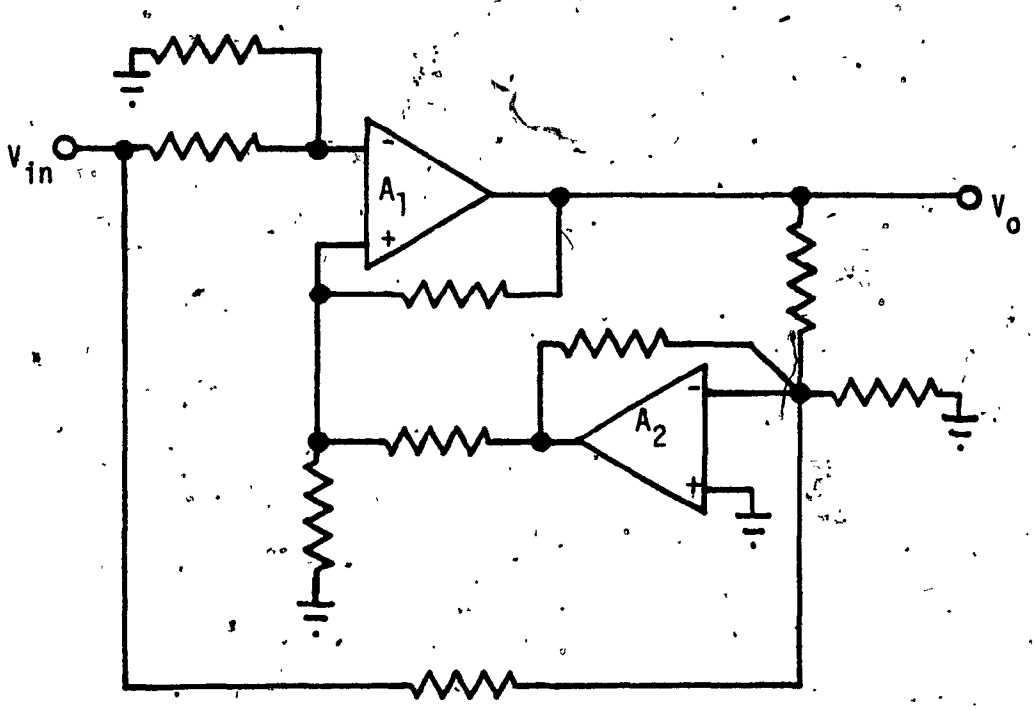

FIG. 3.29: Topological Structure of the Negative Gain Amplifier with $f_1<0$, $F_{22}\leq 0$, $F_{11}\geq 0$, $f_2\leq 0$ and $F_{12}>0$

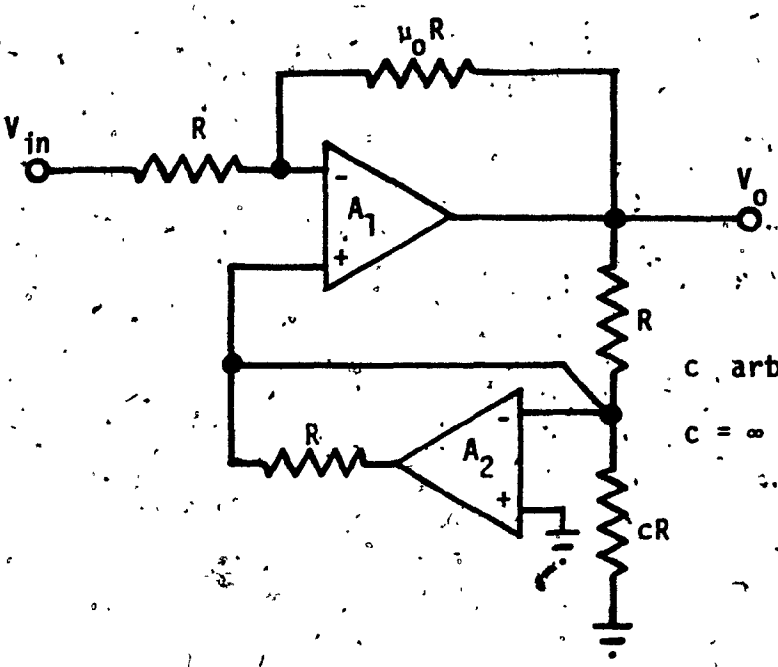

FIG. 3.30: Negative Gain Amplifier with $f_1<0$, $F_{22}\leq 0$, $f_2=0$ and $F_{12}>0$

$$F = \frac{1}{(2+\frac{1}{c})(\mu_0+1)} \tag{3.118}$$

F is maximum when $c = \infty$. Thus, we shall choose this value for future analysis of this circuit.

Case XIV: $f_1 < 0$, $F_{22} \leq 0$, $F_{11} \geq 0$, $f_2 \geq 0$ and $F_{12} < 0$.

Let $F_{12} = -\delta$ and $f_2 = \gamma$. Then the 'f' and 'F' constants can be obtained, which are as follows:

$$\left.\begin{aligned} f_1 &= -\alpha\ , \quad F_{11} = \beta - \frac{\alpha}{\mu_0}\ , \quad F_{12} = -\delta \\ f_2 &= \gamma\ , \quad F_{21} = \frac{\beta^2}{\delta} + \frac{\gamma}{\mu_0}\ , \quad F_{22} = -\beta \end{aligned}\right\} \tag{3.119}$$

and

$$F = \frac{(\alpha\beta + \gamma\delta)}{\mu_0} \tag{3.120}$$

The realizability conditions are given below:

$$\left.\begin{aligned} &\text{(i)}\ \ 0 < \alpha,\ \delta \leq 1\ , \qquad \text{(ii)}\ \ 0 \leq \beta,\ \gamma \leq 1 \\ &\text{(iii)}\ \ \beta \geq \left(\frac{\alpha}{\mu_0}\right)\ , \qquad \text{(iv)}\ \ \gamma \leq \frac{\mu_0(1-\frac{\beta^2}{\delta})}{(\mu_0+1)} \\ &\text{(v)}\ \ \alpha+\delta \leq 1\ , \qquad \text{(vi)}\ \ \beta \leq \left(1+\frac{\alpha}{\mu_0}\right) \end{aligned}\right\} \tag{3.121}$$

Two topological structures that realize (3.119) are suggested in Fig. 3.31. The suboptimal realization is obtained with the following choice for the different parameters:

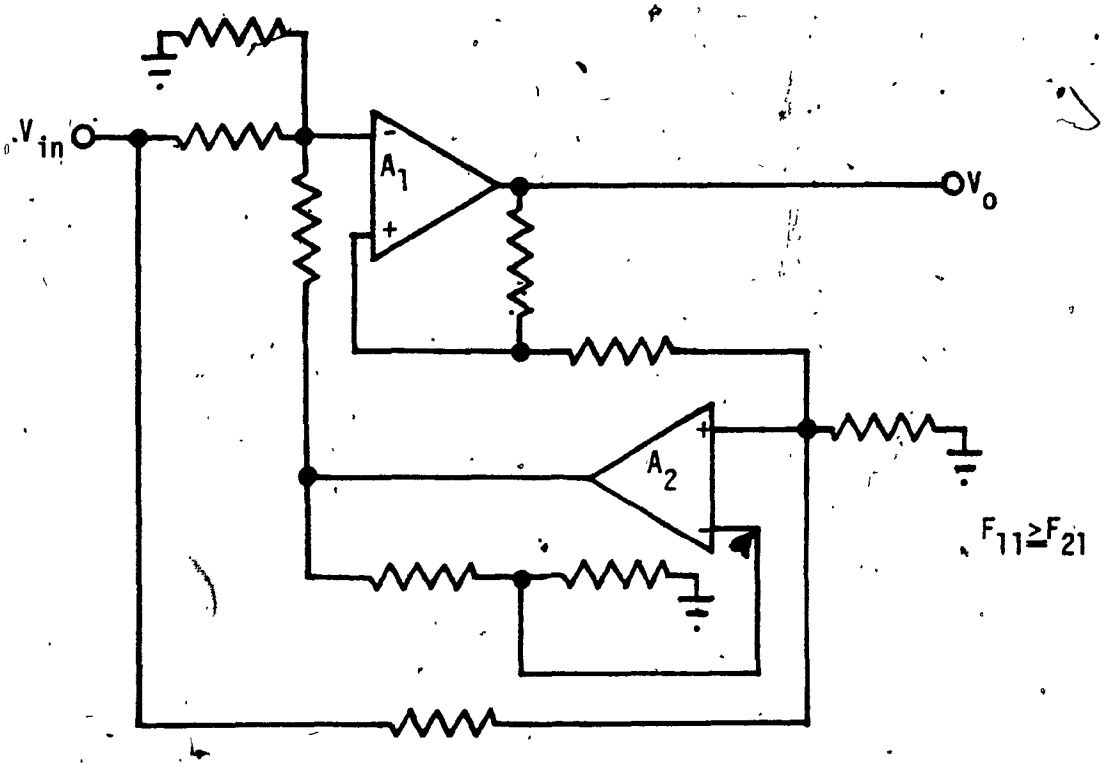

(a)

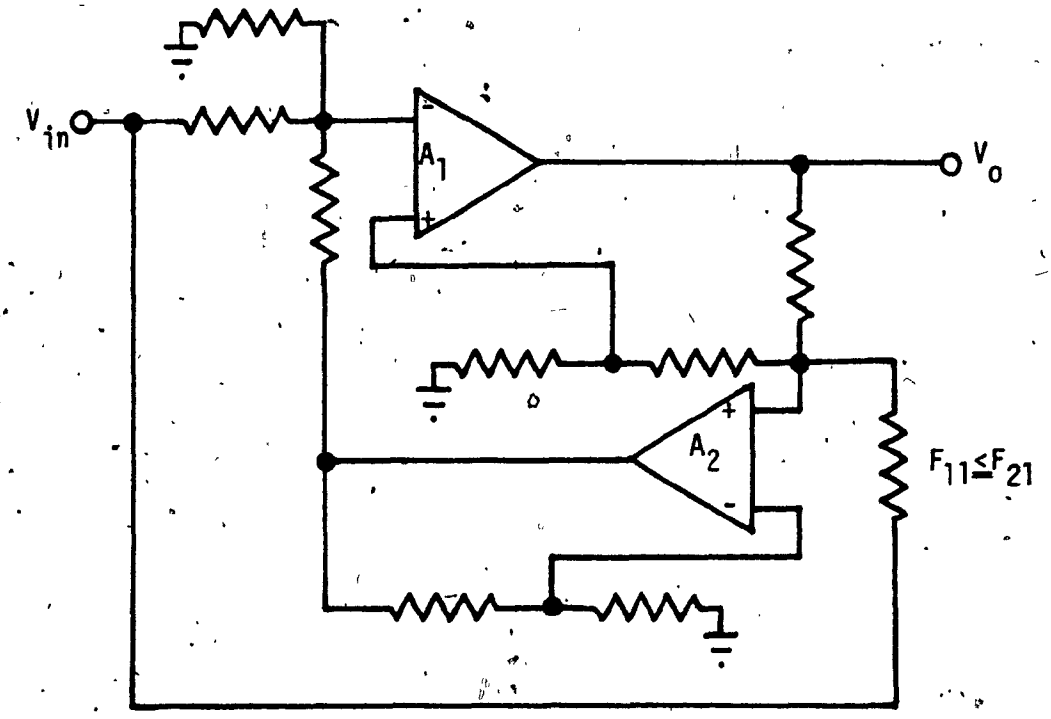

(b)

FIG. 3.31: Topological Structures of the Negative Gain Amplifiers with $f_1<0$, $F_{22}\leq 0$, $F_{11}\geq 0$, $f_2\geq 0$ and $F_{12}<0$

$$\left.\begin{aligned} \alpha &= 2\left(\frac{\mu_0}{\mu_0+1}\right)^2 \left[\left\{1+\left(1+\frac{1}{\mu_0}\right)^2\right\}^{\frac{1}{2}} - 1\right] \\ \beta &= (1-\alpha)^{\frac{1}{2}} \\ \gamma &= 0 \end{aligned}\right\} \quad (3.122)$$

and

$$\delta = (1-\alpha) .$$

The quantity 'F' is given as

$$F = \frac{\alpha\beta}{\mu_0} , \quad (3.123)$$

where α and β are given in (3.122). The suboptimal realization is shown in Fig. 3.32.

Finally, it may be pointed out that there is a degree of arbitrariness present in the realizations of the different cases. This arbitrariness exists at two stages of the realizations. It first appears in the selection process of the 'f' and 'F' constants. This is because, six of these quantities are to be chosen from two equations, while satisfying five inequality constraints. Once a set of 'f' and 'F' constants are chosen, the corresponding topological structure is also not unique; but can be chosen in a number of ways. In fact, the choice is limited by one's own imagination. In all the cases, however, the topological structure corresponding to a particular set of 'f' and 'F' constants has been obtained with an eye to a minimal resistor realization as discussed in Section 3.3.

The suboptimal set of 'f' and 'F' constants, on the other

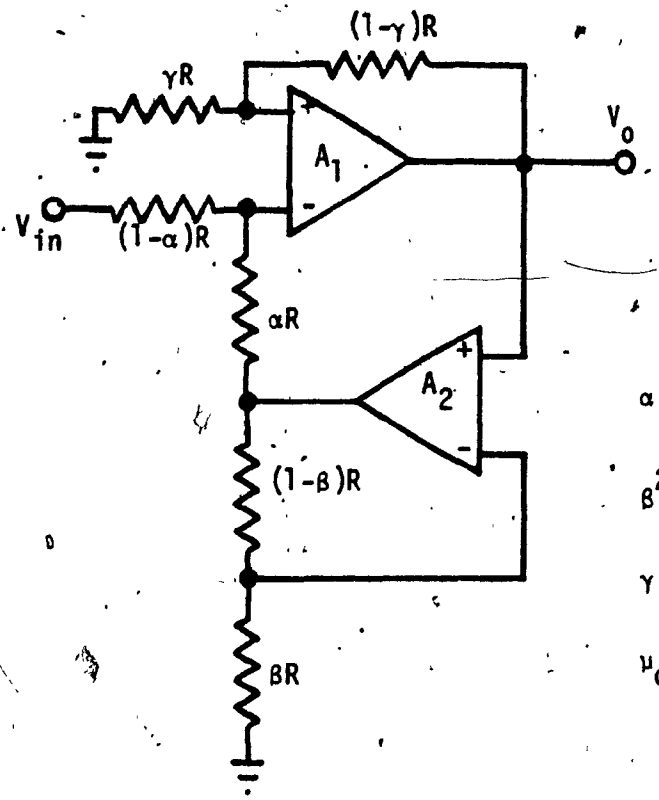

$$\alpha = 2\left(\frac{\mu_0}{\mu_0+1}\right)^2\left[\left\{1+\left(1+\frac{1}{\mu_0}\right)^2\right\}^{\frac{1}{2}}-1\right],$$

$$\beta^2 = 1-\alpha\ ,$$

$$\gamma = \frac{\alpha}{2}\left(1-1/\mu_0\right)\ ,$$

$$\mu_0 \geq 1\ .$$

FIG. 3.32: Suboptimal Realization of the Negative Gain Amplifier with $f_1<0$, $F_{22}\leq 0$, $F_{11}\geq 0$, $f_2\geq 0$ and $F_{12}<0$

hand, corresponding to a given selection of these constants, is unique excepting in two cases, namely, the case I of Section 3.4 and IV of Section 3.7.1. While again, the corresponding circuit implementations of the suboptimal constants in the different cases may not be unique, these realizations are unique if they are derived from a given topological structure.

3.8 A CRITICAL LOOK AT THE SECOND ORDER REALIZATIONS

Now that we have the various second order realizations for the FGA's, let us look for the 'best' circuit for the positive as well as the negative gain amplifiers. Since our aim is to get amplifiers with extended bandwidth operation, obviously the best circuit must be the one having the highest possible bandwidth for a specified deviation in its performance characteristics. However, this bandwidth may not be attainable in practice due to a number of factors. These factors are related to the fact that these amplifiers must be built using practical elements in a given technology. Further, the amplifiers so fabricated are often required to be parts of larger systems such as filters, simulated inductors, oscillators etc. Thus, several other practical aspects of these realizations must also be considered before deciding whether the "apparent" bandwidth based on the theoretical realizations are attainable in a given application. One of them is that the characteristics of the amplifier circuits should be adjustable by trimming some resistors. In addition, when they are used in practical applications, these circuits must have a good relative stability, though all our circuits are stable by themselves. Apart from the above

considerations, there may be a concern (though relatively minor) as to the number of components used in each realization. The maximum bandwidth attainable after satisfying the practical requirements such as the ones discussed above is only of interest. Clearly, a comparison of the different realizations should be thus based on the maximum bandwidth attainable and not on the maximum 'apparent' bandwidth.

A reasonable yardstick, for the purposes of comparison, is determined by the factors given below in the following order of preference:

1. Tunability of the circuits
2. Relative stability
3. Maximum bandwidth, that is, the maximum bandwidth that can be achieved for specified deviations in its performance characteristics.

In order to provide a rationale for such a choice of yardstick, each of the above concepts will now be discussed in some detail.

3.8.1 Tunability

Each of the amplifier circuits has to be designed for a specified d.c. gain of μ_0. When the circuit is built in discrete or IC form, the actual transfer function can be different from the ideally expected transfer function of the form given by (3.6). The performance characteristics of the actual circuit can be different from that of the desired ones in two respects:

(a) The actual d.c. gain may be different from its required nominal value of μ_0.

(b) The success of the improved performance lies in the fact that the first order coefficients of the numerator and denominator polynomials of the transfer function must be equal. However, in the actual circuit they may differ from each other. This difficulty can arise due to two possibilities. (i) the tolerance of the resistors and (ii) the differences in the GB products of the OA's used. The latter one needs an elaboration. In our earlier theoretical development of the amplifier circuits, an assumption was made that all the OA's have the same GB products, equal to B. Though this assumption is a reasonable one, especially when the circuit is made in IC form, it is not valid under all circumstances. The values of GB products of a given type of OA may be close to each other but never equal, particularly when they are built using discrete components. In IC technology, the resistors are not made to exact values. They are, in fact, trimmed to the requirement by using some trimming procedure, such as the one using a laser beam. Obviously, under such circumstances, the difference between the actually realized d.c. gain and the required nominal d.c. gain has to be tuned out to set the performance of the circuit within an allowable tolerance. Similarly, the differences in the first order coefficients of the realized circuit must also be tuned out. Obviously, these two tuning procedures must be independent of each other for ease of control. From the above discussions, it can be appreciated that such an independent tunability of the circuits is an important practical aspect of any realization procedure. Thus, one must look for only such circuits, wherein the d.c. gain and the first order coefficients can be independently controlled.

Among all the suboptimal circuits, there are only a few circuits which possess such a property. These circuits are the ones shown in Figs. 3.4(a), 3.4(b) and 3.7 for positive gain amplifiers and those shown in Figs. 3.11(b), 3.14 and 3.16 for realizing inverting gain amplifiers. If tunability and bandwidth alone are our main concern, we can stop our search within those circuits given above. However, as mentioned earlier, another important practical aspect is their relative stability.

3.8.2 Relative Stability

Since the amplifiers developed previously are intended for use in some applications, such as in active-RC filters, the amplifiers themselves should not only be stable but also must have adequate relative stability for the application at hand. It is not uncommon to see a circuit, employing a stable amplifier, becoming unstable. Thus, one is interested in some quantitative information concerning the 'degree' of stability of these amplifiers [41]. Frequently used measures of relative stability include gain and phase margins of these amplifiers, peak magnitude of the frequency response and the damping ratio associated with the dominant pole pair.

The gain and phase margins, which are calculated based on the loop transmission, give good indications of the relative stability of a system. It is generally found that gain margins of three or more combined with phase margins between 30° and 60° result in a desirable trade-off between the bandwidth and relative stability [41]. For the purposes of comparison of the amplifier circuits, one can use the above figures. Unfortunately, this technique becomes tedious and complex in the cases

of circuits having multiple forward and feedback paths (for example the amplifier circuit shown in Fig. 3.6).

Another quantity of interest for feedback systems is the peak magnitude M_p, equal to the ratio of the maximum magnitude of $G(j\omega)$ to its low-frequency magnitude. A large value of M_p indicates a relatively less stable system, since it shows that there is a frequency at which the characteristic equation approaches zero. This, in turn, indicates that there is a pair of closed-loop poles near the imaginary axis at approximately the peaking frequency. Feedback amplifiers are frequently designed to have M_p's between 1.1 and 1.5 [41]. Lower values for M_p imply greater relative stability while higher values indicate that the stability has been compromised in order to obtain a larger low frequency loop transmission. The above indicated values for M_p can be used only for systems with the form of a transfer function where the numerator is a simple constant. However, in our transfer functions, $G(s)$, the numerator is not a constant. It is a polynomial of first degree. Relative stability depends purely on the relative positions of the dominant poles with respect to the imaginary axis. These poles are determined by the denominator polynomial. Thus, the measure of peak magnitude M_p becomes unsuitable for our purpose, since it will also include information about the numerator polynomial of the concerned transfer function. However, the damping ratio is defined based on the denominator polynomial only. Thus, it can be used. An equivalent quantity, which is more commonly used by the filter designers is the pole-Q factor of the pole pair. This quantity can be easily calculated from the denominator polynomial. Thus, we shall henceforth be concerned

with the pole-Q factor, Q_p . This is defined through the denominator polynomial, $D(s)$, of the transfer function $G(s)$ as follows:

$$G(s) = \frac{N(s)}{D(s)} \tag{3.124}$$

where

$$D(s) = \{1 + (\frac{s}{\omega_p Q_p}) + (\frac{s}{\omega_p})^2\} . \tag{3.125}$$

The information concerning the value of Q_p , that should be used, can be obtained from the acceptable value of M_p , when $N(s) = 1$ in (3.124). The acceptable values of M_p are given in [41] for the transfer function of the form (3.124) with $N(s) = 1$. These are between 1.1 and 1.5 . For the same range of values of M_p , the range of Q_p is between 0.926 and 1.4 . The larger is the value of Q_p , the poorer will be the relative stability. Thus, a reasonable choice for this factor Q_p , seems to be 1 . It is possible that all the sub-optimal realizations have to be rejected because of the attendant un-acceptable relative stability. In such cases, the search for acceptable realizations has to be continued beyond the class of suboptimal realizations into the class of all tunable circuits. With this consideration in mind, Tables 3.1 and 3.2 have been prepared for examining the properties of non-inverting and inverting FGA's. As is observed from these tables, Q_p is a function of μ_0 , the nominal value of d.c. gain and increases with μ_0 except in three cases. Thus there is an upper bound on μ_0 so that Q_p does not exceed a given permissible value. These ranges are also

TABLE 3.1: STUDY OF RELATIVE STABILITY OF NON-INVERTING AMPLIFIERS

Amplifier Configuration Shown in Fig. No.	$\frac{\omega_p}{B}$	Q_p	The range of μ_0 for which	
			the Q_p value does not exceed 1	the Q_p value does not exceed 1.4
3.4	$\frac{1}{\mu_0}$	1.0	$\mu_0 \geq 1$	$\mu_0 \geq 1$
3.6	$\frac{1}{\mu_0}$	1.0	$\mu_0 \geq 2$	$\mu_0 \geq 2$
3.7	$\frac{\sqrt{\mu_0-1}}{\mu_0}$	$\sqrt{\mu_0-1}$	$1 < \mu_0 \leq 2$	$1 < \mu_0 \leq 3$

TABLE 3.2: STUDY OF RELATIVE STABILITY OF INVERTING AMPLIFIERS

Amplifier Configuration Shown in Fig. No.	$\frac{\omega_p}{B}$	Q_p	The range of μ_0 for which	
			the Q_p value does not exceed 1	the Q_p value does not exceed 1.4
3.11(b)	$\{\frac{(\mu_0+1)}{\mu_0(2\mu_0+1)}\}^{\frac{1}{2}}$	$\{\frac{\mu_0(\mu_0+1)}{(2\mu_0+1)}\}^{\frac{1}{2}}$	$\mu_0 = 1.62$	$1.62 \leq \mu_0 \leq 3.56$
3.14	$\frac{1}{(\mu_0+1)^{\frac{1}{2}}}$	$(\mu_0+1)^{\frac{1}{2}}$	$\mu_0 = 0$	$\mu_0 = 1$
3.16	$\frac{1}{(\mu_0+1)}$	$(1+\frac{1}{\mu_0})$	$\mu_0 = \infty$	$\mu_0 \geq 2.5$
3.23(a)	$\{\frac{(\mu_0+1)}{(\mu_0+1)^3-\mu_0}\}^{\frac{1}{2}}$	$\{1-\frac{\mu_0}{(1+\mu_0)^3}\}^{\frac{1}{2}}$	$0 < \mu_0 \leq \infty$	$0 < \mu_0 \leq \infty$
3.23(b)	$\frac{1}{(\mu_0^2+\mu_0+1)^{\frac{1}{2}}}$	$\{1-\frac{\mu_0}{(1+\mu_0)^2}\}^{\frac{1}{2}}$	$0 < \mu_0 \leq \infty$	$0 < \mu_0 \leq \infty$
3.30	$\frac{1}{(2\mu_0+2)^{\frac{1}{2}}}$	$\{\frac{(\mu_0+1)}{2}\}^{\frac{1}{2}}$	$0 < \mu_0 \leq 1$	$0 < \mu_0 \leq 3$

given in the same Tables for each configuration.

Among the positive gain amplifiers, the configuration shown in Fig. 3.4 can realize any value of $\mu_0 \geq 1$ as in the case of conventional realization. The configuration shown in Fig. 3.6 can not realize any gain below 2 and the configuration shown in Fig. 3.7 can not realize an important class of FGA's, viz., unity gain amplifiers with improved bandwidth. If the value of Q_p is restricted to unity and 1.4 , the configuration shown in Fig. 3.7 [31] can realize gains only below 2 and 3 respectively. Only at the risk of poorer relative stability, one can use this configuration for gains above 2 . This is also demonstrated by the fact that when this amplifier was used to realize a Sallen and Key Filter, silicon diodes had to be employed for limiting the signal and to avoid unnecessary locking into oscillation [36]. Reddy, who proposed this configuration [31] and used it in an oscillator circuit, also had to use silicon diodes to limit the signal level so that the OA's will not get saturated. Thus, if Q_p is kept as low as possible in order to prevent stability problems from arising in active-RC filters that use these amplifiers, the useful range of μ_0 available from Reddy's amplifier is very much limited unlike the one obtainable from the amplifier circuit shown in Fig. 3.4.

Among the negative gain amplifiers, the configurations shown in Fig. 3.23 can realize any value of the nominal gain whereas all other amplifier circuits have limited ranges of μ_0 . It should be noted, in particular, that the configuration shown in Fig. 3.14 (due to Reddy) can only realize unity gain inverter, even when the value of Q_p is relaxed

to 1.4 . The configuration shown in Fig. 3.11(b), though it has the advantage of having an infinite input impedance, not only fails to realize an inverter but also its range of μ_0 is rather limited. The configuration shown in Fig. 3.16 can realize any gain beyond 2.5 , if one can risk a Q_p value of 1.4 . The advantage of the configuration shown in Fig. 3.30 is that it can realize an inverter with a good relative stability. Further, if one allows a Q_p value of 1.4, the nominal d.c. gain can be increased up to 3 .

3.8.3 Apparent Bandwidth

Our aim is to design amplifiers that provide us with the maximum possible attainable bandwidth in practice. The attainable bandwidth of an amplifier clearly depends on its apparent bandwidth. The larger is the latter, the greater is the former, assuming, of course, that the other requirements as to the tunability and the relative stability are met. As it has been seen, the amplifiers have frequency dependent gains and that there are changes in the magnitude and the phase of the gains from their nominal values. Further, these changes increase with frequency. Clearly, these changes in the amplifier characteristics determine the maximum frequency up to which a given circuit, containing these amplifiers can be operated within acceptable specifications. The apparent bandwidth of these amplifiers is thus decided, for a given circuit application, by the way these changes affect the performance of the given circuit that uses these FGA's.

In order to derive a quantitative measure for the apparent bandwidth that these amplifiers can offer, let us assume that they are

all used in the same application, say in realizing an active-RC filter. Because of the amplifier imperfections, the transfer function of the realized filter will be different from the ideally expected one, $T(s)$. If we assume that only amplifier imperfections affect the performance of the filter, then the per unit change in the transfer function $(\Delta T/T)$, is given by

$$\frac{\Delta T}{T} = S_K^T \left(\frac{\Delta K}{K}\right) \tag{3.126}$$

where K is the gain of any of the amplifiers and $(\Delta K/K)$ is the per unit change in the gain, K. Since S_K^T depends entirely on the circuit chosen to realize the filter, $(\Delta T/T)$ can only be minimized by minimizing $(\Delta K/K)$. Suppose the amplifier gain K, for real frequencies is written as

$$K(j\omega) = \mu(\omega)\, e^{j\phi(\omega)} \tag{3.127}$$

where $\mu(\omega)$ and $\phi(\omega)$ are frequency dependent magnitude and phase functions of the amplifiers. Nominally, $\mu(\omega) = \mu_0 > 0$ and $\phi(\omega) = 0$ or π. It can easily be shown that

$$\left(\frac{\Delta K}{K}\right) = \left(\frac{\Delta \mu}{\mu_0}\right) + j\Delta\phi \tag{3.128}$$

To minimize the effect of amplifier imperfections we should therefore seek to minimize the magnitude of $(\Delta K/K)$. This function $F(\omega)$, is given

$$F(\omega) = \{(\Delta\mu/\mu_0)^2 + (\Delta\phi)^2\}^{\frac{1}{2}} \tag{3.129}$$

This function $F(\omega)$, can be interpreted as the normalized magnitude of the error vector. The approximate values of this function $F(\omega)$ as a function of frequency are listed in Tables 3.3 and 3.4 for positive and negative gain amplifiers, respectively, along with the conventional realizations. Attention has been restricted only to the amplifiers considered in Tables 3.1 and 3.2. To illustrate how $F(\omega)$ is calculated, let us consider the transfer function of the form given by (3.6). We find that $(\Delta\mu/\mu_0) \cong (\alpha_2\omega^2/B^2)$ and $\Delta\phi \cong -\alpha_1\alpha_2(\omega^3/B^3)$. It is observed that the effect of magnitude change will come into effect, as the frequency increases, long before the effect of the phase change is felt. Thus, we find that

$$F(\omega) \cong \alpha_2 \frac{\omega^2}{B^2} \tag{3.130}$$

In practice, in order for the amplifier imperfections to be acceptable, $F(\omega)$ has to be restricted to a small value. Actual value of $F(\omega)$ depends upon the application at hand and the acceptable tolerance. Restricting the value of $F(\omega)$ to be within a value, say $(1/\sigma)$ (usually $\sigma >> 1$ for active filter applications) the limits on the operating frequencies are also given in Tables 3.3 and 3.4 for positive and negative gain amplifiers, respectively.

TABLE 3.3: BANDWIDTH ANALYSIS OF POSITIVE GAIN AMPLIFIERS

Fig. Number in which the amplifier configuration is shown	$F(\omega)$	ω_L (Approximate value of the limit on the operating frequency)
Fig. 2.1(a) (conventional realization)	$\mu_0 \frac{\omega}{B}$	$\frac{B}{\mu_0 \sigma}$
Fig. 3.4	$\mu_0^2 \frac{\omega^2}{B^2}$	$\frac{B}{\mu_0 \sqrt{\sigma}}$
Fig. 3.6	$\mu_0^2 \frac{\omega^2}{B^2}$	$\frac{B}{\mu_0 \sqrt{\sigma}}$
Fig. 3.7	$\frac{\mu_0^2 \omega^2}{(\mu_0 - 1) B^2}$	$\frac{B}{\mu_0} \sqrt{\frac{\mu_0 - 1}{\sigma}}$

TABLE 3.4: BANDWIDTH ANALYSIS OF NEGATIVE GAIN AMPLIFIERS

Fig. Number in which the amplifier configuration is shown	$F(\omega)$	ω_L (Approximate value of the limit on the operating frequency)
Fig. 2.1(b) (conventional)	$(\mu_0+1)\frac{\omega}{B}$	$\frac{B}{(\mu_0+1)\sigma}$
Fig. 3.11(b)	$\frac{\mu_0(2\mu_0+1)\omega^2}{(\mu_0+1)B^2}$	$B\sqrt{\frac{(\mu_0+1)}{\mu_0(2\mu_0+1)\sigma}}$
Fig. 3.14	$\frac{(\mu_0+1)\omega^2}{B^2}$	$B\sqrt{\frac{1}{(\mu_0+1)\sigma}}$
Fig. 3.16	$(\mu_0+1)^2\frac{\omega^2}{B^2}$	$\frac{B}{(\mu_0+1)}\sqrt{\frac{1}{\sigma}}$
Fig. 3.23(a)	$\{\frac{(\mu_0+1)^3-\mu_0}{(\mu_0+1)}\}\frac{\omega^2}{B^2}$	$B\sqrt{\frac{(\mu_0+1)}{\{(\mu_0+1)^3-\mu_0\}\sigma}}$
Fig. 3.23(b)	$(\mu_0^2+\mu_0+1)\frac{\omega^2}{B^2}$	$B\sqrt{\frac{1}{(\mu_0^2+\mu_0+1)\sigma}}$
Fig. 3.30	$2(\mu_0+1)\frac{\omega^2}{B^2}$	$B\sqrt{\frac{1}{2(\mu_0+1)\sigma}}$

3.9 COMPARISON OF THE SECOND ORDER FGA'S

From the Tables 3.3 and 3.4, a general observation can be made that for $\sigma >> 1$, all the second order realizations will have a wider bandwidth as compared to the conventional realizations of their counterparts. We shall first discuss about the positive gain amplifiers. For the sake of conciseness, the term bandwidth in what follows is used in the sense of the apparent bandwidth. Also, only the properties of tunable amplifier circuits are considered.

3.9.1 Positive Gain Amplifiers

Among the positive gain amplifiers, one can find that the amplifier configurations shown in Fig. 3.6 (henceforth called as NPGA1) will provide the same bandwidth as that of the configuration shown in Fig. 3.4 (henceforth called as NPGA2) for $\mu_0 \geq 2$. NPGA1 is however, not useful for $\mu_0 < 2$. The configuration shown in Fig. 3.7 (Reddy's amplifier, RPGA) will have less bandwidth in the range of μ_0 , such that $1 \leq \mu_0 < 2$ and more bandwidth for $\mu_0 > 2$ compared to the one provided by NPGA2. This increase in the bandwidth is achieved at the risk of poor relative stability. Thus, in order to have better relative stability, one has to use either of NPGA2 or NPGA1.

In the range of $1 \leq \mu_0 < 2$, the only useful configuration is NPGA2, since it has better relative stability and provides more bandwidth than the others. We have two alternatives for $\mu_0 \geq 2$ without risking poor relative stability as mentioned before. Among these two alternatives, the NPGA1 has the minor disadvantage of requiring an additional resistor. However, if one calculates the actual transfer

function of two networks, having unequal GB products of the OA's, it is found that for NPGA1, the first order coefficients of both the numerator and denominator polynomials depend on the same GB product, namely, that of the OA, A_2 . For NPGA2, the first order coefficients of numerator and denominator polynomials depend on the GB products of OA's A_2 and A_1 , respectively. This is not a major disadvantage, since, as we discussed earlier, such differences can be tuned out. After tuning, these GB products as well as the resistor ratios will track with each other with variations in the environmental conditions, such as in power supply voltage and temperature. A detailed analysis of NPGA2 with OA's having different GB products, its tuning process and other details are given in [33].

Considering all the details of practical and theoretical aspects, one comes to the conclusion the among the positive gain amplifiers, in the range of μ_0 such that $1 \leq \mu_0 < 2$, the best circuit is NPGA2. When $\mu_0 \geq 2$, we have two alternatives among NPGA1 and NPGA2 and there is not really much to choose. If one can risk poorer relative stability, one can use RPGA for $\mu_0 \geq 2$. At this point it is worth noting that RPGA fails to improve the properties of the unity gain amplifier, which is an important element by itself. In this connection it is worth noting that when the GB products of the OA's are equal, we can realize a unity gain amplifier using the configuration of NPGA2 without the use of additional resistors and just with two OA's. Laboratory tests have shown that significant extension of the bandwidth over conventional realizations is achieved even when the OA's used have

unequal GB products and no additional resistors are used to compensate for this. These conclusions will be more clearly demonstrated by considering some applications later. Before concluding this paragraph, it is worth noting that all these second order realizations can also be used as variable phase shift amplifiers.

Finally, to get an idea of the amount of improvement achieved by the new designs, let us consider a particular value of σ . For example, if the error should not exceed 0.1% , then the value of $\sigma = 1000$. This turns out to be a typical value for active-RC filter applications. For this value of σ and for d.c. gain of $\mu_0=1$, 1.55 (which will be used later in our applications in Chapter V) and 3.0, the limiting frequencies have been calculated. These are given in Table 3.5. The corresponding values of Q_p are also included in the Table. In this Table CPGA refers to the conventional realization of positive gain amplifier. Referring to this Table, one can note that there is an order of magnitude improvement in the bandwidth provided by NPGA2 compared to the one given by the CPGA. All our previous conclusions are also confirmed by this Table. We shall now proceed to compare the performances of negative gain amplifiers.

3.9.2 Negative Gain Amplifiers

From the point of view of bandwidth, the amplifier configuration shown in Fig. 3.14 (henceforth called RNGA) (31) gives the maximum bandwidth for any value of μ_0 . Unfortunately, it is the worst circuit from the point of view of relative stability. As is obvious from Table 3.2, it's application has to be limited to low values of μ_0 . The

TABLE 3.5: LIMITING FREQUENCIES IN THE CASES OF POSITIVE GAIN AMPLIFIERS WITH $\sigma = 1000$.

Configuration	$\mu_0 = 1.00$		$\mu_0 = 1.55$		$\mu_0 = 3.00$	
	ω_L	Q_p	ω_L	Q_p	ω_L	Q_p
CPGA	0.001B	-	6.45×10^{-4}B	-	3.33×10^{-4}B	-
NPGA 2	0.0316B	1	0.0204B	1	0.0105B	1
RPGA	0.001B	-	0.0151B	0.742	0.0149B	1.414
NPGA1	-	-	-	-	0.0105B	1

ω_L = Limiting frequency

Q_p = Pole-Q factor

B = GB product of the OA's

configurations shown in Fig. 3.23 (hence forth referred to as NNGA1 and NNGA2 respectively) are found to have good relative stability and useful for any value of gain, μ_0 . These also provide significant improvement in the bandwidth over the conventional realization (CNGA). We shall compare the performances by taking a particular value of $\sigma = 1000$ for $\mu_0=1$ (an inverter) and $\mu_0=10$. The corresponding set of limiting frequencies is given in Table 3.6. The appropriate values for Q_p are also included in this Table. A general conclusion can immediately be drawn from this Table; all second order realizations provide improvement in the bandwidth, which is an order of magnitude. As an inverter, the configurations shown in Figs. 3.16, 3.23 and 3.30 all provide more or less same bandwidth and is comparable to that of RNGA. However, they have better relative stability compared to that of RNGA. For large gains, however, the only useful configurations are NNGA1 and NNGA2, because they possess superior relative stability. In the realization of NNGA2, the element spread is of the order of μ_0^2 and hence it is useful only for low values of μ_0 . It is observed that, as an inverter, the optimum circuit is NNGA2. If the slightly poorer relative stability of RNGA is acceptable, then it is a better circuit. For gains $\mu_0 > 1$, the configurations shown in Figs. 3.11(b) ($1.62 \leq \mu_0 \leq 3.56$) and 3.30 ($1 \leq \mu_0 \leq 3$) seem to be better, if their poorer relative stability are acceptable. However, for $\mu_0 > 3.56$, the only useful configuration is NNGA1 because of its superior relative stability.

3.10 EXPERIMENTAL RESULTS

The positive gain elements of NPGA2, RPGA and CPGA were built

TABLE 3.6: LIMITING FREQUENCIES FOR NEGATIVE GAIN AMPLIFIERS WITH $\sigma = 1000$

Fig. Number in which the amplifier configuration is shown	$\mu_0 = 1.00$		$\mu_0 = 10.00$	
	ω_L	Q_p	ω_L	Q_p
Fig. 2.1(b) (CNGA)	$5\times10^{-4}B$	-	9.1×10^{-5}	-
Fig. 3.11(b)	-	-	$7.2\times10^{-3}B$	2.29
Fig. 3.14 (RNGA)	$2.2\times10^{-2}B$	1.414	$9.5\times10^{-3}B$	3.32
Fig. 3.16	$1.6\times10^{-2}B$	2	$2.9\times10^{-3}B$	1.1
Fig. 3.23(a) (NNGA1)	$1.7\times10^{-2}B$	0.935	$2.9\times10^{-3}B$	0.996
Fig. 3.23(b) (NNGA2)	$1.8\times10^{-2}B$	0.866	$3\times10^{-3}B$	0.958
Fig. 3.30	$1.6\times10^{-2}B$	1	$6.7\times10^{-3}B$	2.345

ω_L = Limiting frequency

Q_p = Pole-Q factor

B = GB product of the OA's

to realize a nominal value of $\mu_0 = 1.55$ and tested in the laboratory. Discrete resistors of 1% tolerance and μA741 (Motorola) OA's with a nominal GB product of 1MHz were used. In none of the cases was any attempt made to compensate for the unequal GB products. The theoretically expected magnitude and phase characteristics are shown in Fig. 3.33. The experimentally obtained points are marked over these curves. It is observed that for frequencies near the peak of each curve and at higher frequencies, the experimental results differ significantly from the theoretical ones. This is to be expected since the one pole model is no longer valid in this region and the second pole of the amplifier [33], which has been neglected, should be taken into consideration. This effect of the second pole on the amplifier characteristics is considered in detail in Chapter IV.

Inverting unity gain amplifiers, with the same OA's and discrete resistors of 1% tolerance, were also constructed and tested. The theoretically expected characteristics, with the one pole model, of NNGA2 and RNGA are shown in Fig. 3.34 along with the characteristics of CNGA. Experimentally obtained values are marked on the curves.

3.11 CONCLUSION

In this Chapter, starting with a general five port active-R network in which two OA's are embedded, all possible circuits for realizing second order positive and negative gain amplifiers, of the form given by (3.6), are enumerated. These circuits have also been compared to the (a) tunability, (b) relative stability and (c) the maximum apparent bandwidth that can be provided by each circuit. From

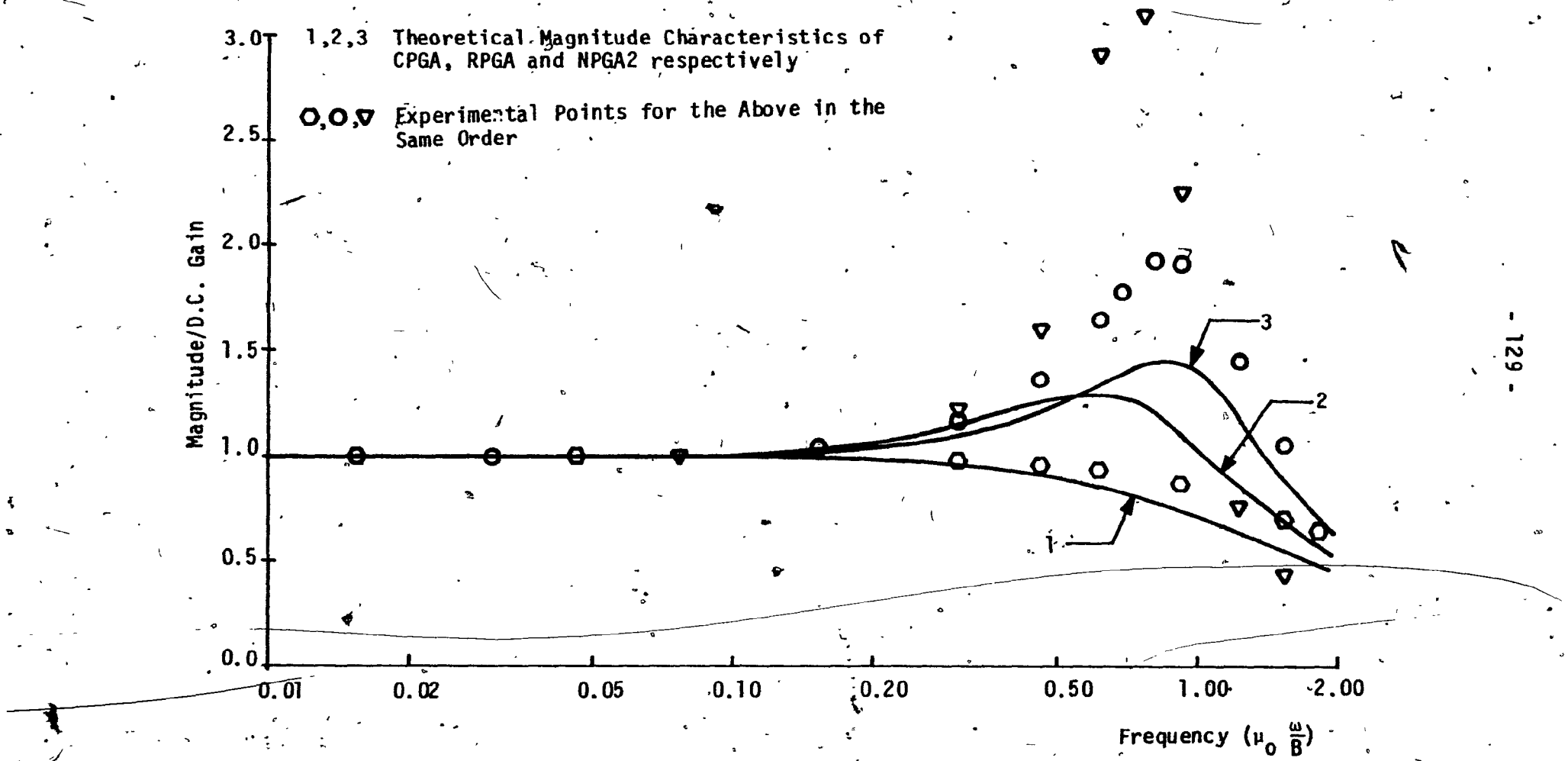

FIG. 3.33(a): Magnitude Characteristics of Positive Gain Amplifiers

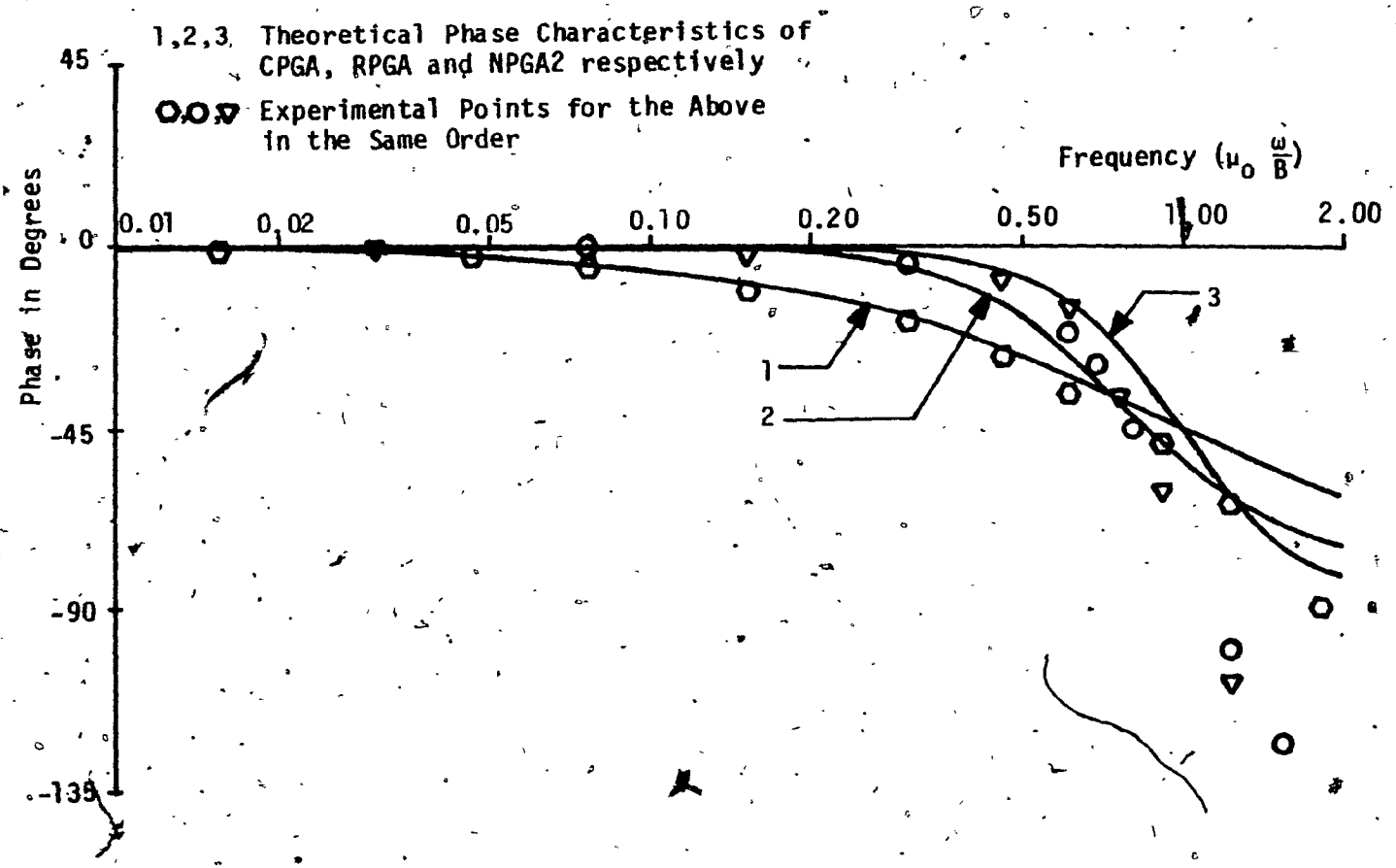

FIG. 3.33(b): Phase Characteristics of Positive Gain Amplifiers

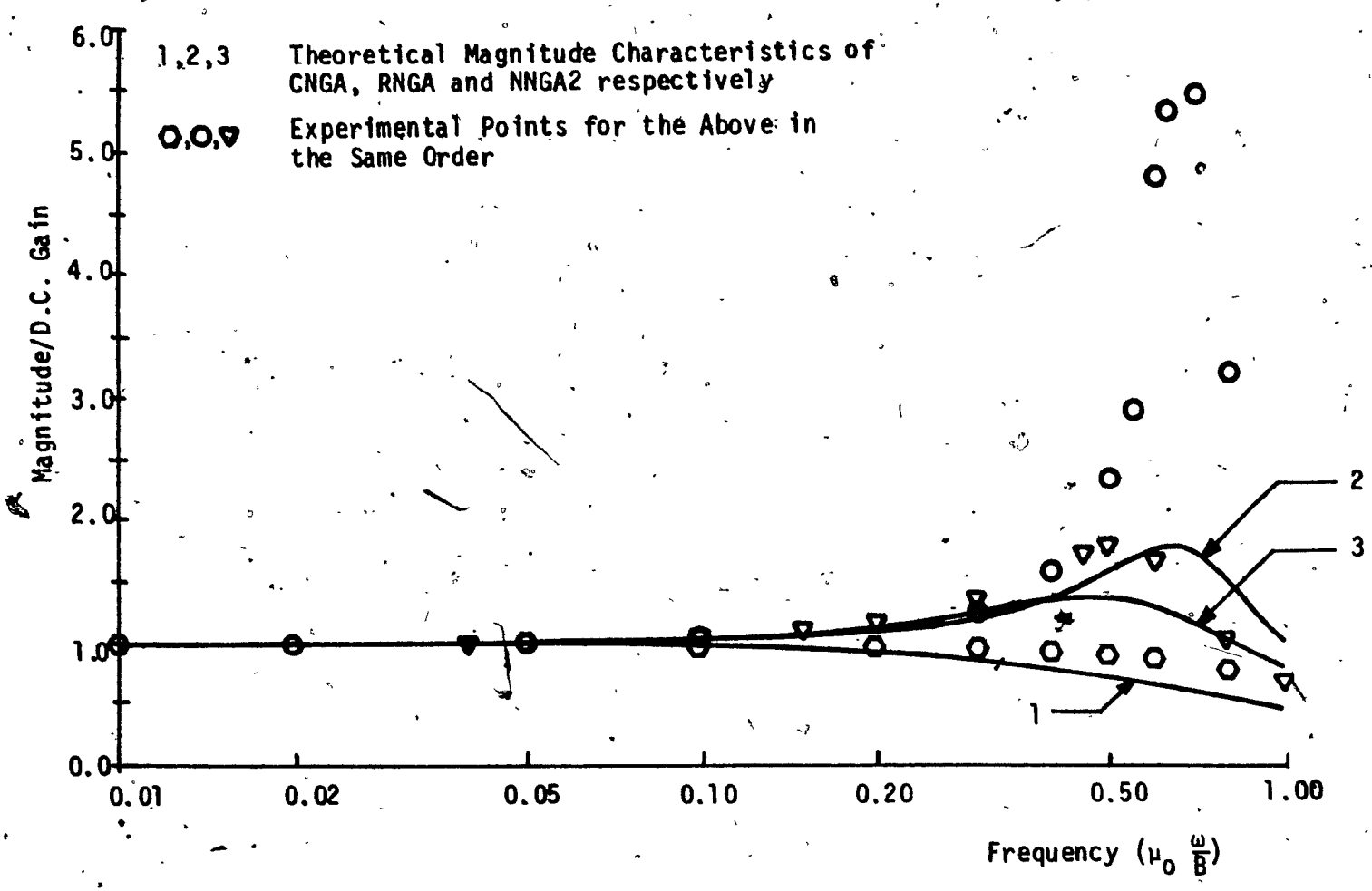

FIG. 3.34(a): Magnitude Characteristics of Negative Gain Amplifiers

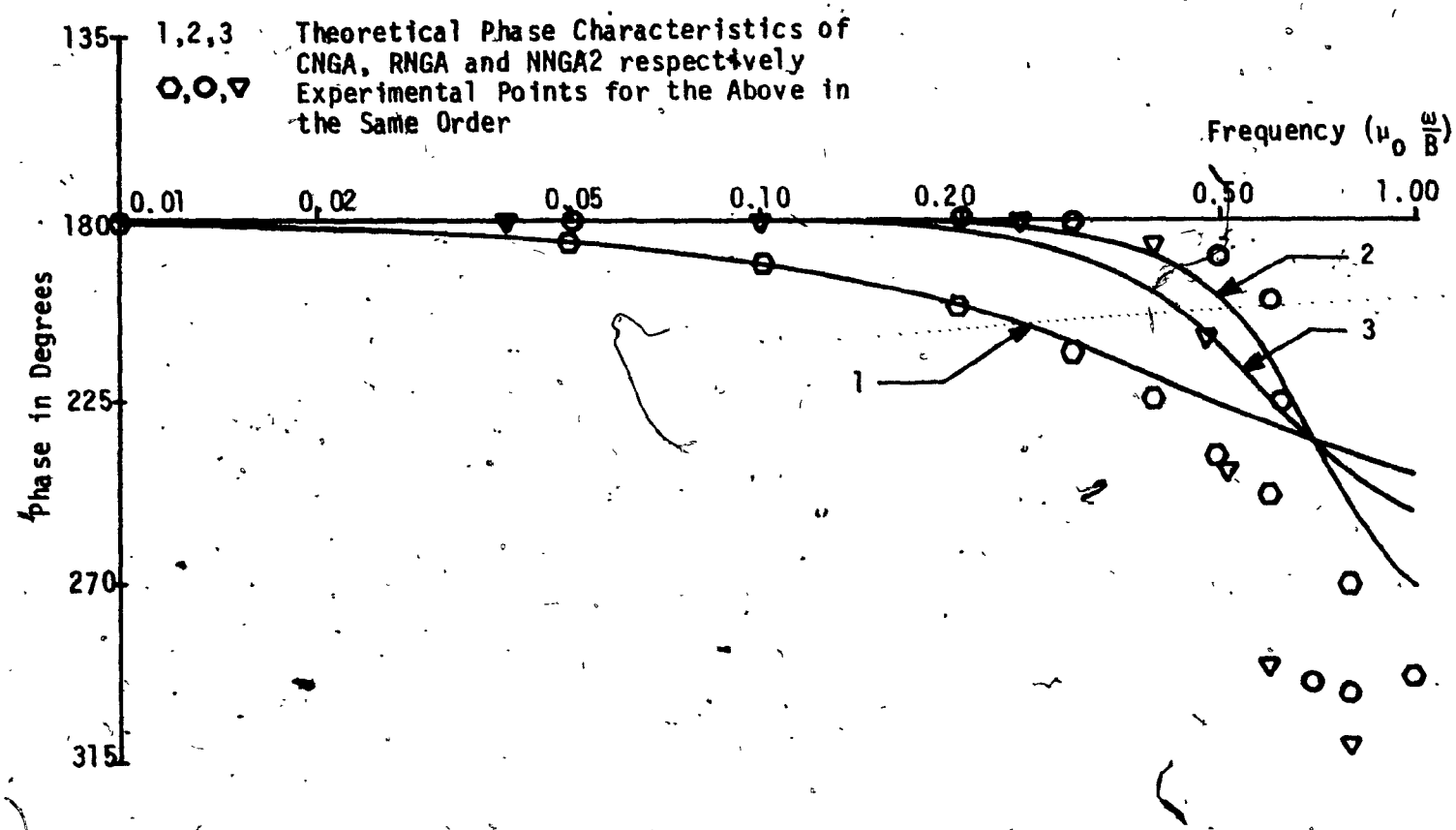

FIG. 3.34(b): Phase Characteristics of Negative Gain Amplifiers

these studies, a set of optimum circuits has been selected for positive as well as negative gain realizations. It has been found that the optimum circuit depends upon the range of the nominal gain desired. Both theoretical and experimental characteristics of the magnitude and phase responses of these amplifiers have been provided to show the superiority of these amplifiers over their counterparts in the conventional realization.

The superiority of these new amplifiers will be further established through some applications in Chapter V. Before doing that, let us take a look at the nature of some of these new realizations. It should be noted that originally a control model with a single forward path and a single feedback path was assumed to obtain (3.6). However, in implementing (3.6), some circuits that employ multiple forward as well as feedback paths are obtained.

Our basic theory of active compensation of FGA's in Chapter II was based on single feedback system. The realization of higher order transfer functions was abandoned based on the stability of such a system. However, if one introduces multiple feedbacks in the basic model, it might be possible to get stable higher order realizations that extend the frequency range of the FGA's beyond what can be achieved by second order FGA's. Another way of interpreting the same situation would be that the additional feedback paths might pull the right hand side (in s-plane) poles of the higher order realizations of the basic control model back to the left hand side, in the process providing improved operating frequency range for the FGA's. This is the subject matter of the next chapter.

CHAPTER IV

HIGHER ORDER REALIZATIONS OF FINITE GAIN AMPLIFIERS

4.1 INTRODUCTION

The possibility of realizing stable higher order FGA's was mentioned in the last chapter. This possibility is investigated in this chapter. Towards this end, two general network configurations are assumed. These two configurations are obtained as generalizations of NPGA2 and NNGA1, where additional feedbacks have been introduced. It is shown that a stable amplifier of any order can be realized by one or the other of these configurations. However, phase margin and gain margin studies lead to the fact that only 3OA configurations are useful. These 3OA circuits realize a third order transfer function. Thus, we restrict ourselves to the realization of configurations with 3OA's. The elemental characteristics are provided which show the superiority of these amplifiers compared to the conventional as well as the second order realizations.

4.2 TWO GENERAL CONFIGURATIONS

Let us consider the circuits shown in Figs. 4.1 and 4.2 for realizing positive and negative gain amplifiers, respectively. These two circuits are obtained, as mentioned before, by generalizing the configurations of NPGA2 and NNGA1. For simplicity, let us assume that the GB products of all the OA's A_1 , A_2 ... A_{n-1} , A_n are same and its value is equal to B . The gain equation of each OA , in the frequency range of interest, is given by (2.2). Then the transfer functions of

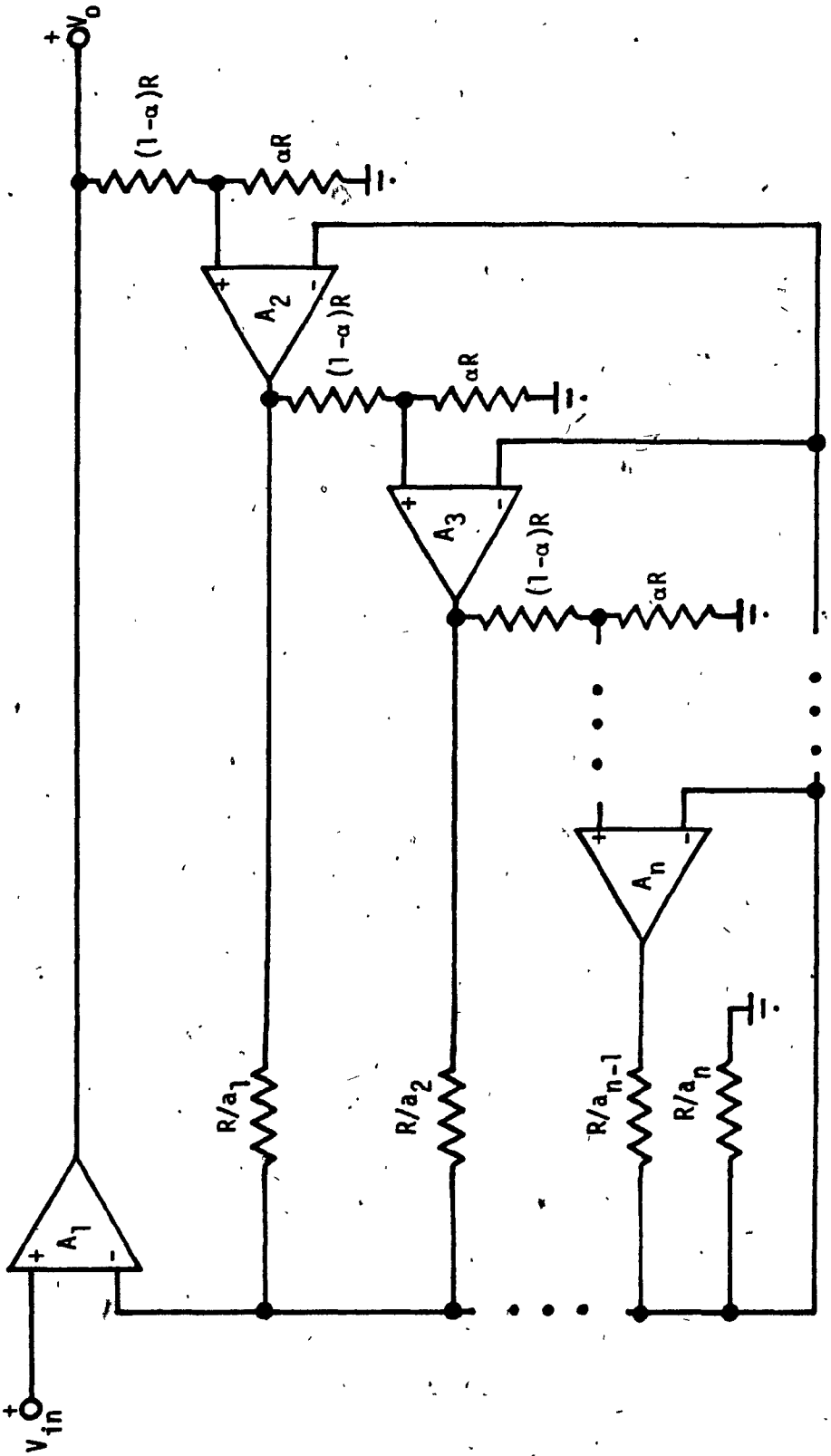

FIG. 4.1: Generalized Structure of the Positive Gain Amplifier with 'n' OA's

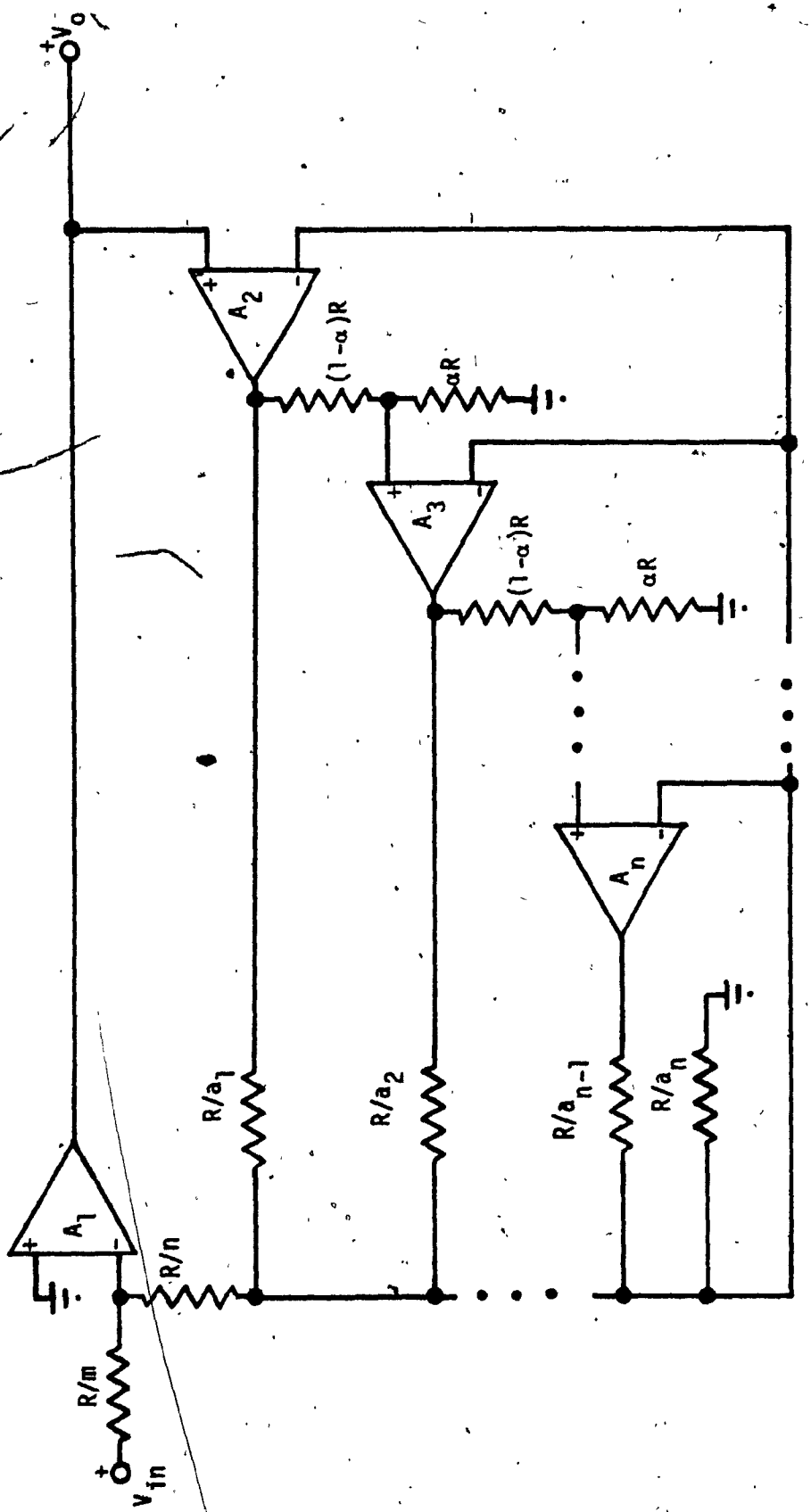

FIG. 4.2: Generalized Structure of the Negative Gain Amplifier with 'n' OA's

the networks can be derived in terms of the parameters given in the network and these are given below:

$$\frac{V_0}{V_{in}} = G_I(s) = \frac{1}{\alpha} \frac{1+\sum_{i=1}^{n-1} N_i x^i}{1+\sum_{j=1}^{n} D_j x^j} \tag{4.1}$$

where

$$\left.\begin{aligned} N_i = D_i &= \frac{(a_{n-1}+a_{n-2}+\cdots+a_{n-i-1})}{a_{n-1}}, \quad i=1,2,\ldots,n-2 \\ N_{n-1} &= \alpha\left(N_{n-2}+\frac{a_n}{a_{n-1}}\right) \\ D_{n-1} &= N_{n-2} \\ D_n &= N_{n-1} \end{aligned}\right\} \tag{4.2}$$

and

$$x = \left(\frac{s}{\alpha B}\right)$$

$$\frac{V_0}{V_{in}} = G_{II}(s) = -\frac{m}{n} \frac{1+\sum_{i=1}^{n-1} N_i x^i}{1+\sum_{j=1}^{n} D_j x^j} \tag{4.3}$$

where

$$
\left.
\begin{aligned}
N_i = D_i &= \frac{(a_{n-1}+a_{n-2}+\cdots+a_{n-i-1})}{a_{n-1}}, \quad i=1,2,\ldots,n-2 \\
N_{n-1} &= \alpha\{N_{n-2}+\frac{(a_n+n)}{a_{n-1}}\} \\
D_{n-1} &= N_{n-2} \\
D_n &= N_{n-1} - \frac{n\alpha^2}{a_{n-1}} \\
x &= (\frac{s}{\alpha B})
\end{aligned}
\right\} \qquad (4.4)
$$

and

$$
\alpha = \frac{1}{(1+\frac{m}{n})}
$$

The equations (4.1) and (4.2) give the transfer function of the circuit shown in Fig. 4.1 and the equations (4.3) and (4.4) describe that of the circuit of Fig. 4.2. By observing (4.2) and (4.4), one can note that only the ratios of resistors affect the transfer functions and thus, without loss of generality, we shall assume $a_{n-1} = 1.0$ in both the circuits. In order to realize a d.c. gain of μ_0, we need to have, in the circuit of Fig. 4.1,

$$
\mu_0 = (\frac{1}{\alpha}) \qquad (4.5)
$$

and in the circuit of Fig. 4.2,

$$
m = 1 \quad \text{and} \quad n = (\frac{1}{\mu_0}) \qquad (4.6)
$$

In order that the coefficients of the numerator and denominator polynomials are equal up to (n-1)th power, the condition for the positive gain amplifier turns out to be

$$a_n = N_{n-2}(\mu_0 - 1) \tag{4.7}$$

and for the negative gain amplifier, it is

$$a_n = \mu_0 N_{n-2} - \frac{1}{\mu_0} \tag{4.8}$$

The conditions (4.5) through (4.8) can be satisfied in practice and if these conditions are satisfied, then the transfer functions given by (4.1) and (4.3) reduce to (4.9) and (4.10) respectively, as given below:

$$G_I(s) = \mu_0 \frac{1 + \sum_{i=1}^{n-1} N_i x^i}{1 + \sum_{j=1}^{n} D_j x^j} \tag{4.9a}$$

where

$$\left.\begin{aligned} N_i = D_i &= (1 + a_{n-2} + \cdots + a_{n-i-1}), \quad i = 1, 2, \ldots, n-2 \\ \text{and} \\ N_{n-1} &= D_{n-1} = D_n = N_{n-2} \end{aligned}\right\} \tag{4.9b}$$

$$G_{II}(s) = \frac{1 + \sum_{i=1}^{n-1} N_i x^i}{1 + \sum_{j=1}^{n} D_j x^j} \tag{4.10a}$$

where

$$\left.\begin{aligned} N_i = D_i &= (1+a_{n-2}+\cdots+a_{n-i-1}) \ , \quad i=1,2,\ldots,n-2 \\ N_{n-1} &= D_{n-1} = N_{n-2} \\ D_n &= N_{n-1} - \frac{1}{\mu_0(\mu_0+1)^2} \end{aligned}\right\} \quad (4.10b)$$

and

The equations (4.9) and (4.10) indicate that the circuits of Figs. 4.1 and 4.2 can, respectively, realize an nth order positive gain amplifier and an nth order negative gain amplifier. It is obvious from (4.9b) and (4.10b) that (n-2) parameters of the amplifiers can be chosen arbitrarily. However, before proceeding further, the stability of these amplifiers should be examined.

4.3 STABILITY OF THE HIGHER ORDER AMPLIFIERS

We shall consider in detail the case of the positive gain amplifiers only. Similar discussions apply to the case of the negative gain amplifier also.

Considering the denominator polynomial of $G_I(s)$ given by (4.9), it is our aim to show that the constants a_1 , a_2 ,..., a_{n-2} can always be chosen such that its zeros lie in the L.H.S. of the x plane. The denominator polynomial, $D(x)$, can be rewritten as shown below:

$$D(x) = \frac{[1+\sum_{i=1}^{n-2} a_i x^i - x^{n+1}(1+\sum a_i)]}{(1-x)} \qquad (4.11)$$

In the polynomial $\{1+\sum_{i=1}^{n-2} a_i x^i\}$, each coefficient can be chosen arbitrarily (i.e. each a_i can be chosen arbitrarily) and thus, by a proper choice, its zeros can be placed any where in the x-plane. Hence, the choice of a_i's can be made such that this polynomial has its zeros in the L.H.S. of the x-plane. To be specific and for simplicity, let us choose the a_i's so that all the zeros of the polynomial are repeated and lie on the negative real axis (though this is not necessary for our argument). Thus we can write that

$$1+\sum_{i=1}^{n-2} a_i x^i = (1+\alpha x)^{n-2} \qquad (4.12)$$

Changing the variable as in the following

$$y = \alpha x \qquad (4.13)$$

and substituting (4.12) in (4.11), we get

$$D(y) = \frac{\alpha[(1+y)^{n-2} - y^{n+1}\frac{(1+\alpha)^{n-2}}{\alpha^{n+1}}]}{(\alpha-y)}$$

$$= \frac{(1+\alpha)^{n-2} y^{n+1}}{\alpha^n (y-\alpha)}\left[1 - \frac{\alpha^{n+1}}{(1+\alpha)^{n-2}}\frac{(1+y)^{n-2}}{y^{n+1}}\right] \qquad (4.14)$$

Obviously, $(y-\alpha)$ is a factor of the part $1-\{\alpha^{n+1}(1+y)^{n-2}\}/\{(1+\alpha)^{n-2}y^{n+1}\}$

in (4.14). Thus, clearly, $y = \alpha$ is not a solution of the characteristic equation $D(y) = 0$. Thus, we have to concentrate on the modified characteristic equation,

$$[1-\eta \frac{(1+y)^{n-2}}{y^{n+1}}] = 0 \qquad (4.15)$$

where

$$\eta = \frac{\alpha^{n+1}}{(1+\alpha)^{n-2}}$$

and check whether, by properly choosing η, all the roots excepting the one $y = \alpha$, can be placed in the left half of the y-plane.

This characteristic polynomial has $(n+1)$ roots at $y = 0$ for $\eta = 0$. For increasing values of η, the roots start moving away from this point. As $\eta \to \infty$ (corresponding to $\alpha \to \infty$), $(n-2)$ of these roots terminate on $y = -1$ and the remaining three approach $y = \infty$. For any value of η (determined by a particular value of α), there is a root at $y = \alpha$. However, as indicated earlier, this root can be ignored. The loci of the roots of the characteristic equation for the case when n is odd, are shown in Fig. 4.3. The root-locus diagram for the case, when n is even is the same excepting for the fact that the branch on the negative real axis between 0 and -1 is absent.

It is observed from the root-locus diagram that there can be only one root of the modified characteristic polynomial at $y = \alpha$ and the rest of the n roots can always be placed in the L.H.S. of the

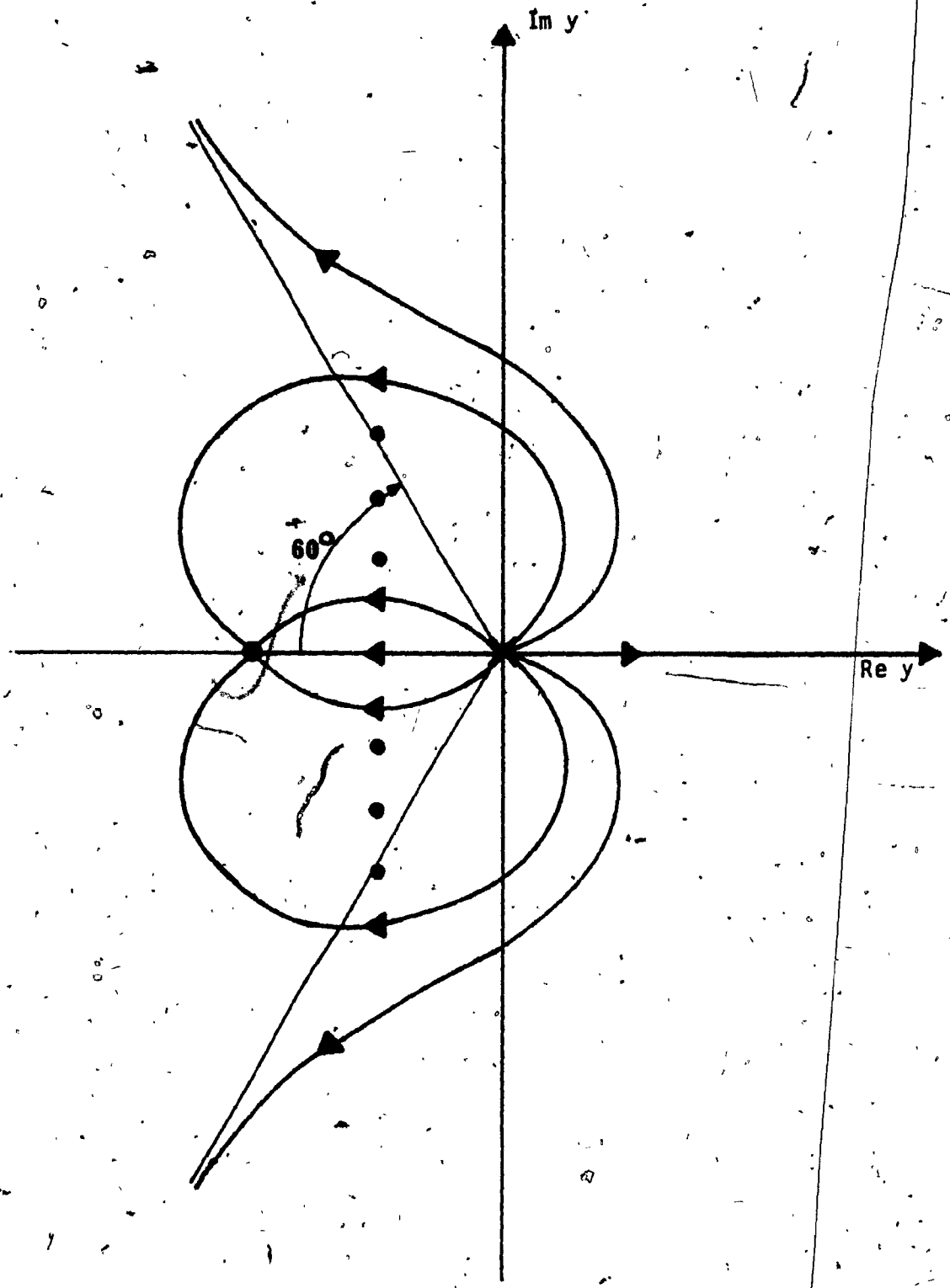

FIG. 4.3: Root-Loci of the Characteristic Equation (4.15) when n is odd

y-plane by choosing a sufficiently larger value of n, that is, α. These remaining n roots are the roots of the original characteristic polynomial, $D(y)$. The parameter α can be increased to any value by properly choosing a_i's. Thus, it is always possible to choose a_1, a_2, ..., a_{n-2} such that the transfer function given by (4.9) is stable. Similar arguments hold good for the higher order negative gain amplifiers, that is, for the transfer function described by (4.10). Thus, it can be concluded that by a proper choice of a_i's, the structures in Figs. 4.1 and 4.2 can be used to realize stable positive as well as negative gain amplifiers of any order n. It is worth noting that these amplifier configurations reduce to those of NPGA2 and NNGA1, described in Chapter 3, when $n = 2$.

The constants a_i's should be so chosen as to get maximum bandwidth. As has been seen in the second order cases, the maximum bandwidth is obtained when the coefficient of the highest order term of s in the denominator polynomial is minimum. Thus, the aim should be to minimize this coefficient, while at the same time, ensuring a good relative stability. In order to do so, the relative stability of the higher order realizations are next studied.

To this end, we shall refer, as in the cases of second order FGA's, to the realizations, where the coefficient of the highest power of s in the denominator polynomial has been minimized as suboptimal realizations.

4.4 SUB-OPTIMAL REALIZATIONS AND RELATIVE STABILITY

Mathematically, the transfer functions of the negative gain FGA's are different from those of the positive gain FGA's only in the coefficient of the highest power of x. This difference is $1/\{\mu_0(\mu_0+1)^2\}$ and is constant for a given μ_0. Further, either the maximum bandwidth or the degree of relative stability of these FGA's are affected only negligibly by this difference, especially for $\mu_0 \geq 1$. These conclusions have also been verified by computer simulations. In view of the foregoing discussion, attention will be restricted to only non-inverting FGA's. Whatever values of a_i's are obtained for these amplifiers will also be adopted for the inverting FGA's.

For reasons that will subsequently be evident, higher order realizations only up to $n = 5$ are examined.

4.4.1 Three OA Structure (n = 3)

In this case the transfer function given by (4.9) reduces to the one given below:

$$G(s) = \mu_0 \frac{1+(1+a_1)x+(1+a_1)x^2}{1+(1+a_1)x+(1+a_1)x^2+(1+a_1)x^3} \qquad (4.16)$$

The maximum bandwidth is obtained when $a_1 = 0$. However, this choice of a_1 leads to an unstable circuit. Thus, for stability, one has to choose

$$a_1 > 0 \qquad (4.17)$$

4.4.2 Four OA Structure (n = 4)

The equation (4.9) reduces as follows when $n = 4$.

$$G(s) = \mu_0 \frac{1+px+qx^2+qx^3}{1+px+qx^2+qx^3+qx^4} \tag{4.18}$$

where

$$\left.\begin{aligned} p &= 1+a_2 \\ \text{and} \\ q &= 1+a_2+a_1 \end{aligned}\right\} \tag{4.19}$$

The quantity q is minimized while ensuring stability, if a_1 and a_2 are selected as given below:

$$\left.\begin{aligned} a_2 &= 1 \\ a_1 &= 1+E \\ \text{and} \\ E &> 0 \end{aligned}\right\} \tag{4.20}$$

Substituting (4.20) and (4.19) into (4.18), the transfer function $G(x)$ becomes,

$$G(s) = \mu_0 \frac{1+2x+(2+E)x^2+(2+E)x^3}{1+2x+(2+E)x^2+(2+E)x^3+(2+E)x^4} \tag{4.21}$$

where

$$E > 0$$

for stability.

4.4.3 Five OA Structure (n = 5)

For the five OA circuit, the transfer function is a fifth order one. This function can easily be obtained from (4.9). The following choices for a_1, a_2 and a_3 will minimize the coefficient of the fifth order term of x in the denominator polynomial of the transfer function.

$$\left.\begin{aligned} a_1 &= 2p \\ a_2 &= 3+p+E \\ \text{and} \quad a_3 &= p \end{aligned}\right\} \qquad (4.22)$$

where

$$p, E > 0 .$$

With these choices, the corresponding transfer function is given as

$$G(s) = \mu_0 \frac{1+N_1x+N_2x^2+N_3x^3+N_3x^4}{1+N_1x+N_2x^2+N_3x^3+N_3x^4+N_3x^5} \qquad (4.23)$$

where

$$\left.\begin{aligned} N_1 &= (1+p) \\ N_2 &= (4+2p+E) \\ N_3 &= (4+4p+E) \end{aligned}\right\} \qquad (4.24)$$

and

$$p, E > 0 .$$

In each of the above realizations, there are still some unknown parameters to be determined. The conditions obtained before in each case ensure stable operation of the amplifiers. However, as discussed in the previous chapter, it is the degree of relative stability that is important, if these amplifiers are to be part of any larger system.

In the case of second order FGA's, the pole-Q factor, Q_p was found to be suitable to predict the degree of relative stability. As we are now dealing with higher order FGA's, this is no longer appropriate. Thus the measures of gain and phase margins will be used. In all the above realizations, the phase and gain margins can be calculated from the loop transmission. The values of these measures can then be used to fix the unknown quantities. In an attempt to do that, let us choose $a_1 = 4$ in (4.16), $E = 6$ in (4.20); and $p = 5$ and $E = 5$ in (4.24). These values were chosen so that there will be an improvement in the bandwidth as the order of FGA is increased. Then the Nyquist plots were obtained to determine the gain and phase margins of these amplifiers. These plots are shown in Fig. 4.4.

In the case of 50A structure, the gain margin and phase margin are 1.67 and 5.6° respectively. These values are much lower than even the minimum, quoted in Chapter III (which are 3 and 30°), for good relative stability. If we attempt to increase the values of p and E to improve the relative stability, the increase in the bandwidth compared to the 30A and 40A structures becomes insignificant. This, along with the fact that there is a considerable increase in the component count, makes the 50A structure unattractive in practice. Hence, this

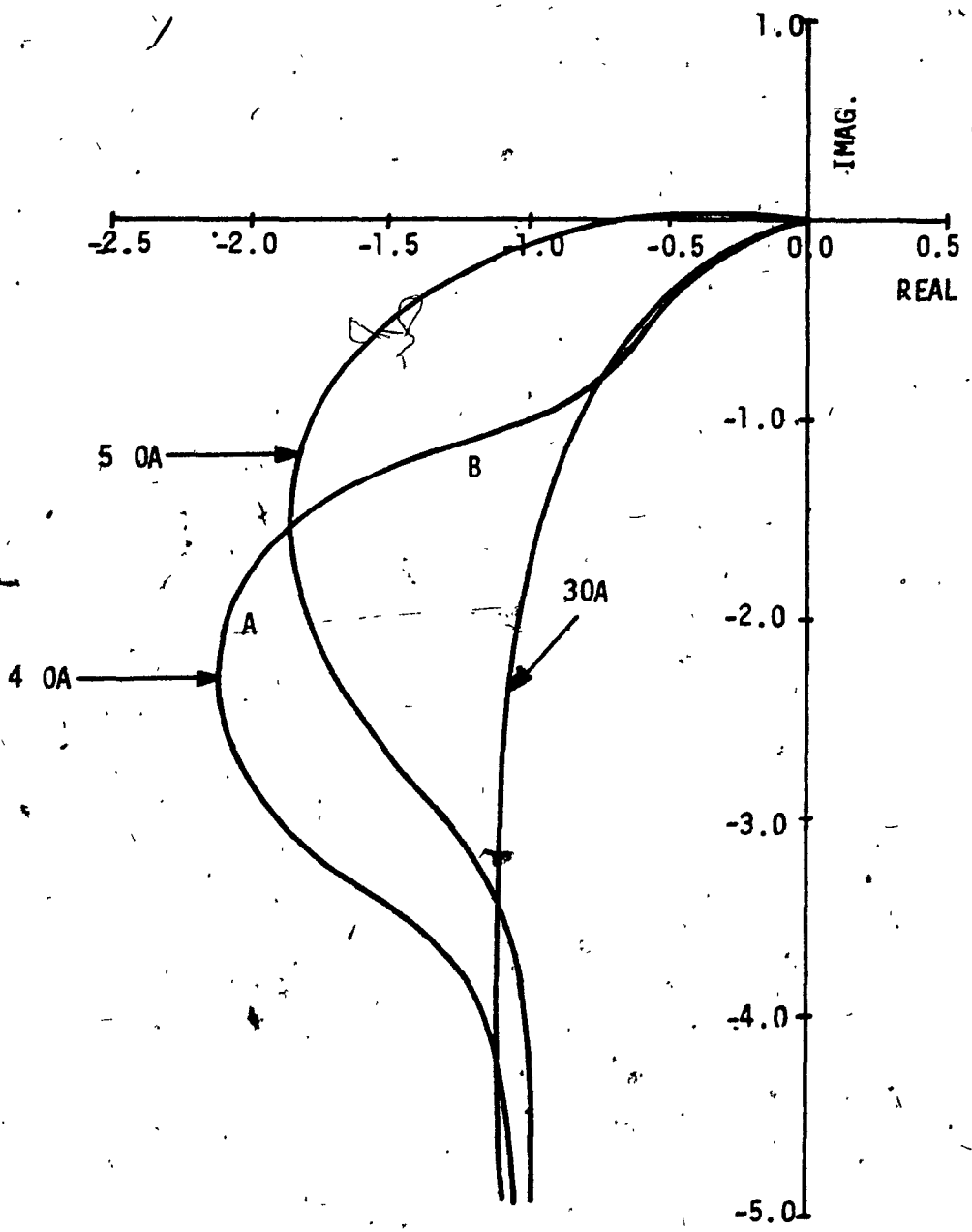

FIG. 4.4: Nyquist Plots for 3,4 and 5OA Positive Gain Amplifiers

case is not considered any further. Incidentally, the relative stability of six and higher order FGA's is poorer still. In fact, for a sixth order realization, the phase margin is less than 1°.

Moving now to the case of 40A structure, the phase margin is measured by the angle subtended by the tangent to curve in the portion A and B passing through the origin with the negative real axis [42]. Though the gain margin in this case is ∞, the phase margin is only about 28°. Increasing the value of E beyond 6 in (4.20) will increase the phase margin. In that case, however, the improvement in the bandwidth provided by this structure becomes negligible compared to the one provided by the 30A structure.

Clearly then, any further studies should be restricted only to the third order realizations. These correspond to the case $n = 3$. Henceforth, the third order positive and negative gain FGA's will be referred to as NPGA3 and NNGA3 respectively.

In the case of NPGA3 as well as NNGA3, the gain margin is always infinity and the phase margin can be controlled by a proper choice of the constant a_1. As mentioned earlier, the feedback amplifiers are usually designed with a phase margin to be anywhere between 30° and 60°. The constant a_1 in (4.16) can be chosen to give a phase margin within this range. Before choosing a particular value of a_1 it should be observed that to maximize the phase margin, the quantity a_1 has to be maximized while to maximize the bandwidth, a_1 has to be minimized. A good compromise between these two conflicting requirements can be effected by choosing

$$a_1 = 4 \tag{4.24}$$

The above choice yields a value of 45° for the phase margin for NPGA3. In our subsequent analysis, (4.24) will be used in (4.16). In the case of NNGA3, the phase margin will be slightly more than 45° for the choice of $a_1 = 4$ in (4.10) with $n = 3$.

Let us now examine in detail the 3OA structures. For the sake of generality, the GB products of the OA's will now be assumed to be different from each other. A tuning procedure will also be described to account for this difference.

4.5 ANALYSIS OF 3OA STRUCTURES

The new 3OA realizations for positive and negative gain amplifiers can be derived from the general structures shown in Figs. 4.1 and 4.2. These are shown in Fig. 4.5. A slight modification has been made to account for the differences in the GB products of the OA's. Let B_1, B_2 and B_3 be the GB products of the OA's A_1, A_2 and A_3 respectively, in both the circuits. Again, let us assume that, in the frequency range of interest, the gain of each OA is described by (2.2), which is reproduced below for convenience

$$A_i(s) = \frac{B_i}{s} \quad , \quad i=1,2 \text{ and } 3$$

Then the transfer function of the circuit shown in Fig. 4.5(a) can be derived to be

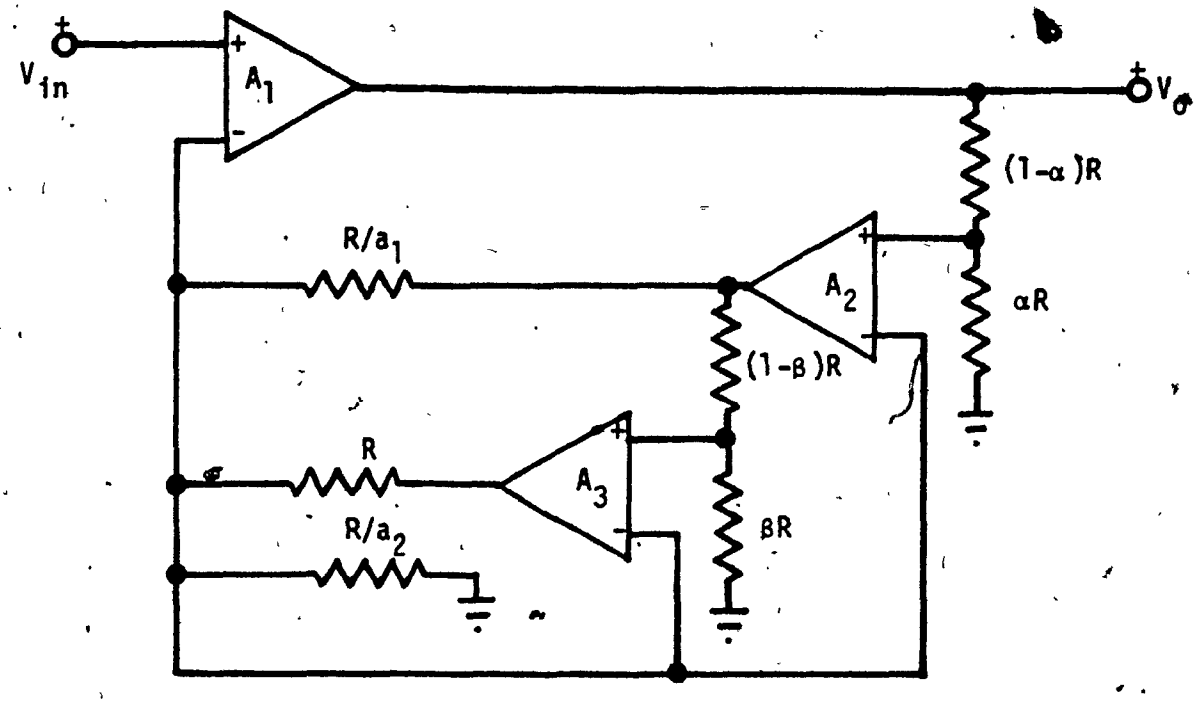

(a)

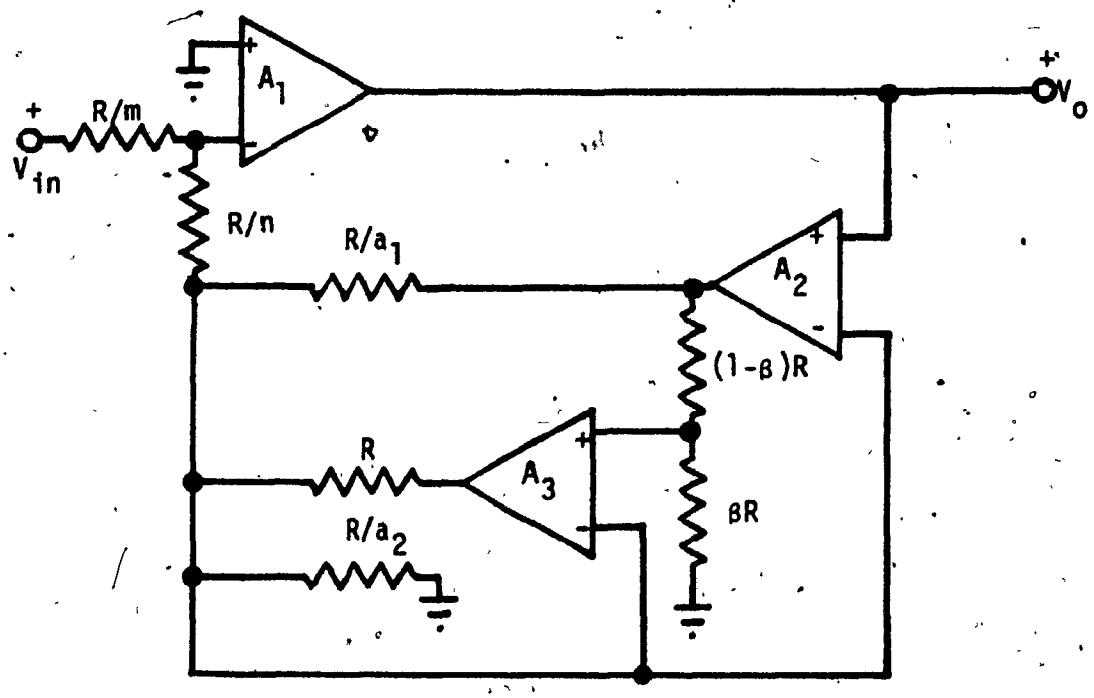

(b)

FIG. 4.5: Finite Gain Amplifiers with 3OA's

(a) Positive Gain Amplifier

(b) Negative Gain Amplifier

$$G_a(s) = \frac{1}{\alpha} \frac{1+\frac{s}{\beta B_2}\left(1+a_1\frac{B_2}{B_3}\right)+\frac{s^2}{\beta B_2 B_3}(1+a_1+a_2)}{\left[1+\frac{s}{\alpha B_1}\left(1+\frac{a_1\alpha B_1}{\beta B_3}\right)+\frac{s^2}{\alpha\beta B_1 B_2}\left(1+\frac{a_1 B_2}{B_3}\right)\right.} \qquad (4.25)$$

$$\left.+\frac{s^3}{\alpha\beta B_1 B_2 B_3}(1+a_1+a_2)\right]$$

and that of the negative gain amplifier shown in Fig. 4.5(b) is given by the following equation.

$$G_b(s) = -\frac{m}{n} \frac{1+\frac{s}{\beta B_2}\left(1+a_1\frac{B_2}{B_3}\right)+\frac{s^2}{\beta B_2 B_3}(1+a_1+a_2+n)}{\left[1+\frac{s}{\gamma B_1}\left(1+a_1\frac{\gamma B_1}{\beta B_3}\right)+\frac{s^2}{\gamma\beta B_1 B_2}\left(1+a_1\frac{B_2}{B_3}\right)\right.} \qquad (4.26)$$

$$\left.+\frac{s^3}{\gamma\beta B_1 B_2 B_3}\{(1+a_1+a_2+n)-n\gamma\}\right]$$

where

$$\gamma = \frac{1}{\left(1+\frac{m}{n}\right)}$$

The d.c. gains of the amplifiers are fixed by α in the circuit of Fig. 4.5(a) (NPGA3) and the ratio (m/n) in the circuit of Fig. 4.5(b) (NNGA3). If the required d.c. gain is μ_0, then we have for NPGA3,

$$\mu_0 = \frac{1}{\alpha} \qquad (4.27)$$

and for NNGA3,

$$m = 1 \quad \text{and} \quad n = \frac{1}{\mu_0} \qquad (4.28)$$

The conditions on (4.25) for the numerator and denominator coefficients to be equal are as follows:

$$\alpha B_1 = \beta B_2 = \frac{B_3(1+a_1 \frac{B_2}{B_3})}{(1+a_1+a_2)} \tag{4.29}$$

Similar conditions on (4.26) are given below:

$$\gamma B_1 = \beta B_2 = \frac{B_3(1+a_1 \frac{B_2}{B_3})}{(1+a_1+a_2+n)} \tag{4.30}$$

These conditions will reduce to the same as given before in (4.5) through (4.8) when $\alpha = \beta$ and $B_1 = B_2 = B_3$ in the case of NPGA3 and when $\beta = \gamma$ and $B_1 = B_2 = B_3$ in the case of NNGA3. It is easy to show that the above conditions can be met easily in practice and if these are met, then the transfer functions given by (4.25) and (4.26) will reduce to the following:

$$G_a(s) = \mu_0 \frac{1+Ex+Ex^2}{1+Ex+Ex^2+Ex^3} \tag{4.31}$$

and

$$G_b(s) = -\mu_0 \frac{1+Ey+Ey^2}{1+Ey+Ey^2+y^3\{E-\frac{1}{\mu_0(\mu_0+1)^2}\}} \tag{4.32}$$

where

$$E = (1+\frac{a_1 B_2}{B_3})$$

$$x = \frac{\mu_0 s}{B_1}$$

and

$$y = \frac{(1+\mu_0)s}{B_1}$$

One can verify that (4.31) reduces to the same as given by (4.16) for equal GB products. It is reasonable to assume that the GB products of the OA's are equal for a given type of OA. However, this analysis shows that even if the values of the GB products are different, by properly choosing the resistor ratios, it is possible to compensate for the differences in the GB products. Thus, there is no loss of generality in assuming that the values of the GB products are equal. An interesting point to note is that when the GB products are equal, a positive unity gain amplifier can be realized with just 3 OA's and two resistors as shown in Fig. 4.6.

The above results have been reported in [34] and [38]. As discussed at length earlier, the value of E can be chosen as 5 in (4.31) and (4.32) to give a phase margin $\geq 45^\circ$. Once this choice is made, then the constants α, β and a_2 can be chosen to fix the nominal value of the d.c. gain and to satisfy the conditions given by (4.29) in the case of NPGA3. Similarly, the various parameters m, n, β and a_2 can be chosen to meet the d.c. gain requirement and the conditions of (4.30) for NNGA3. Let us now discuss a procedure for tuning these circuits.

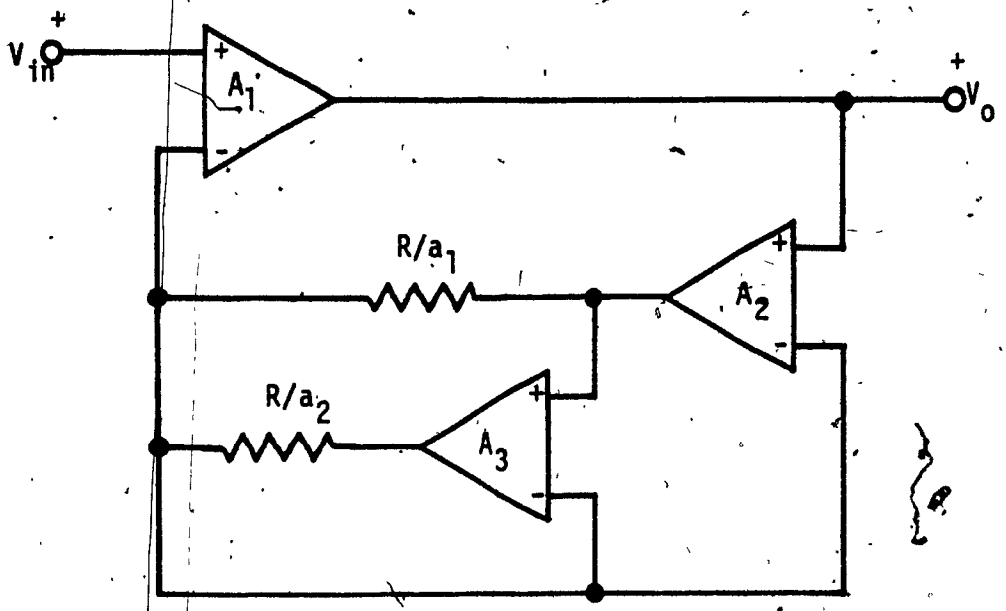

FIG. 4.6: Voltage Follower Circuit using NPGA3 Configuration with OA's Having Equal GB Products

4.5.1 Tuning Procedure

The d.c. gain requirement of μ_0 can be met by adjusting α and n in NPGA3 and NNGA3 respectively. Then setting a frequency such that

$$E\left(\frac{\mu_0\omega}{B_1}\right)^2 << 1 \quad \text{in the case of NPGA3}$$

and

$$E\left\{\frac{(\mu_0+1)\omega}{B_1}\right\}^2 << 1 \quad \text{in the case of NNGA3}$$

the value of β can be adjusted to give a zero phase shift between the input and output signals. Now at a frequency such that,

$$E\left(\frac{\mu_0\omega}{B_1}\right)^3 << 1 \quad \text{in the case of NPGA3}$$

and

$$E\left\{\frac{(\mu_0+1)\omega}{B_1}\right\}^3 << 1 \quad \text{in the case of NNGA3}$$

a_2 can be adjusted to give again a phase shift of zero between the input and output signals.

In order now to gain an idea as to the effectiveness of these circuits, we shall proceed to compare them with conventional as well as second order realizations.

4.6 COMPARISON OF THE 3 OA CIRCUITS WITH CONVENTIONAL AND SECOND ORDER FGA'S

It should be pointed out at the outset that the problem of relative stability in these structures does not depend on the nominal

value of d.c. gain, μ_0 as was the case in some of the second order realizations. These structures being the generalizations of NPGA2 and NNGA1 are useful for realizing any given d.c. gain value without having the problem of relative stability.

The next aspect that we have to consider is that of the bandwidth of the amplifier for a given permissible deviation in the magnitude and phase characteristics. One may recall that the function $F(\omega)$ given by (3.115) was derived independently of any amplifier configuration. Thus, this function can be used for the purposes of comparison. In the case of these new amplifiers, NPGA3 and NNGA3, the change in phase $(\Delta\phi)$, is of the order of $(\omega/B)^3$ whereas the per unit change in the magnitude $(\Delta\mu/\mu_0)$, from the nominal d.c. value is of the order of $(\omega/B)^4$. Obviously, when $(\omega/B) < 1$ the change in the phase, $\Delta\phi$ dominates over $(\Delta\mu/\mu_0)$ and the approximate value of $F(\omega)$ for NPGA3, can be derived as

$$F(\omega) = E \left(\frac{\mu_0\omega}{B}\right)^3 \tag{4.33}$$

and for NNGA3, we have

$$F(\omega) = H \left\{\frac{(\mu_0+1)\omega}{B}\right\}^3 \tag{4.34}$$

where

$$H = \left\{E - \frac{1}{\mu_0(\mu_0+1)^2}\right\}$$

At this point, it is obvious that, while the performance of conventional realizations and those of the second order realizations are affected by the first and second order terms of (ω/B), that is, by (ω/B) and $(\omega/B)^2$, respectively, our new amplifier circuits are affected only by the third order term of (ω/B), namely $(\omega/B)^3$. Clearly then, the third order structures should possess a wider bandwidth compared to those of the other ones. However, let us try to obtain a quantitative comparison by calculating the limiting frequencies as was done in Chapter III. Thus, limiting the $F(\omega)$ to be within a value, say $(1/\sigma)$, we can get the limiting frequencies and they are given by (4.35) and (4.36) for NPGA3 and NNGA3, respectively.

$$\omega_L = \frac{B}{\mu_0(E\sigma)^{1/3}} \tag{4.35}$$

$$\omega_L = \frac{B}{(\mu_0+1)(H\sigma)^{1/3}} \tag{4.36}$$

To get a more precise feeling about the performance of the new circuits, let us now consider only the non-inverting FGA's. Similar conclusions can be obtained about negative gain FGA's. Let $\sigma = 1000$. For the values of $\mu_0 = 1$, 1.55 and 3 (the same values were considered in Chapter III), the corresponding limiting frequencies are 0.0585B, 0.0385B and 0.0195B respectively. Now referring to Table 3.5, it can be noted that NPGA3 extends the operating frequency range by about 58.5 times in comparison to CPGA, whereas, under the same circumstances, NPGA2 improves the operating range only by about 31.6 times. This ratio

of 58.5 can be increased still further by choosing a smaller value for E , at the risk of poorer relative stability. In comparison with RPGA, referring again to Table 3.5, the improvement offered by NPGA3 will be 58.5 times for a d.c. gain of $\mu_0 = 1$, while it is 2.5 times for a d.c. gain of 1.55 . This ratio decreases with the increase in gain. However, one might recall from section 3.7 that RPGA has very poor relative stability for $\mu_0 > 2$.

It will be demonstrated in the following chapter that the changes in the phase and magnitude in the gain of the amplifiers affect the performance of the active filters differently. It turns out that these estimates in the case of CPGA and NPGA3 are on the pessimistic side. In actual applications this ratio of improvement in the bandwidth provided by NPGA3 will be more compared to the one provided by the second order realizations.

4.7 EXPERIMENTAL RESULTS

The positive gain amplifiers CPGA, RPGA, NPGA2 and NPGA3 were all constructed to realize a d.c. gain of $\mu_0 = 1.55$ by using μA741 OA's (Motorola) whose nominal GB products are 1 MHz and with fixed resistors of 1% accuracy. The theoretical frequency responses of both magnitude and phase characteristics are shown in Fig. 4.7. The experimental points are marked on these curves. It is seen that there is a good agreement between the theoretical predictions and the experimental results. However, there is a significant divergence between the two in the high frequency region particularly in the neighbourhood of $(\frac{\mu_0 \omega}{\beta}) = 1$. This is because of the second pole in the OA gain as mentioned in Chapter III.

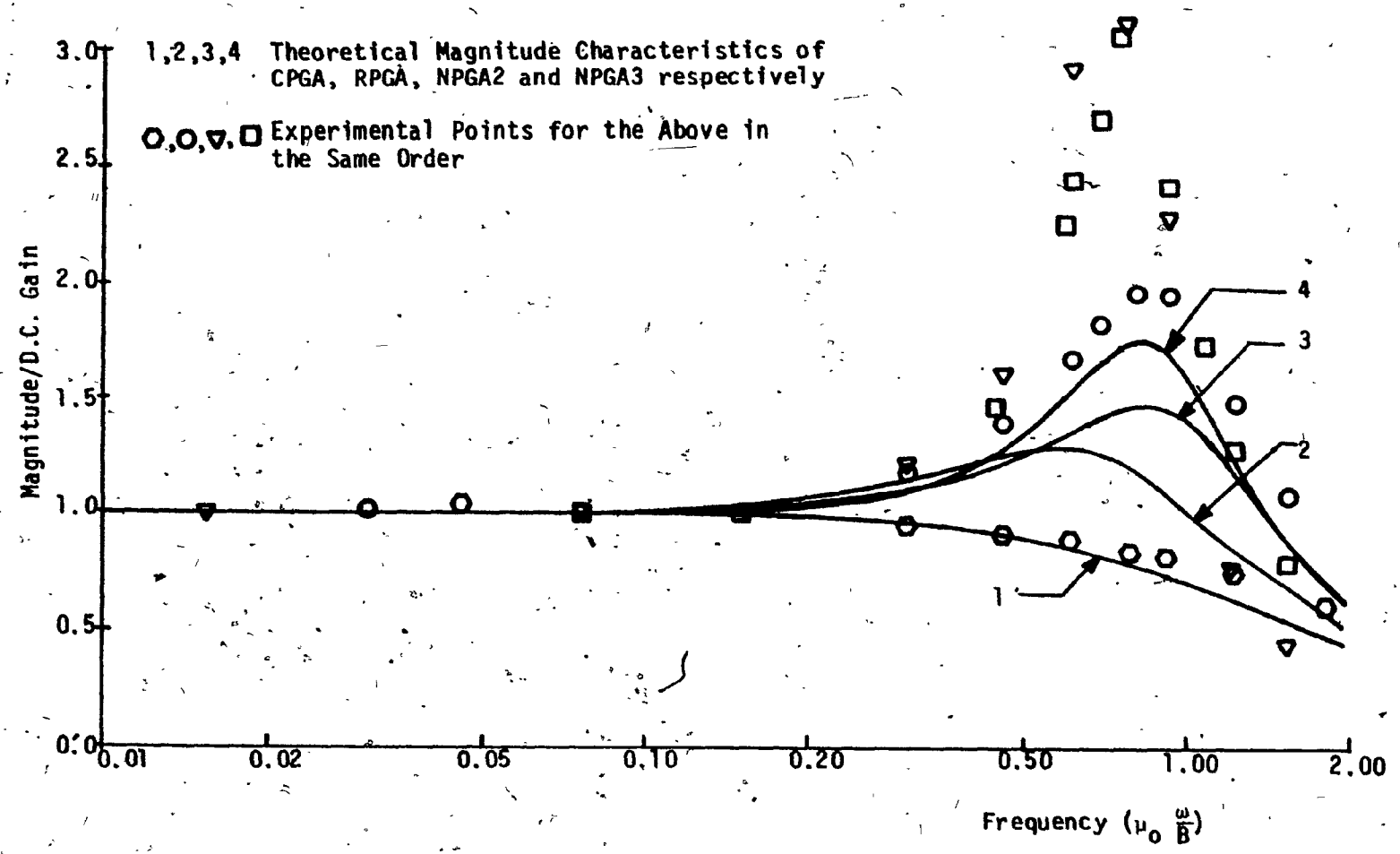

FIG. 4.7(a): Magnitude Characteristics of the Positive Gain Amplifiers with Single Pole Model for the OA's

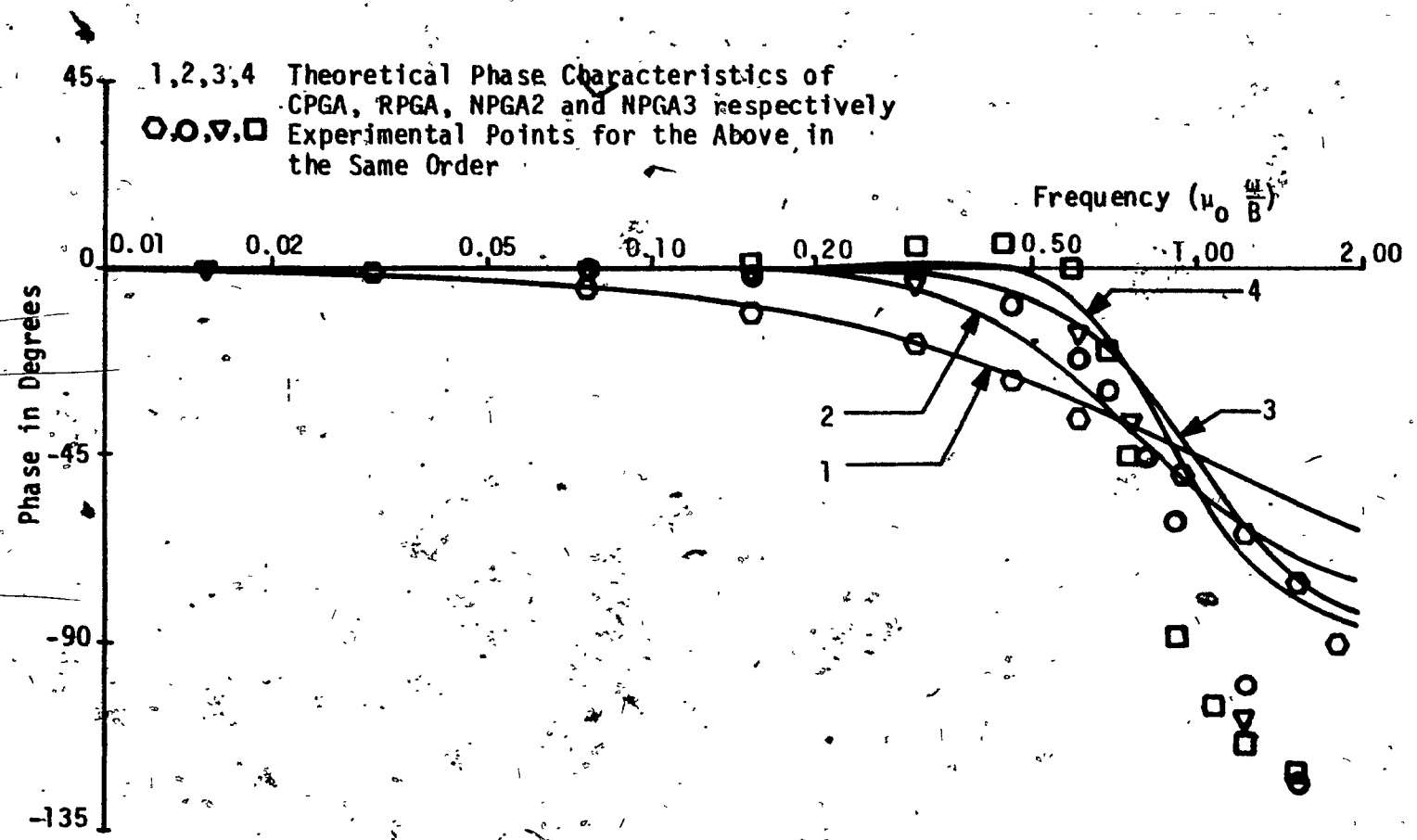

FIG. 4.7(b): Phase Characteristics of the Positive Gain Amplifiers with Single Pole Model for the OA's

Thus, this divergence can be explained with a two pole model of OA gain instead of the single pole model. This two pole model is discussed in [43] under a different context, wherein a simple method of measuring the second pole and the GB product of an OA has also been suggested. Using the method, the second poles and the GB products of the OA's were measured. The GB products of the OA's A_1, A_2 and A_3 in Fig. 4.5 were measured to be 1.04 MHz, 1.088 MHz and 1.055 MHz, respectively. The second poles of the OA's were measured to be 1.8 MHz, 1.95 MHz and 1.96 MHz, respectively, in the same order.

Incorporating the revised OA model with these values of the GB products and second poles, the theoretical magnitude and phase characteristics are shown in Fig. 4.8, where again the practically obtained points are marked on these curves. These figures still show a difference between the theory and experiment at the high frequency range. However, there is a closer agreement now. The apparent difference can be attributed to the measurement errors, especially in the measurement of the second poles, which in turn critically depends on the phase measurement in the high frequency range.

4.8 CONCLUSIONS

In this Chapter, two general structures, which employ 'n' OA's for realizing FGA's with an nth order transfer function have been examined. Though these amplifiers are stable by themselves, attention had to be restricted to $n = 3$ because of the requirements of the relative stability. A detailed analysis of the structures with $n = 3$ has been given. Comparisons have also been made with the conventional as well as the second order

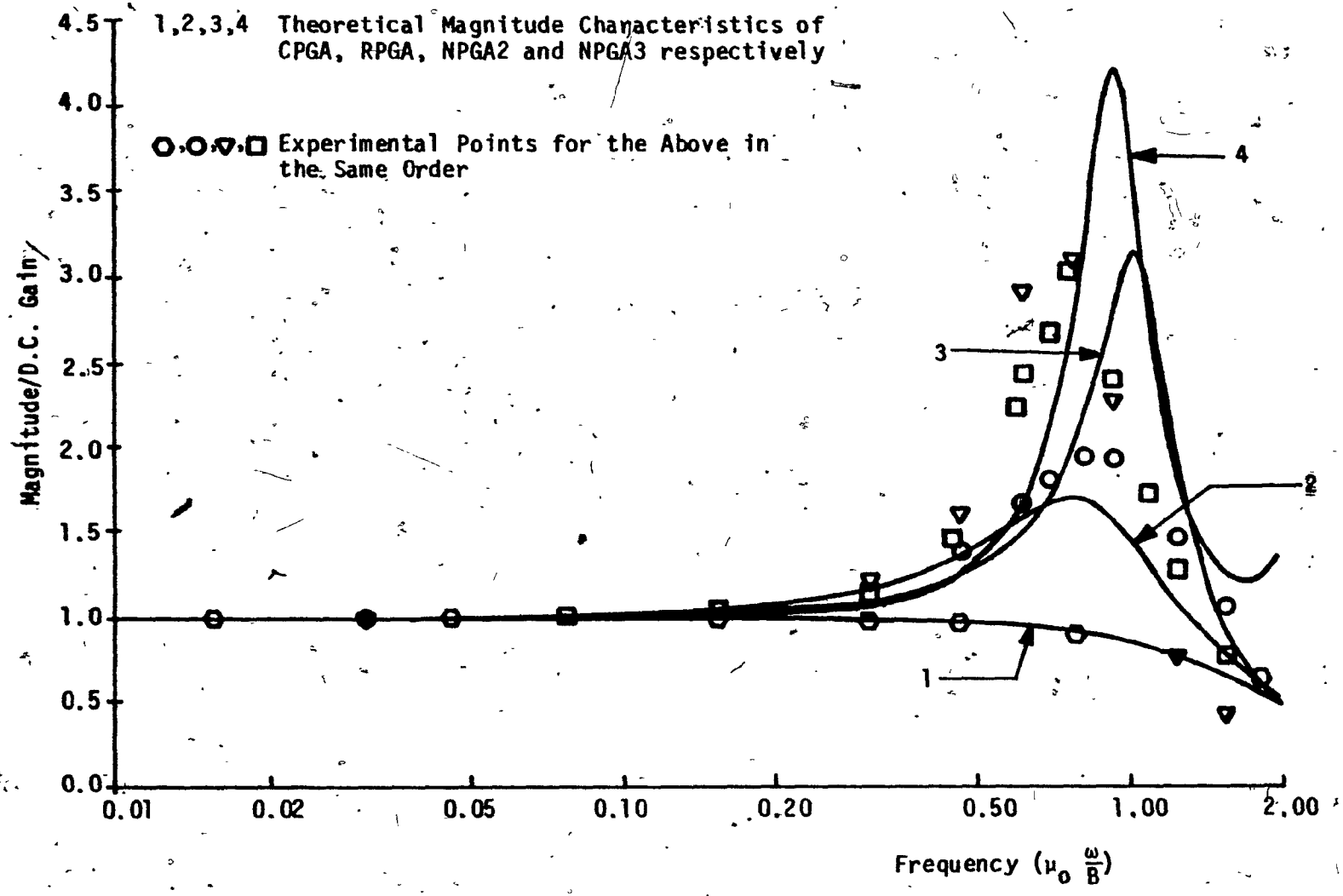

FIG. 4.8(a): Magnitude Characteristics of the Positive Gain Amplifiers with 2-Pole Model for the OA's

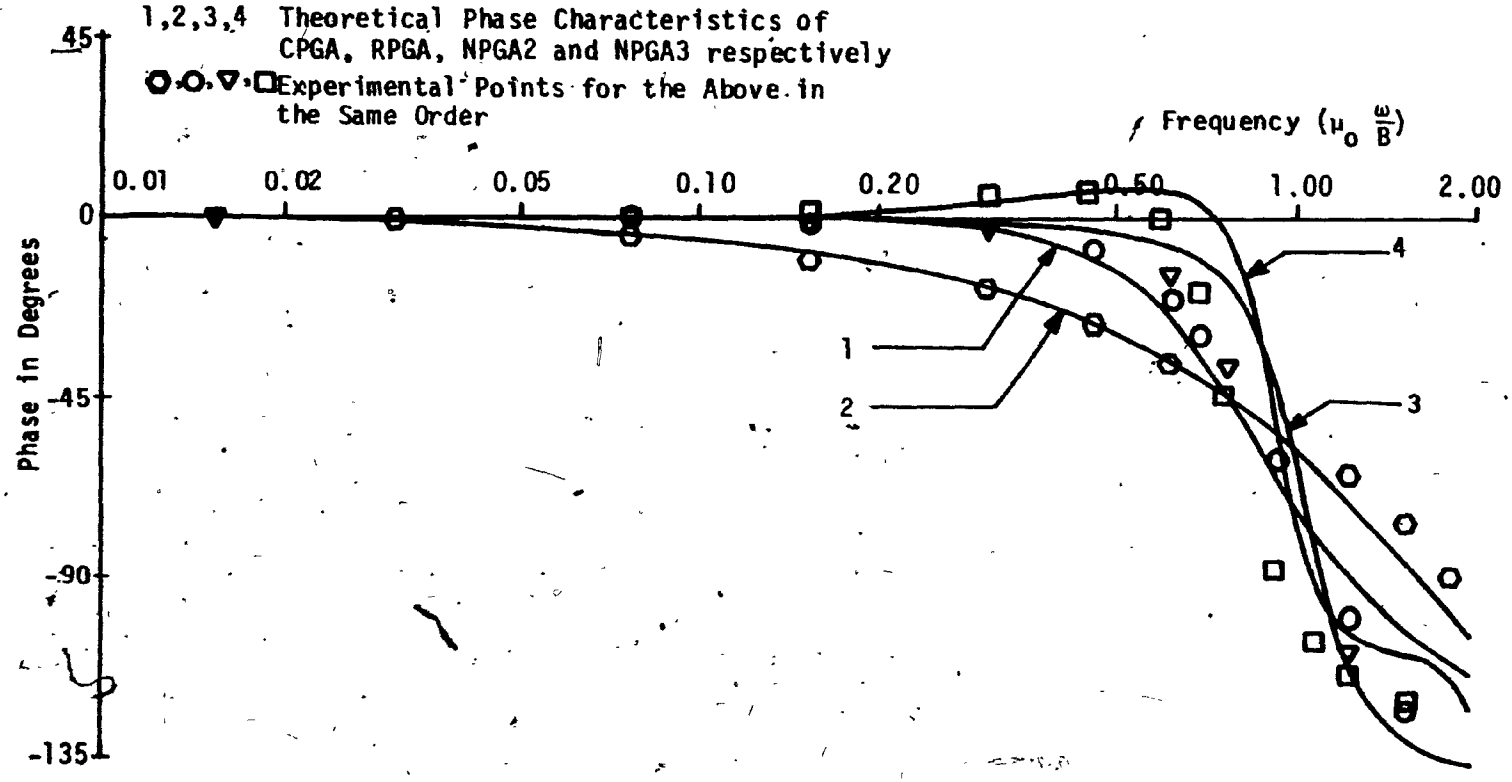

FIG. 4.8(b): Phase Characteristics of the Positive Gain Amplifiers with 2-Pole Model for the OA's

realizations. It is shown that these new structures improve the operating frequency range significantly over the ones provided by the other realizations. Experimental results of positive gain amplifiers have also been given to demonstrate the superiority of the new FGA's.

A major objective of this thesis, as discussed in the beginning, is to extend the operating frequency range of active-RC filters employing FGA's. Thus, to demonstrate the usefulness of these new amplifier circuits, it is appropriate to investigate the performance of some practical filters in which the new FGA's are used. This is the subject matter of the following chapter.

CHAPTER V

SOME APPLICATIONS OF FINITE GAIN AMPLIFIERS

5.1 INTRODUCTION

Several new procedures have been suggested in the preceding chapters for designing FGA's with an improved bandwidth. The improvement in their bandwidth should result in an extension of the operating frequency range of the circuits that employ them. The purpose of this chapter is to demonstrate this fact by considering a few applications of the FGA's in active-RC filters. It is shown that when the new amplifiers replace the conventional ones in the filter circuits, there is a substantial improvement in the operating frequency range of these filters.

5.2 SELECTING THE FILTER APPLICATIONS

The active filter circuits that employ the positive gain amplifiers are likely to have the best high frequency performance. This is because these circuits place the mildest requirements on the amplifiers used [5]. However, the highest operating frequency of even such filters, for reasonable changes in ω_p and Q_p, will be only a few kilo hertz, when the conventional amplifiers are used in these circuits. Even among the filter realizations employing positive gain amplifiers, it has been shown [44] that the effect of the GB products will be minimum, if the nominal value of the d.c. gain, μ_0 is as low as possible. This fact will later emerge in our derivations too. Obviously then, the realizations with unity gain amplifiers will be the ones where the effect of the GB

products will be minimum. Further, such filters are an important class by themselves. In addition, the realization of the unity gain amplifiers requires no additional resistors in the case of CPGA and NPGA2 and only two resistors in the case of NPGA3. Thus, these elements turn out to be more desirable than the realization of non-unity gain (>1) FGA's. Hence, we shall first consider the application of unity gain NPGA2 and NPGA3 (since RPGA can not realize an improved unity gain amplifier). For purposes of comparison, the unity gain CPGA is also included in our analysis.

In order to gain an insight into the applications of non-unity gain elements, a single amplifier filter circuit is also considered. As a by-product of the analysis in this chapter, a new method is also developed for comparing single amplifier filter circuits.

5.3 AN APPLICATION OF UNITY GAIN AMPLIFIERS*

Consider the circuit shown in Fig. 5.1. This circuit is due to Bach [7,8] and is a popular lowpass filter, which employs voltage followers as active elements. If the gains of the active elements are ideally equal to unity, the transfer function of the circuit can be derived to be

$$T(s) = \frac{\omega_p^2}{s^2 + (\frac{\omega_p}{Q_p})s + \omega_p^2} \qquad (5.1)$$

---

*The analysis given in this section is based on the materials given in [33] and [34].

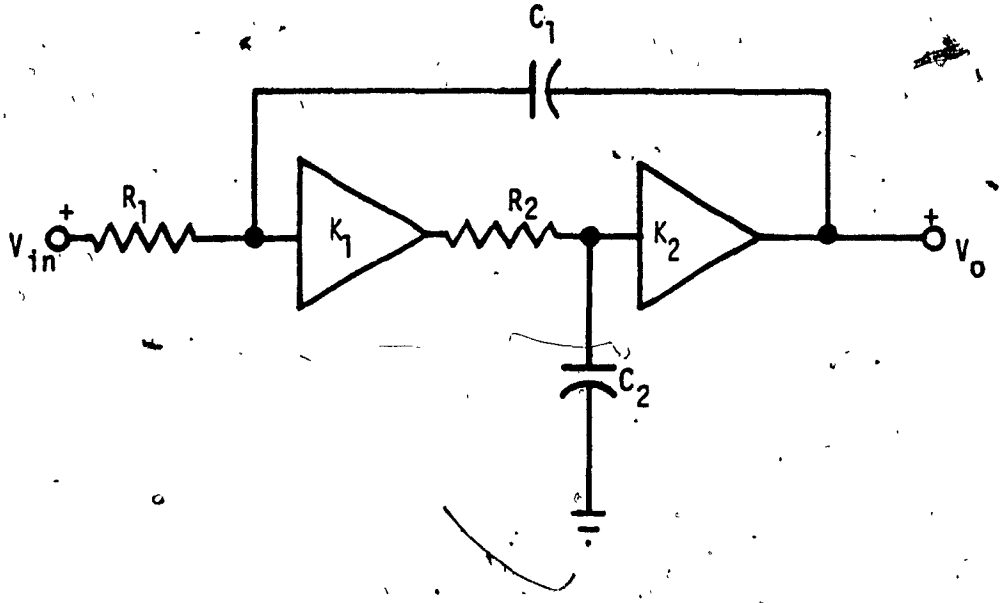

FIG. 5.1: Bach's Lowpass Filter

where ω_p and Q_p are the pole frequency and pole Q, respectively and they are given by

$$\omega_p = \frac{1}{\sqrt{R_1 R_2 C_1 C_2}} \tag{5.2}$$

and

$$Q_p = \sqrt{\frac{R_1 C_1}{R_2 C_2}} \tag{5.3}$$

If the gains K_1 and K_2 depart from unity, then the transfer function of this circuit becomes,

$$T_A(s) = \frac{K_1 K_2 \omega_p^2}{s^2 + \{(\frac{\omega_p}{Q_p}) + (1-K_1 K_2)\omega_p Q_p\}s + \omega_p^2} \tag{5.4}$$

To find the effect of the GB products of the OA's used in the realizations of the voltage followers, we shall assume that all passive components have been properly chosen so as to realize the given ω_p and Q_p. If the gains K_1 and K_2 are each realized with a single OA in the conventional way (CPGA's), we have

$$K_1 = \frac{1}{(1 + \frac{s}{B_1})} \quad \text{and} \quad K_2 = \frac{1}{(1 + \frac{s}{B_2})}$$

where B_1 and B_2 are the GB products of the OA's. For simplicity, let us assume that both the OA's have the same values of GB products,

say B . Then the transfer function given by (5.4) becomes as follows:

$$T_A(s) = \frac{\omega_p^2}{a_4 s^4 + a_3 s^3 + a_2 s^2 + a_1 s + a_0} \qquad (5.5)$$

where

$$a_4 = \frac{1}{B^2} \quad , \quad a_3 = \frac{2}{B} + \frac{\omega_p}{B^2}\left(Q_p + \frac{1}{Q_p}\right)$$

$$a_2 = 1+2\,\frac{\omega_p}{B}\left(Q_p + \frac{1}{Q_p}\right) + \left(\frac{\omega_p}{B}\right)^2$$

$$a_1 = \omega_p\left(\frac{1}{Q_p} + \frac{2\omega_p}{B}\right) \text{ and } a_0 = \omega_p^2$$

Extracting the dominant poles of the denominator polynomial of (5.5), the effective pole frequency, ω_{pe} and pole Q , Q_{pe} can be obtained. Thus following a procedure given in [5] and neglecting terms beyond second order, we get the expressions for ω_{pe} and Q_{pe} as follows (for $Q_p >> 1$):

$$\left(\frac{\omega_{pe}}{\omega_p}\right) \simeq \frac{1}{\sqrt{1+2x}} \qquad (5.6a)$$

and

$$\left(\frac{Q_{pe}}{Q_p}\right) \simeq \sqrt{1+2x} \qquad (5.6b)$$

where

$$x = \left(\frac{\omega_p Q_p}{B}\right) .$$

Now let us consider the case when the active elements are the unity gain amplifiers using the configuration of NPGA2. Again for simplicity, let us assume that all the OA's have the same GB products and the unity gain amplifiers are described by the following gain equation

$$K_1 = K_2 = \frac{1+\frac{s}{B}}{1+\frac{s}{B}+\frac{s^2}{B^2}} \tag{5.7}$$

Substitution of (5.7) in (5.4) gives the actual transfer function $T_A(s)$ as follows:

$$T_A(s) = \frac{(1+\frac{s}{B})^2\omega_p^2}{\sum_{i=0}^{6} a_i s^i} \tag{5.8}$$

where

$$a_6 = \frac{1}{B^4}, \quad a_5 = \frac{2}{B^3} + \frac{\omega_p}{B^4}(Q_p + \frac{1}{Q_p})$$

$$a_4 = \frac{3}{B^2} + \frac{2\omega_p}{B^3}(Q_p + \frac{1}{Q_p}) + \frac{\omega_p^2}{B^4}$$

$$a_3 = \frac{2}{B} + \frac{\omega_p}{B^2}(Q_p + \frac{3}{Q_p}) + 2\frac{\omega_p^2}{B^3}$$

$$a_2 = 1 + (\frac{2\omega_p}{Q_p B}) + 3\frac{\omega_p^2}{B^2}$$

$$a_1 = \omega_p(\frac{1}{Q_p} + \frac{2\omega_p}{B}) \quad \text{and} \quad a_0 = \omega_p^2$$

Following the same procedure as adopted in the previous case and neglecting terms beyond second order, the effective values of pole frequency, ω_{pe} and pole-Q, Q_{pe} are given as follows (for $Q_p \gg 1$):

$$\left(\frac{\omega_{pe}}{\omega_p}\right) \simeq \frac{1}{\sqrt{1-\frac{2\omega_p^2}{B^2}}} \tag{5.9a}$$

and

$$\left(\frac{Q_{pe}}{Q_p}\right) \simeq \frac{1}{(1-2x^2)} \tag{5.9b}$$

Let us now consider the case when the amplifiers used are NPGA3, namely, the 3 OA structures. When the GB products of the OA's are equal, the voltage followers are described by the gain equation, which is derived from (4.31) as

$$K_1 = K_2 \simeq \frac{(a+\frac{s}{B}+\frac{s^2}{B^2})}{(a+\frac{s}{B}+\frac{s^2}{B^2}+\frac{s^3}{B^3})} \tag{5.10}$$

where $a = \frac{1}{E}$.

As discussed earlier in Chapter IV a phase margin of 45° is chosen and hence the value of $E = 5$. This corresponds to a value of $a = 0.2$. Substituting (5.10) in (5.4) gives the actual transfer function, $T_A(s)$ as follows:

$$T_A(s) = \frac{(a + \frac{s}{B} + \frac{s^2}{B^2})^2 \omega_p^2}{\sum_{i=0}^{8} a_i s^i} \qquad (5.11)$$

where

$$a_8 = \frac{1}{B^6}, \quad a_7 = \frac{2}{B^5} + \frac{\omega_p}{B^6}\left(Q_p + \frac{1}{Q_p}\right)$$

$$a_6 = \frac{3}{B^4} + 2\frac{\omega_p}{B^5}\left(Q_p + \frac{1}{Q_p}\right) + \frac{\omega_p^2}{B^6}$$

$$a_5 = \frac{2(1+a)}{B^3} + \frac{\omega_p}{B^4}\left(2Q_p + \frac{3}{Q_p}\right) + \frac{2\omega_p^2}{B^5}$$

$$a_4 = \frac{(1+2a)}{B^2} + \frac{\omega_p}{B^3}\left\{2aQ_p + \frac{(1+a)}{Q_p}\right\} + \frac{3\omega_p^2}{B^4}$$

$$a_3 = \frac{2a}{B} + \frac{\omega_p}{B^2}\frac{(1+2a)}{Q_p} + 2(1+a)\frac{\omega_p^2}{B^3}$$

$$a_2 = a^2 + \frac{2a}{Q_p}\cdot\frac{\omega_p}{B} + \frac{(1+2a)\omega_p^2}{B^2}$$

$$a_1 = a^2\frac{\omega_p}{Q_p} + 2a\frac{\omega_p^2}{B}$$

and

$$a_0 = a^2\omega_p^2$$

As before, the effective values of pole frequency and pole Q can be derived and are given as follows (for $Q_p >> 1$):

$$\left(\frac{\omega_{pe}}{\omega_p}\right) \simeq \frac{1}{D} \qquad (5.12a)$$

and

$$\left(\frac{Q_{pe}}{Q_p}\right) \simeq \frac{D}{\{1+\frac{2Q_p}{a}\left(\frac{\omega_p}{B}\right)^3 - 2\left(\frac{Q_p}{a}\right)^2\left(\frac{\omega_p}{B}\right)^4\}} \tag{5.12b}$$

where

$$D = \{1-\left(\frac{Q_p}{a}\right)\left(\frac{\omega_p}{B}\right)^3 - \frac{2}{a^2}\left(\frac{\omega_p}{B}\right)^4\} \tag{5.12c}$$

Extensive computer simulations have been carried out to verify the expressions given by (5.6), (5.9) and (5.12). The expressions for the normalized changes in ω_p and Q_p can be obtained from the above equations. They are given below for the three cases in the same order, by (5.13) through (5.15).

$$\left(\frac{\Delta\omega_p}{\omega_p}\right) = \left(\frac{\omega_{pe}}{\omega_p}\right) - 1 \simeq \frac{-\left(\frac{\omega_p Q_p}{B}\right)}{\left(1+\frac{\omega_p Q_p}{B}\right)} \tag{5.13a}$$

and

$$\frac{\Delta Q_p}{Q_p} = \left(\frac{Q_{pe}}{Q_p} - 1\right) \simeq \frac{\omega_p Q_p}{B} \tag{5.13b}$$

when

$$\frac{\omega_p Q_p}{B} \ll 1 .$$

$$\left(\frac{\Delta\omega_p}{\omega_p}\right) \simeq \left(\frac{\omega_p}{B}\right)^2 \tag{5.14a}$$

$$\left(\frac{\Delta Q_p}{Q_p}\right) \simeq \frac{2\left(\frac{\omega_p Q_p}{B}\right)^2}{\left[1 - 2\left(\frac{\omega_p Q_p}{B}\right)^2\right]} \qquad (5.14b)$$

when

$$\left(\frac{\omega_p Q_p}{B}\right)^2 << 1 .$$

$$\left(\frac{\Delta\omega_p}{\omega_p}\right) \simeq \left(\frac{Q_p}{a}\right)\left(\frac{\omega_p}{B}\right)^3\left[1 - 2\left(\frac{Q_p}{a}\right)\left(\frac{\omega_p}{B}\right)\right] \qquad (5.15a)$$

$$\left(\frac{\Delta Q_p}{Q_p}\right) \simeq \left(\frac{Q_p}{a}\right)\left(\frac{\omega_p}{B}\right)^3\left[-3 + 2\left(\frac{Q_p}{a}\right)\left(\frac{\omega_p}{B}\right)\right] \qquad (5.15b)$$

when

$$\frac{Q_p}{a}\left(\frac{\omega_p}{B}\right)^3 << 1 .$$

The expressions (5.13) through (5.15) give an idea about the changes in ω_p and Q_p from their nominal values. For a given Q_p, the changes are of the orders of (ω_p/B), $(\omega_p/B)^2$ and $(\omega_p/B)^3$ in the three cases that use CPGA, NPGA2 and NPGA3, respectively.

Thus, we note that the frequency up to which the circuit can be employed without ω_p and Q_p exceeding a particular percentage variation from their nominal values, is extended by using NPGA 2 and considerably extended by employing NPGA3 over the one obtained by using CPGA. In order to obtain a meaningful and quantitative comparison of the circuits, we proceed as given in the following section.

5.3.1 Comparison of Bach's Filter using the Different Unity Gain Amplifiers

When there are changes in both ω_p and Q_p, as is the case when the filter uses CPGA and NPGA3, the maximum change in the magnitude of a high Q second order transfer function in the passband occurs at the 3 db points and is given by [15]

$$\left| \frac{\Delta|T|}{|T|} \right|_{max} = Q_p \left| \frac{\Delta\omega_p}{\omega_p} \right| + \frac{1}{2} \left| \frac{\Delta Q_p}{Q_p} \right| \qquad (5.16)$$

When the normalized change in ω_p is negligible and the change in Q_p is considerable, as it happens to be the case when the NPGA2's are used in the network, the maximum change in the transfer function occurs at the center frequency and is given by [15]

$$\left| \frac{\Delta|T|}{|T|} \right|_{max} = \left| \frac{\Delta Q_p}{Q_p} \right| \qquad (5.17)$$

Further, it may be noted that the normalized changes in ω_p and Q_p are of the same order in (5.13) and (5.15). Thus in these cases for $Q_p >> 1$, (5.16) can be further simplified as given below:

$$\left| \frac{\Delta|T|}{|T|} \right|_{max} \approx Q_p \left| \frac{\Delta\omega_p}{\omega_p} \right| \qquad (5.18)$$

Let the deviation in the magnitude response of the filter in the passband be constrained to be within x%. Let ω_{pc}, ω_{pn} and ω_{pN} be the maximum operating frequencies that can be obtained employing CPGA, NPGA2 and NPGA3, respectively, under the above constraint. Then, one can find

that

$$\omega_{pc} \cong \frac{xB}{100\, Q_p^2} \tag{5.19}$$

$$\omega_{pn} \cong \frac{B}{Q_p} \left\{\frac{x}{(200+2x)}\right\}^{1/2} \tag{5.20}$$

and

$$\omega_{pN} \cong B \left\{\frac{xa}{100\, Q_p^2}\right\}^{1/3} \tag{5.21}$$

Hence,

$$\left(\frac{\omega_{pn}}{\omega_{pc}}\right) \cong Q_p \left\{\frac{100}{2x}\right\}^{1/2} \tag{5.22}$$

and

$$\left(\frac{\omega_{pN}}{\omega_{pc}}\right) \cong \left\{\frac{a\, 10^4\, Q_p^4}{x^2}\right\}^{1/3} \tag{5.23}$$

For the filter performance to be acceptable, $x \ll 100$. Thus, from (5.22) and (5.23), it is clear that a considerable improvement can be achieved in the maximum operating frequency of the filter by using NPGA2 and NPGA3, even for moderate values of Q_p. To cite a particular example, when $Q_p = 10$ and $x = 10$, the ratios given by (5.22) and (5.23) are 22.3 and 58.5 respectively. Thus the maximum operating frequency of the filter using NPGA2 is 22.3 times the one that can be obtained by using conventional voltage followers. This ratio is increased to 58.5 times when we employ NPGA3. To put these figures

into proper perspective, it should be noted that in order to obtain a comparable performance from the conventional designs of voltage followers, the OA's that are used in these designs, should have a value of GB product equal to 22.3 times that of the OA's employed in NPGA2 and 58.5 times that of the OA's employed in NPGA3.

5.3.2 Experimental Results

The Bach's lowpass filter circuit with a nominal value of $Q_p = 10$ was constructed and tested with all the three types of voltage followers. The Texas instrument μA741 OA's along with resistors of 1% accuracy and capacitors with 5% accuracy were used in the circuit. The GB products of the OA's were about $2\pi \times 10^6$ rads/sec. With this value of GB product, the values of f_{pc}, f_{pn} and f_{pN} are calculated to be 1 KHz, 22.3 KHz and 58.5 KHz, respectively, for a maximum permissible deviation of 10% of the transfer function magnitude in the passband of the filter characteristic. The voltage followers using the configuration of NPGA2 were realized with just two OA's and those using the configuration of NPGA3 were realized with just three OA's and two resistors as shown in Fig. 4.6. No attempt was made to compensate for the unequal GB products of the OA's.

The theoretical magnitude characteristics are shown in Fig. 5.2(a) with a nominal value of the pole frequency, $f_p = 5$ KHz, along with the experimentally obtained values marked on them.

We note from these characteristics that even though $(f_p/B) = 0.005$, the change in f_p of the realized filter characteristic with the use of CPGA's is about 5% from the ideally expected value and this amounts to a

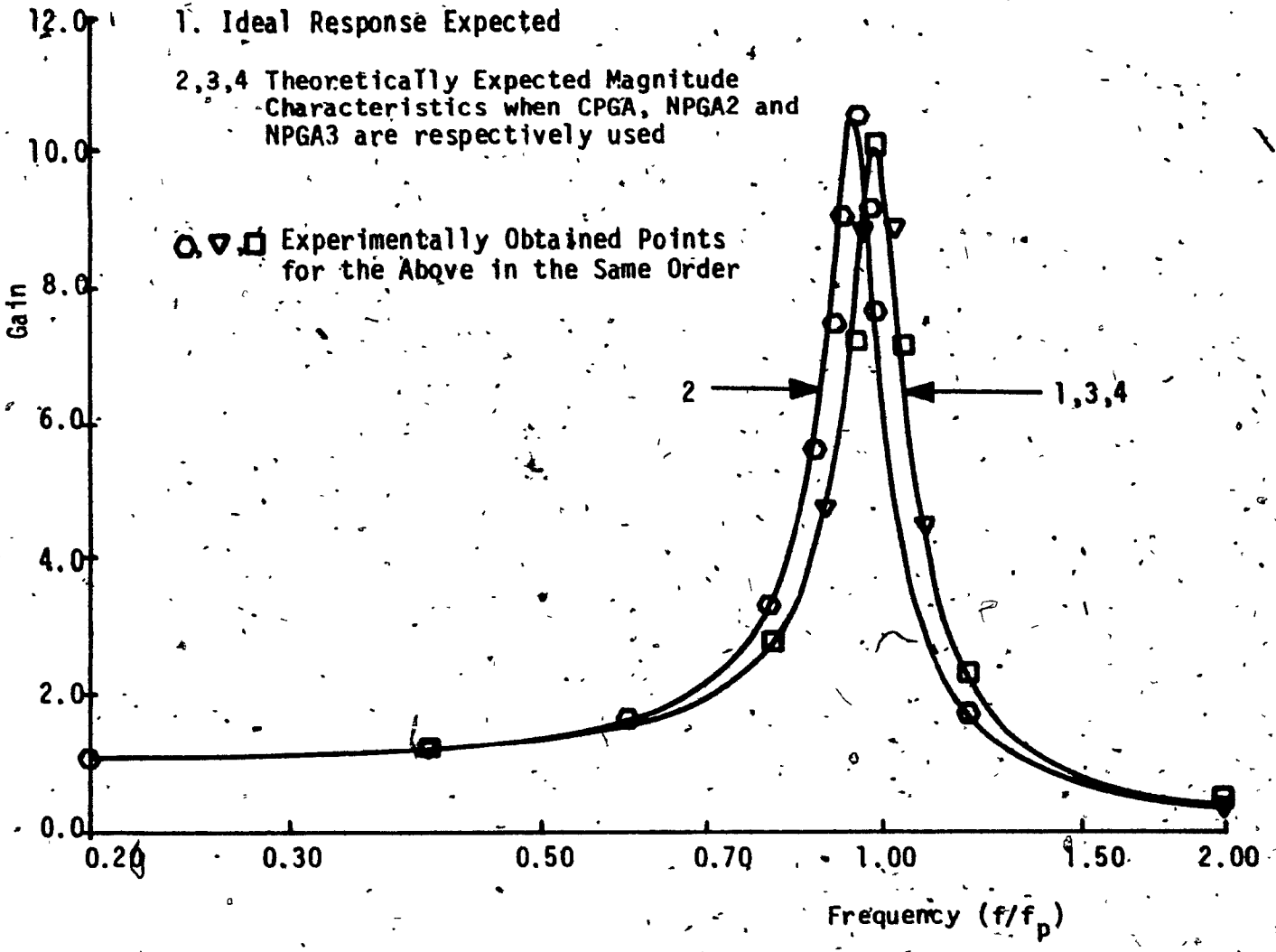

FIG. 5.2(a): Magnitude Characteristics of Bach's Lowpass Filter with a Nominal Value of f_p = 5 KHz

change of 50% in the required bandwidth. On the other hand, the magnitude characteristics obtained with the use of NPGA2 and NPGA3 follow almost exactly the desired ideal characteristic.

Another set of readings were taken at a nominal pole frequency of 25 KHz . The theoretically expected magnitude characteristics along with the experimental points are shown in Fig. 5.2(b). From this figure one can easily visualize the total failure of the circuit employing CPGA. Also, the characteristic of the circuit using NPGA2 exceeds the specified deviation in the transfer function magnitude at the center frequency; the change being approximately 14.5% instead of 10% . This Q-enhancement becomes more prominent with increasing values of f_p . However, the filter characteristic with the use of NPGA3 follows again the ideally expected characteristic almost exactly.

Finally, a set of readings were taken at f_p = 50 KHz to compare the performances of NPGA2 and NPGA3. The results are shown in Fig. 5.2(c). One can easily see the severe Q-enhancement in the filter characteristic obtained with NPGA2. It can also be observed that even though we are near the theoretically predicted maximum frequency, the filter characteristic obtained by using NPGA3 is very close to the ideal characteristic desired. These results serve to demonstrate the superiority of NPGA3 over the other configurations of positive gain amplifiers.

From the theoretical study and the experimental verifications of the above filter characteristics, it can be noted that the use of NPGA2 increases the operating frequency range of the filter by an order of magnitude compared to the one that can be obtained with the use of

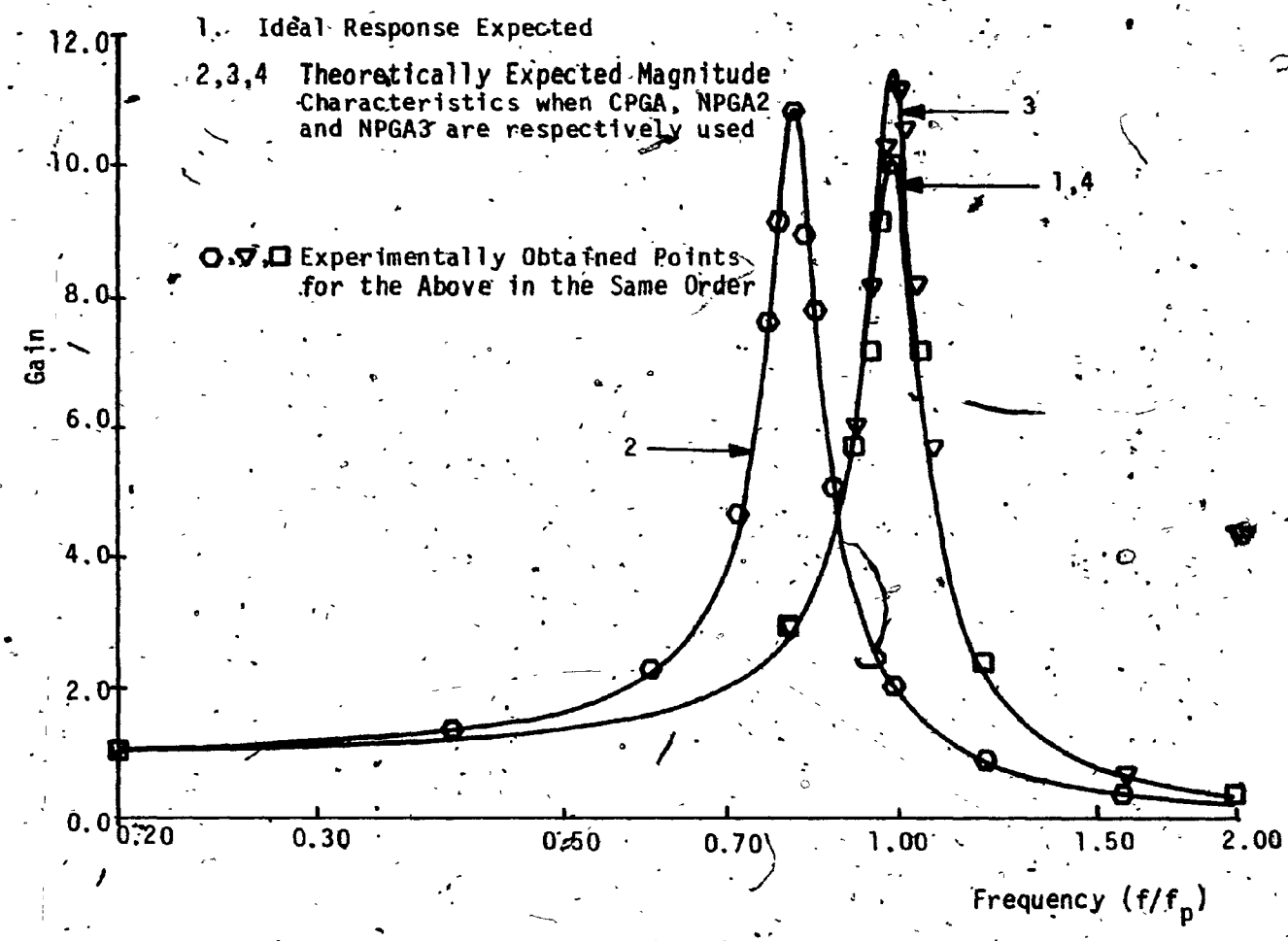

FIG. 5.2(b): Magnitude Characteristics of Bach's Lowpass Filter with a Nominal Value of f_p = 25 KHz

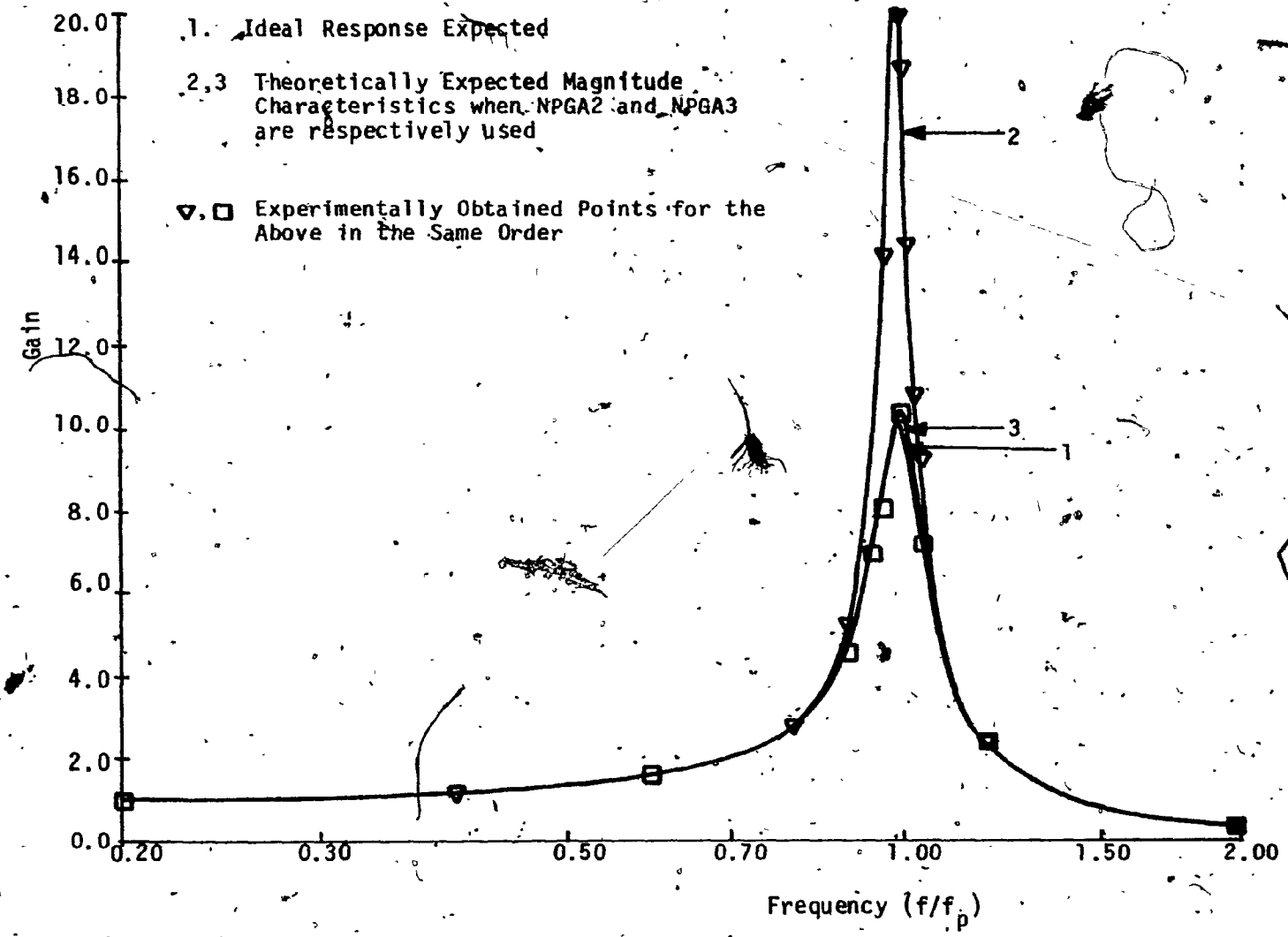

FIG. 5.2(c): Magnitude Characteristics of Bach's Lowpass Filter with a Nominal Value of f_p = 50 KHz

CPGA. The use of NPGA3 increases the frequency range still further and the maximum operating frequency is increased to about 58.5 times the one that can be obtained with the use of CPGA. This is about 3 times higher than the one that can be obtained with the use of NPGA2. Thus, among all the amplifier configurations, NPGA3 gives the maximum operating frequency. With this conclusion, let us proceed to the next section to consider another application wherein we can compare the performance of RPGA also along with these configurations.

5.4 AN APPLICATION OF NON-UNITY ($\mu_0 > 1$) POSITIVE GAIN AMPLIFIERS*

The filter circuit shown in Fig. 5.3 is a bandpass filter due to Sallen and Key [6]. Such filters are extensively used in practice. In this case also, let us assume that the passive components and the nominal value of the d.c. gain, μ_0 are properly chosen to realize a particular pole frequency, ω_p and pole-Q factor, Q_p. The design of this circuit is entirely based on [3]. If the amplifier gain is real and equal to μ_0, the circuit will realize an ideal second order bandpass transfer function, given by the following equation:

$$T(s) = \frac{\mu_0 \omega_p s}{\{s^2 + (\frac{\omega_p}{Q_p})\, s + \omega_p^2\}} \qquad (5.24)$$

---

*The material presented in this section is based on [38].

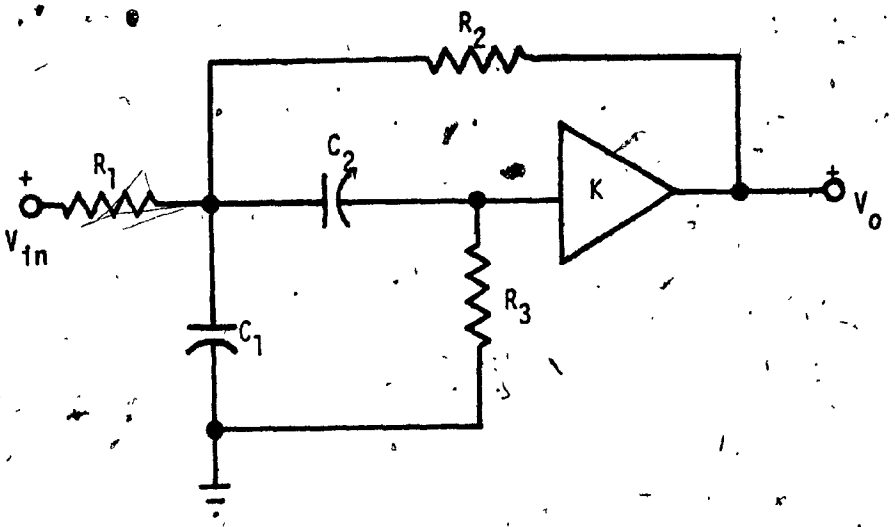

FIG. 5.3: Sallen and Key Bandpass Filter

For the filter circuit that is now considered, the equation (5.24) can be written in the following form where the gain of the finite gain amplifier is expressed explicitly.

$$T(s) = \frac{K\omega_p s}{\{s^2 + a\omega_p s + \omega_p^2 - bK\omega_p s\}} \qquad (5.25)$$

where the constants a and b depend upon the design; and

$$Q_p = \frac{1}{(a - b\mu_0)}$$

and where ω_p, Q_p and μ_0 are nominal values of the pole frequency, pole Q-factor and the gain of the amplifier, respectively. To generalize the analysis, let us now substitute (3.127) in (5.25). Then, the transfer function for the real frequencies becomes

$$T(j\omega) = \frac{-j\omega\omega_p\mu e^{j\phi}}{\{\omega_p^2 - \omega^2 + ja\omega\omega_p - jb\omega\omega_p\mu e^{j\phi}\}} \qquad (5.26)$$

In filter applications, as discussed earlier, one is mainly interested in the change in magnitude of the transfer function and thus we are interested in limiting this change to be within a specified value in the entire passband of the filter. Towards that end, we will have to find the normalized per unit change in $|T|$ and this will be a function of ω. For small changes in $|T|$, we can write

$$\frac{\Delta|T|}{|T|} = \frac{1}{|T|}\left[\left.\frac{\partial|T|}{\partial\mu}\right|_{\substack{\mu=\mu_0\\ \phi=0}} \Delta\mu + \left.\frac{\partial|T|}{\partial\phi}\right|_{\substack{\mu=\mu_0\\ \phi=0}} \Delta\phi\right] \tag{5.27}$$

Thus, for the transfer function given by (5.26), we get

$$\frac{\Delta|T|}{|T|} = F_1(\omega)\left(\frac{\Delta\mu}{\mu_0}\right) + F_2(\omega)\,\Delta\phi \tag{5.28}$$

where

$$F_1(\omega) = \left\{1 - \frac{\mu_0 b(a-\mu_0 b)\left(\frac{\omega}{\omega_p}\right)^2}{\left[\left\{1-\left(\frac{\omega}{\omega_p}\right)^2\right\}^2 + (a-b\mu_0)^2\left(\frac{\omega}{\omega_p}\right)^2\right]}\right\}$$

and

$$F_2(\omega) = \frac{-b\mu_0\left\{1-\left(\frac{\omega}{\omega_p}\right)^2\right\}\left(\frac{\omega}{\omega_p}\right)}{\left[\left\{1-\left(\frac{\omega}{\omega_p}\right)^2\right\}^2 + (a-b\mu_0)^2\left(\frac{\omega}{\omega_p}\right)^2\right]}$$

We find that $F_1(\omega)$ reaches its maximum at ω_p and this maximum value is

$$|F_{1max}| \cong b\mu_0 Q_p \tag{5.29}$$

whereas $F_2(\omega)$ reaches its maximum at $\omega_p\left(1 \pm \frac{1}{2Q_p}\right)$ (3 db frequencies) in the passband and its maximum value is

$$|F_{2max}| = \frac{b\,\mu_0\,Q_p}{2} \tag{5.30}$$

Thus we can write from (5.28),

$$\left|\frac{\Delta|T|}{|T|}\right|_{max} \leq |F_{1max}| \left|\frac{\Delta\mu}{\mu_0}\right| + |F_{2max}| \, |\Delta\phi| \tag{5.31}$$

Now we can substitute the expressions for $(\frac{\Delta\mu}{\mu_0})$ and $(\Delta\phi)$, evaluated at $\omega = \omega_p$, for the different amplifier configurations in (5.31) and determine the maximum ω_p in each case such that $|\Delta|T|/|T||_{max}$ does not exceed a particular value, say $x\%$.

Before doing that, it is useful to recall that, in the case of CPGA and NPGA3, the phase change $(\Delta\phi)$ affects the performance of the amplifier characteristics predominantly. Thus, in these two cases, we get

$$\left|\frac{\Delta|T|}{|T|}\right|_{max} \cong |F_{2max}| \, |\Delta\phi| \tag{5.32}$$

The magnitude change $(\frac{\Delta\mu}{\mu_0})$ is the predominant factor in changing the amplifier characteristics of NPGA1, NPGA2, and RPGA. In case $\mu_0 < 2$, NPGA1 is not realizable and when $\mu_0 \geq 2$, the analysis of NPGA1 and that of NPGA2 are same. In any case, in such cases where $(\frac{\Delta\mu}{\mu_0})$ is predominant, we get

$$\left|\frac{\Delta|T|}{|T|}\right|_{max} \cong |F_{1max}| \left|\frac{\Delta\mu}{\mu_0}\right| \tag{5.33}$$

At this point, it should be noted that (5.32) or (5.33), as the case may be, is not only applicable to the application that is considered now, but also to any other filter for which the decomposition indicated in the denominator of (5.25) is valid. This includes a large variety of single amplifier lowpass, highpass and bandpass Sallen and Key type of filters. Let us now proceed to compare the performances of the different amplifier configurations by obtaining the maximum ω_p's with the use of (5.32) or (5.33) as the case may be.

5.4.1 Comparison of the Sallen and Key Filter Circuits using the Different Amplifier Configurations

Proceeding to find the maximum ω_p's, we can write from (5.32) and (5.33)

$$|\Delta\phi| \leq \frac{2x}{(100\ \mu_o bQ_p)} \tag{5.34}$$

and

$$\left|\frac{\Delta\mu}{\mu_o}\right| \leq \frac{x}{(100\ \mu_o bQ_p)} \tag{5.35}$$

in the appropriate cases. At this stage, let us recall a statement, made earlier in section (4.6), that the phase and magnitude changes in the amplifier characteristics affect differently the performance of the filter circuit. This is evident by comparing (5.34) and (5.35). However, the comparison that was made earlier in sections (3.8) and (4.6) as to the bandwidths depended on the change in the transfer function $(\frac{\Delta T}{T})$, whereas

here the maximum operating frequency, that is of interest, is based on the change $\left(\frac{\Delta|T|}{|T|}\right)$. It is easy to show that

$$\left|\frac{\Delta|T|}{|T|}\right| \leq \left|\frac{\Delta T}{T}\right|$$

This is the reason why the estimates in the cases of CPGA and NPGA3 turn out to be pessimistic.

The changes $\Delta\phi$ for CPGA and NPGA3 are available from Table 3.3 and (4.33) respectively. The changes $(\Delta\mu/\mu_o)$ are available from Table 3.3 for both NPGA2 and RPGA. Using these changes and (5.34) and (5.35), we can find the maximum ω_p's that can be obtained in each case. Let ω_{pc}, ω_{pR}, ω_{pn} and ω_{pN} be the maximum operating frequencies obtained by using CPGA, RPGA, NPGA2 and NPGA3, respectively, in the filter circuit. Then, they are given by the following:

$$\omega_{pc} \cong \left(\frac{B}{\mu_o}\right) \frac{2x}{(100\ \mu_o bQ_p)} \tag{5.36}$$

$$\omega_{pR} \cong \left(\frac{B}{\mu_o}\right) \left\{\frac{(\mu_o-1)x}{(100\ \mu_o bQ_p)}\right\}^{1/2} \tag{5.37}$$

$$\omega_{pn} \cong \left(\frac{B}{\mu_o}\right) \left\{\frac{x}{100\ \mu_o bQ_p}\right\}^{1/2} \tag{5.38}$$

and

$$\omega_{pN} \approx \left(\frac{B}{\mu_{o}}\right) \left\{\frac{2x}{100\, E\mu_{o} bQ_{p}}\right\}^{1/3} \qquad (5.39)$$

where $E=5$ and $\mu_{o} bQ_{p} >> 1$ in practice.

Since $\{x/(100\ \mu_{o} bQ_{p})\}$ is a small fraction, it is evident from (5.36) through (5.39) that the maximum operating frequencies of the filter circuit using NPGA2 and RPGA will be higher compared to the one obtained with the use of CPGA. Further, the greatest increase in the maximum operating frequency is attained using NPGA3. To quote an example, taking the design given in [3] for our network, $Q_{p} = 10$ and $\mu_{o} = 1.55$, $\mu_{o} bQ_{p} = 46.5$. Suppose, the value of x is fixed as 10, as was done in the previous application, then we get

$$\left.\begin{aligned} f_{pC} &= 2.8 \text{ KHz} \\ f_{pR} &= 22.2 \text{ KHz} \\ f_{pn} &= 29.9 \text{ KHz} \end{aligned}\right\} \qquad (5.40)$$

and

$$f_{pN} = 61.35 \text{ KHz}$$

The value of B in the evaluation of each of the above has been assumed to be $2\pi \times 10^{6}$ rad/sec, which is typical of the GB product values of μA741. However, computer simulations show that these values are 2.8 KHz, 21.5 KHz, 28.5 KHz and 52.5 KHz respectively for CPGA, RPGA, NPGA2 and NPGA3. These results are quite close to the predicted ones except in the last case. The error in the last case is due to the fact that the magnitude error $(\Delta\mu/\mu_{o})$, which has been neglected, also

contributes to some extent, especially at high frequencies.

5.4.2 Experimental Results

The Sallen and Key filter circuit employing CPGA, RPGA, NPGA2 and NPGA3, were all realized by using Motorola μA741C OA's with a nominal value of the GB product equal to $2\pi \times 10^6$ rads/sec. The circuits were built with 1% resistors and 5% capacitors to realize a nominal value of $Q_p = 10.0$. The theoretically expected magnitude characteristics will all the four amplifiers along with the ideally expected characteristic with a nominal pole frequency of $f_p = 10$ KHz are shown in Fig. 5.4 (a). Experimentally obtained points are marked on these curves. It can be seen that the magnitude characteristic with the use of CPGA is widely different from the ideally expected one, whereas the characteristics of the filter circuit employing RPGA, NPGA2 and NPGA3 closely follow the ideal one. Another set of characteristics at a nominal value of $f_p = 25$ KHz are shown in Fig. 5.4(b). At this frequency also, the characteristic using CPGA in the filter circuit differs widely from the ideal characteristic. The performance of the circuit employing RPGA exceeds the specified maximum deviation of 10% from the ideal characteristic. The characteristic with the use of NPGA2 also deviates from the ideal one. However, the maximum deviation is well within 10%. The one with NPGA3 closely follows the desired characteristic. A final set of characteristics were obtained at $f_p = 50$ KHz and these are given in Fig. 5.4(c). At this frequency no meaningful result could be obtained using CPGA and the filter with RPGA simply oscillated due to severe Q enhancement, even after grounding the input. Thus, the characteristics with NPGA2 and NPGA3 are only given

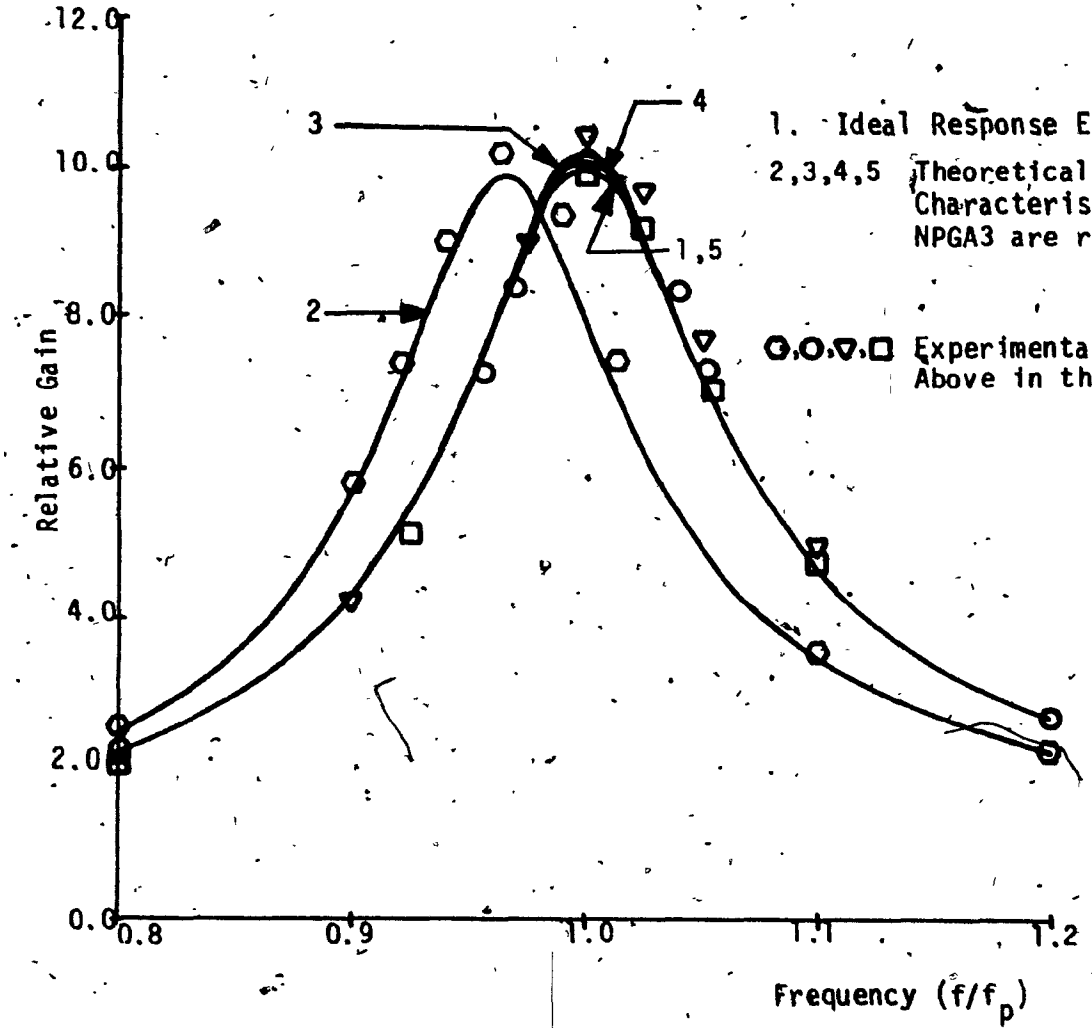

FIG. 5.4(a): Magnitude Characteristics of Salien and Key Bandpass Filter with a Nominal Value of f_p = 10 KHz

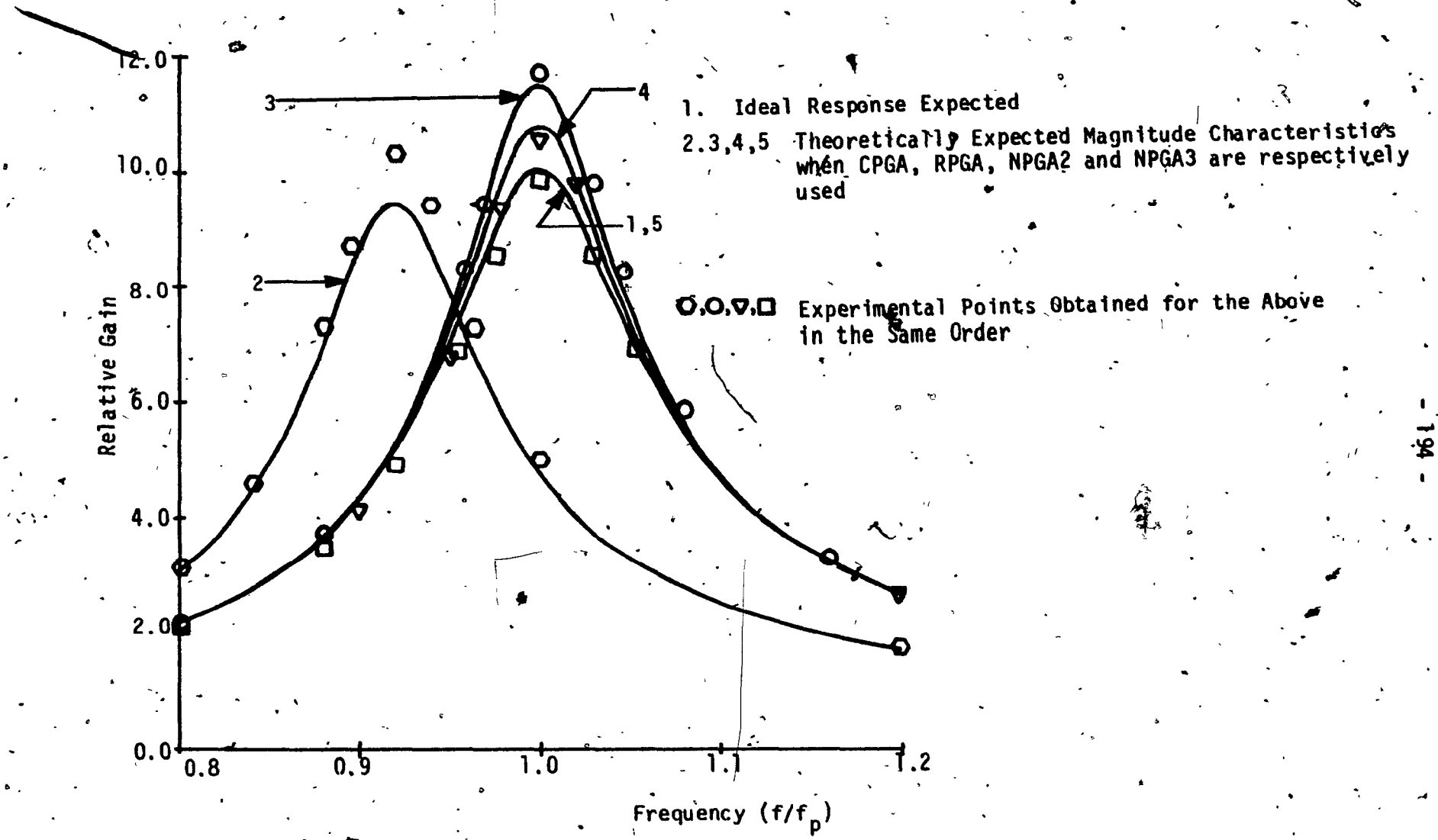

FIG. 5.4(b): Magnitude Characteristics of Sallen and Key Bandpass Filter with a Nominal Value of f_p = 25 KHz

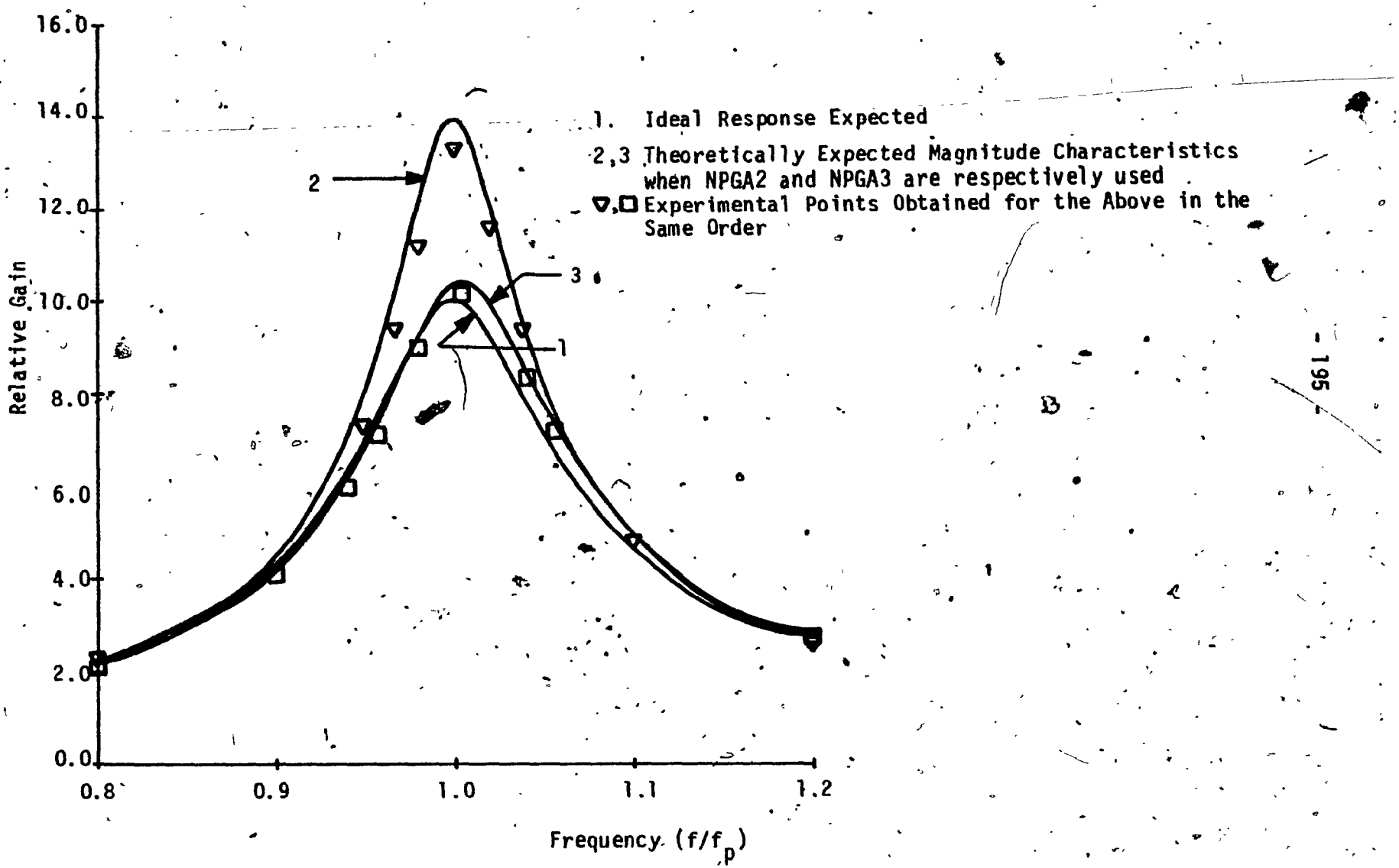

FIG. 5.4(c): Magnitude Characteristics of Sallen and Key Bandpass Filter with a Nominal Value of f_p = 50 KHz

along with the ideal one. The experimental points are marked on these curves. It is remarkable, however, to observe that at this frequency too, the filter characteristic with the use of NPGA3 follows quite closely the ideal characteristic. The above results again convincingly demonstrate the superiority of NPGA3 over other amplifier realizations.

The filter characteristics were obtained with an input signal of 10 mv . The d.c. supply voltages to the OA's were maintained at ±12 V . At this stage, it is resonable to inquire into the signal handling capability of these filter circuits. This will be discussed at length in the next section. Now we shall examine the effect of power supply voltage variations on the filter responses. The power supply voltages were increased from ±12 VDC to ±18 VDC . Over this range, the GB product changed, on an average by 11% . The changes in the effective pole frequencies and pole-Q factors were measured for all the filters at f_p = {10, 25} and 50 KHz . These results are given in Tables 5.1(a), 5.1(b) and 5.1(c) .

Before taking a close look at these figures, let us recall a comment made by Mostchytz [15] that "frequency stability is far more (at least 20 times more) crucial, for both amplitude and phase response of a second order network than the Q stability". Examining now Table 5.1(a) with f_p = 10 KHz , we observe that the percentage change in f_p for the filter circuit with CPGA is the worst compared to all other filter circuits. The combined effect of the changes in both f_p and Q_p is much lower in the case of the filters using NPGA2 and NPGA3 than in the ones corresponding to RPGA and CPGA. However, it may be noted that if frequency stability alone is of consideration, then the circuit

TABLE 5.1(a). THE EFFECT OF SUPPLY VOLTAGE VARIATIONS ON THE SALLEN AND KEY FILTER RESPONSES

Nominal pole frequency, f_p = 10 KHz

Nominal pole-Q, Q_p = 10.0

Amplifier Configuration with which the filter is realized	Measured effective pole frequency, f_{pe} at ±12 V (KHz)	Measured effective pole-Q, Q_{pe} at ±12 V	With increase in supply voltage from ±12 V to ±18 V	
			Measured % age change in f_{pe}	Measured % age change in Q_{pe}
CPGA	9.634	10.39	0.26	0.29
RPGA	10.002	10.33	0	1:16
NPGA2	10.008	10.0	0.07	0.25
NPGA3	10.005	10.0	0.07	0.025

TABLE 5.1(b). THE EFFECT OF SUPPLY VOLTAGE VARIATIONS ON THE SALLEN AND KEY FILTERS RESPONSES

Nominal pole frequency, f_p = 25 KHz

Nominal pole-Q, Q_p = 10.0

Amplifier Configuration with which the filter is realized	Measured effective pole frequency, f_{pe} at ±12V (KHz)	Measured effective pole-Q, Q_{pe} at ±12V	With increase in supply voltage from ±12V to ±18V	
			Measured % age change in f_{pe}	Measured % age change in Q_{pe}
CPGA	23.009	10.39	0.513	0.813
RPGA	24.998	11.45	0.056	2.2
NPGA2	25.004	10.57	0.04	2.17
NPGA3	25.011	10.2	0.088	0.784

TABLE 5.1(c). THE EFFECT OF SUPPLY VOLTAGE VARIATIONS ON THE SALLEN AND KEY FILTER RESPONSES.

Nominal pole frequency, f_p = 50 KHz

Nominal pole-Q , Q_p = 10.0

Amplifier Configuration with which the filter is realized	Measured effective pole frequency, f_{pe} at ±12 V (KHz)	Measured effective pole Q, Q_{pe} at ±12 V	With increase in supply voltage from ±12 V to ±18 V	
			Measured % age change in f_{pe}	Measured % age change in Q_{pe}
CPGA	42.886	9.71	0.846	1.75
RPGA	-	-	-	-
NPGA2	50.0	14.08	0.15	9.23
NPGA3	50.17	10.23	0.155	1.76

of RPGA may be desirable.

Now moving to the next table, one can easily note that NPGA3 performs very well even at 25 KHz because of the very low changes in f_p and Q_p. Though the changes in f_p, corresponding to the cases of NPGA2 and RPGA, are lower than that of NPGA3, the changes in Q_p are quite large. These limit the operating frequencies of these filters. Moving now to Table 5.1(c), the changes in f_p and Q_p for NPGA3 are larger now, but still acceptable. It is also observed that the filter circuits using CPGA and NPGA2 are severely affected by the variations in the power supply voltage. In the former, the poor performance is due to the significant effect of f_p, while in the latter, it is due to the strong influence on Q_p, of the variations in the power supply voltage. However, as discussed shortly before, NPGA3 performs quite well at this high frequency also. The frequency shift and the Q-enhancement can be avoided by appropriately accounting for these effects. The designer, however, has no control over these changes themselves. Thus the amplifier configuration of NPGA3 again appears to be the most desirable of all the positive gain amplifiers.

Let us now proceed to compare the signal handling capabilities of the filter circuits employing the different amplifiers. This comparison will be done only briefly based on some experimental results.

5.5 SOME RESULTS ON THE SIGNAL HANDLING CAPABILITY

It may appear that the signal handling capability of the filter circuits may be reduced significantly as the number of OA's used increases. However, it may also be noted that the OA's are not connected in tandem,

when this is likely to happen. The additional OA's are connected in the feedback paths. Further, these OA's often have their own self feedbacks. Thus, it is not unreasonable to expect that the signal handling capabilities of the filter circuits employing the new actively compensated FGA's will not be drastically reduced. A few experimental results are now presented that tend to support the above conjecture. These results were obtained with the Sallen and Key filters discussed in the previous section.

Let us first consider the filter circuits designed to operate at f_p = 25 KHz . At this frequency, the filter circuit with RPGA started oscillating when the input signal was increased beyond 120 mv (rms) . No such difficulty was experienced with the filter circuits employing CPGA, NPGA2 and NPGA3. The output signals were only distorted when the input signals were increased beyond 200 mv , 200 mv and 100 mv in CPGA, NPGA2 and NPGA3, respectively. It is to be noted that the performance of NPGA2 (two OA configuration) is the same as that of the CPGA with reference to the signal handling capability. Also we note that the signal handling capability of the filter using NPGA3 (3OA configuration) is comparable to the one of CPGA.

To get further insight into their operation, each of these amplifiers, with the nominal gain of μ_0 = 1.55 , was isolated from the filter circuit and then tested for their signal handling capabilities both at 25 KHz and at 50 KHz . These results are given in Table 5.2. A study of this table reveals that the signal handling capabilities of the amplifier units with 2OA's and 3OA's are lower than the one of CPGA (the conventional design). However, the reduction is not significant.

TABLE 5.2. SIGNAL HANDLING CAPABILITY OF THE DIFFERENT AMPLIFIERS FOR $\mu_o = 1.55$

Amplifier Configuration	Max. Input Signal for Distortion at the Output	
	at 25 KHz	at 50 KHz
CPGA	1.9 V	0.7 V
RPGA	1.4 V	0.6 V
NPGA2	1.4 V	0.6 V
NPGA3'	1 V_o	0.5 V

The above results seem to indicate that the signal handling capabilities of the new amplifier configurations are not significantly different from that of the conventional amplifier configurations. A similar comment applies to the circuits that use them.

5.6 CONCLUSIONS

In this Chapter, two applications of FGA's in active-RC filter circuits, namely, Bach's lowpass and Sallen and Key bandpass filters, have been considered. Through these applications, a comparison of various amplifier configurations in extending the operating frequency range of active-RC filters has been attempted. It has been shown, through the theoretical studies as well as experimental verifications of the two circuits, that the two OA configurations extend the operating frequency ranges of the filters by an order of magnitude or more, while the circuits employing the 3OA configurations have these ranges extended even further. In the applications considered, the extension in the operating frequency is a minimum of 10 times and a maximum of 60 times over the one obtained with the use of conventional realizations. Thus, clearly the operating frequency range of the class of filters requiring FGA's can be considerably extended by using actively compensated FGA's.

In the above applications, the designs of the filters were adopted from elsewhere. As these designs assume ideal FGA characteristics, they are incapable as such to compensate for the non-ideal OA characteristics. The only way, as has been shown, to improve the performance of these circuits is to improve the characteristics of the FGA's themselves. On the

other hand, given a particular filter configuration employing a set of OA's (with finite GB products), one can also attempt to derive the design values of the circuit elements in such a way as to maximize the operating frequency range of the filter subject to a set of circuit specifications. Clearly, this procedure if successful, will minimize the effect of the finite GB products of the OA's on the circuit response and hence will result in an extension of the operating frequency range of the circuit. The practical implementation of this philosophy forms the subject matter of the next chapter.

CHAPTER VI

OPTIMIZATION OF ACTIVE-RC FILTERS

6.1 INTRODUCTION

It has been shown in the previous chapters that the performance of the conventional designs of FGA's is restricted by the first order term of (ω/B). Consequently, the performance of active-RC filters using these FGA's will also be dominated by the first order term of (ω/B). This is the reason why the operating frequency range is so severely limited in the case of the filters that employ the conventional FGA's. This dependence on the first order term can be eliminated by designing filters employing the actively compensated FGA's suggested in this thesis. Specifically, the use of second order FGA's in the filters will eliminate the dependence on the first order term of (ω/B). Further, using third order FGA's will not only remove the dependence of the filter transfer function on the first order term of (ω/B) but also on the second order term of the same. However, in all such schemes, the maximum operating frequency will still be restricted by the higher order terms of (ω/B), such as by the second and higher order terms in those employing second order FGA's; and by the third and higher order terms in those using third order FGA's.

There is another way by which one might attempt to improve the high frequency performance of the filters. In this technique, the effect of the finite GB products (for example on ω_p and Q_p) is minimized by introducing additional elements in the circuit. It is apparent that this

is a compensation technique for the overall network as opposed to the one discussed so far in this thesis, namely, the one for the active element. Several methods have already been reported in the literature [25, 29, 30, 39] along this line. However, all of them attempt to minimize the circuit dependence on the first order term of (ω/B). As mentioned earlier, the improvement in circuit performance in such cases will be prevented in realizing its full potential by the higher order terms of (ω/B).

It is thus logical to seek a design procedure where the values of the circuit elements, particularly those of the compensating elements, are chosen in such a way that the overall effect of the GB products of the OA's, not just the effect of the first order term of (ω/B) but also that of the higher order terms of (ω/B), on the circuit response is minimized. Only such a procedure can realize to the fullest extent, the improvement in the operating frequency range of a filter for a given type of OA. Clearly, a closed form mathematical solution to this problem is not feasible and an optimization procedure should be attempted. This optimization technique should try, in effect to "match" the amount of compensation to the properties of the filter circuit at hand, in the process delivering the optimal values of the circuit parameters, including those of the compensating elements. Obviously this technique can only be used for a specific circuit configuration with a given set of specifications.

The purpose of this chapter is to present three optimization algorithms. Each of these algorithms can be used to maximize the operating frequency range of active-RC filters that employ OA's. These algorithms are also compared as to the accuracy and the required execution time by considering a particular application:

6.2 PROBLEM STATEMENT AND ALGORITHM I

In this section, the first of the three optimization techniques, termed Algorithm I, is presented. In all the three techniques, the goal is to minimize an error function, F. In this process, the design values of the circuit elements are obtained such that a maximum frequency range of operation of the concerned circuit is achieved. The minimum value sought for F is zero in each case. As the basic philosophy is the same in each case and as all the techniques seek to solve the same problem, it is not surprising to find that all of them have many steps in common. However, the techniques are different from each other in the crucial aspect of the actual formulation of the error function, F. Consequently, this function is calculated differently in each method. This being the case, there are important differences too, in many respects, between the techniques.

Thus, while presenting Algorithm I, an attempt is also made to develop the basic steps that will be found to be common to all the three techniques.

The objective of the optimization is to maximize the operating frequency range of active-RC filters subject to a given permissible value of deviation of the response from the desired one. As discussed before, in filter applications one is interested in keeping the variations of the magnitude of the actual transfer function from the desired one within acceptable limits. In particular, the passband of the filter is more important. Thus, the problem can be stated as follows:

Maximize the operating frequency range such that the deviation in the magnitude of the actual transfer function (which includes the effects of the GB products of the OA's) from that of the ideally desired one is within a specified limit in the entire passband of the filter.

The above problem statement is independent of the order of the filter or the number of OA's employed in the circuit. However, in this thesis, we shall consider the case of only a second order filter. Any second order transfer function can be written in the following form:

$$T_i(s) = \frac{N(s)}{s^2 + (\frac{\omega_p}{Q_p})\, s + \omega_p^2} \qquad (6.1)$$

where the form of $N(s)$ depends on the type of the filter, such as lowpass, highpass and bandpass, etc. In practice, the actual transfer function realized, $T_a(s)$ will be different from $T_i(s)$ due to the finite GB products of the OA's. In this case, the above objective can be restated as follows:

Maximize ω_p *(with proper choice of circuit parameters) such that the deviation in the magnitude of* $T_a(j\omega)$ *, that is* $|T_a(j\omega)|$ *is within a certain percentage (say* $x\%$ *) of* $|T_i(j\omega)|$ *, as given by (6.1), in the entire passband of the filter.*

Let ω_{pm} be the maximum ω_p up to which the circuit can be operated. The above problem statement then means that

$$\left| \frac{|T_a(j\omega)| - |T_i(j\omega)|}{|T_i(j\omega)|} \right| \leq (\frac{x}{100})$$

in the entire passband, for every ω_p in the range $0 < \omega_p \leq \omega_{pm}$. This is because the aim is to minimize the effect of the finite GB products of the OA's on the filter response over the maximum possible range of frequencies up to which the filter may be used and not just over a given passband for a particular ω_p.

The Algorithm I can now be implemented by following the steps described below in order.

1. Start with a small value of ω_p, with a proper choice of the circuit parameters as variables.

2. Calculate

$$e = \left| \frac{T_a}{T_i} - 1 \right| - \alpha ,$$

where

$$\alpha = \frac{x}{100}$$

and T_a and T_i refer to the magnitude responses of the actual transfer function and the ideally expected one respectively; x is the magnitude of the percentage deviation allowed in the passband. This quantity e will be a function of frequency ω, for a given ω_p.

3. Calculate $f = \int_W e^2 d\omega$,

where $W = \{\omega: \omega_{-3db} \leq \omega \leq \omega_{3db}\} \cap \{e: e > 0\}$ and where ω_{-3db} and ω_{3db} refer to the lower and upper 3db points of the filter characteristic between which the passband of the filter lies. It is to be noted that

the integration is carried out only in the region where $e > 0$. In order to clarify the above step more fully, let us consider the filter characteristic curves shown in Fig. 6.1(a). The magnitude characteristics I and A represent the ideally expected and the actual characteristics of a second order bandpass filter in the passband of interest. U and L represent the upper and lower limits within which the actual characteristic A is supposed to lie so that the error in the actual magnitude characteristic from the ideally desired one will be within a specified percentage, x%. The step 3 corresponds to the hatched portion of this diagram, where e_i and T_i are marked for a particular frequency, ω_i. From this e^2 can be calculated in the range of frequency where $e > 0$ and this is shown in Fig. 6.1(b). The step 3 above will give a value proportional to the area under the curve shown in Fig. 6.1(b).

In Algorithm I, this is the crucial step in the formulation of the error function to be minimized. The other two algorithms are different from this one in this step only, as will be seen later.

4. Obtain $F = \int_0^{\omega'_p} f \, d(\omega_{p\nu})$

The above step (4) is necessary to ensure that the error function to be minimized takes into account the passband of not only a given filter designed with a particular pole frequency, ω_p but also of every filter designed with any $\omega_{p\nu}$ such that $0 < \omega_{p\nu} \leq \omega_p$.

5. Minimize the function, F using any one of the standard techniques such as the one given in [46]. The minimum value of F_{min},

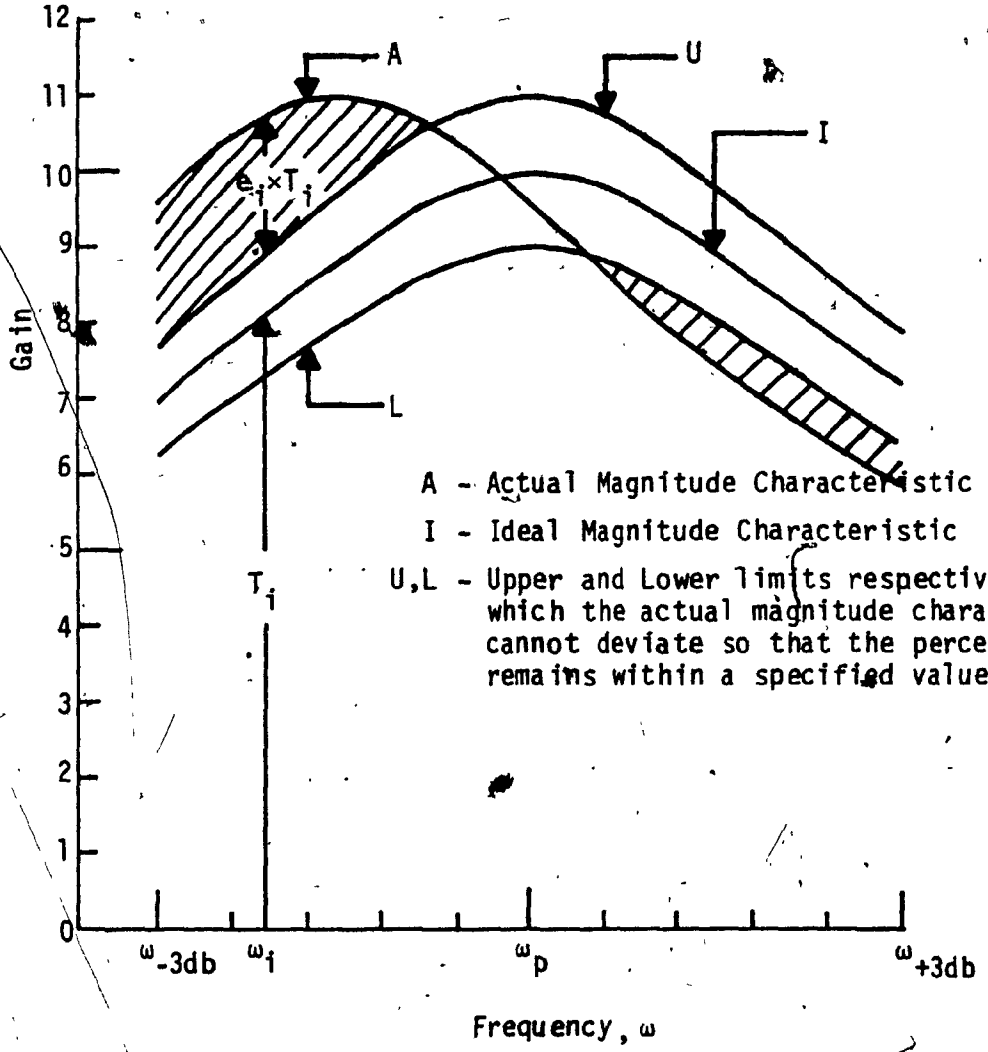

FIG. 6.1(a): A Pictorial Representation of Step 3 in Section 6.2

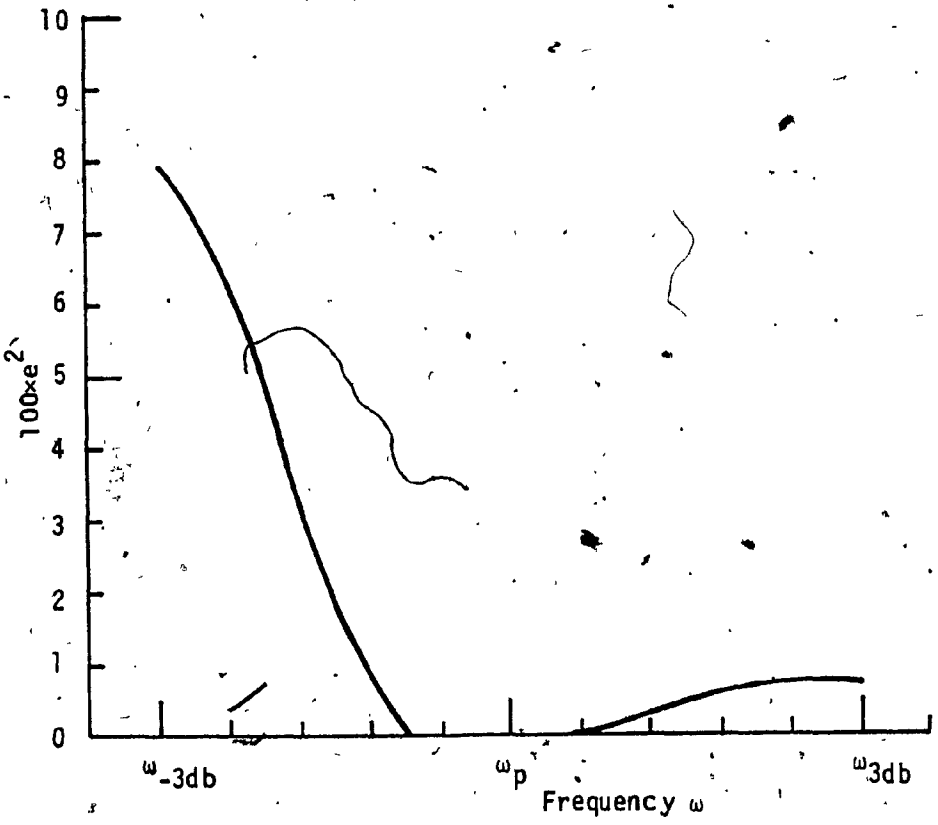

FIG. 6.1(b): A Pictorial Representation of Step 3 in Section 6.2 - continued

should be zero for a proper choice of the circuit parameters. A zero value of F_{min} implies that $e \leq 0$ in step (3) not only for all ω between ω_{-3db} and ω_{3db} for a given $\omega_{p\nu}$ and it is true for any $\omega_{p\nu}$ such that $0 < \omega_{p\nu} \leq \omega_p$.

6. Increase ω_p in small steps and go to step 2. Repeat this cycle till F_{min} can no longer be made zero by any further increase in the value of ω_p. Exit the cycle at this stage.

The non-zero value of F_{min} implies that a set of values of the variables (circuit parameters) can no longer be found such that $e \leq 0$ in the frequency range $\omega_{-3db} \leq \omega \leq \omega_{3db}$ for a given ω_p and for all $\omega_{p\nu}$ in the range $0 < \omega_{p\nu} \leq \omega_p$.

7. Note the maximum value of ω_p, ω_{pm} for which F_{min} is zero. This value of ω_{pm} will be the maximum usable frequency of operation of the filter. The values of the variables (circuit parameters) corresponding to this ω_{pm} will be the desired and optimum values of the variables.

The above steps are summarized in the flow chart shown in Fig. 6.2. A few additional details are given in the flow chart so that the initial step size can be large and be decreased to small values as ω_{pm} is approached. The steps 3 and 4 are included in the box "Calculate new F and minimize F". All the seven steps and this flow chart can be programmed easily in a computer.

Before using this Algorithm, let us consider a simplification of the step (3). The simplification will lead us to Algorithms II and III.

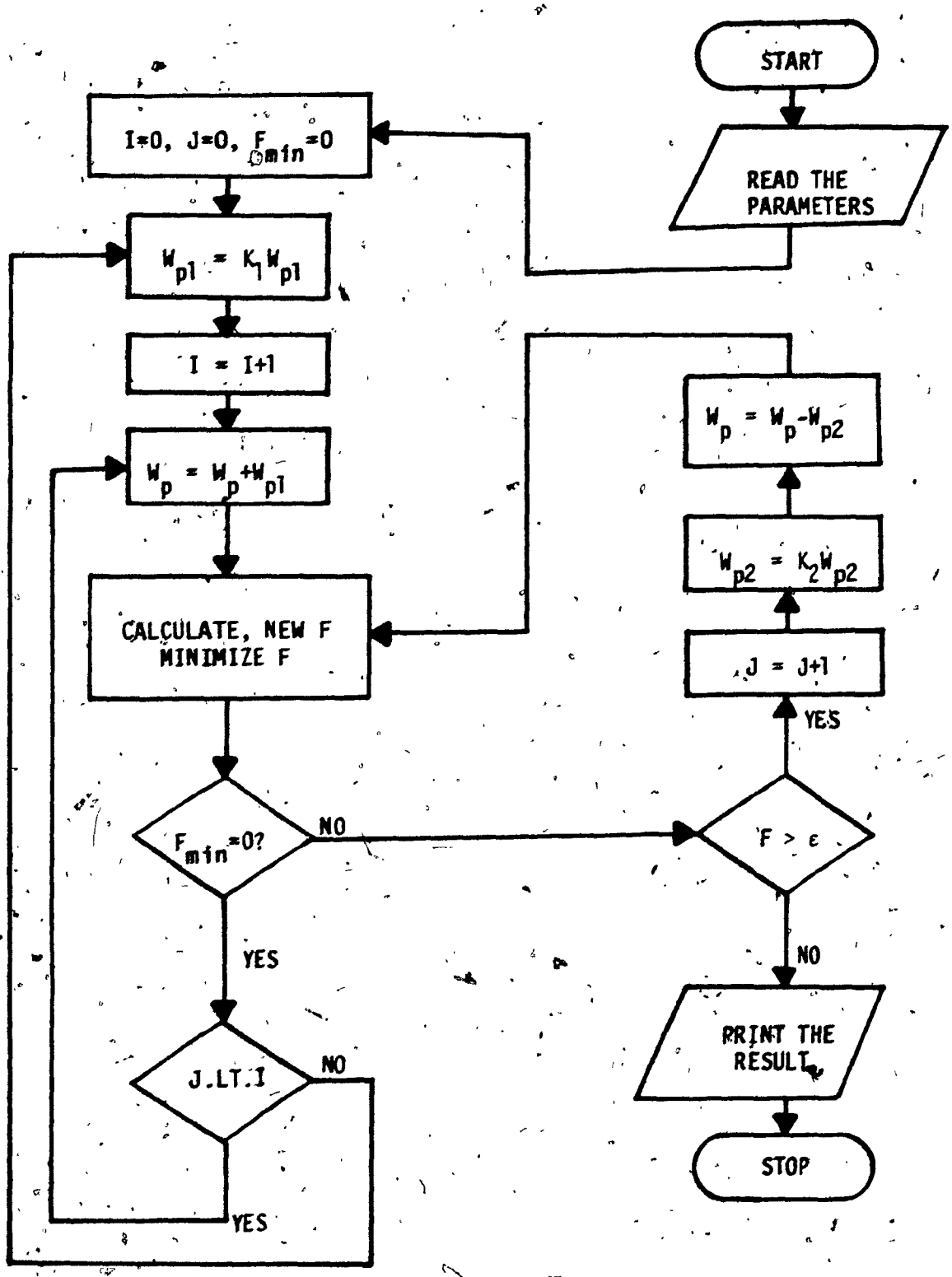

FIG. 6.2: Flow Chart for Algorithm I

These simplifications are aimed at reducing the computing time required. To implement step 3 in the Algorithm I in a computer, it is required that the passband be divided into small intervals, say N and the magnitudes, T_a and T_i of the actual and ideal transfer functions be evaluated at $(N+1)$ frequencies. The required value of N depends upon the desired accuracy. However in practice, for a reasonable accuracy, it has been found that N must be chosen as high as 20 or more. Then at each frequency ω_i we find

$$e_i = \left|\frac{T_a}{T_i} - 1\right| - \alpha \tag{6.2}$$

and the quantity f is found using the following:

$$f = \sum_{i \in I} e_i^2 \tag{6.3}$$

where $I = \{i: e_i > 0\}$. To get one value of f, the transfer functions are to be evaluated 21 or more times. Clearly then, if the value of N can be decreased without significantly affecting the desired accuracy, the required computing time will also be reduced. To achieve this, let us note that the quantity given by

$$E = \frac{T_a}{T_i} - 1 \tag{6.4}$$

is a function of ω. Thus, if the frequency at which the maximum value of $|E|$ occurs in the passband can be located, it is sufficient to calculate the value of $|E|$ and the error magnitude, $e = |E| - \alpha$ at

this frequency to evaluate the function, f . This is because, if the error $e > 0$, then it implies that the magnitude characteristic of the actual transfer function exceeds the limits set by either U or L as shown in the Fig. 6.1. However, by limiting the maximum of $|E|$ to be within α , we are assured that the error magnitude at other frequencies is also within α . Thus, one has to find only the frequencies at which $(T_a/T_i - 1)$ is most positive and most negative.

As one does not know, a priori, at which one of these frequencies $e = |E| - \alpha > 0$, in general one has to evaluate the transfer functions at both these frequencies. However, it should be noted that the amount of computing time required is greatly reduced because of the considerable decrease in the number of transfer function evaluations, viz., by ten or more times. This reduction is achieved at the expense of some added complexity in Algorithm I. The Algorithm I is required to be modified so as to find the frequencies at which E , given by (6.4) is most negative and most positive. This modification results in Algorithm II which is discussed in the next section.

6.3 DEVELOPMENT OF ALGORITHM II

Let us assume that a filter is designed to yield a transfer function of the form given by (6.1). The effect of the finite values of the GB products of the OA's used causes the actual transfer function to be of a higher order. Thus the actual filter response may be quite different from the desired one. However, if the maximum permissible deviation of the actual characteristic from the desired one is limited to be within a few percent, then within the passband, the filter response

is mainly decided by the dominant pole pair of the actual transfer function, the other poles being far away from these poles. Under these circumstances, the denominator polynomial of the filter transfer function may be assumed to be of a second order, the coefficients of which are determined by the dominant pole pair.

The numerator polynomial, say $N'(s)$ will also be different from that of the desired one, due to the effect of the finite GB products of the OA's. However, in most cases, the dominant roots of $N'(s)$ are very close to those of $N(s)$, while the additional roots, if any are far away from the dominant ones. Thus, without any substantial effect on the transfer function, it can be assumed that $N'(s) \cong N(s)$.

Let ω_{pe} and Q_{pe} be the effective pole frequency and pole Q of the actual transfer function. Then such a transfer function can be approximated by the one given below:

$$T_a(s) \cong \frac{N(s)}{s^2 + (\frac{\omega_{pe}}{Q_{pe}})s + \omega_{pe}^2} \qquad (6,5)$$

Once we approximate the actual transfer function as given by (6.5), then it can be shown that, for a given ω_p, the frequencies at which the error $E = (T_a/T_i - 1)$ becomes most positive and negative are given by the solution of the following equation

$$A y^2 + B y + C = 0 \qquad (6.6)$$

where

$$A = 2(1-p) + \frac{1}{Q_p^2}\left(\frac{p}{q} - 1\right)$$

$$B = 2(q^2 - 1)$$

$$C = 2p(1-p) + \frac{p}{Q_p^2}\left(p - \frac{1}{q}\right)$$

$$p = \left(\frac{\omega_{pe}}{\omega_p}\right)^2$$

$$q = \left(\frac{Q_{pe}}{Q_p}\right)^2$$

$$y = x^2$$

and

$$x = \left(\frac{\omega}{\omega_p}\right)$$

From (6.6), it is possible to show that when $\omega_{pe} = \omega_p$ $(p = 1)$, the frequency at which the maximum deviation occurs is at $\omega = \omega_p$. For large Q_p values, when $Q_{pe} = Q_p$ $(q = 1)$, the maximum deviation occurs either at $\omega = \omega_{pe}$ or at ω_p.

As one will not know beforehand about the nature of the values of p and q, we will have to solve (6.6) in general and obtain the positive values of y, since $y = x^2$ can not be negative. The solution of this equation requires the values of A, B and C, which in turn require the values of ω_{pe} and Q_{pe} for a given set of values of ω_p and Q_p. All these computations can be implemented in a computer. The step 3 of Algirithm I has to be changed suitably so as to implement

the above considerations. The required modifications are only given below.

3(a) From the coefficients of the denominator polynomial of the actual transfer function, determine the values of ω_{pe} and Q_{pe}.

These coefficients are required at any rate for the calculation of the transfer function magnitude. The values of ω_{pe} and Q_{pe} can be calculated through an iteration process [5]. In practice, it has been found that one or two iterations in this technique yields very good accuracy in the computed values. For this purpose a subroutine was also developed and used. The flow chart for the subroutine is given in Fig. 6.3.

3(b) Solve (6.6) to find the frequencies at which the error given by (6.4) becomes the most positive and the most negative.

3(c) Calculate the error magnitude $|E_i| = |T_a/T_i - 1|$ at the above frequencies which are inside the passband.

3(d) Use (6.2) and (6.3) to evaluate f.

When the above 4 steps replace step (3) in the first Algorithm, that is, Algorithm I, the second algorithm, namely, Algorithm II is obtained. In this algorithm, the number of evaluations of the magnitudes of the transfer functions are reduced at the expense of additional steps, namely, 3(a) and 3(b) given above.

For very highly selective filters, the optimizing algorithm can further be simplified resulting in additional saving of computing time. Before considering an application of Algorithm II, this simplification

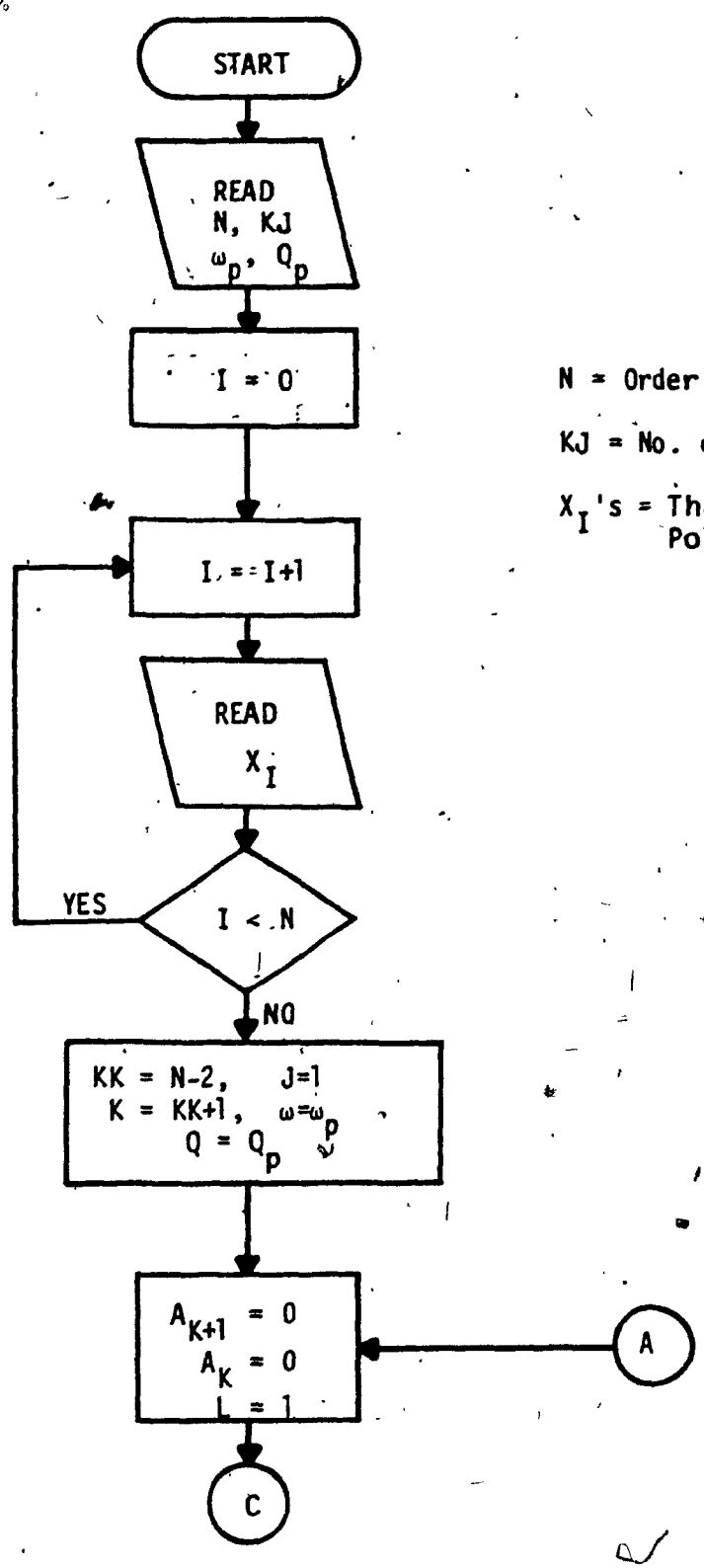

N = Order of the Polynomial +1

KJ = No. of Iterations Required

X_I's = The Coefficients of the Polynomial

FIG. 6.3: Flow Chart of the Subroutine Developed to Find ω_{pe} and Q_{pe}

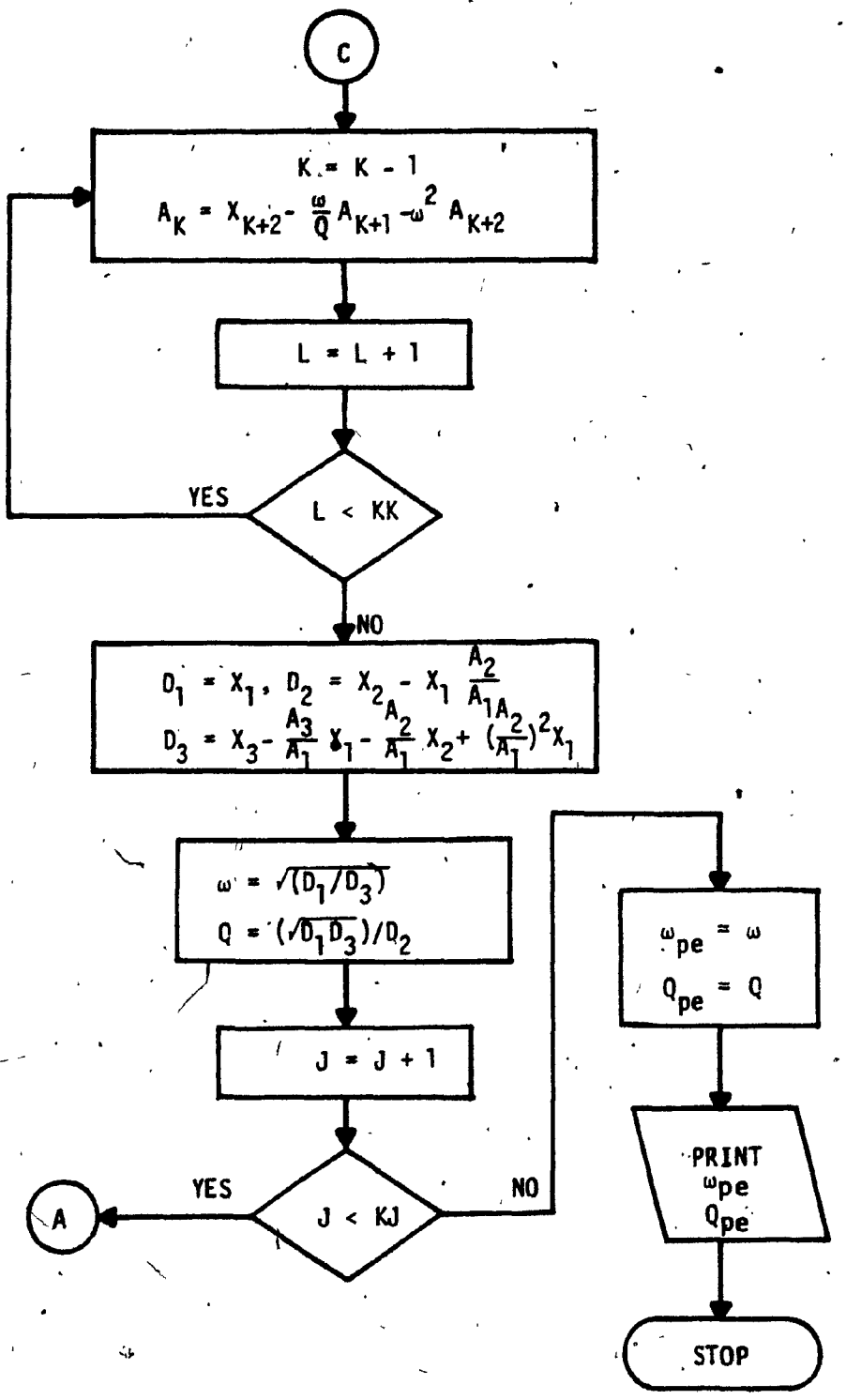

FIG. 6.3: Flow Chart of the Subroutine to Find ω_{pe} and Q_{pe} - continued

will be presented yielding the final algorithm, that is, Algorithm III.

6.4 DEVELOPMENT OF ALGORITHM III*

The actual transfer function has been approximated by a second order one in the previous section. This process is carried further in this section. The second order approximation of the actual transfer function becomes more accurate when the nominal pole Q-factor, Q_p is large.

The magnitude response of a highly selective network can be closely approximated in the passband by a bandpass second order transfer function $T(s)$, that is, by a transfer function of the form given by (6.5), where $N'(s) = H's$. It has been shown [15,47] that with changes in both ω_p and Q_p, $|\Delta|T|/|T||$ or $(\Delta\phi/\phi)$ where $\phi = \text{Arg } T(j\omega)$ is maximum at the 3db points in the passband and is given by

$$\left|\frac{\Delta|T|}{|T|}\right|_{max} = \left|\frac{\Delta\phi}{\phi}\right|_{max}$$

$$= \left|\frac{\Delta Q_p}{2Q_p}\right| + Q_p \left|\frac{\Delta\omega_p}{\omega_p}\right| \qquad (6.7)$$

In case there is no change in ω_p (i.e.) $\Delta\omega_p = 0$, the maximum change in $|T|$ occurs at ω_p (as shown in the last section also) and this is

$$\left|\frac{\Delta|T|}{|T|}\right|_{max} = \left|\frac{\Delta Q_p}{Q_p}\right| \qquad (6.8)$$

---

*This algorithm is essentially the same as the optimization procedure given in [45].

The above expressions giving the maximum deviation in the magnitude characteristic of the actual transfer function from the ideal one can be used instead of evaluating transfer functions as was done in the previous two cases. Further, for evaluating ΔQ_p and $\Delta\omega_p$ one can also use the subroutine that was used to find Q_{pe} and ω_{pe} in Algorithm II, since

$$\left.\begin{aligned} \frac{\Delta Q_p}{Q_p} &= \frac{Q_{pe}}{Q_p} - 1 \\ \text{and} \\ \frac{\Delta\omega_p}{\omega_p} &= \frac{\omega_{pe}}{\omega_p} - 1 \end{aligned}\right\} \quad (6.9)$$

Now proceeding further to give the Algorithm III, let us define two functions G_1 and G_2 as follows:

$$\left.\begin{aligned} G_1 &= \left|\frac{\Delta Q_p}{Q_p}\right| \\ \text{and} \\ G_2 &= Q_p \left|\frac{\Delta\omega_p}{\omega_p}\right| \end{aligned}\right\} \quad (6.10)$$

Then the equations (6.7) and (6.8) become as follows:

$$\left|\frac{\Delta|T|}{|T|}\right|_{max} = \frac{G_1}{2} + G_2 \quad (6.11)$$

and

$$\left|\frac{A|T|}{|T|}\right|_{max} = G_1 \qquad (6.12)$$

As it will not be known which of the above two expressions are to be used beforehand in evaluating the function 'f' in step (3) of Algorithm I, we have to use both of them. Thus, let us define

$$e_1 = \frac{G_1}{2} + G_2 - \alpha \qquad (6.13)$$

and

$$e_2 = G_1 - \alpha \qquad (6.14)$$

With the theoretical background given above, we are ready to discuss the steps for the Algorithm III. As mentioned before, the only change that is required is in step (3). Thus the necessary modifications in step (3) of Algorithm I are given below.

3(a) Obtain ω_{pe} and Q_{pe} and use (6.9) through (6.14) to evaluate e_1 and e_2.

(b) Use (6.3) to evaluate f.

Thus replacing the step (3) in Algorithm I with the above two steps, the Algorithm III results. It should be noted that in this algorithm, the transfer function is not evaluated at any stage. Thus, in terms of the computational effort needed, this is the fastest of all the three algorithms.

Before comparing the different algorithms, let us first consider an application of these algorithms to illustrate how these can be used advantageously in extending the frequency range of active-RC filters.

6.5 AN APPLICATION OF VARIOUS ALGORITHMS

The algorithms developed in the previous sections can be used to improve the high frequency performance of any type of active-RC filters that use OA's not just of any particular type such as the ones using FGA's. To emphasize this point, the filter circuit of Fig. 6.4 was chosen for optimization. This is an actively compensated double integrator loop, recently reported by Reddy [39].

Reddy chose the parameters n and b shown in Fig. 6.4 as 4 and 1 respectively and this choice eliminates only the first order effects of the GB products of the OA's. However, in Algorithms I, II and III, the parameters n and b are assumed to be variables.

Assuming μA741 OA's with a typical value of GB product of $2\pi\times10^6$ rad./sec. and a value of 5 for Q_p the maximum frequency of operation f_p, for a maximum change of 10% in the transfer function in the passband is found to be 26 KHz for the choice of $n = 4$ and $b = 1$. Using the three algorithms discussed we get the optimum choice of the parameters and the maximum f_p's as shown in Table 6.1, for the same values of α, GB products and Q_p. The effectiveness of the optimization procedures for the filter circuit is obvious from the Table 6.1. The maximum operating frequency is extended from 26 KHz to 74 KHz, which is about 285%.

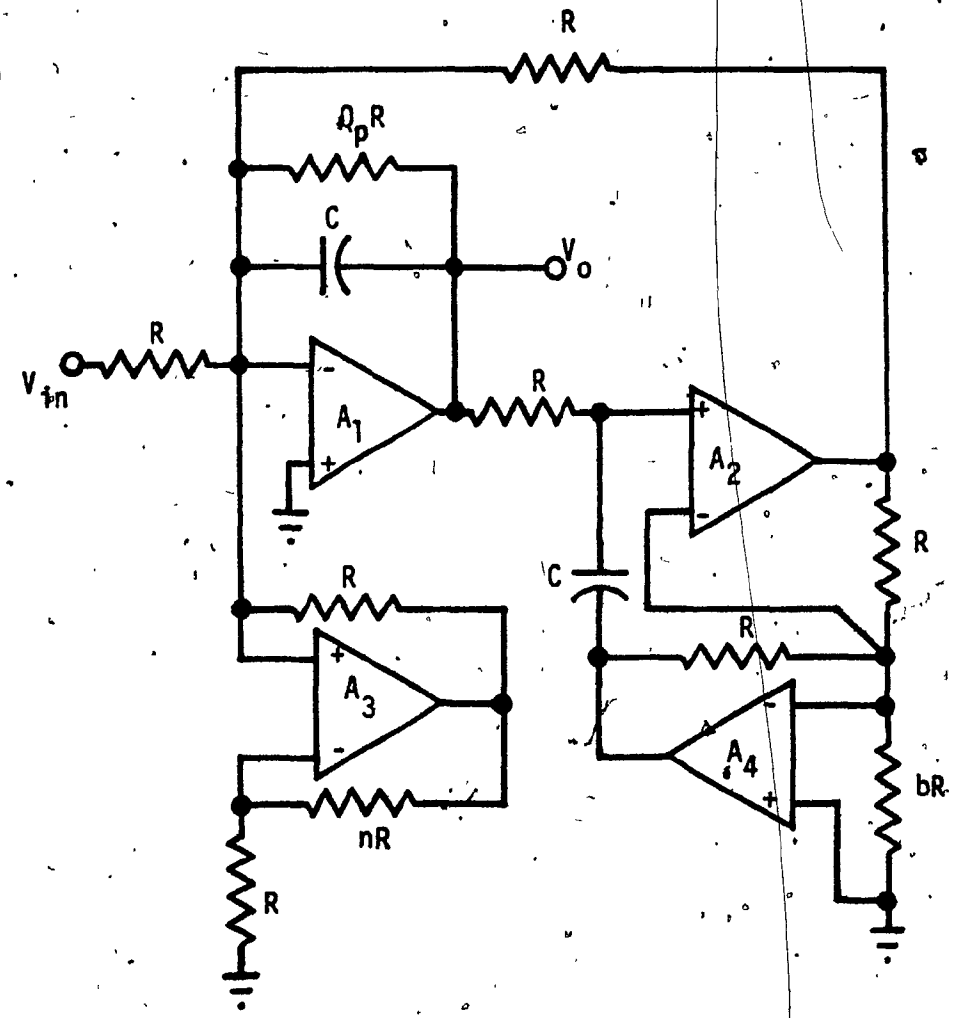

FIG. 6.4: Double Integrator Filter for High Frequency Applications Given in [7]

To verify the results obtained, the filter circuit was designed and tested with a nominal value of $Q_p = 5.0$ at the pole frequencies with nominal values of 26 KHz and 74 KHZ. The elements that were used, were ±1% resistors and ±2% capacitors. Motorola μA741 OA's, whose nominal GB products is $2\pi \times 10^6$ rad./sec. were employed in the circuit. One can easily notice from the Table 6.1 that the values of n and b obtained using Algorithms I and II are almost same, the differences being less than 0.2%. Thus, the filter was tested only with pairs of values obtained from Algorithms II and III, and with the pair of values suggested by Reddy. The theoretically expected magnitude characteristics along with the ideally expected one are shown in Figs. 6.5(a) and 6.5(b) at $f_{pn} = 26$ KHz and $f_{pn} = 74$ KHz respectively. The experimentally obtained points are marked on them.

The foregoing results, both theoretical and experimental confirm that the optimization technique extends the maximum operating frequency range significantly.

The maximum f_p's that are given by the different algorithms being about the same, the question naturally arises as to which one of these algorithms should be used in practice. In order to answer this question, the performances of these algorithms are compared in the next section through the same application.

6.6 COMPARISON OF THE DIFFERENT ALGORITHMS

The Algorithm I and the basic steps therein were developed directly from the problem statement and no approximation was involved. Obviously it is the most direct and hence the simplest method. Clearly,

TABLE 6.1. RESULTS OF OPTIMIZATION OF THE FILTER SHOWN IN FIG. 6.4 WITH $Q_p = 5.0$.

Technique Used	n	b	Maximum value of f_p that can be obtained
Algorithm I	3.471	0.4023	74 KHz
Algorithm II	3.465	0.4031	74 KHz
Algorithm III	3.328	0.4852	73.3 KHz
Reddy's Choice	4	1	26 KHz

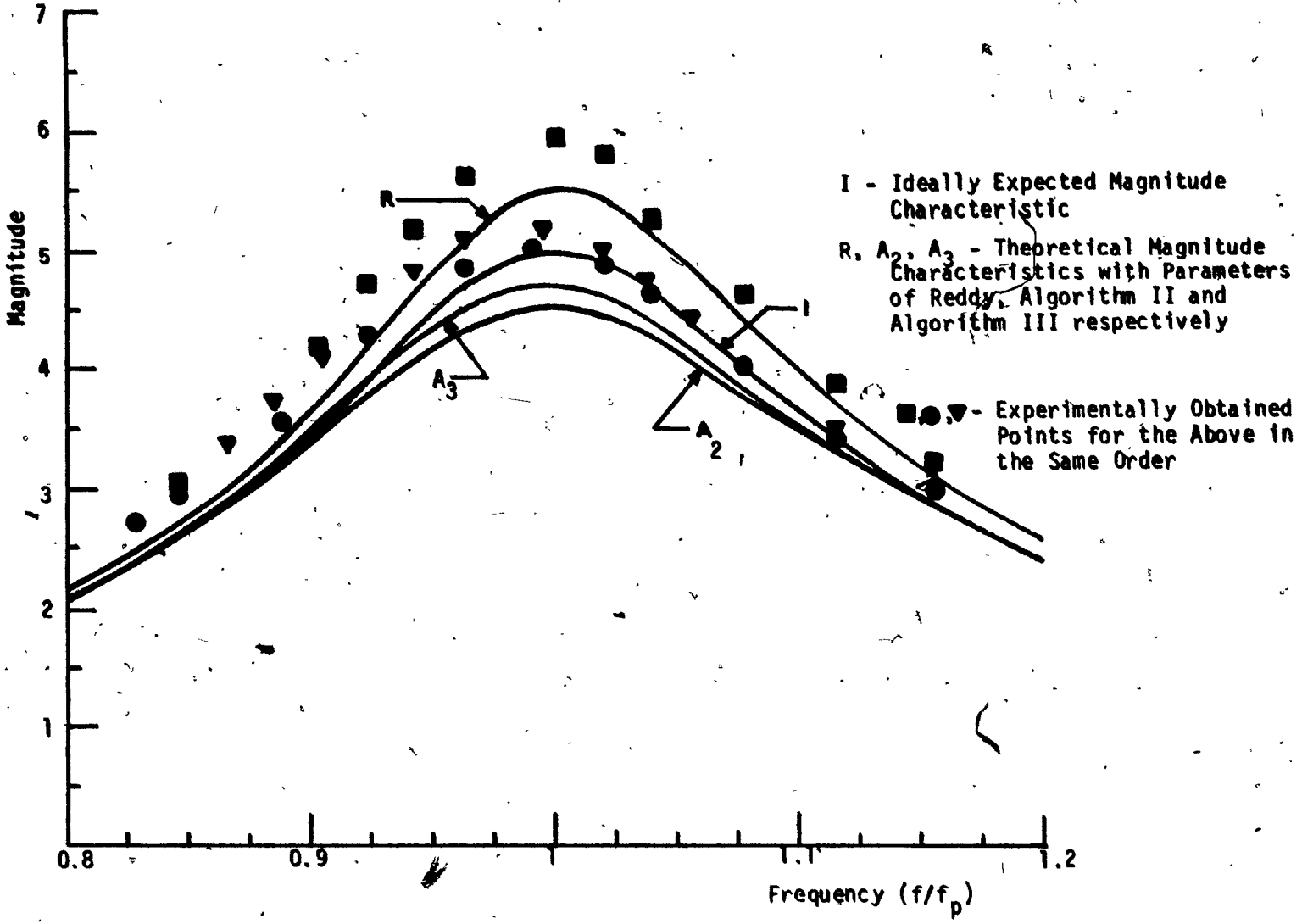

FIG. 6.5(a): Magnitude Characteristics of the Filter Shown in Fig. 6.4 with a Nominal Value of f_p=26 KHz

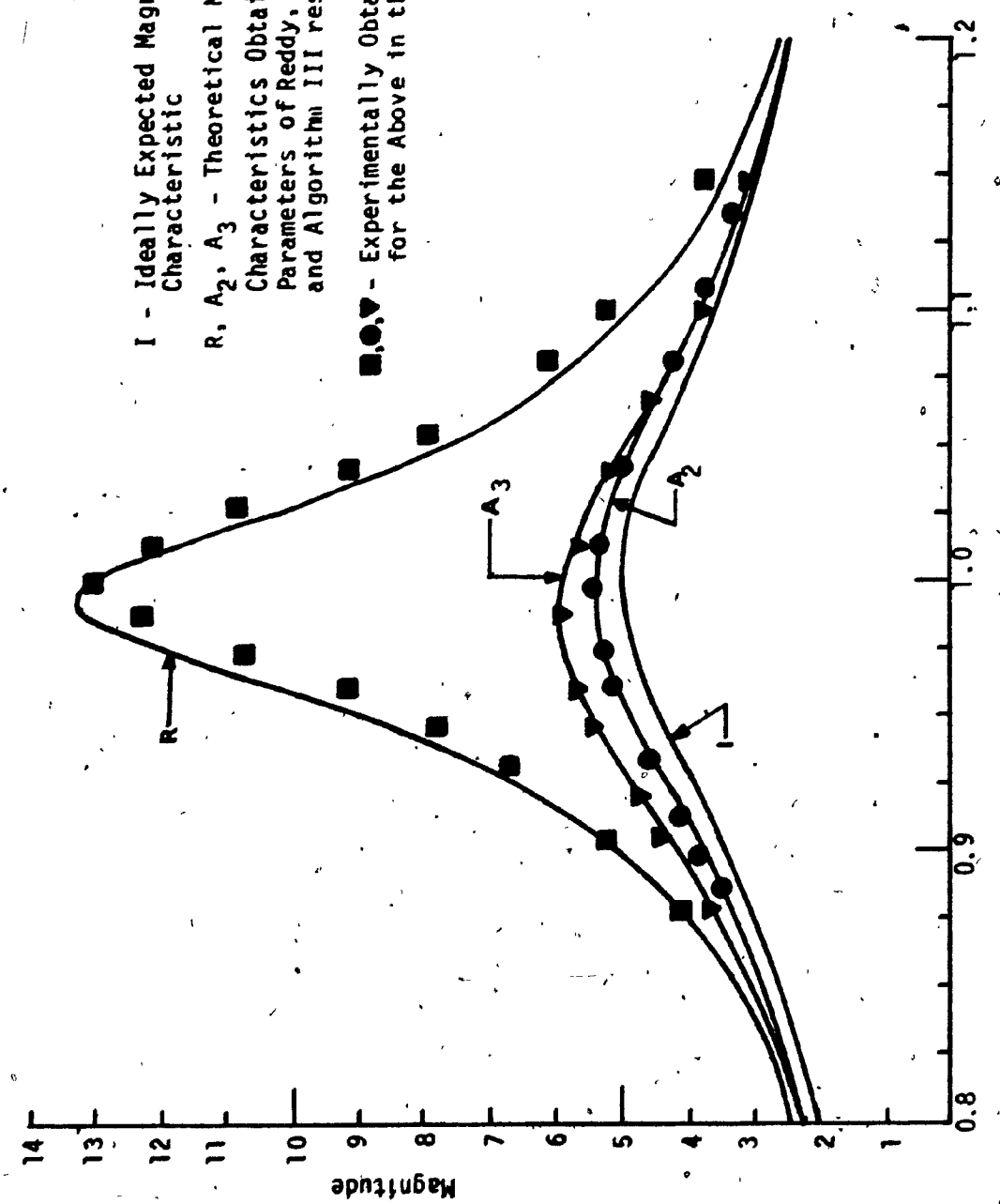

FIG. 6.5(b): Magnitude Characteristics of the Filter Shown in Fig. 6.4 with a Nominal Value of f_p=74 KHz

it is the most accurate method. This algorithm can also be employed for extending the operating frequency range of higher order filters with some simple modifications. However, the computational work in calculating the function to be optimized is quite complex. Thus the execution time required is also considerable.

In order to reduce the computational effort, the Algorithm II was then developed, as explained at length in section 6.2. This algorithm involves an approximation in it. However, by referring to Table 6.1, we find that, in this application, the errors involved in the optimized parameters are less than 0.2% . Thus, it appears that the accuracy is negligibly affected by using the approximation. The maximum frequency expected is also found to be same as that given by Algorithm I. However, the computational time required is very much reduced.

The approximation was carried to the fullest extent in developing Algorithm III so as to reduce the computational effort still further. However the accuracy in the values of the parameters obtained suffers significantly. Again referring to Table 6.1, we find that the error involved in n is found to be about 4.2% and that in b is about 20.6% , which is quite high. In this connection it is worth remembering that the approximations that are involved are really true only for high Q filters. Since the Q_p of the filter considered is rather low, that is 5 , the failure of the Algorithm III can be expected. These errors that are involved must have some effect on the highest operating frequency. This is just what has happened. Thus, in order to carry out the comparisons more fully the three algorithms were tested in the same application as

used in the previous section for different values of Q_p, one at a low value of Q_p, namely at $Q_p = 5$ and another at a high value of Q_p, that is, at $Q_p = 50$. The aim of the tests is to determine the accuracy of the parameters obtained and the computational time required in each case. The details of the results are given in Tables 6.2(a) and (b) for $Q_p = 5$ and $Q_p = 50$ respectively.

The parameters obtained through the optimization procedure using Algorithm I are directly based on the problem statement. Hence these parameters can be taken as the basis for finding the accuracy of the other set of parameters. Referring to Table 6.2(a), when $Q_p = 5$, the parameters obtained through the Algorithm II are different from those of the Algorithm I by 0.17% in n and 0.198% in b', whereas the set of parameters obtained through Algorithm III is erroneous by 4.2% in n and 20.6% in b. The maximum f_p's, that can be obtained with each set of these parameters so that the error magnitude does not exceed the prescribed 10%, were calculated. They are 74 KHz, 74 KHz and 57 KHz respectively, as given in Table 6.2(a).

Examining the execution time required, we find that Algorithm II requires 6.2 times less execution time and Algorithm III requires about 22 times less execution time than that required by Algorithm I. However, it is observed that while Algorithms I and II predict the performances quite closely, Algorithm III fails completely to predict the performance. There is an error of about 23% in the maximum f_p that was predicted by Algorithm III. Thus, for optimizing low Q_p filters, it appears that Algorithm II is the 'best', because of the fact that it requires much less

TABLE 6.2(a). DETAILS OF THE OPTIMIZATION OF THE FILTER CIRCUIT WITH A NOMINAL Q_p VALUE OF 5 WITH DIFFERENT ALGORITHMS

Technique used for optimization	Values of the optimized parameters		Execution time required for optimization with the same initial values (CP secs)	Maximum f_p, given by the optimization (KHz)	Maximum frequency expected by actual evaluation of the transfer function so that the error magnitude does not exceed the 10% (KHz)
	n	b			
Algorithm I	3.471	0.4023	297.82	74.33	74
Algorithm II	3.465	0.4031	48.18	74.2	74
Algorithm III	3.328	0.4852	13.78	73.3	57

TABLE 6.2(b). DETAILS OF THE OPTIMIZATION OF FILTER CIRCUIT WITH A NOMINAL Q_p VALUE OF 50 WITH DIFFERENT ALGORITHMS

Technique used for optimization	Values of the optimized parameters		Execution time required for optimization with the same initial values (CP secs)	Maximum f_p, given by the optimization (KHz)	Maximum f_p, expected f_p by actual evaluation of the transfer function so that the error magnitude does not exceed 10% (KHz)
	n	b			
Algorithm I	3.8714	0.6829	66.0	21.5	21.5
Algorithm II	3.868	0.6762	29.98	21.6	21.5
Algorithm III	3.7911	0.6985	9.866	21.8	19.6

execution time compared to that required by Algorithm I without sacrificing the accuracy.

Now, from Table 6.2(b), we observe that the differences in the set of optimized parameters obtained using Algorithms I and II are 0.09% in 'n' and 0.98% in b . These differences are quite acceptable in Engineering practice. Also the maximum f_p's predicted by both these algorithms are again quite close. At the same time, we find that Algorithm II requires an execution time which is less than half of the time taken by Algorithm I. Let us now compare Algorithm III with Algorithm I. The set of parameters given by the optimization using Algorithm III are different from those obtained with Algorithm I by 2.1% in 'n' and 2.3% in 'b' . Thus, in the case of high 'Q_p' filters, the errors are considerably less and this fact is also reflected in the maximum f_p given by these set of parameters. With actual calculation of transfer function with these parameters, we get the maximum f_p as 19.6 KHz . This is different from the predicted one only by 8.8% , which is well accepted in engineering practice. Also we find that Algorithm III requires an execution time that is, 1/3 of the one required by Algorithm II and (1/6.7) of the one required by Algorithm I. Thus for optimizing filters with high Q_p , the use of Algorithm III appears to be acceptable.

Thus, in conclusion, it may be observed that Algorithm II performs very well for filters with both high and low Q_p's , whereas Algorithm III, which is the fastest, is quite acceptable for high Q_p filters.

In order to verify some of these results, experimentally, the error magnitudes of both the filters with the nominal values of $Q_p = 5$

and f_p = 74 KHz constructed and tested earlier with parameters obtained from Algorithms II and III were calculated. They are shown in Fig. 6.6(a) along with the theoretically expected error magnitudes in the passband of the filter. The maximum error in the parameters given by Algorithm III is more than 20% , as we expected. However, the theoretical error magnitude characteristic of the filter constructed with parameters obtained through Algorithm II shows that the maximum error is well within 10% and the experimental results closely agree with it.

Similar results were obtained from the characteristics of the same filter, shown in Fig. 6.4 constructed using the two sets of parameters with nominal values of Q_p and f_p as 50 and 21.22 KHz respectively. They are shown in Fig. 6.6(b). The error magnitude characteristics show that the Algorithm III is also quite acceptable. Both theoretical and experimental results show that the difference in the maximum errors obtained with Algorithms II and III continues to decrease with increasing values of Q_p .

6.7 CONCLUSIONS

In this Chapter, three optimization algorithms have been developed for extending the frequency range of operation of active-RC filters. These techniques are applicable to any second order active-RC filter using OA's. It has been shown, through an application, that the operating frequency range of active-RC filters can be significantly improved by using these techniques. In particular, by considering an actively compensated double integrator loop, it has been found that such an optimization extends the frequency range by about three times

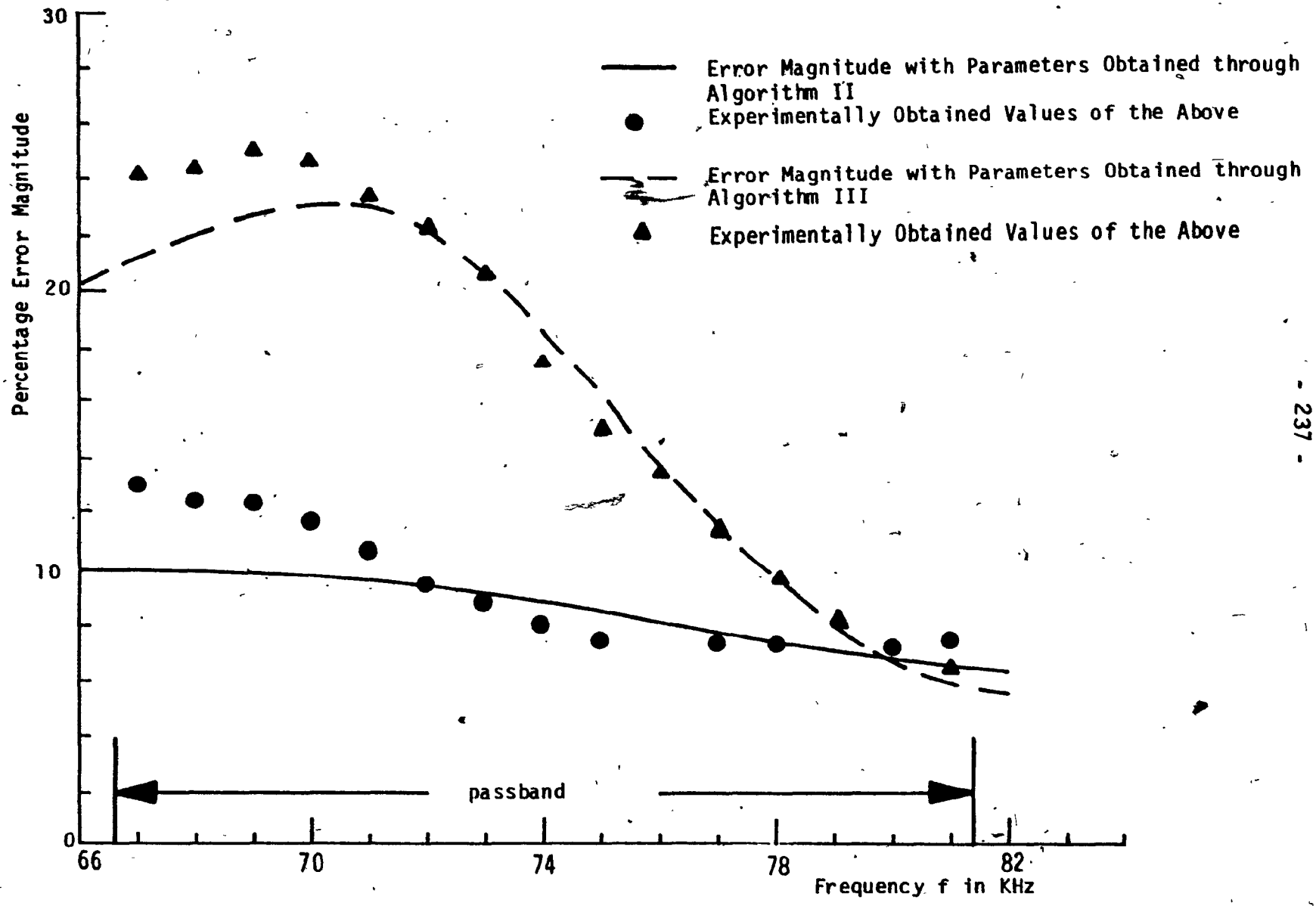

FIG. 6.6(a): Error Magnitude Characteristics in the Passband with Q_p=5 and f_p=74.00 KHz

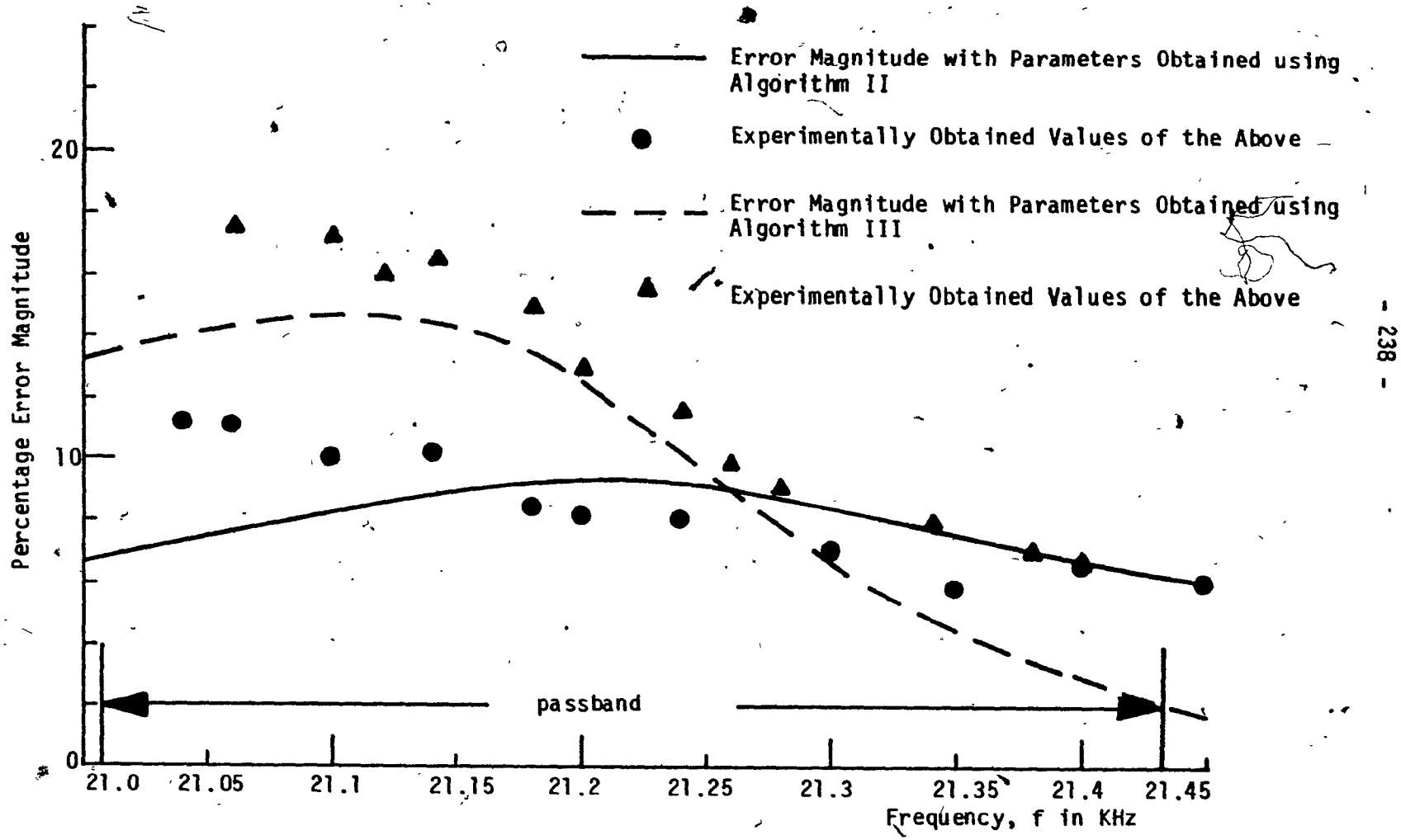

FIG. 6.6(b): Error Magnitude Characteristics in the Passband with Q_p=50 and f_p=21.22 KHz

the one that can be obtained without optimization. These algorithms are also compared as to their accuracy and the execution time required. This is done by testing these algorithms through an application. Algorithm I is the most accurate and it can be used to optimize any filter of any order. However, its execution time is very large. Algorithm II reduces the execution time considerably without sacrificing the accuracy significantly. Algorithm III can be used only for high Q_p filters. However, for such filters, Algorithm III is fastest. On the other hand, Algorithm II can be used for any Q_p value. From all considerations, Algorithm II is the optimal one.

CHAPTER VII
CONCLUSIONS

The operating frequency ranges of active-RC filters employing OA's are limited by the finite GB products of the OA's. This thesis has suggested and examined in detail two possible techniques for minimizing the effect of the finite GB products on the responses of the active-RC filters.

The first method suggests ways of improving the bandwidth of the FGA's that use OA's. This will help to extend the frequency range of operation of the popular and practically useful class of active-RC filters which employ FGA's as active elements.

In order to develop design procedures for improved FGA's, first a general theory of active compensation of FGA's is presented in Chapter II. This theory yields the general form of the transfer function for the FGA's to possess improved bandwidth of operation. A stability study of this transfer function leads, unfortunately, to the conclusion that only the second order transfer functions are practically realizable.

Consequently, an exhaustive set of realization procedures is given in Chapter III for such second order FGA's. For this purpose, a general five port resistive network in which two OA's are embedded is investigated in detail. From this investigation, a set of tunable second order FGA's is obtained. These amplifiers, in addition, possess a good relative stability and their properties have been optimized to yield maximum operating bandwidths. The second order FGA's reported earlier

in the literature are also shown to be special cases of the realizations presented in this chapter. Amongst the second order non-inverting FGA's, NPGA2 is found to be optimal for any d.c. gain from the points of view of (i) tunability, (ii) relative stability and (iii) bandwidth. A similar statement holds good for NNGA1, which realizes a second order inverting FGA.

Theoretical as well as experimental results have been provided for these FGA's along with those of the conventional realizations. The comparison shows that the new designs improve the operating bandwidths of the FGA's by an order of magnitude or more over the one that can be obtained with the conventional designs.

The general theory presented in Chapter II assumes a control configuration which employs a single forward path along with a single feedback path. This theory also suggests that the coefficients of the corresponding powers of s in the denominator and the numerator polynomials of an mth order transfer function should be equal up to $(m-1)$th term. While implementing the second order FGA's possessing the above property for the transfer function, the existence of circuits with multiple feedbacks is revealed. The feedback factor β as given by (2.13), where $(m-1)$ terms are only retained is only one of the required forms for the transfer function to possess such a property. However, it can be visualized that as long as the higher order transfer functions possess the above mentioned property and they are stable, whatever might be the feedback factor or the form of the circuit realization, further extension of bandwidths of FGA's may be possible by implementing the higher order transfer functions.

Thus, in Chapter IV circuits with multiple feedback paths are considered. Two circuits are presented for realizing FGA's with stable transfer functions of any order - one for realizing higher order positive gain amplifiers and the other for obtaining negative gain amplifiers. While the FGA's obtained from these circuits are, for any order, stable by themselves, the considerations such as relative stability, improvement of the operating bandwidth and economy of the designed circuits indicate that it is not worthwhile to examine realizations beyond third order. Consequently, detailed design procedures are given only for the third order FGA's in this chapter. Theoretical and experimental results are given to show that these FGA's are superior in bandwidth to any other type of FGA's, second order or conventional.

In order to demonstrate the usefulness of the new designs of the FGA's proposed in this thesis, some applications in active-RC filters are presented in Chapter V. These applications clearly show that the greatest improvement in the operating frequency ranges in active-RC filters is obtained by using the third order FGA's in them. However, active-RC filters using the second order FGA's also achieve an extension in their operating frequency ranges of an order of magnitude or more over the ones using conventional FGA's. Extensive theoretical and experimental results have been provided to support the above conclusions. The experimental results also show that the second order FGA's are less affected by the changes in power supply voltages than the conventional FGA's. Also, the effect of these variations is the least in the case of third order FGA's. Further, it has been shown that, in practice, the signal handling capabilities of the new FGA's compare favourably with those

of the conventional FGA's.

The designs of the foregoing FGA's are attractive from the point of view of implementing them in IC technology, since circuit implementation of the new FGA's require only OA's and resistors. Further, their characteristics depend on the ratios of the resistors and GB products of the OA's. As the values of resistors and GB products of the OA's track closely with each other with respect to aging, variations in power supply voltage, temperature etc., the ratios are likely to remain constant. Thus, the properties of these FGA's, once tuned, are not likely to be affected by varying environmental conditions. This characteristic is highly desirable for mass production of active-RC filters in IC technology.

In the first method, the performance of the filters is sought to be improved by improving the active elements, viz. the FGA's contained in them. In the second method, presented in Chapter VI, the performance of the active-RC filters is sought to be improved by suitably designing the given circuit so as to minimize the dependence of the response on the GB products of the OA's. In this procedure, it is suggested that the values of the circuit elements, particularly the values of the compensating elements, may be chosen in such a way as to "match" the amount of the "compensation" that is just required for the given circuit at hand. Specifically, the suggestion is made to the effect that the compensating elements may be chosen through an optimization technique so as to minimize the overall effect of the GB products of the OA's and not just of the first or second order effects of (ω/B) on the response. In this way, it is expected that a maximum possible improvement in the operating frequency range can be achieved for a given filter circuit and for a given type of OA's.

Three optimization algorithms, Algorithms I, II and III, are given to implement the above design philosophy. These algorithms can be used for any type of active-RC filters using OA's. To emphasize this fact, an actively compensated double integrator loop reported by Reddy [39] is chosen for application. The optimized designs for this circuit result in significant improvement in the performance over the one available from the design of Reddy. The algorithms are also compared as to their accuracies and the required execution times. It is shown that Algorithm I is the most accurate and the simplest of all the algorithms. Also, this algorithm can be used for designing filters of any order with simple modifications to the one suggested in this thesis. However, for second order filters, Algorithm II seems to be "optimal" and Algorithm III is acceptable for only highly selective filters. It should also be noted that, when acceptable, Algorithm III is the fastest requiring the least execution time.

An obvious fruitful future direction of research is the investigation of improvement in the operating frequency range obtained when the optimization algorithms are applied to filter circuits that employ the higher order FGA's. In such a case, the technique will choose not only the optimal parameters of the circuit but will also yield an optimal design for the FGA's suitable to the circuit in which they are used.

Only experimental results for signal handling capabilities of the FGA's have been presented. However, a complete theoretical analysis of this aspect as well as noise properties of the new FGA's should prove to be useful in predicting the dynamic ranges of these elements. In addition, the limitations imposed by the slew rate of the OA's should also be examined.

The effect of the second pole of the OA's on the FGA's has been but briefly examined. These two effects become important in the high frequency range. Thus, a detailed look into these problems might be rewarding.

Finally the applications of the new FGA's only in active-RC filters, have been considered. It may be worthwhile to look into the other areas of potential applications such as instrumentation, control etc. In such areas of applications, the time domain response may be of improtance. Thus, it may be desirable to investigate the time domain behaviour of the new FGA's.

In conclusion, in view of the fact that the active-RC filters find numerous and varied applications in several areas such as telephony and switching circuits, instrumentation, data processing equipments, PCM systems, control systems etc., the author hopes that the techniques presented and the results obtained in this thesis should be useful in practice.

REFERENCES

1. Mitra, S.K., *Analysis and Synthesis of Linear Active Networks*, New York, Wiley, 1969.

2. Newcomb, R.W., *Active Integrated Circuit Synthesis*, Englewood Cliffs, N.J., Prentice-Hall, 1968.

3. Huelsman, L.P., *Theory and Design of Active RC Networks*, Bombay, Tata McGraw-Hill, 1968.

4. Widlar, R.J. and Giles, J.N., "Designing with off-the-Shelf Linear Microcircuits", Fairchild Applications Bulletin, App. -124, Jan., 1966.

5. Heinlein, W. and Holmes, H., *Active Filters for Integrated Circuits*, New York, Springer-Verlag, 1974.

6. Sallen, R.P. and Key, E.L., "A practical method of designing RC-Active filters", IRE Trans. Circuit Theory, Vol. CT-2, pp. 74-85, March 1955.

7. Bach, R.E., "Selecting RC Values for Active Filters", Electronics, Vol. 33, pp. 82-85, May 1960.

8. Solid State Variable Filter, Model 3200(R), Krohn-Hite Corporation, Cambridge, Mass. 02139, 1973.

9. Natarajan, S. and Murti, V.G.K., "RC-Active Network Synthesis using an Amplifier", Int. J. Electronics, Vol. 26, No.5, pp. 423-435, 1969.

10. Natarajan, S. and Murti, V.G.K., "Realization of Transfer Functions using one Amplifier", Electronics Letters, Vol. 15, No. 19, 18th Sept., 1969.

11. Prescott, A.J., "Loss Compensated Active Gyrator using Differential Input OA's", Electronics Letters, Vol. 2, pp. 283-284, July 1966.

12. Dutta Roy, S.C. and Nagarajan, V., "On Inductor Simulation using a Unity Gain Amplifier", IEEE J. Solid-State Circuits, Vol. SC-5, pp. 95-98, June 1970.

13. Millman, J. and Halkias, C.C., *Integrated Electronics: Analog and Digital Circuits and Systems*, New York, McGraw-Hill, 1972.

14. Budack, A. and Petrela, D.M., "Frequency Limitations of Active Filters using OA's", IEEE Trans. Circuit Theory, Vol. CT-19, pp. 322-329, July 1972.

15. Moschytz, G.S., *Linear Integrated Circuits-Design*, New York, Van Nostrand, 1975.

16. Thomas, L.C., "Biquad: Part-I-Some Practical Design Considerations", IEEE Trans. Circuit Theory, Vol. CT-17, pp. 358-367, August 1970.

17. Antoniou, A. and Naidu, K.S., "A Compensation Technique for a Gyrator and its use in the Design of a Channel Bank Filter", IEEE Trans. Circuits and Systems, Vol. CAS-22, pp. 316-323, April 1975.

18. Srinivasagopolan, R. and Martens, G.O., "A Comparison of a Class of Active Filters with Reference to the OA GB Product", IEEE Trans. Circuits and Systems, Vol. CAS-21, pp. 377-381, May 1974.

19. Tarmi, R. and Ghausi, M.S., "Very High Q Insensitive Active-RC Networks", IEEE Trans. Circuit Theory, Vol. CT-17, pp. 358-366, August 1970.

20. Mikhael, W.B. and Bhattacharyya, B.B., "A Practical Design for Insensitive RC-Active Filters", IEEE Trans. Circuits and Systems, Vol. CAS-22, pp. 407-415, May 1975.

21. Rao, K.R. and Srinivasan, S., "A Bandpass Filter using the OA Pole", IEEE J. of Solid State Circuits, Vol. 8, pp. 245-246, June 1973.

22. Mitra, A.K. and Aatre, V.K., "Low Sensitivity High Frequency Active-R Filters", IEEE Trans. Circuits and Systems, Vol. CAS-23, pp. 670-676, Nov., 1976.

23. Brand, J.R. and Schaumann, R., "Active-R Filters: Review of Theory and Practice", IEE J. on Electronics and Systems, Vol. 2, No. 4, pp. 89-101, July 1978.

24. Wilson, G., "Compensation of OA Based RC-Active Networks", IEEE Trans. Circuits and Systems, Vol. CAS-23, pp. 443-446, July 1976.

25. Abougabal, M.S., Bhattacharyya, B.B. and Swamy, M.N.S., "An Optimal Design of RC-Active Filters using Grounded Capacitors", Intl. Journal of Circuit Theory and Applications, Vol. 6, pp. 31-40, Jan., 1978.

26. Soliman, A.M. and Ismail, M., "Phase Correction in two Integrator Loop Filters using a Single Compensating Resistor", Electronics Letters, Vol. 14, pp. 375-376, June 1978.

27. Wupper, H., "Extending the Frequency Range of some RC-Active Filters", Proc. IEEE Intl. Symposium on Circuits and Systems, pp. 324-327, April 1977.

28. Vogel, P.M., "Method for Phase Correction in Active-RC Circuits using Two Integrators", Electronics Letters, Vol. 7, pp. 273-275, May 1971.

29. Akerberg, D. and Mossberg. K., "A Versatile Active-RC Building Block with Inherent Compensation for Finite Bandwidth of the Amplifier", IEEE Trans. Circuits and Systems, Vol. CAS-21, pp. 75-78, Jan., 1974.

30. Reddy, M.A., "An Insensitive Active-RC Filter for High Q and High Frequencies", IEEE Trans. Circuits and Systems, Vol. CAS-23, pp. 429-433, July 1976.

31. Reddy, M.A., "OA Circuits with Variable Phase Shift and Their Application to High Q Active-RC Filters and RC-Oscillators", IEEE Trans. Circuits and Systems, Vol. CAS-23, pp. 384-389, June 1976.

32. Brackett, P.O. and Sedra, A.S., "Active Compensation for High Frequency Effects in OA Circuits with Applications to Active-RC Filters", IEEE Trans. Circuits and Systems, Vol. CAS-23, pp. 68-72, Feb., 1976.

33. Natarajan, S. and Bhattacharyya, B.B., "Design and Some Applications of Extended Bandwidth Finite Gain Amplifiers", Journal of Franklin Institute, Vol. 305, No. 6, pp. 321-341, June 1978.

34. Bhattacharyya, B.B. and Natarajan, S., "An Improved Design of Voltage Follower Circuits using Operational Ampliffers", Proc. 21st Midwest Symposium on Circuits and Systems, pp. 188-192, August 1978.

35. Geiger, R.L., "Amplifiers with Maximum Bandwidth", IEEE Trans. Circuits and Systems, Vol. CAS-24, pp. 510-512, Sept., 1977.

36. Geiger, R.L., "Zero Sensitivity Active Filter Employing Finite Gain Voltage Amplifiers", Proc. IEEE Intl. Symposium on Circuits and Systems, pp. 1064-1068, May 1978.

37. Geiger, R.L. and Budak, A., "Biquadratic Active Filters with Zero Amplifier-Sensitivity", Proc. 21st Midwest Symposium on Circuits and Systems, pp. 536-540, August 1978.

38. Natarajan, S. and Bhattacharyya, B.B., "Design of Finite Gain Amplifiers using OA's for Improved Bandwidth", sent for publication.

39. Reddy, M.A., "An Active-RC Filter for High-Q and High Frequencies with Zero-Q-Frequency Sensitivity to Amplifier Gain Bandwidth Product", Proc. IEEE Vol. 65, pp. 814-815, May 1977.

40. Bhattacharyya, B.B. and Natarajan, S., " A New Continuously Tunable Sinusoidal Oscillator without External Capacitors", Proc. IEEE, Vol. 65, pp. 1726-1727, Dec., 1977.

41. Roberge, J.K., *Operational Amplifiers, Theory and Practice*, New York, Wiley, 1975.

42. Ghausi, M.S., *Principles and Design of Linear Active Networks*, New York, McGraw-Hill, 1965.

43. Kapustian, V., Bhattacharyya, B.B. and Swamy, M.N.S., "Frequency Limitations of Active-R Filters using Operational Amplifiers", Proc. European Conference on Circuit Theory and Design, pp. 150-154, Sept., 1978.

44. Fuji, N., "On the Minimum Gain Pole-Sensitivity Product of Single Amplifier RC-Active Networks", IEEE Trans. on Circuits and Systems, Vol. CAS-24, pp. 504-510, Sept., 1977.

45. Natarajan, S. and Bhattacharyya, B.B., "Optimization of RC-Active Filters for Extended Bandwidth Operation", Proc. IEEE, Vol. 66, pp. 260-261, Feb., 1978.

46. Fletcher, R., "A New Appraoch to Variable Metric Algorithms", Computer Journal, Vol. 13, pp. 317-322, August 1970.

47. Hilberman, D., "An Approach to Sensitivity and Statistical Variability of Biquadratic Filters", IEEE Trans. on Circuit Theory, Vol. CT-20, pp. 382-390, July 1973.